The Dissertation Committee for Stephen Richard Marek Certifies that this is the approved version of the following dissertation:

Intelligent Delivery via Enzyme Active Hydrogels

Committee:

Nicholas A. Peppas, Supervisor

Donald R. Paul

Benny D. Freeman

Jennifer A. Maynard

Muhammad H. Zaman

Intelligent Delivery via Enzyme Active Hydrogels

by

Stephen Richard Marek, B.S.

Dissertation

Presented to the Faculty of the Graduate School of

The University of Texas at Austin

in Partial Fulfillment

of the Requirements

for the Degree of

Doctor of Philosophy

The University of Texas at Austin

December 2009

Dedication

To my wife Beth.

Acknowledgements

First and foremost, I want to thank my graduate advisor, Professor Nicholas Peppas, for all the support and guidance he provided me during my graduate studies. His countless hours of teaching and assistance have helped make me who I am today.

I would not have made it here without the support of my parents. They taught me the value of an education and hard work, and helped me through all of my studies.

I also want to thank my current and former lab mates. Hunter taught me my first polymerization, Kristy kept me humble, Don taught me how *not* to do things, Brock made my work ethic look bad, Terry applauded all of my questioning and Omar showed me how many more questions I could ask. Daniel always stole half of the glory on my birthday, while Justin kept us rockin' till the wee hours. Adam, thanks for the polymer help. Carolyn, thanks for listening and the thesis help. Marty, I'm glad I no longer deal with the DLS. Thank you Maggie for trying to run some cells, and Bill for doing SEM because I was too busy. Brandon, I'm never riding with you again. Diana, your vote for crazy sky gave me the tie. David, Penny misses you. Cody and Anh, good luck. Thanks to everyone for their friendship and support during these difficult times.

Last, but definitely not least, I would like to thank my loving wife Beth. Her warmth and support helped me through some of the most stressful parts of my life. Without her, I would be lost, adrift at sea. Dr. H will always be there for you.

Finally, I would like to acknowledge the financial support of The University of Texas at Austin, Cockrell School of Engineering in the form of graduate fellowships.

Intelligent Delivery via Enzyme Active Hydrogels

Publication No._____

Stephen Richard Marek, Ph.D.

The University of Texas at Austin, 2009

Supervisor: Nicholas A. Peppas

Advances in medical treatment are leading away from generalized care towards intelligent systems or devices which can sense and respond to their environment. With these devices, the burden of monitoring and dosing for treatment can be removed from the doctor (or the patient) and be placed on the device itself. Implicit closed-loop control systems will allow the device to respond to its environment and release a therapeutic agent in response to a specific stimulus. Environmentally responsive hydrogels show great promise in being incorporated in such an intelligent device, such as pH-responsive hydrogels which can swell and deswell in response to changes in the pH of the media. Thus, pH changes can be exploited for controlled and intelligent drug delivery when used in combination with these pH-responsive hydrogels.

In this work, heterogeneous, thermal-redox initiated free-radical polymerizations were developed to synthesize novel pH-responsive hydrogels, microparticles, and nanogels. The specific disease of interest was type I diabetes, which requires daily doses of insulin both at a basal amount and either a postprandial or preprandial bolus in order to maintain blood glucose levels within safe limits. To allow pH-responsive

hydrogels to be sensitive to glucose, glucose oxidase was incorporated which oxidizes glucose to gluconic acid.

A novel inverse-emulsion polymerization method was developed for the synthesis of poly[2-(diethylaminoethyl methacrylate)-grafted-polyethylene glycol monoethyl ether monomethacrylate] (P(DEAEM-g-PEGMMA)) nanogels (100-400 nm) for intelligent insulin delivery. The new polymerization method allowed the incorporation of hydrophilic components, such as glucose oxidase and catalase, as well as PEG surface tethers of lengths 400 Da up to 2000 Da. Surface tethers successfully decreased the surface charge of the nanogels. Insulin loading and release was determined for microparticles which were able to imbibe substantial amounts of insulin from solution when swollen, entrap the insulin when collapsed, and then release the insulin in response to either a pH or glucose stimulus.

Table of Contents

LIST OF FIGURES

CHAPTER 1

1.1 INTRODUCTION

There is a growing need in the medical field for devices that can provide patients with custom doses of a therapeutic agent [1] in response to high concentrations of selected biomarkers. More importantly, these devices need to be "intelligent;" they need to only release the drug when the patient is in need of its therapeutic effects. To provide this automatic and customized dosing, these devices must be able to first sense a specific biomarker associated with the diseased state and then release the drug at a predetermined biomarker level. Once the biomarker concentration drops and signals the end of the dosing period, the device must then limit its release of the therapeutic agent. Thus, a closed-loop system involving sensors, transducers, and actuators must be synthesized to provide this desired response.

The detection of a biomarker can be implemented in numerous ways. Molecularly imprinted polymers (MIPs) have shown great promise as "artificial antibodies" that can recognize specific substrates [2-6]. The polymer is formed around the desired substrate, which allows monomer moieties to form interactions, generally noncovalent, with the substrate. Cavities are left behind once the template molecules are rinsed out of the polymer; thus, the polymer is able to preferentially absorb molecules that fit these cavities. A major drawback to MIPs is the high crosslinking ratio necessary to prevent the cavities from "forgetting" their imprint [7, 8] a crosslinking ratio that decreases the magnitude of swelling and thus decreases the possible increase of release of a drug molecule.

A second possible sensing mechanism incorporates competitive binding of a ligand [9-11]. One such instance is the use of concanavalin A (ConA), which is a lectin

that binds sugar molecules. It has a very high affinity for glucose, which leads to numerous methods of delivering insulin. Hydrogels can be synthesized containing crosslinks of ConA complexed with either glucosyloxyethyl methacrylate [10] or some other glycosylated monomer unit [12]. In the presence of glucose, the glucosyloxyethyl methacrylate-ConA complex dissociates, and ConA reassociates with glucose in solution. This process leads to the dissolution of the polymer complex, which can be combined with the release of imbibed insulin. ConA can also be used to bind a bioactive glycosylated insulin conjugate which, in the presence of glucose, is released from the system [13, 14]. However, over time, most systems slowly lose ConA to the surrounding fluid, thus decreasing sensitivity.

The toxicity of such devices has been questioned, though a recent review [15] has concluded that, provided the devices are not injected intravenously, a functional amount of ConA could safely be incorporated. Another method incorporates phenylboronic acid moieties, which can also reversibly bind to diols, forming repulsive charges on the polymeric backbone [16, 17]. One other complication with these ligand-binding based sensors is their affinity for other saccharides such as mannose. It has been shown that oral ingestion of mannose increases blood mannose levels [18], which could undermine the glucose sensitivity of a ConA based device and possibly prove dangerous.

There are numerous methods proposed and used for sensing glucose. However, enzymes have evolved to have a highly specific affinity for certain biomolecules, and exploiting this specificity could prove to be an ideal method of detection in pharmaceutical devices. Of the sensors currently being researched, enzyme-based sensors appear to be the most promising; their specificity does not allow “forgetting” of the biomarker, and they also tend to have orders of magnitude more specificity for one molecule compared to similar molecules. *For this thesis, type I diabetes will be used as a*

model disease, using glucose as the biomarker and glucose oxidase as the sensor enzyme.

Type I diabetes mellitus is a disease in which the patient's pancreas is no longer able to produce the required insulin for glucose cellular uptake, and thus the patient requires supplemental insulin for survival. Typically, this is due to an autoimmune response to the patient's own β-islet cells.

The current standard method of insulin delivery is subcutaneous injection of an insulin solution multiple times per day, primarily before consuming a meal. The insulin pump is a second method, in which the patient has a catheter implanted for prolonged periods of time that is connected to an external insulin delivery device. The patient can easily control the dosing of insulin to account for his current activities. In both of these treatments, for optimal glucose control, the patient must know precisely how much insulin is needed at any given time. The extraction of a small amount of blood, most commonly via needle prick, is necessary for glucose measurements.

To provide patients with optimal blood glucose control, a closed loop delivery device is ideal. The device itself can continuously monitor the patient's glucose levels, and then deliver insulin when necessary. The inconvenience of forcing the patient to monitor his or her glucose levels can thus be eliminated, along with the requirement that the patient knows how much insulin to dose himself or herself in any given situation. The patient's blood glucose levels can remain within healthy physiological limits, which significantly decrease secondary complications such as blindness, renal failure, microvascular problems, nerve damage, and more [19-25]. The cost of treating these complications has been shown to be significantly more than the cost of treating diabetes itself [26].

This thesis focuses on determining whether enzyme-based hydrogel carriers can be used for intelligent closed-loop drug delivery. The hypothesis of the research was that *polymeric carriers using enzymes to sense specific biomarkers will provide*

intelligent, feedback-controlled closed-loop release of a pharmaceutical agent, ultimately resulting in better control of the diseased state. Type I diabetes mellitus was used as a model disease, and tighter glycemic control that will thus improve the living standards of type I diabetics was be the final goal. It was important to determine whether the specificity of an enzyme can be coupled to a polymeric device to provide the desired sensing and release properties necessary for a pharmaceutical device.

1.2 REFERENCES

1. Heller, A., *Integrated medical feedback systems for drug delivery.* AIChE J., 2005. **51**(4): p. 1054-1066.

2. Hilt, J.Z., M.E. Byrne and N.A. Peppas, *Microfabrication of intelligent biomimetic networks for recognition of D-glucose.* Chem Mater, 2006. **18**(25): p. 5869-5875.

3. Byrne, M.E., E. Oral, J.Z. Hilt and N.A. Peppas, *Networks for recognition of biomolecules: molecular imprinting and micropatterning poly(ethylene glycol)-Containing films.* Polym Advan Technol, 2002. **13**(10-12): p. 798-816.

4. Mosbach, K., *Molecular Imprinting.* Trends Biochem Sci, 1994. **19**(1): p. 9-14.

5. Sellergren, B., M. Lepisto and K. Mosbach, *Highly Enantioselective and Substrate-Selective Polymers Obtained by Molecular Imprinting Utilizing Noncovalent Interactions - Nmr and Chromatographic Studies on the Nature of Recognition.* J Am Chem Soc, 1988. **110**(17): p. 5853-5860.

6. Oya, T., T. Enoki, A.Y. Grosberg, S. Masamune, T. Sakiyama, Y. Takeoka, et al., *Reversible molecular adsorption based on multiple-point interaction by shrinkable gels.* Science, 1999. **286**(5444): p. 1543-1545.

7. McCluskey, A., C.I. Holdsworth and M.C. Bowyer, *Molecularly imprinted polymers (MIPs): sensing, an explosive new opportunity?* Organic & Biomolecular Chemistry, 2007. **5**(20): p. 3233-3244.

8. Miyata, T., T. Uragami and K. Nakamae, *Biomolecule-sensitive hydrogels.* Adv Drug Deliver Rev, 2002. **54**(1): p. 79-98.

9. Zhang, R., M. Tang, A. Bowyer, R. Eisenthal and J. Hubble, *Synthesis and characterization of a d-glucose sensitive hydrogel based on CM-dextran and concanavalin A.* Reactive and Functional Polymers, 2006. **66**(7): p. 757-767.

10. Miyata, M., A. Jikihara, K. Nakamae, T. Uragami, A.S. Hoffman, K. Kinomura and M. Okumura, *Preparation of Glucose-Sensitive Hydrogels by Entrapment or Copolymerization of Concanavalin A in a Glucosyloxyethyl Methacrylate Hydrogel*, in *Advanced biomaterials in biomedical engineering and drug delivery systems*, N. Ogata, Editor. 1996, Springer: Tokyo ; New York. p. 237-240.

11. Sung, W.K., M.P. Chaul, K. Makino, L.A. Seminoff, D.L. Holmberg, J.M. Gleeson, D.E. Wilson and E.J. Mack, *Self-Regulated Glycosylated Insulin Delivery.* J Control Release, 1990. **11**(1-3): p. 193-201.

12. Lee, S.J. and K. Park, *Synthesis and characterization of sol-gel phase-reversible hydrogels sensitive to glucose.* J Mol Recognit, 1996. **9**(5-6): p. 549-557.

13. Brownlee, M. and A. Cerami, *Glucose-Controlled Insulin-Delivery System - Semi-Synthetic Insulin Bound to Lectin.* Science, 1979. **206**(4423): p. 1190-1191.

14. Seminoff, L.A., G.B. Olsen and S.W. Kim, *A Self-Regulating Insulin Delivery System .1. Characterization of a Synthetic Glycosylated Insulin Derivative.* Int J Pharm, 1989. **54**(3): p. 241-249.

15. Ballerstadt, R., C. Evans, R. McNichols and A. Gowda, *Concanavalin A for in vivo glucose sensing: A biotoxicity review.* Biosens Bioelectron, 2006. **22**(2): p. 275-284.

16. Siegel, R.A., Y.D. Gu, A. Baldi and B. Ziaie, *Novel swelling/shrinking behaviors of glucose-binding hydrogels and their potential use in a microfluidic insulin delivery system.* Macromol Symp, 2004. **207**: p. 249-256.

17. Kataoka, K., H. Miyazaki, M. Bunya, T. Okano and Y. Sakurai, *Totally synthetic polymer gels responding to external glucose concentration: Their preparation and application to on-off regulation of insulin release.* J Am Chem Soc, 1998. **120**(48): p. 12694-12695.

18. Alton, G., S. Kjaergaard, J.R. Etchison, F. Skovby and H.H. Freeze, *Oral Ingestion of Mannose Elevates Blood Mannose Levels: A First Step toward a Potential Therapy for Carbohydrate-Deficient Glycoprotein Syndrome Type I.* Biochem Mol Med, 1997. **60**(2): p. 127-133.

19. Schaumberg, D.A., R.J. Glynn, A.J. Jenkins, T.J. Lyons, N. Rifai, J.E. Manson, P.M. Ridker and D.M. Nathan, *Effect of intensive glycemic control on levels of markers of inflammation in type 1 diabetes mellitus in the diabetes control and complications trial.* Circulation, 2005. **111**(19): p. 2446-2453.

20. Genuth, S., J. Lipps, G. Lorenzi, D.M. Nathan, M.D. Davis, J.M. Lachin and P.A. Cleary, *Effect of intensive therapy on the microvascular complications of type 1 diabetes mellitus.* Jama-J Am Med Assoc, 2002. **287**(19): p. 2563-2569.

21. Albers, J.W., D.J. Kenny, M. Brown, D. Greene, P.A. Cleary, J.M. Lachin and D.M. Nathan, *Effect of intensive diabetes treatment on nerve conduction in the diabetes control and complications trial.* Ann Neurol, 1995. **38**(6): p. 869-880.

22. *Effect of Intensive Therapy on the Development and Progression of Diabetic Nephropathy in the Diabetes Control and Complications Trial.* Kidney Int, 1995. **47**(6): p. 1703-1720.

23. Shamoon, H., H. Duffy, N. Fleischer, S. Engel, P. Saenger, M. Strelyzn, et al., *The Effect of Intensive Diabetes Treatment on the Progression of Diabetic-Retinopathy in Insulin-Dependent Diabetes-Mellitus - the Diabetes Control and Complications Trial.* Arch Ophthalmol-Chic, 1995. **113**(1): p. 36-51.

24. *Influence of intensive diabetes treatment on quality-of-life outcomes in the diabetes control and complications trial.* Diabetes Care, 1996. **19**(3): p. 195-203.

25. *Effect of Intensive Diabetes Management on Macrovascular Events and Risk-Factors in the Diabetes Control and Complications Trial.* Am J Cardiol, 1995. **75**(14): p. 894-903.

26. Bjork, S., *The cost of diabetes and diabetes care.* Diabetes Res Clin Pr, 2001. **54**: p. S13-S18.

CHAPTER 2

Background

2.1 DIABETES MELLITUS

2.1.1 Pathology

Diabetes mellitus is a disorder in which the patient has elevated blood glucose levels, either due to the inability to produce enough insulin or the inability to efficiently use the insulin produced [1]. The body uses glucose as the main metabolite for generating adenosine triphosphate (ATP), the energy source for most cellular activity. The typical level of blood glucose in healthy individuals is around 80-90 mg/dL. Even after consuming a meal, a healthy individual will rarely have glucose levels above about 120-140 mg/dL. Excess glucose is removed from the plasma and either used or stored as glycogen. During fasting conditions, the body will regenerate this glucose, either from the breakdown of glycogen, amino acids, or fatty acids. In order to help cells uptake and use glucose, the pancreas secretes the regulating hormone insulin from the β-cells in the Islets of Langerhans.

At the onset of a blood glucose level spike, the β-islet cells release insulin to accelerate glucose usage and prevent hyperglycemia (Figure 2.1). The response of these cells to elevated blood glucose levels is not zero order. There is an initial spike in insulin release, which is then followed by a large decrease in the insulin concentration. As the islet cells synthesize more insulin, it is released to the surroundings, eventually reaching the maximum amount to be delivered. This response has been characterized as having both a proportional and a derivative response to the glucose input [2]. While increased

blood glucose levels are a strong factor in determining how much insulin is released, other metabolites are important as well. Amino acids, free fatty acids, as well as numerous proteins and hormones all contribute to the islet cells' insulin production. Diabetes sets in when the pancreatic cells are no longer able to operate as normal, and thus blood glucose levels rise above normal.

There are two main types of diabetes mellitus. Type 1 diabetes is characterized by either a severe or total lack of insulin production. This disease is usually caused by an autoimmune attack of the patient's β-islet cells where insulin is produced. The cells are destroyed, leaving the individual unable to produce insulin. Thus, the patient must take insulin supplements to survive. Type 2 diabetes is caused by a resistance to the effects of normal insulin levels. Patients can have a genetic predisposition for this disease, and it is more common in obese patients. While diet and exercise were the normal treatments for type 2 diabetes, insulin supplements have recently become more commonly prescribed. Diabetes is a serious disease afflicting over 180 million people worldwide with estimates that this number will double by 2030, according to the World Health Organization. This diabetes epidemic has therefore influenced numerous researchers to try to improve upon current treatment options. Because type 1 diabetes is always insulin dependent, it will be the focus of this research.

2.1.2 Current Treatments

Current treatments for type 1 diabetes consist of dosing the patient with exogenous insulin. The most common method of delivering the insulin is subcutaneously via syringe. The patient must first test his or her blood glucose level with a sample of blood, usually obtained by a needle stick to the finger or some other body part. Once the current glucose level is known, the patient must decide whether an insulin dose is necessary. If a dose is necessary, the patient must calculate how much

insulin is needed depending on what activities are planned in the near future. Consuming a meal, exercising, and many other activities affect how much insulin the patient will need. If instead it is determined that hypoglycemia has set in, a small amount of sugar is necessary to prevent the condition from becoming dangerous, which could lead to fainting or even a coma. This treatment regime is an open-loop control of blood glucose levels, since the patient must both measure his or her glucose levels and then use that measurement to decide what action must be taken.

There are other methods available for diabetic patients to combat insulin deficiency, though nearly every one is also an open loop control. Insulin pumps have become more common over the years. Instead of having to repeatedly inject oneself with insulin, a cannula is implanted subcutaneously for a number of days and a continuous supply of insulin is provided. When the patient needs to adjust the infusion rate, the pump can be reprogrammed and the patient can receive insulin without using a new syringe accompanied by an injection. However, blood glucose levels need to still be monitored by the patient to know when the insulin dosage needs to be altered. Higher risks of ketoacidosis have been reported, especially when the pump malfunctions. The device usually must be removed during certain physical activities such as strenuous exercise or bathing. Recently, implantable insulin pumps (IIP) have been released in Europe and America. These devices solve many of the problems of external pumps, yet still require user intervention to change insulin infusion rates. Also, new problems have arisen, such as scarring or fibrotic tissue formation near the implant site [3].

These insulin delivery routes both pose numerous problems. Needles are involved with both methods, which decrease patient compliance and comfort due to pain and/or needle phobia [4]. Needles also pose a biohazard risk. Exubera®, an inhalable form of insulin, was recently released, but it had problems with product bulkiness and a limited number of patients that could actually use the device. Smaller

than average lung capacity, such as a child's, or even damaged lungs from being a smoker or having uncontrolled asthma, rendered the patient unable to use inhalable insulin. Even for those patients lucky enough to qualify for inhalable insulin, the dosing was a fixed amount, and the patient had to take the inhalation ten minutes before every meal. These problems, among others, forced Pfizer to halt production and sales of Exubera. Oral delivery of insulin has been labeled as the holy grail for insulin delivery, since the patient would no longer need to inject insulin. The problem of protein degradation in the stomach has been solved using methacrylic acid based complexation hydrogels, but low bioavailability still remains an issue [5]. Also, all of these treatments are part of an open loop control of the patient's blood glucose levels, where the patient must first check his glucose levels and then dose himself accordingly.

2.1.3 Closed-Loop Diabetes Control

Patient inconvenience is not the only problem associated with the open-loop control of a diabetic's blood glucose levels. Severe complications have been associated with chronically poor blood glucose control. Tissue damage occurs after years of high glucose levels. Blood vessels can be damaged on both the microvasculature and macrovasculature levels, leading to numerous other problems such as loss of sight, kidney failure, and nerve damage. The Centers for Disease Control and Prevention have stated that diabetes-caused nerve damage is the leading reason for the non-traumatic amputation of lower limbs in the United States. Preventing these complications not only helps improve the quality of life of diabetics, but it also helps decrease healthcare needs. Thus, diabetic patients need to have their blood glucose levels monitored and controlled on a continuous basis, bringing treatment closer to the response of an actual pancreas.

In order to provide the ideal control of blood glucose levels, the device must continuously monitor glucose and release insulin. This concept is the basis for closed-loop control devices for the treatment of diabetes. A logical option would be to transplant a healthy pancreas into the patient; however, due to shortages of healthy pancreases as well as severe problems with immune responses, a pancreas transplant is not typically a feasible route. Encapsulating the β-cells in a semipermeable membrane has been heavily researched [6], which could possible act as an artificial pancreas. The membrane prevents cells or antibodies from destroying the encapsulated cells, yet allows glucose into the device and insulin out of the device. However, cell viability and immune responses are still major problems. Different geometries are being researched to maximize the response of these cells to the blood glucose levels while still protecting them from the immune response.

Entirely synthetic devices have also been researched and manufactured. The Biostator® is one such device, with both a glucose sensor and an insulin infusion pump, acting as an artificial pancreas. A computer algorithm controls the insulin infusion, depending on the needs of the patient. However, the device is too large to be implanted and is thus extracorporeal. More problems with this device included catheter fouling, maintaining insulin activity in the reservoir, and needing to tune the algorithm for the specific patient, among others. While it is impractical for daily use, it is a significant contribution to the medical field and academic community. More work is being conducted, attempting to combat these issues while miniaturizing the whole device by linking an IIP with a continuous glucose monitoring device.

Another alternative to these devices is an implicit closed-loop insulin delivery device based on a chemical system that can perform all three functions of the artificial pancreas in one unit. The device can detect the surrounding glucose levels, and then alter the infusion rate of insulin based on this concentration. It acts as a sensor for glucose, a control algorithm by mechanically changing in response to the glucose levels,

and an infusion system by passively allowing the diffusion of insulin out of the device. Since the device itself must respond appropriately to its surroundings, the design and fabrication of the device, both chemically and physically, is integral to providing the necessary therapeutic effects.

The field of novel diabetes treatment research is continually evolving and resides at an exciting forefront of medicinal research. Diabetes was initially diagnosed by a patient having sweet-tasting urine, from ancient times up until about the 20th century. Initial treatments were also just as crude and thus life expectancy was quite short. Around the 1920s several milliliters of crudely purified insulin was discovered to effectively treat patients. Significant advancements have occurred over the last century, though there is still plenty of room for improvement. Improving the lives of diabetic patients will continually be sought until a cure for the disease itself is discovered.

2.2 HYDROGELS IN DRUG DELIVERY

2.2.1 Hydrogels

Hydrogels are hydrophilic polymers that have been crosslinked to form a three-dimensional polymer matrix. Under the correct environmental conditions, these materials can imbibe significant amounts of water, often over two orders of magnitude more water than polymer by weight. Due to the large water content, hydrogels are currently the synthetic material most resembling living tissue [7]. These properties help make hydrogels ideal for use in tissue engineering, as well as numerous other applications such as drug delivery, surface coatings, contact lenses, wound dressings, and even polluted water treatment [8-11].

There are several important physical parameters of hydrogels that alter the properties and ultimately can determine the potential uses of a polymer system. One of

the most important parameters is the average molecular weight between crosslinks, $\overline{M_c}$, which indicates how frequently crosslinks have formed along the polymer backbone. However, for diffusion studies, it is more important to know the physical size between the polymer chains. By using Equation (2.1), $\overline{M_c}$ can be manipulated to find the mesh size, ξ, which essentially indicates what sized particle could theoretically diffuse through the polymer network.

$$\xi = Q^{-1/3}\left(C_n l^2 \frac{\overline{M}_c}{M_r}\right)^{1/2} \tag{2.1}$$

In this equation, Q is the volume swelling ratio, C_n is the Flory characteristic ratio, l is the length of a bond on the polymer backbone, and M_r is the molecular weight of the repeat unit. As a hydrogel swells, its mesh size increases allowing larger solutes to diffuse through its macromolecular chain network. This swelling is characterized by the polymer volume fraction in the swollen state, $v_{2,s}$, which is the inverse of the volume swelling ratio.

The study of hydrogel use in drug delivery applications has been in place for decades [12-15]. It was realized early on that reservoir devices yielded zero-order release kinetics, that is, a release rate that was not a function of time. Transport through the membrane shell is the diffusion-limiting step, and so the rate of release can be controlled by changing the thickness or type of membrane. These devices tend to have either a burst-effect or lag-effect, depending on whether or not the drug had time to dissolve in the membrane during storage. Since many diseased states can be treated with a constant, therapeutic level of drug, reservoir devices seemed ideal. However, difficulties in manufacturing as well as problems with membrane rupture were significant hindrances. Also, large molecular weight drugs such as proteins are not able to diffuse at an appreciable rate through the biocompatible polymers used in reservoir devices.

Non-degrading matrix type systems, on the other hand, typically yield first-order release kinetics. A matrix system has the drug homogeneously dispersed or dissolved throughout the polymer. For these devices, the release profile is a function of the square root of time. Thus, the drug is released faster at earlier time points compared to later ones. This is because the drug has to diffuse through the whole polymer system in order to be released, and so the diffusional path length increases with time as the drug concentration decreases. The burst and lag effects tend to not be present, and the manufacturing of these devices can be less intricate than reservoir systems. There is also no need to worry about the polymer rupturing, since the drug is dispersed throughout the whole polymer system and it is less likely to cause a significant overdose. These devices permit site-specific drug delivery and others can even permit tissue targeting [16].

2.2.1.1 Neutral Hydrogels

Depending on their charges, hydrogels can be divided into two types: neutral and ionic. Neutral hydrogels are a class of polymer gels that do not have any ionizable moieties on their side chains, such as poly(vinyl alcohol) (PVA). These polymers swell due to a balance between the elastic retractive forces of the polymer chains and the thermodynamic mixing of the polymer chains with the solvent molecules. These polymers can be used as bioadhesives or in both reservoir and matrix drug delivery systems, among other applications.

Certain hydrogels exhibit environmental sensitivity due to these forces being functions of temperature [17, 18] or some other variable. One such polymer, poly(N-isopropyl acrylamide), exhibits a lower critical solution temperature (LCST); at temperatures above this LCST, the polymer is hydrophobic and remains in a collapsed state. Below the LCST, the hydrogel is hydrophilic and imbibes large amounts of water.

Thus, if a drug is dissolved or suspended in the polymer, it is more easily able to diffuse out when the polymer is swollen. A similar swelling behavior is observed with polymers that exhibit an upper critical solution temperature (UCST), though these systems swell above the threshold temperature and collapse below it (Figure 2.2).

Poly(ethylene glycol) (PEG) is a neutral polymer that does not exhibit pH sensitivity but is still quite important to mention. It is a highly biocompatible polymer of repeating ethylene glycol units. In an aqueous environment, each ethylene glycol repeat unit is able to bind multiple molecules of water. This phenomenon allows the PEG chains to repel each other and form a "brush-like" conformation when the appropriate PEG density is achieved [19]. It is believed that the chains form a mushroom morphology when the surface density of PEG is much lower. Thus, a high surface density of PEG grafts is usually desired.

PEG has long been known for its resistance to protein adsorption [20-22] which can be attributed to its steric repulsion, hydrophilicity, and chain mobility [23]. Two surfaces coated with PEG will develop repulsive forces when brought close enough, due to the steric stabilization of each PEG chain. The interaction between infinitely sized [21] to small sized [20] proteins has been modeled, showing that van der Waals interactions between the PEG and protein are negligible. Materials coated with PEG tethers have been shown to decrease opsonization and often complement system activation [24]. These properties can allow the prolonged use of medical devices *in vivo* while preventing coagulation, protein binding, or severe immune response. Thus, these properties have made PEG the most widely used polymer to impart biocompatibility and stealth properties to materials. For a more in-depth review of PEG, see Appendix A.

2.2.1.2 Ionic Hydrogels

One of the interesting types of environmentally-sensitive hydrogels is the ionic hydrogel [25]. These polymers exhibit extensive swelling when in certain media, in part due to electrostatic forces. Changes in environmental conditions such as pH [26, 27], ionic strength [28], buffer species [29, 30], temperature [31, 32], or other conditions cause swelling of these systems. Anionic pH-sensitive hydrogels are neutral at a pH below their pK_a, where the backbone and/or pendant groups are uncharged. When in this state, hydrogen bonding between moieties is possible, especially when acidic and ethereal groups are present such as methacrylic acid and PEG. It is interesting to note that the pK_a can be a slight function of temperature, thus adding some temperature dependence to pH-sensitive polymers.

Once the pH rises above the pK_a of the pendant groups they become charged. Usually, a carboxylic acid becomes deprotonated which imparts a negative charge on the system. Often, hydrogen bonds are broken and electrostatic repulsion ensues. The polymer also tends to become more hydrophilic, thus imbibing more water as it swells. Osmotic forces also play a role in the extent of swelling. Thus, the pH, buffer species, and ionic strength are all important parameters in determining the extent of swelling of a given polymer system. Common anionic polymers consist of methacrylic acid (MAA) or acrylic acid (AA), which have carboxylic acid functional groups that can deprotonate to form carboxylate anions (Figure 2.3). It has also been shown that copolymers of acrylic acid and acrylamide exhibit both a pH and very significant temperature swelling response [33].

Cationic hydrogels function in the opposite manner as anionic hydrogels. When the pH of the medium is above the pK_a of the polymer, the polymer is in its uncharged, deprotonated state. Many polymers are also fairly hydrophobic in this state. The polymer is collapsed, excluding a significant amount of water from the interior of the

system. Once the pH is dropped below the pK_a, significant portions of the polymer become protonated, thus taking on a positive charge. This positive charge can then induce swelling due to charge repulsion and an increase in hydrophilicity of the system, imbibing significant amounts of water. These hydrogels can then be collapsed again by raising the pH. Many cationic hydrogels are based on amines since the lone electron pair on the nitrogen is able to capture a hydrogen ion, imparting a positive charge to the nitrogen atom (Figure 2.3).

Significant research has been conducted on cationic systems based on either polymers or copolymers of N,N-diethylaminoethyl methacrylate (DEAEM) or N,N-dimethylaminoethyl methacrylate (DMAEMA) [30, 34-40]. The pK_a of PDEAEM at physiological temperature is very close to physiological pH, between about 7.0 and 7.3; therefore, a slight drop in local pH from physiological will cause significant swelling of the hydrogel system. This swelling is coupled to an increase in the mesh size of the system, allowing imbibed solutes to more easily diffuse out. One important limitation that Siegel *et al.* observed is that Donnan equilibrium excludes hydrogen ions from the hydrogels, which can be partly overcome by using buffered media. In high ionic strength media, Donnan equilibrium also limits the extent of swelling, due to the partitioning of the dissolved salts. Mallapragada and Anderson have synthesized copolymers of DEAEM and PEG via anionic polymerizations [41]. The initiator potassium *t*-butoxide was used to produce very monodisperse linear pH responsive polymers. Cytocompatibility tests were also conducted. While polymers of pure DEAEM were cytotoxic, polymers containing PEG tethers were shown to be cytocompatible at concentrations as high as 3 mg/L. Thus, the PEG tethers act as expected and can help decrease cell toxicity.

2.2.2 Hydrogels in Insulin Delivery

Insulin delivering hydrogels have been heavily researched, though the success of these systems is variable. Ishihara *et al.* characterized the permeation of insulin through membranes made of 2-hydroxyethyl methacrylate (HEMA) with methyl methacrylate (MMA) as a comonomer [42]. These devices exhibited zero order release profiles of insulin, and permeability increased with increasing HEMA content. However, the insulin needs of a patient that has just consumed a meal are not met with a zero order release. They also showed the responsiveness of a poly(amine) membrane to glucose using immobilized glucose oxidase [43, 44]. The diffusion of insulin through the membrane was shown to increase as the glucose concentrations increased. This concept was later used to form polymer capsules of 1.5 mm diameter synthesized out of complexed random copolymers of DEAEM, 2-hydroxyethyl acrylate (HEA), and 4-trimethylsilylstyrene (TMS) with entrapped glucose oxidase [45]. These capsules were loaded with insulin when synthesized, and release rates were determined. A cyclic response was observed when the capsules were repeatedly exposed to glucose solutions.

Most hydrogel based insulin delivery systems rely on glucose oxidase coupled with environmentally sensitive hydrogels to detect glucose. Glucose oxidase (GOx) is approximately a 160 kDa dimeric enzyme for oxidizing glucose into gluconic acid (Figure 2.4). Dissolved oxygen is reduced to hydrogen peroxide in the process of glucose oxidation (Figure 2.5). Since an acid is produced from glucose, it is possible to use the decrease in pH as a signal for increased glucose levels. Glucose oxidase has been used for decades in the determination of blood glucose levels for diabetic patients. It has also been demonstrated that molecules other than oxygen can be reduced, thus allowing the transfer of charge along a conductive material to directly operate as a sensor. Due to the toxicity of hydrogen peroxide, catalase (CAT), a 250 kDa tetrameric

enzyme, has been incorporated in some devices to prevent a toxic buildup (Figure 2.5). Catalase also regenerates the consumed dissolved oxygen, thus helping to eliminate one limitation of the glucose oxidase/glucose sensor. Both enzymes occur naturally in many organisms, though the mold *Aspergillus niger* is a common source for industrial and medical uses.

A graphical representation of how a pH responsive cationic polymer with immobilized glucose oxidase and catalase responds to glucose levels is shown in Figure 2.6. An appropriate hydrogel needs to be selected such that the system is collapsed at normal physiological pH, with a relatively small mesh size. Thus, the pK_a of the hydrogel needs to be at or below about 7.4. As the glucose levels rise, the glucose oxidase catalyzes more oxidations of glucose and therefore the concentration of gluconic acid increases. Locally, this gluconic acid buildup drops the pH. The hydrogel absorbs these excess hydrogen ions, imparting a positive charge along the polymer backbone. The governing thermodynamics force the polymer to swell. Larger quantities of gluconic acid cause larger amounts of swelling. As the hydrogel swells, the mesh size increases, thus allowing imbibed insulin to diffuse out of the system. Once the released insulin starts to cause a drop in glucose levels, the concentration of gluconic acid inside the system decreases and the insulin release slows or stops.

Horbett *et al.* designed systems based on crosslinked DMAEMA with HEMA and glucose oxidase [46]. These films were synthesized by first freezing the monomer mixture and then exposing it to radiation from a ^{60}Co source to initiate the polymerization. Glucose oxidase was entrapped in the hydrogel structure, thus imparting glucose sensitivity to the pH sensitive hydrogel. Storage of the systems for 300 days in buffer still retained more than a third of the enzymatic activity, whereas storage in blood for 60 days retained almost half of the enzymatic activity. Thus, long term usage of such devices may be possible, since the enzyme remains stable over long periods of time. ^{125}I labeled insulin was used for release studies, which were performed

in vitro as well as *in vivo*. They concluded that insufficient amounts of insulin were being released, however, and that macroporous structures may be necessary. Further work showed that these macroporous structures were able to regulate insulin release at more relevant levels [47].

Siegel and Firestone [40] also used polybasic gels based on DMAEMA. Oscillatory swelling and deswelling was demonstrated, yielding an ultimate collapsed state. These systems were then used to selectively release caffeine as a model drug [38]. At a very low pH, release continued for almost two hours. At slightly acidic and neutral pH, the gels took nearly twice as long to fully release the caffeine. Thus, the collapsed hydrogels were able to trap the small molecular weight drug significantly more than the swollen hydrogels. When they copolymerized DMAEMA with methyl methacrylate [35], they showed that temperature and ionic strength also affected swelling and deswelling. Significant amounts of water were able to be imbibed in these systems. As the amount of MAA or the alkyl chain length of n-alkyl methacrylate esters increased, swelling volume decreased [28]. This effect was attributed to an increase in the overall hydrophobicity of the system, which decreased the total amount of water able to be imbibed.

Siegel and Firestone also studied the effects of the ionic strength and buffer composition of the swelling media [30, 34, 36]. They tested how different ions affected swelling extent and rates using a 70/30 gel of MMA/DMAEMA. These systems exhibited significant sensitivities to the different ions tested, especially the multivalent ions. Increased ion concentrations decreased overall swelling. Weak electrolytes allowed faster swelling than strong electrolytes. A rigorous application of the ideal Donnan equilibrium theory was unsuccessfully able to fit all the data, and so a heuristic approach was taken to qualitatively describe the responses of the systems to different ionic species [30].

Kinetic experiments were performed using DMAEMA and n-alkyl methacrylate esters [35]. The alkyl chain length was altered to vary the overall hydrophobicity of the systems. A biphasic means of swelling was observed in glassy disks, having an initial slow uptake of water followed by a rapid volume expansion. This initial swelling rate was observed to increase with four factors: increased temperature, decreased pH, decreased n-alkyl methacrylate content, and decreased alkyl chain length. When the opposite conditions are met, a non-Fickian zero-order behavior is observed. Weak electrolytes were observed to increase swelling kinetics substantially compared to strong electrolytes, which was attributed to the ease of ion transport through the membranes. Initially rubbery disks, on the other hand, did not exhibit these biphasic swelling fronts. Instead, they had monophasic but still non-Fickian sorption of the solvent.

More recently, Siegel has moved away from a hydrogel for releasing insulin towards one that acts as an actuator for a glucose sensing device based on phenylboronic moieties [48]. The glucose reversibly bound to the phenylboronic groups, imparting a charge to the boron atom. This charge induced swelling in the system similarly to the cationic hydrogels. As the gel swelled in the presence of glucose, it pressed against a plate attached to a variable capacitor, thus altering the resonant frequency of an LC resonator. This device had a response time of 90 min, though this should be improved by decreasing the thickness of the responsive hydrogel layer. They have also been working on a P(NIPAAm-co-MAA) membrane that could temporarily shut off glucose transport at low pH [49]. Glucose flux resumed after equilibration at this low pH, albeit at much lower rates. These results were attributed to a collapsed “skin” that formed on the acidic side of the membrane.

Goldraich and Kost [50] studied systems based on DEAEM and HEMA, crosslinked with tetraethylene glycol dimethacrylate (TEGDMA). Glucose oxidase, either immobilized or entrapped, was included in these systems. Swelling as a function of the

comonomer and crosslinking ratios was determined, and insulin release was tested. In high pH media, little insulin was released. Unfortunately, the collapse of a gel was much slower than the swelling, and thus the cutoff of insulin release was much slower than the initiation of insulin release. This slowed collapse may be due to Donnan equilibrium effects, which make it more difficult to remove the hydrogen ion from the swollen gel. Other problems noticed were low physiological oxygen concentrations and possible encapsulation after implantation. Since glucose oxidase is dependent on dissolved oxygen as a reactant, low physiological levels significantly hinders the kinetic rate of the glucose oxidation.

Imanishi and associates took a different approach to releasing insulin. Porous cellulose films were grafted with poly(acrylic acid) and glucose oxidase [51]. At neutral pH, the chains were charged and extended due to charge repulsion, thus blocking the pores of the cellulose membrane. Once the glucose levels increased, glucose oxidase catalyzed the formation of gluconic acid. The pH dropped, and the acrylic acid groups became protonated and lost their charge. This decrease in electrostatic repulsion between polymer chains allowed the opening of the pores, releasing insulin. A second method of insulin release consisted of insulin immobilized to a polymer membrane using a disulfide bond [52]. Glucose dehydrogenase (GDH) was used to ultimately reduce the disulfide bond in the presence of glucose, thus releasing insulin. NAD was also incorporated to help with the charge transfer from the GDH to the insulin disulfide bond. Released insulin activity was reported to be the same as untreated insulin.

Heller *et al.* also took a different route to release insulin [53]. A bioerodible poly(ortho ester) was used, which should have degraded in response to very slight pH decreases. Thus, with the incorporation of glucose oxidase would render the system glucose erodible, since it would degrade much faster in the presence of glucose. This degradation could be coupled to the release of infused insulin. However, it was noticed that the poly(ortho ester) was not terribly specific for its degradation. The inclusion of

tertiary amine components solved this problem by increasing the hydrophilicity of the system when in an acidic pH. The increased hydrophilicity allowed higher water penetration, which in turn led to a faster erosion rate. This erosion was coupled to a release of the impregnated insulin. They demonstrated cyclic responses as well, and these data suggest the possibility of a long-term device that could release insulin in bursts, in response to high glucose concentrations.

Peppas *et al.* have been studying both anionic and cationic hydrogels for the delivery of insulin and other drugs for decades. Hariharan and collaborators [54-56] studied copolymers of DEAEM and HEMA, N,N-diethylaminoethyl acrylate (DEAEA) and HEMA, methacrylaminopropyl ammonium chloride and HEMA, and acrylic acid (AA) and HEMA. Model drugs such as insulin, oxprenolol, lysozyme, and bovine serum albumin (BSA) were used in the studies. As the crosslinking amount increased, the mesh size decreased and solute release was either decreased or slowed. For the cationic gels, solute release increased with a decrease in pH. Anionic gels exhibited the opposite behavior, where solute release increased with an increase in pH. Release of solutes was by a diffusion-controlled process.

Dorski *et al.* took another approach to insulin release [57-59]. Instead of coupling glucose oxidase to a cationic hydrogel for insulin release in the presence of glucose, an anionic gel was studied. Since the decrease in pH still needed to illicit the release of insulin, a tighter network was used. Thus, upon constriction of the hydrogel, insulin was “squeezed” out of the system. Copolymers of methacrylic acid (MAA) and ethylene glycol (EG) were synthesized, containing immobilized glucose oxidase and catalase. The system exhibited strong complexation at acidic pH, thus providing a means of insulin release in the presence of glucose.

There is great promise in DEAEM based devices, as shown by Podual *et al.* [60-66]. Hydrogels were synthesized with DEAEM and PEG grafts, and crosslinked with TEGDMA. Glucose oxidase and catalase were chemically immobilized in the systems

using acryloyl chloride. Both films and microparticles were synthesized, both of which showed pH and glucose sensitivity. The films were made via UV initiated polymerization between two glass plates. The particles were synthesized via suspension polymerization in silicone oil with redox initiators, and different sized particles were formed depending on the speed of mixing and the amount of surfactant used. Smaller particles swelled faster, whereas larger particles and disks swelled slower. The films were determined to have too slow a response time for physiological need; however, the microparticles did have a fast enough response time.

Other parameters were also changed, such as crosslinking ratio and PEG graft length. Varying the crosslinking ratio was shown to alter the swelling rates and maxima. It was found that a crosslinking ratio of 3 mol % gave the highest ratio of diffusion of insulin out of the swollen hydrogel to the collapsed hydrogel. Systems with longer PEG grafts were determined to have swelling responses dominated by relaxation of chains, whereas shorter PEG grafted systems had diffusion-controlled swelling rates. Modeling of these systems was performed, which provided a means of estimating insulin release profiles. It was determined that a reasonable amount of polymer particles could be loaded and delivered to a patient.

Hydrogels have also been used in the oral delivery of proteins. Lowman *et al.* showed that copolymers of MAA and PEG form significant complexation in their collapsed states [67, 68]. Hydrogen bonding at low pH between the hydrogen on the MAA group to an etheric oxygen on the PEG unit was observed. This complexation was broken once the pH rose above the pK_a of the material and the acid moiety became deprotonated and negatively charged. These systems were also very efficient at loading insulin. Since these hydrogels were collapsed at a low pH and swollen at a neutral pH, they were ideal for oral insulin delivery to the small intestines. The stomach has a low pH as well as peptidases that are designed to destroy proteins. Thus, when insulin was encapsulated in the collapsed hydrogel at low pH values, it was protected from the

harsh environment of the stomach. The environment in the upper small intestines is much more hospitable to insulin, with fewer peptidases and a much higher pH. Thus, after being protected in the stomach, the insulin was released in the neutral environment of the small intestines when the complexation of the MAA and PEG broke down.

One last example worth mentioning, though not for insulin delivery, is the detection of glucose levels using glucose oxidase imbedded in a conductive polymer [69]. Instead of coupling glucose oxidase with acid production to generate a signal, the reduction of redox hydrogels was used to capture electrons from the enzymatic reaction and pass them along the polymer to an electrode. The polymer backbone itself was not conductive, contrary to standard conductive polymers such as polyaniline. Rather, long flexible pendant chains off the polymer backbone had a functional group susceptible to redox reaction, which allowed the charge to diffuse by swinging from pendant chain to pendant chain towards the imbedded electrode, as shown in Figure 2.7. This arrangement allowed the enzyme to be throughout the entire hydrogel contrary to monolayers coating an electrode.

2.3 CONCLUSIONS

It is apparent from the above literature survey that designing a device to release insulin in a physiological manner is highly desirable. Hydrogels seem a logical building block, since their parameters can be precisely tuned to provide specific key features, such as mesh size, response time, and release rates. They also can easily be made biocompatible, either by choosing already biocompatible materials or by grafting chains such as PEG to the surface (see Appendix A). The environmental sensitivity of the many hydrogels being studied also provides a means of incorporating a drug reservoir, a

sensor, and an actuator all into one device with minimal components. Thus, designing an optimal insulin-releasing device with hydrogels is quite a promising endeavor.

2.4 FIGURES

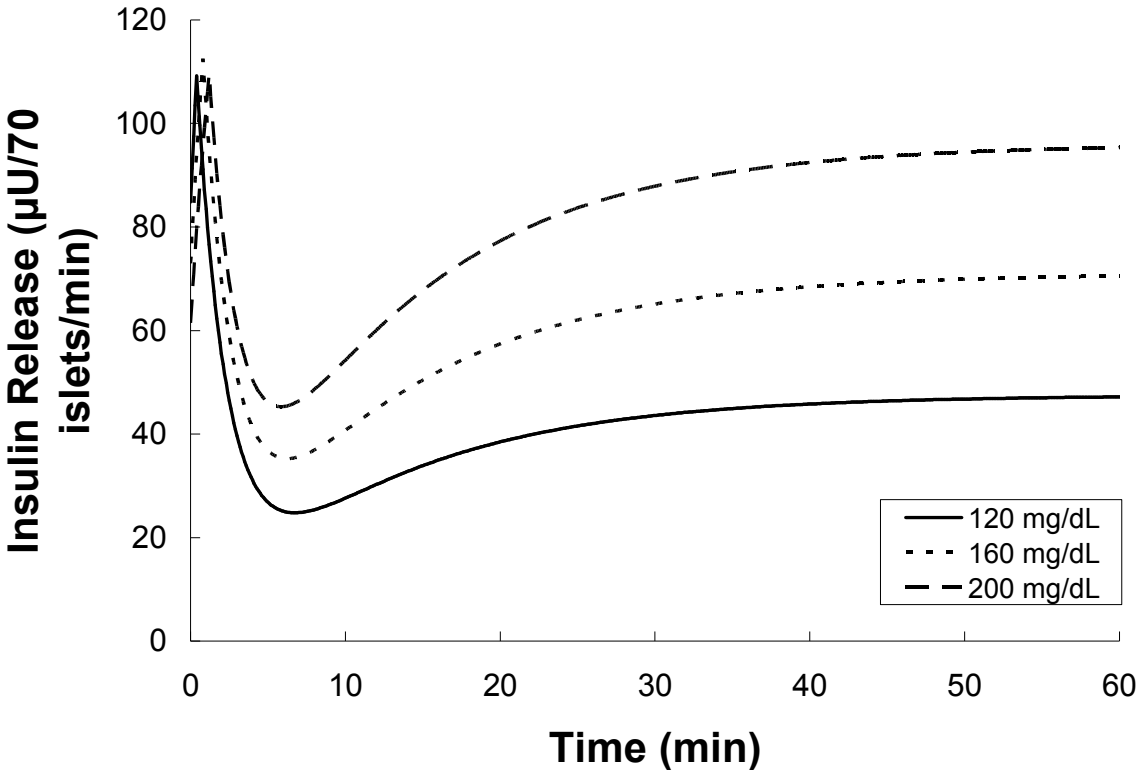

Figure 2.1. Insulin Infusion of a Healthy Individual

Increase in blood insulin levels in isolated rat pancreatic islets in response to different increases in blood glucose levels. Glucose levels were initially 80 mg/dL and were ramped to a final constant value. The initial high rate of infusion is due to the rapid dumping of previously synthesized insulin, while the secondary release is from currently synthesized insulin. Model is adapted from ref [2].

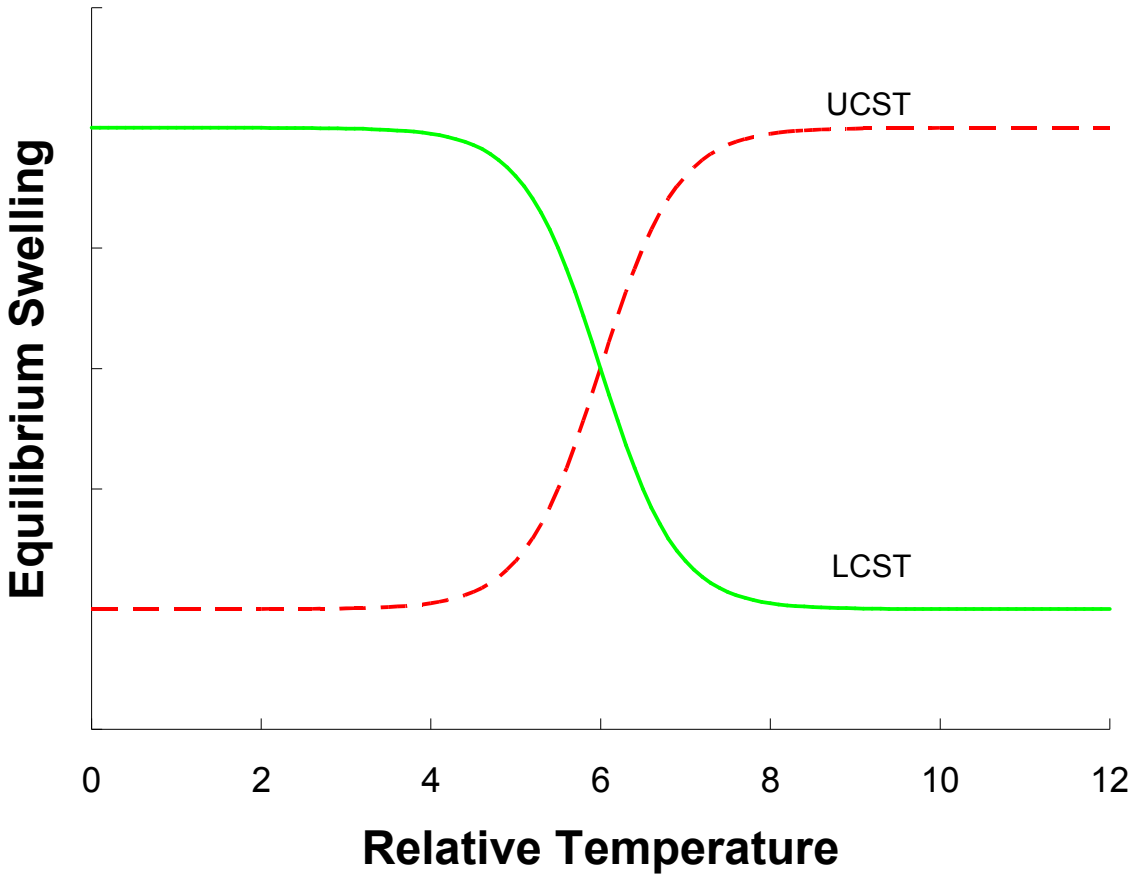

Figure 2.2. Swelling of Theoretical Temperature-Sensitive Polymers.

The solid line represents a theoretical polymer exhibiting a lower critical solution temperature (UCST), the hashed line represents a theoretical polymer exhibiting an upper critical solution temperature (LCST).

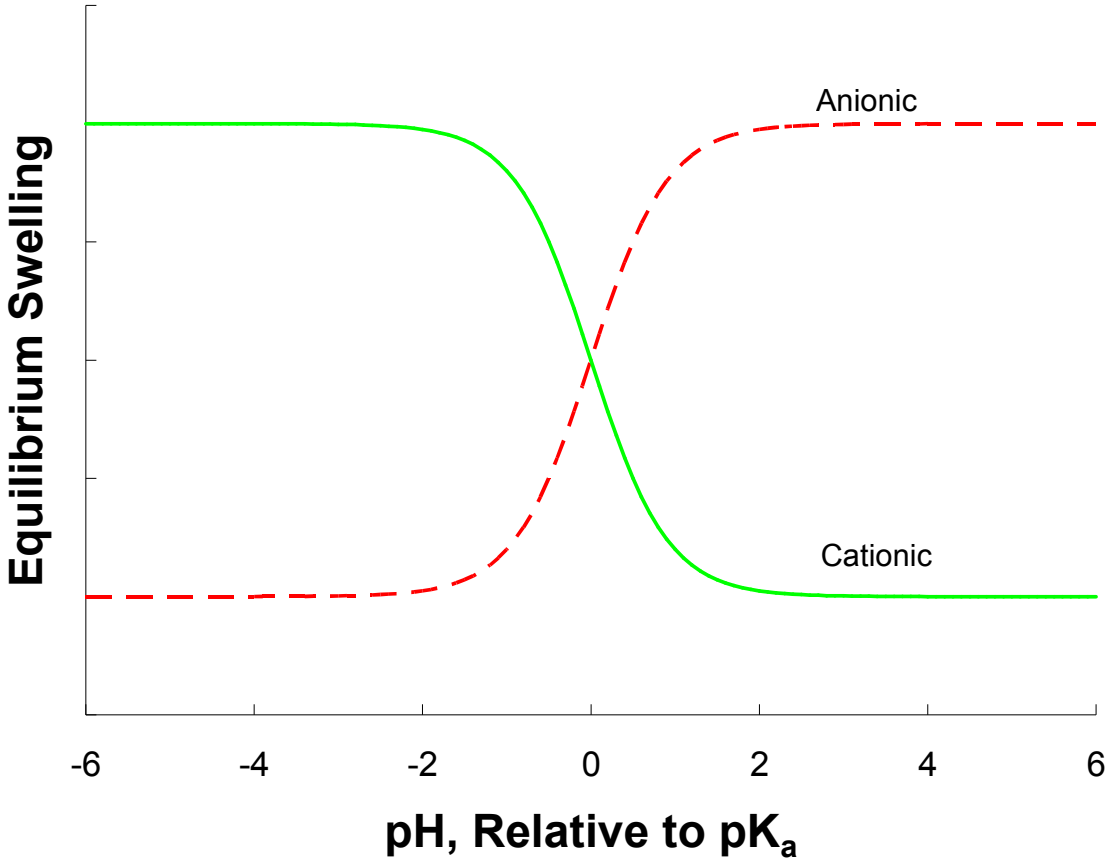

Figure 2.3. Swelling of Theoretical pH-Sensitive Polymers.

The solid line represents a theoretical anionic polymer; the hashed line represents a theoretical cationic polymer. Both polymers have a pKa of about 5.

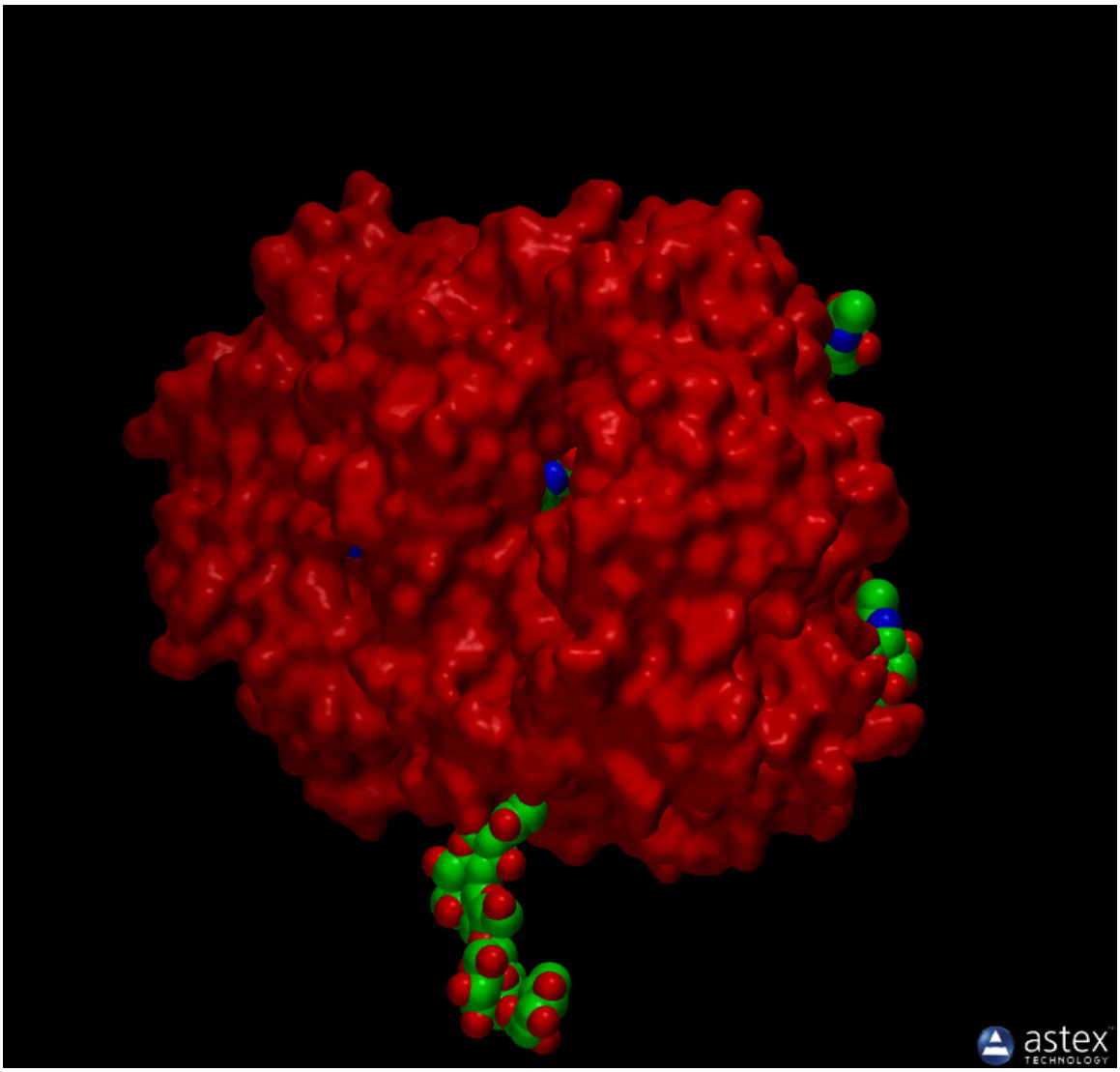

Figure 2.4. Molecular Computer Model of Glucose Oxidase from Aspergillus Niger.

The red atoms represent the surface mapping of the enzyme glucose oxidase. The green spheres are typical glycosylation molecules. The blue in the center of the image is an oxygen atom on the FAD at the center of the active site.

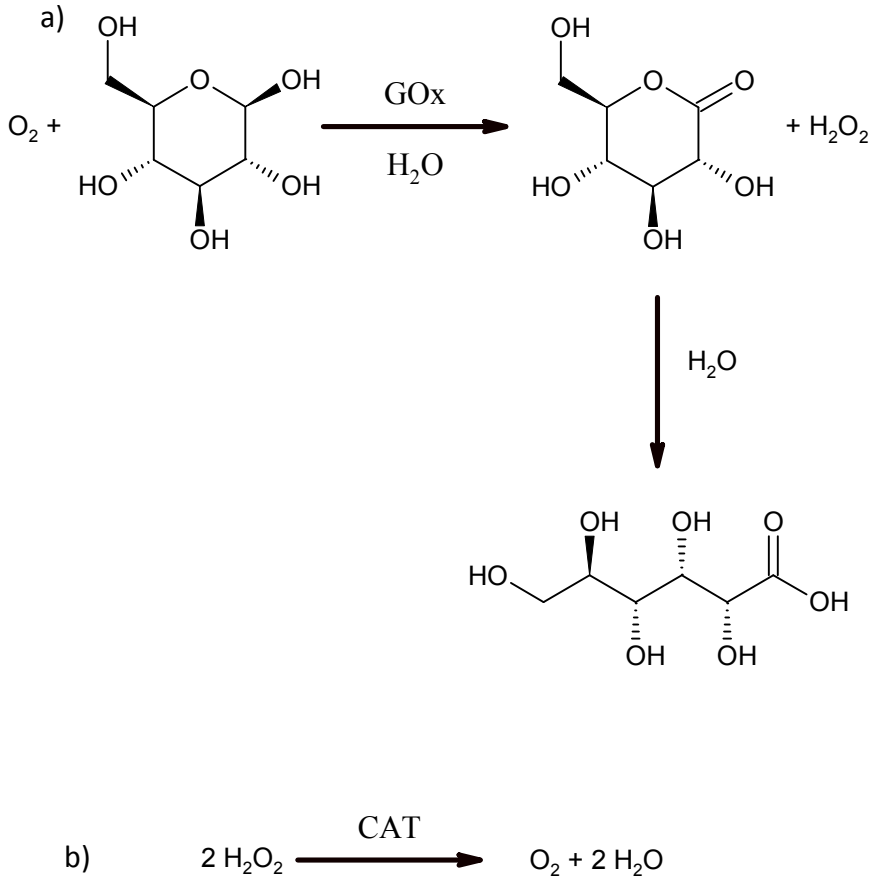

Figure 2.5. Chemical Reaction Catalyzed by Glucose Oxidase

(a) β-D-glucose is first oxidized to β-D-glucono-1,5-lactone while dissolved oxygen is reduced to hydrogen peroxide by the enzyme glucose oxidase (GOx). β-D-glucono-1,5-lactone is then hydrolyzed to gluconic acid in the presence of water.
(b) Hydrogen peroxide is oxidized back into water by catalase (CAT), evolving molecular oxygen in the process.

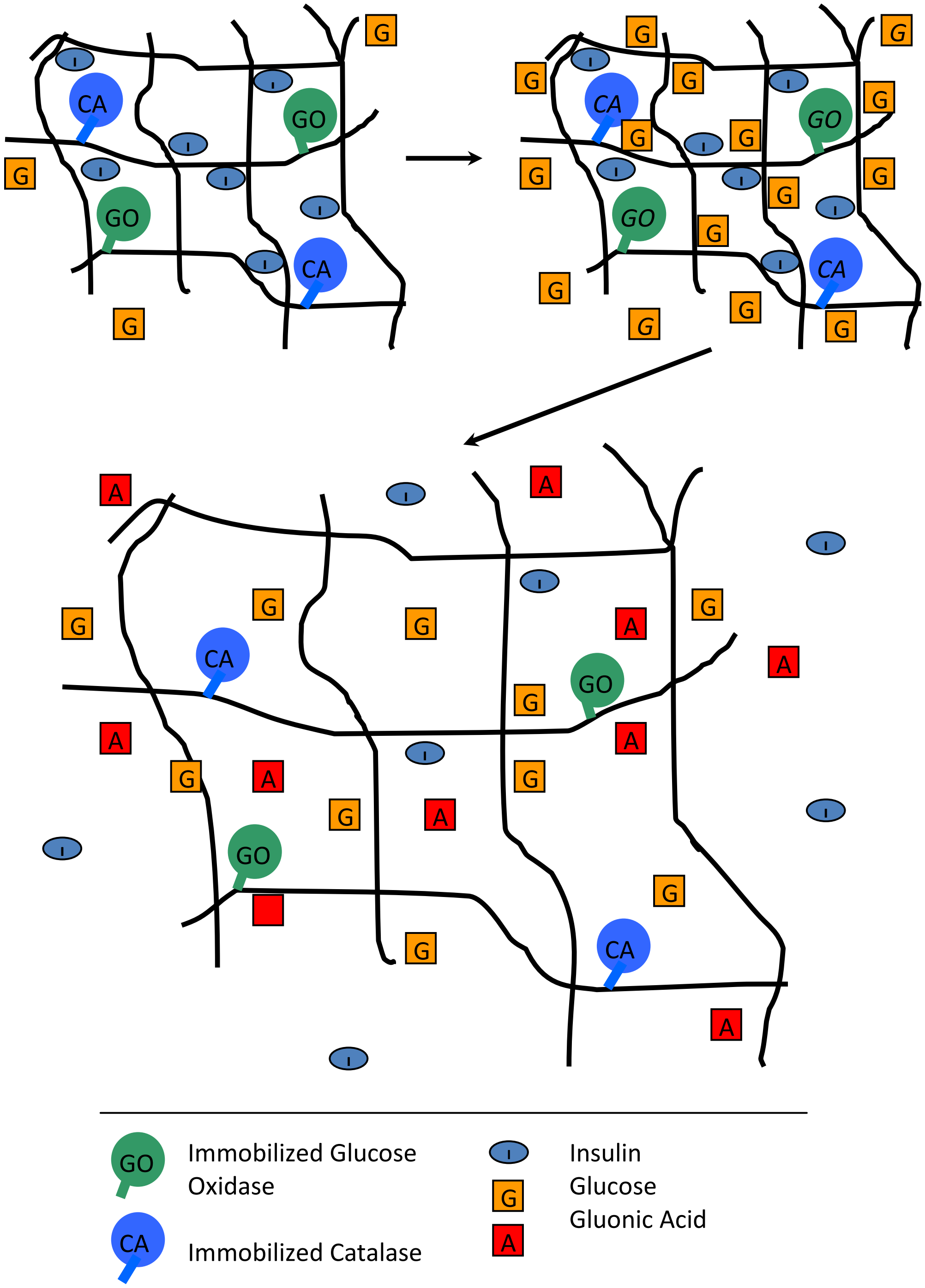

Figure 2.6. Diagram of a Cationic Hydrogel System Response to a Glucose Stimulus

As glucose concentrations rise, gluconic acid production increases. The system swells and releases insulin.

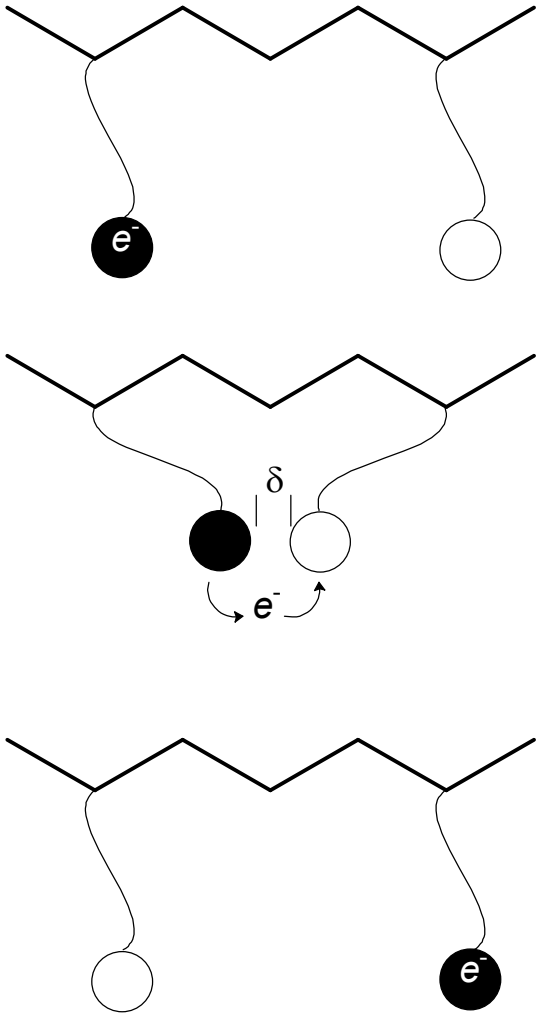

Figure 2.7. Electron Diffusion in Redox Hydrogels

Electrons diffuse in the redox hydrogels by collisions between mobile redox centers tethered to the backbone of the cross-linked and hydrated polymer. When the tethers are long enough, the reduced (black) and the oxidized (white) members of the couple can come within the Marcus theory-defined distance δ that the electron can cross (adapted from ref [69]).

2.4 REFERENCES

1. Guyton, A.C. and J.E. Hall, *Textbook of medical physiology*. 11th ed. 2006, Philadelphia: Elsevier Saunders. xxxv, 1116 p.

2. Nomura, M., M. Shichiri, R. Kawamori, Y. Yamasaki, N. Iwama and H. Abe, *A mathematical insulin-secretion model and its validation in isolated rat pancreatic islets perifusion.* Comput Biomed Res, 1984. **17**(6): p. 570-579.

3. Moore, K.B., C.D. Saudek, A. Greene and A. Dackiw, *Implantable insulin pump therapy: An unusual presentation of a catheter-related complication.* Diabetes Technology & Therapeutics, 2006. **8**(3): p. 397-401.

4. Nir, Y., A. Paz, E. Sabo and I. Potasman, *Fear of injections in young adults: Prevalence and associations.* Am J Trop Med Hyg, 2003. **68**(3): p. 341-344.

5. Lowman, A.M., M. Morishita, M. Kajita, T. Nagai and N.A. Peppas, *Oral delivery of insulin using pH-responsive complexation gels.* J Pharm Sci, 1999. **88**(9): p. 933-937.

6. Parker, R.S., *Insulin Delivery*, in *Encyclopedia of Biomaterials and Biomedical Engineering*, G.E. Wnek and G.L. Bowlin, Editors. 2004, Marcel Dekker: New York. p. 857-866.

7. Ratner, B.D., A.S. Hoffman, F.J. Schoen and J.E. Lemons, eds. *Biomaterials Science: An Introduction to Materials in Medicine*. 2nd ed. 2004, Elsevier Academic Press: Amsterdam ; Boston.

8. Wheeler, J.C., J.A. Woods, M.J. Cox, R.W. Cantrell, F.H. Watkins and R.F. Edlich, *Evolution of hydrogel polymers as contact lenses, surface coatings, dressings, and drug delivery systems.* J Long-Term Eff Med, 1996. **6**(3-4): p. 207-217.

9. Chen, J., Y.Q. Yang, P.B. Qian, Z.T. Ma, W.B. Wu, P.Z. Sung, X.G. Wang and J.H. Li, *Drug Carrying Hydrogel Base Wound Dressing.* Radiat Phys Chem, 1993. **42**(4-6): p. 915-918.

10. Hoffman, A.S., *Hydrogels for Biomedical Applications.* Ann Ny Acad Sci, 2001. **944**(1): p. 62-73.

11. Shawky, H.A., M.H. El-Sayed, A.E. Ali and M.S.A. Mottaleb, *Treatment of polluted water resources using reactive polymeric hydrogel.* J Appl Polym Sci, 2006. **100**(5): p. 3966-3973.

12. Bodde, H.E., E.A.C. Vanaalten and H.E. Junginger, *Hydrogel Patches for Transdermal Drug Delivery - Invivo Water Exchange and Skin Compatibility.* J Pharm Pharmacol, 1989. **41**(3): p. 152-155.

13. Kim, S.W., *Hydrogel Drug Delivery Systems.* Pharm Int, 1983. **4**(7): p. 182-182.

14. Lee, P.I., *Kinetics of drug release from hydrogel matrices.* J Control Release, 1985. **2**: p. 277-288.

15. Rosiak, J., K. Burozak and W. Pekala, *Polyacrylamide hydrogels as sustained release drug delivery dressing materials.* Radiation Physics and Chemistry (1977), 1983. **22**(3-5): p. 907-915.

16. Kopecek, J. and R. Duncan, *Targetable polymeric prodrugs.* J Control Release, 1987. **6**(1): p. 315-327.

17. Rice, C.V., *Phase-transition thermodynamics of N-isopropylacrylamide hydrogels.* Biomacromolecules, 2006. **7**(10): p. 2923-2925.

18. Hirotsu, S., *Coexistence of Phases and the Nature of 1st-Order Phase-Transition in Poly-N-Isopropylacrylamide Gels.* Adv Polym Sci, 1993. **110**: p. 1-26.

19. Halperin, A., *Polymer brushes that resist adsorption of model proteins: Design parameters.* Langmuir, 1999. **15**(7): p. 2525-2533.

20. Jeon, S.I. and J.D. Andrade, *Protein--surface interactions in the presence of polyethylene oxide : II. Effect of Protein Size.* J Colloid Interf Sci, 1991. **142**(1): p. 159-166.

21. Jeon, S.I., J.H. Lee, J.D. Andrade and P.G. De Gennes, *Protein--surface interactions in the presence of polyethylene oxide : I. Simplified theory.* J Colloid Interf Sci, 1991. **142**(1): p. 149-158.

22. Seifert, L.M. and R.T. Greer, *Evaluation of in vivo adsorption of blood elements onto hydrogel-coated silicone rubber by scanning electron microscopy and fourier transform infrared spectroscopy.* J Biomed Mater Res, 1985. **19**(9): p. 1043-1071.

23. Sharma, S., K.C. Popat and T.A. Desai, *Controlling nonspecific protein interactions in silicon biomicrosystems with nanostructured poly(ethylene glycol) films.* Langmuir, 2002. **18**(23): p. 8728-8731.

24. Owens, D.E. and N.A. Peppas, *Opsonization, biodistribution, and pharmacokinetics of polymeric nanoparticles.* Int J Pharm, 2006. **307**(1): p. 93-102.

25. Peppas, N.A., P. Bures, W. Leobandung and H. Ichikawa, *Hydrogels in pharmaceutical formulations.* Eur J Pharm Biopharm, 2000. **50**(1): p. 27-46.

26. Zhao, B. and J.S. Moore, *Fast pH- and ionic strength-responsive hydrogels in microchannels.* Langmuir, 2001. **17**(16): p. 4758-4763.

27. Baker, J.P., L.H. Hong, H.W. Blanch and J.M. Prausnitz, *Effect of Initial Total Monomer Concentration on the Swelling Behavior of Cationic Acrylamide-Based Hydrogels.* Macromolecules, 1994. **27**(6): p. 1446-1454.

28. Siegel, R.A. and B.A. Firestone, *pH-dependent equilibrium swelling properties of hydrophobic polyelectrolyte copolymer gels.* Macromolecules, 1988. **21**(11): p. 3254-3259.

29. Zhao, Y.B., W.Y. Chen, Y.J. Yajiang, X.L. Yang and H.B. Xu, *Swelling behavior of ionically cross-linked polyampholytic hydrogels in varied salt solutions.* Colloid Polym Sci, 2007. **285**(12): p. 1395-1400.

30. Firestone, B.A. and R.A. Siegel, *Ph, Salt, and Buffer Dependent Swelling in Ionizable Copolymer Gels - Tests of the Ideal Donnan Equilibrium-Theory.* J Biomat Sci-Polym E, 1994. **5**(5): p. 433-450.

31. Ju, H.K., S.Y. Kim and Y.M. Lee, *pH/temperature-responsive behaviors of semi-IPN and comb-type graft hydrogels composed of alginate and poly (N-isopropylacrylamide).* Polymer, 2001. **42**(16): p. 6851-6857.

32. Yu, H. and D.W. Grainger, *Thermosensitive Swelling Behavior in Cross-Linked N-Isopropylacrylamide Networks - Cationic, Anionic, and Ampholytic Hydrogels.* J Appl Polym Sci, 1993. **49**(9): p. 1553-1563.

33. Owens, D.E., Y.C. Jian, J.E. Fang, B.V. Slaughter, Y.H. Chen and N.A. Peppas, *Thermally responsive swelling properties of polyacrylamide/poly(acrylic acid) interpenetrating polymer network nanoparticles.* Macromolecules, 2007. **40**(20): p. 7306-7310.

34. Siegel, R.A., I. Johannes, C.A. Hunt and B.A. Firestone, *Buffer Effects on Swelling Kinetics in Polybasic Gels.* Pharmaceut Res, 1992. **9**(1): p. 76-81.

35. Firestone, B.A. and R.A. Siegel, *Kinetics and Mechanisms of Water Sorption in Hydrophobic, Ionizable Copolymer Gels.* J Appl Polym Sci, 1991. **43**(5): p. 901-914.

36. Siegel, R.A., B.A. Firestone, I. Johannes and J. Cornejo, *Weak Ionic Hydrogels - Effects of Ph, Ionic-Strength and Buffer Composition on Swelling Equilibria, Kinetics and Solute Release.* Abstr Pap Am Chem S, 1990. **199**: p. 119-POLY.

37. Siegel, R.A. and B.A. Firestone, *Mechanochemical Approaches to Self-Regulating Insulin Pump Design.* J Control Release, 1990. **11**(1-3): p. 181-192.

38. Siegel, R.A., M. Falamarzian, B.A. Firestone and B.C. Moxley, *Ph-Controlled Release from Hydrophobic Poly-Electrolyte Copolymer Hydrogels.* J Control Release, 1988. **8**(2): p. 179-182.

39. Siegel, R.A. and B.A. Firestone, *Ph-Dependent Equilibrium Swelling Properties of Hydrophobic Poly-Electrolyte Copolymer Gels.* Macromolecules, 1988. **21**(11): p. 3254-3259.

40. Firestone, B.A. and R.A. Siegel, *Dynamic Ph-Dependent Swelling Properties of a Hydrophobic Poly-Electrolyte Gel.* Polym Commun, 1988. **29**(7): p. 204-208.

41. Anderson, B.C. and S.K. Mallapragada, *Synthesis and characterization of injectable, water-soluble copolymers of tertiary amine methacrylates and poly(ethylene glycol) containing methacrylates.* Biomaterials, 2002. **23**(22): p. 4345-4352.

42. Ishihara, K., M. Kobayashi and I. Shinohara, *Insulin Permeation through Amphiphilic Polymer Membranes Having 2-Hydroxyethyl Methacrylate Moiety.* Polym J, 1984. **16**(8): p. 647-651.

43. Ishihara, K., M. Kobayashi, N. Ishimaru and I. Shinohara, *Glucose-Induced Permeation Control of Insulin through a Complex Membrane Consisting of Immobilized Glucose-Oxidase and a Poly(Amine).* Polym J, 1984. **16**(8): p. 625-631.

44. Ishihara, K., M. Kobayashi and I. Shionohara, *Control of Insulin Permeation through a Polymer Membrane with Responsive Function for Glucose.* Makromol Chem-Rapid, 1983. **4**(5): p. 327-331.

45. Ishihara, K. and K. Matsui, *Glucose-Responsive Insulin Release from Polymer Capsule.* J Polym Sci Pol Lett, 1986. **24**(8): p. 413-417.

46. Kost, J., T.A. Horbett, B.D. Ratner and M. Singh, *Glucose-Sensitive Membranes Containing Glucose-Oxidase - Activity, Swelling, and Permeability Studies.* J Biomed Mater Res, 1985. **19**(9): p. 1117-1133.

47. Albin, G., T.A. Horbett and B.D. Ratner, *Glucose sensitive membranes for controlled delivery of insulin: Insulin transport studies.* J Control Release, 1985. **2**: p. 153-164.

48. Lei, M., A. Baldi, E. Nuxoll, R.A. Siegel and B. Ziaie, *A hydrogel-based implantable micromachined transponder for wireless glucose measurement.* Diabetes Technology & Therapeutics, 2006. **8**(1): p. 112-122.

49. Dhanarajan, A.P. and R.A. Siegel, *Time-dependent permeabilities of hydrophobic, pH-sensitive hydrogels exposed to pH gradients.* Macromol Symp, 2005. **227**: p. 105-114.

50. Goldraich, M. and J. Kost, *Glucose-sensitive polymeric matrices for controlled drug delivery.* Clin Mater, 1993. **13**(1-4): p. 135-142.

51. Ito, Y., M. Casolaro, K. Kono and Y. Imanishi, *An Insulin-Releasing System That Is Responsive to Glucose.* J Control Release, 1989. **10**(2): p. 195-203.

52. Chung, D.J., Y. Ito and Y. Imanishi, *An Insulin-Releasing Membrane System on the Basis of Oxidation Reaction of Glucose.* J Control Release, 1992. **18**(1): p. 45-53.

53. Heller, J., A.C. Chang, G. Rood and G.M. Grodsky, *Release of insulin from pH-sensitive poly(ortho esters).* J Control Release, 1990. **13**(2-3): p. 295-302.

54. Hariharan, D. and N.A. Peppas, *Characterization, dynamic swelling behaviour and solute transport in cationic networks with applications to the development of swelling-controlled release systems.* Polymer, 1996. **37**(1): p. 149-161.

55. Amende, M.T., D. Hariharan and N.A. Peppas, *Factors Influencing Drug and Protein-Transport and Release from Ionic Hydrogels.* React Polym, 1995. **25**(2-3): p. 127-137.

56. Hariharan, D., N.A. Peppas, R. Bettini and P. Colombo, *Mathematical-Analysis of Drug-Delivery from Swellable Systems with Partial Physical Restrictions or Impermeable Coatings.* Int J Pharm, 1994. **112**(1): p. 47-54.

57. Hassan, C.M., F.J. Doyle and N.A. Peppas, *Dynamic behavior of glucose-responsive poly(methacrylic acid-g-ethylene glycol) hydrogels.* Macromolecules, 1997. **30**(20): p. 6166-6173.

58. Dorski, C.M., F.J. Doyle and N.A. Peppas, *Preparation and characterization of glucose-sensitive P(MAA-g-EG) hydrogels.* Abstr Pap Am Chem S, 1997. **213**: p. 172-PMSE.

59. Dorski, C.M., F.J. Doyle and N.A. Peppas, *Glucose-responsive, complexation hydrogels.* Abstr Pap Am Chem S, 1996. **211**: p. 417-POLY.

60. Podual, K., *Glucose-sensitive cationic hydrogels for insulin release*. 1998, Purdue University, CHE, DEC, 1998. p. xviii, 263 p.

61. Podual, K. and N.A. Peppas, *Relaxational behavior and swelling-pH master curves of poly[(diethylaminoethyl methacrylate)-graft-(ethylene glycol)] hydrogels.* Polym Int, 2005. **54**(3): p. 581-593.

62. Podual, K., F. Doyle and N.A. Peppas, *Modeling of water transport in and release from glucose-sensitive swelling-controlled release systems based on poly(diethylaminoethyl methacrylate-g-ethylene glycol).* Ind Eng Chem Res, 2004. **43**(23): p. 7500-7512.

63. Podual, K., F.J. Doyle and N.A. Peppas, *Dynamic behavior of glucose oxidase-containing microparticles of poly(ethylene glycol)-grafted cationic hydrogels in an environment of changing pH.* Biomaterials, 2000. **21**(14): p. 1439-1450.

64. Podual, K., F.J. Doyle and N.A. Peppas, *Glucose-sensitivity of glucose oxidase-containing cationic copolymer hydrogels having poly(ethylene glycol) grafts.* J Control Release, 2000. **67**(1): p. 9-17.

65. Podual, K., F.J. Doyle and N.A. Peppas, *Preparation and dynamic response of cationic copolymer hydrogels containing glucose oxidase.* Polymer, 2000. **41**(11): p. 3975-3983.

66. Podual, K., F.J. Doyle and N.A. Peppas, *Release of insulin from glucose-sensitive hydrogels.* Abstr Pap Am Chem S, 1996. **211**: p. 221-PMSE.

67. Morishita, M., A.M. Lowman, K. Takayama, T. Nagai and N.A. Peppas, *Elucidation of the mechanism of incorporation of insulin in controlled release systems based on complexation polymers.* J Control Release, 2002. **81**(1-2): p. 25-32.

68. Lowman, A.M. and N.A. Peppas, *Molecular analysis of interpolymer complexation in graft copolymer networks.* Polymer, 2000. **41**(1): p. 73-80.

69. Heller, A., *Electron-conducting redox hydrogels: design, characteristics and synthesis.* Curr Opin Chem Biol, 2006. **10**(6): p. 664-672.

CHAPTER 3

Research Objectives

The main objective of this Ph.D. thesis was to contribute to the medical field through the evaluation of enzyme-containing systems for intelligent, feedback-controlled drug delivery. This work had several goals: a) synthesize novel self-regulating polymeric systems consisting of pH-responsive moieties, as well as immobilized enzymes to impart sensitivity of a specific biomarker; and b) study the release kinetics from these systems.

We proposed that a new intelligent polymeric system can have the ability to regulate its drug release and provide closed-loop control of the intended disease. As a model case, type I diabetes was evaluated. Closed-loop control should decrease complications typically associated with poor glucose control by preventing spells of severely high or low glucose levels [1]; the system will be able to respond to its environment and only release insulin when necessary. The specific aims of this research project were to

1. Identify systems where enzymes can be used to help detect biomarkers.
2. Apply concepts to glucose oxidase containing systems for intelligent response to glucose, using type I diabetes as the model disease.
3. Prepare and characterize the systems, including under physiologically relevant conditions.
4. Provide guidance for the design and development of devices using these concepts.

Each of these specific aims was covered in a chapter below. The first two specific aims were covered in Chapter 4. The third specific aim was broken down into several chapters; the macro- and microscopic polymer synthesis and characterization was

discussed in Chapter 5, the nanoparticle polymer synthesis and characterization was discussed in Chapter 6, Chapter 7 discusses the insulin loading and release behavior of all polymer systems, and monomer and crosslinker synthesis was discussed in Chapter 8. Chapter 9 provides conclusions of the work as well as guidance on possible device development.

3.1 REFERENCES

1. Shamoon, H., H. Duffy, N. Fleischer, S. Engel, P. Saenger, M. Strelzyn, et al., *The Effect of Intensive Treatment of Diabetes on the Development and Progression of Long-Term Complications in Insulin-Dependent Diabetes-Mellitus.* New Engl J Med, 1993. **329**(14): p. 977-986.

CHAPTER 4

Enzyme Selection for Biomarker Detection in Hydrogel Devices

4.1 HYDROGELS FOR CONTROLLED DRUG DELIVERY

There are two main methods of using enzymes paired with hydrogels to control drug delivery; one system swells in acidic media (cationic), the other swells in basic media (anionic). The pK_a of an ionic polymer indicates the critical swelling pH, where the hydrogel will transition between its fully collapsed to its fully swollen state. Cationic hydrogels typically contain a basic moiety such as an amine which causes the swelling. In basic media, above the pK_a, the amine is deprotonated and in its collapsed, hydrophobic states. In an acidic medium, below the pK_a of the polymer, the amine is protonated and carries a net positive charge. This net charge causes an increase in hydrophilicity and net repulsive forces that increase the osmotic pressure inside the hydrogel. A balance is struck between the elasticity, mixing, and ionic Gibbs free energies which results in a swollen hydrogel. This swelling is reversible upon increasing the pH back to above the pK_a, causing a collapse in the system.

Anionic hydrogels typically contain an acidic moiety such as a carboxylic acid which causes the swelling. In acidic media, below the pK_a, the carboxylic acid is protonated and in its collapsed, possibly complexed state (hydrogen bonding between the acid hydrogen and electron pairs on nearby oxygen atoms). In basic media, above the pK_a of the polymer, the acid is deprotonated and carries a net negative charge. This net charge causes a breakdown in hydrogen bonding and net repulsive forces that increase the osmotic pressure inside the hydrogel. A balance is struck between the elasticity, mixing, and ionic Gibb's free energies which results in a swollen hydrogel.

This swelling is reversible upon decreasing the pH back to below the pK_a, causing a collapse in the system and reformation of hydrogen bonded complexes.

Cationic monomers which could be used in controlled drug delivery devices include N,N-dimethylaminoethyl methacrylate, N,N-diethylaminoethyl methacrylate, 2-(diisopropylamino)ethyl methacrylate, 2-(N-morpholino)ethyl methacrylate. The associated pK_a values of the polymers of these monomers are 8.0, 7.3, 6.0, and 4.9, respectively [1]. Reduction of the pK_a of the hydrogel shifts the critical pH at which it will swell, and also dictates the sensitivity of the system to slight perturbations in local pH. It is possible to slightly shift any of these pK_a values to either higher or lower values by copolymerization with more hydrophilic or hydrophobic monomers, or by synthesizing similar molecules with differing structures. These modifications allow one to tune the way the system responds to a given stimulus.

Anionic hydrogels, on the other hand, are capable of swelling in elevated pH ranges. These gels have also been investigated for "squeezing out" a drug at low pH values, since they collapse in acidic media. Possible monomers for such delivery devices are acrylic acid (AA), methacrylic acid (MAA), ethacrylic acid (EAA), and so on. The pK_a values of these monomers are 4.8, 6.2, and 7.2, respectively [2-4]. Obviously, polymers containing EAA have a substantial biological potential due to physiological pH being 7.4.

4.2 SPECIFIC ENZYMES FOR BIOMARKER DETECTION

Typically, an enzyme is selected that is inherently specific to a certain biomarker of interest. This process provides maximum selectivity and specificity for the desired biomarker, reducing the chance of unwanted

Urease is an oxidoreductase that converts urea to carbon dioxide and ammonia (Figure 4.1). High levels of urea, while not toxic, may indicate problems with a patient's kidneys [5]. Increased urea production has also been shown to accompany moderate to

severe bleeding from gastric ulcers [6]. Thus, when one of these two conditions occurs, an increase in urea in the presence of urease would cause an increase in ammonia. Since ammonia is a base, it could be coupled to anionic hydrogels to induce swelling and then release a drug to combat the symptoms. Since both conditions are chronic, the use of an enzyme system could prove quite promising as a long-term solution that would require little to no intervention from the patient.

Cholesterol oxidase is another enzyme that may be promising to the controlled drug delivery field. The enzyme oxidizes cholesterol to cholest-4-en-3-one (Figure 4.2), which has been shown to significantly reduce body weight gain and body fat accumulation [7]. Hydrogen peroxide is also produced as a byproduct of this reaction. While the conversion of cholesterol itself is of therapeutic importance, this process could possibly be coupled to the release of a drug for high cholesterol. Due to the toxicity of hydrogen peroxide and the dependence on the reaction rate on dissolved oxygen, catalase is often used to consume excess hydrogen peroxide that is formed in such reactions. However, it may be possible to use a second enzyme, such as horseradish peroxidase, to instead couple the hydrogen peroxide production with the swelling of the hydrogel. Horseradish peroxidase is able to oxidize numerous substrates, and thus it may be possible to oxidize another molecule imbibed in the system or an aldehyde monomer unit to a carboxylic acid, which could in turn cause swelling of the hydrogel system. This route could be coupled with either a cationic or an anionic hydrogel, depending on the compound to be oxidized.

Finally, one of the most promising biomarker-enzyme combinations to date for intelligent drug delivery is the glucose-glucose oxidase pair. Glucose oxidase will oxidize glucose, forming gluconic acid. Since the presence of glucose causes a drop in pH, the combination of this enzyme with pH sensitive hydrogels has been studied for intelligent insulin delivery. In this body of work, the main monomer of interest was N,N-

diethylaminoethyl methacrylate, since the pK_a is just below physiological pH of 7.4 and thus is expected to allow maximum swelling in response to a glucose level increase.

4.3 FIGURES

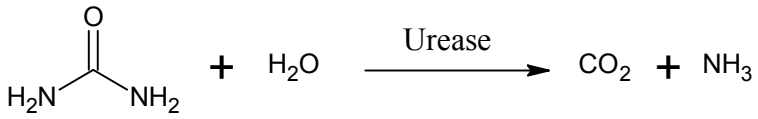

Figure 4.1. Urease Oxoreduction

Chemical reaction catalyzed by the urease enzyme. Urea is hydrolyzed into carbon dioxide and ammonia in the presence of the urease enzyme.

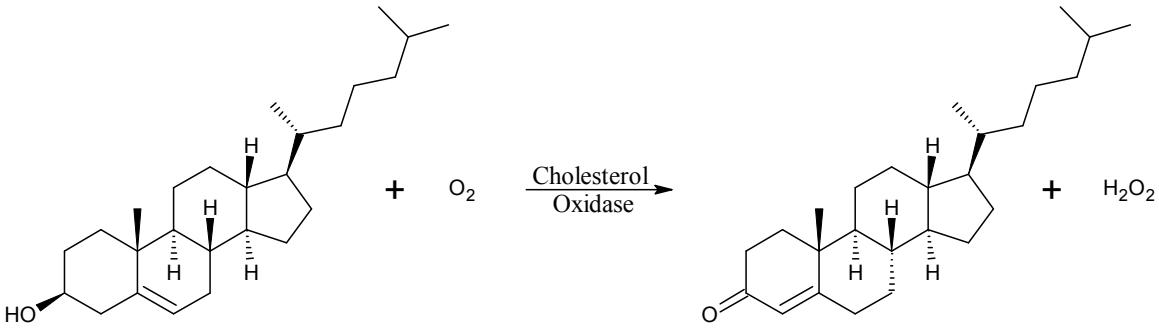

Figure 4.2. Cholesterol Oxidation via Cholesterol Oxidase

Chemical reaction catalyzed by the cholesterol oxidase enzyme. Cholesterol is oxidized into hydrogen peroxide and cholest-4-en-3-one in the presence of the cholesterol oxidase enzyme.

4.4 REFERENCES

1. Butun, V., S.P. Armes and N.C. Billingham, *Synthesis and aqueous solution properties of near-monodisperse tertiary amine methacrylate homopolymers and diblock copolymers.* Polymer, 2001. **42**(14): p. 5993-6008.

2. Mandel, M., *The potentiometric titration of weak polyacids.* Eur Polym J, 1970. **6**(6): p. 807-822.

3. Joyce, D.E. and T. Kurucsev, *HYDROGEN-ION EQUILIBRIA IN POLY(METHACRYLIC ACID) AND POLY(ETHACRYLIC ACID) SOLUTIONS.* Polymer, 1981. **22**(3): p. 415-417.

4. Stayton, P.S., A.S. Hoffman, N. Murthy, C. Lackey, C. Cheung, P. Tan, L.A. Klumb, A. Chilkoti, F.S. Wilbur and O.W. Press. *Molecular engineering of proteins and polymers for targeting and intracellular delivery of therapeutics*. 2000.

5. Bagshaw, S.M. and R.T.N. Gibney, *Conventional markers of kidney function.* Crit Care Med, 2008. **36**(4): p. S152-S158.

6. Bermejo, F., D. Boixeda, J.P. Gisbert, V. Defarges, J.M. Sanz, C. Redondo, C.M. de Argila and A.G. Plaza, *Rapid urease test utility for Helicobacter pylori infection diagnosis in gastric ulcer disease.* Hepato-Gastroenterol, 2002. **49**(44): p. 572-575.

7. Suzuki, K., T. Shimizu and T. Nakata, The cholesterol metabolite cholest-4-en-3-one and its 3-oxo derivatives suppress body weight gain, body fat accumulation and serum lipid concentration in mice. Bioorg Med Chem Lett, 1998. **8**(16): p. 2133-2138.

CHAPTER 5

Preparation and Characterization of Poly(Diethyaminoethyl methacrylate) Based Hydrogels

5.1 INTRODUCTION

The monomer 2-(diethylamino)ethyl methacrylate (DEAEM) is a well studied methacrylate monomer that easily undergoes free-radical polymerizations [1-3]. Several research groups have studied the macroscopic properties of hydrogels based on DEAEM, either as a homopolymer or copolymerized with such monomers as methyl methacrylate (MMA) [4], 2-hydroxyethyl methacrylate (HEMA) [5], and others [6, 7]. These polymers have an increased hydrophilicity at pH values near and below the pKa of the polymer due to the protonation of the tertiary amine. This process is reversible, and hydrophobicity increases with increased pH.

Initial studies with DEAEM were performed by Shatkay and Michaeli [8], who identified the phase separation of PDEAEM at 7.48 and measured a pKa of 7.68 via titration. Several factors can influence this pKa value such as polymer chain length, comonomer composition (and thus hydrophobicity), and crosslinking ratio, with other groups reporting values in the range of 7.0 to 7.4. These polymers also have a T_g below ambient temperature, with values ranging from 16-24°C [4, 9].

In order to accomplish the second specific aim, free-radical initiated cationic hydrogel films and microparticles were synthesized. One of the most promising polymeric systems for closed-loop insulin delivery is based on PDEAEM. These polymers are cationic, with a pKa value very near physiological pH. To impart glucose sensitivity, glucose oxidase (GOx) is typically entrapped in these hydrogels. GOx oxidizes β-D-glucose (which remains in equilibrium with α-D-glucose while in solution [10]) into

gluconic acid, reducing dissolved oxygen into hydrogen peroxide in the process, as shown in Figure 2.5 and Equation (5.1):

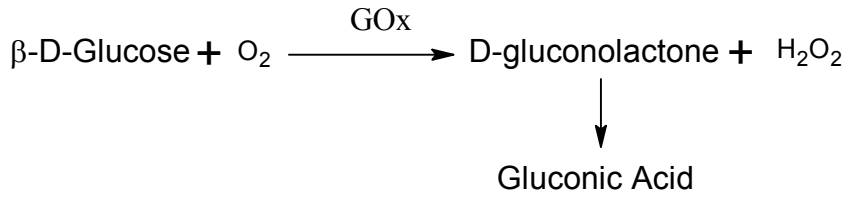

(5.1)

With an increase in glucose concentration, glucose oxidase catalyzes the formation of gluconic acid. Therefore, the local pH drops, protonating the tertiary amines and swelling the polymer due to charge repulsion and polymer hydration. However, it has been shown that the depletion of dissolved oxygen will affect the reaction kinetics, and that saturating the reaction solution with oxygen can increase reaction rate by as much as 100%. Also, hydrogen peroxide is toxic to biological systems and has a poisoning effect on this reaction. Thus, the incorporation of Catalase (CAT) allowed the oxidation of hydrogen peroxide back into dissolved oxygen, removing the toxic byproduct and regenerating oxygen, a reactant. This reaction can be seen in Equation (5.2):

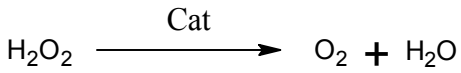

(5.2)

Optimization was performed to determine the optimal concentrations of glucose oxidase and catalase, as well as the ratio of functional monomers to PEG grafts and crosslinks. The structures of the monomers used can be seen in Figure 2.5.

Currently, most attempts at designing DEAEM-based closed-loop drug delivery devices have involved the physical entrapment of both glucose oxidase and catalase in the device. This procedure may allow the slow release of these enzymes into the surrounding medium, thus decreasing the effectiveness of the device as time progresses. The hydrogels reported here have chemically bound enzymes, which prevent the loss of enzyme over time. It has also been shown that chemically bound

enzymes may have increased specific activities when compared to physically entrapped enzymes [11]. The N-terminus of each enzyme was functionalized with acryloyl chloride, essentially turning each enzyme into a very large monomer.

5.2 MATERIALS AND METHODS

5.2.1 Poly(Diethylaminoethyl methacrylate) Polymer Film Synthesis

Hydrogels of N,N-diethylaminoethyl methacrylate and poly(ethylene glycol)-n monomethyl ether monomethacrylate, henceforth P(DEAEM-g-EGn) were synthesized using a free radical thermal polymerization in solution, where 'n' refers to the average molecular weight of the ethylene glycol repeat units. To synthesize these hydrogels, a solution of DEAEM (Sigma-Aldrich, St. Louis. MO), PEGnMMA (Polysciences, Warrington, PA) and the crosslinking agent tetraethylene glycol dimethacrylate (TEGDMA) or polyethylene glycol 400 dimethacrylate (PEG400DMA) (Acros Organics, Morris Plains, NJ) was made. The DEAEM was passed through a column of basic alumina (Fisher Scientific, Fair Lawn, NJ) prior to use to remove inhibitor. All other reagents were used as received. Phosphate buffered saline (PBS) (Fisher Scientific) was used as the solvent to prevent autoacceleration and was reconstituted from a 10X concentrate with deionized water (Milli-Q Plus system, Millipore, Bedford, MA), in a ratio of about 1:1 by weight of the monomers. Hydrochloric acid (ca. 37 wt%, Fisher Scientific) was used to increase solubility. Ammonium persulfate (APS) (Fisher Scientific) and sodium metabisulfite (NaMBS) (Fisher Scientific) were used to initiate the polymerization.

Several different polymers were synthesized with varying compositions. The ratio of DEAEM to PEG grafts was either 10:1, 25:1, or no PEG grafts. Crosslinking ratios varied from 3 mol% up to 15 mol%. Once all compounds had been well mixed in a test tube, the solution was transported to a glove box where it was purged with nitrogen for

20 min to remove dissolved oxygen, a free-radical scavenger. The initiator solution was then added, mixed via aspiration, and then pipette between two glass slides, separated by a 760 µm Teflon spacer. The glass slide assembly was then placed in an acrylic air-tight polymerization box, sealed, and transported to an incubator at 37°C for 24 h. This procedure resulted in polymer films which were either cut into small discs (ca. 11 mm diameter) or crushed into microparticles via a wet-sieving technique. The discs were then washed in a jar of PBS for one week to remove unreacted monomers and small molecular weight polymers. The microparticles were suspended in fresh ddH_2O, spun on a rotary mixer for 45 min, and then centrifuged at 3200 rcf (relative centrifugal force) for 20 min. The pellets were resuspended and this process was repeated 5 times total. The polymers were then either stored in buffer or dried in a vacuum oven (discs) or freeze dried (particles) and stored in a dessicator until use.

The DEAEM is hydrophobic at a pH above its pKa; thus, hydrochloric acid (ca. 37 wt%, Fisher Scientific) was used to protonate the monomer to make it hydrophilic. An alternate route to improving the solubility of DEAEM was to precipitate solid DEAEM-HCl from a 2 N HCl solution in ethyl ether. The precipitate was recovered, washed with dry ethyl ether, excess solvent removed under reduced pressure, and then stored in vials at -20 °C until used.

The redox initiator ammonium persulfate (APS) (Fisher Scientific) was used to initiate the polymerization, along with the accelerant sodium metabisulfite (NaMBS) (Fisher Scientific) to prevent the need of elevated temperatures. The ratio of the two compounds was usually 4:1 by mole to prevent premature polymerization, and the chemicals were pre-mixed before polymerization in distilled deionized water (ddH_2O) at a 1 wt% concentration of APS. The initiator solution was used in an amount of 0.5% by moles of monomers.

Several different polymers were synthesized with varying compositions. The ratio of DEAEM to PEG grafts was either 10:1, 25:1, or no PEG grafts. Crosslinking ratios

varied from 3 mol% up to 15 mol%. Glucose oxidase concentrations were either 3.3 x 10^{-4} mg/g polymer or 6.6 x 10^{-4} mg/g polymer. Catalase concentrations were always five times the glucose oxidase concentration.

Numerous steps were taken to provide the optimal polymerization conditions. The monomer solution was mixed in a glass test tube wrapped with aluminum foil to help decrease the chances of premature polymerization from light. Acidifying the monomer was an exothermic reaction, so small quantities of acid were added to an ice cold monomer solution and then mixed. This prevented premature thermally-induced polymerization of the uninhibited DEAEM. Once all compounds had been well mixed in the test tube, it was transported to a glove box where it was purged with nitrogen for 20 min to remove dissolved oxygen, a free-radical scavenger. The initiator solution was then added, mixed via aspiration, and then pipette between two glass slides, separated by a 760 µm Teflon spacer. The glass slide assembly was then placed in an acrylic air-tight polymerization box, sealed, and transported to an incubator at 37°C for 24 h. Polymer films were synthesized in this way, and were washed in a jar of PBS for one week to remove unreacted monomers and small molecular weight polymers. The polymers were then either stored in buffer or dried in a vacuum oven and stored in a dessicator until use. The wash water was analyzed for residual, unreacted enzyme content.

Polymer films had two fates: small discs (ca. 11 mm diameter), or crushed microparticles. Polymer discs were formed by placing the hydrated polymer film on a Teflon slab and cutting it into discs with a cork-borer of inner diameter 11 mm. Microparticles were formed via a wet-sieving technique. The hydrated polymer was placed in a sieve of a specific mesh size (typically 150 µm) and then forced through the sieve with a pestle. If a smaller particle size was desired, the particles were placed in an even smaller mesh sieve and again forced through the screen. Particle sizes as small as sub-30 µm were obtained using this method.

5.2.2 Incorporation of Enzymes into Polymer Structure

Polymers were also synthesized with both glucose oxidase and catalase in order to render these polymeric systems glucose sensitive. The enzymes were suspended in PBS and allowed to chill in an ice bath for 30 min. Gentle stirring was used to allow mixing but to prevent flocculation. After chilling, a small amount of acryloyl chloride (Alfa Aesar) was added to the solution. The acid chloride moiety of acryloyl chloride has been shown to be preferentially attacked by the N-terminus of GOx and presumably CAT as well, as shown by the mechanism in Figure 5.3. This step essentially converts the enzymes into very large monomers; the acrylate groups on the enzymes allow them to participate in the copolymerization, incorporating the enzymes covalently into the polymer backbone. It has been reported that chemically immobilizing some enzymes has shown increased stability, and the loss of activity over time due to leeching of enzymes is no longer a concern.

To synthesize these hydrogels, a solution of DEAEM, PEGnMMA and the crosslinking agent TEGDMA or PEG400DMA was made. The DEAEM was passed through a column of basic alumina prior to use to remove inhibitor. All other reagents were used as received. Instead of neat PBS, the enzyme solution as prepared above was used as the solvent to prevent autoacceleration, in a ratio of about 1:1 by weight of the monomers. Hydrochloric acid was used to increase solubility and was added slowly to reduce temperature spikes. APS and NaMBS were used to initiate the polymerization in a ratio of 4:1 by mole, and the chemicals were pre-mixed before polymerization in ddH_2O at a 1 wt% concentration of APS. The initiator solution was used in an amount of 0.5% by moles of monomers.

Several different hydrogels were synthesized with varying compositions. The ratio of DEAEM to PEG grafts was either 10:1, 25:1, or no PEG grafts. Crosslinking ratios varied from 3 mol% up to 15 mol%. Once all compounds had been well mixed in a test

tube, the solution was transported to a glove box where it was purged with nitrogen for 20 min to remove dissolved oxygen, a free-radical scavenger. The initiator solution was then added, mixed via aspiration, and then pipette between two glass slides, separated by a 760 µm Teflon spacer. The glass slide assembly was then placed in an acrylic air-tight polymerization box, sealed, and transported to a refrigerator at 4°C for 24 h to reduce any chance of enzyme denaturation. This procedure resulted in polymer films which were either cut into small discs (ca. 11 mm diameter) or crushed into microparticles via a wet-sieving technique. The discs were then washed in a jar of PBS for one week, refrigerated, to remove unreacted monomers and small molecular weight polymers. The microparticles were suspended in fresh ddH_2O, spun on a rotary mixer for 45 min, and then centrifuged at 3200 rcf for 20 min. The pellets were resuspended and this process was repeated 5 times total. The polymers were then either stored in buffer or dried in a vacuum oven (discs) or freeze dried (particles) and stored in a dessicator until use.

5.2.3 Polymer Characterization via FT-IR

Fourier transform infrared (FT-IR) spectra were obtained on a ThermoNicolet Nexus 470 spectrometer (Thermo Electron Corp., Waltham, MA) with a deuterated triglycine sulfate (DTGS) detector and potassium bromide (KBr) beam splitter. Typically, 128 scans were performed in the wavenumber range of 4000-400/cm, both forward and backward at 10 kHz, with a manual gain of one. Pellets of ca. 10 mg polymer and 200 mg KBr (spectroscopy grade, Acros Organics) were pressed at 15,000 psi using a Carver laboratory press. Crushed microparticles were used for generating the spectra.

5.2.4 Polymer Characterization via NMR

Nuclear magnetic resonance (NMR) spectra were obtained on a Varian Unity+ 300 MHz spectrometer. Deuterated water (D_2O, Cambridge Isotope Laboratories, Inc., Andover, Ma.) was used to suspend nanoparticles for tether analysis. Water suppression was used via the PRESAT macro with a saturation power of -2 and a saturation time of 5 s on any samples with significant water signals. Small molecule analysis was obtained by using a suitable deuterated solvent, such as chloroform (CDCl3), dimethylsulfoxide (d6-DMSO), or d¬6-acetone, all obtained from Cambridge Isotope Laboratories. Unless otherwise stated, for all ^1H NMR spectra, the sample was spinning at 20 Hz, the number of transients was 8, and line broadening was 0.1.

5.2.5 Polymer Characterization via DSC

A PerkinElmer DSC 7 differential scanning calorimeter (PerkinElmer, Waltham, MA) using a heat/cool/heat method was used to characterize the polymers. A rapid heating cycle was used to erase any thermal history from the samples, after which the samples were cooled back down to the starting temperature. The final heating cycle had a ramp rate of 10^oC/min, which was slow enough to detect a T_g in some samples. Since room temperature was above the T_g of most samples, a nitrogen cooling unit was used with an initial temperature of -55°C.

5.2.6 Polymer Characterization via SEM

A LEO Model 1530 SEM was used to determine the morphology of the synthesized particles. Samples were prepared for imaging in one of two methods. Method one consisted of suspending the particles in a volatile non-solvent and then placing a drop on an aluminum stage. Method two required the use of double-sided

conductive carbon tape to hold the lyophilized samples on the aluminum stage. To prevent charging of the samples, they were sputter coated with gold using a Pelco Model 3 sputter coater. Stages were stored in a dessicator until loading into the SEM.

5.2.7 Polymer Swelling Characterization

As stated above, nanoparticles were sized via DLS as a function of pH. The swelling response of microparticles and disks was obtained gravimetrically. The polymer samples were titrated to the desired pH with either 0.1N HCl or 0.1N NaOH, and the pH was measured with an ISFET probe as with the nanoparticles. Swelling media was PBS with an ionic strength of 154 mM and initial pH of 7.4. Microparticles were centrifuged at a relative centrifugal force of 3200g (Centra CL3R, Thermo IEC) and the supernatant was removed to obtain the mass of the particles.

5.3 RESULTS AND DISCUSSION

5.3.1 Poly(Diethylaminoethyl methacrylate) Polymer Film Synthesis

Films, which were then either cut into discs or crushed into microparticles, were successfully synthesized. Wet sieving yielded irregularly-shaped particles with sizes of sub-150 µm or sub-45 µm in the relaxed state, depending on which sized sieve was used. It is necessary to note that all polymers in this work are referred to by their feed (pre-polymerization) compositions rather than polymer compositions due to the difficulty in quantitatively analyzing crosslinked copolymer compositions.

5.3.2 Incorporation of Enzymes into Polymer Structures

The inclusion of the immobilized enzymes did not appear to alter the pK_a of the hydrogels significantly, both films and microparticles. Temperature, however, did affect the pK_a. At 20 °C, the pK_a was very close to 7.4. At a temperature of 37 °C, the pK_a dropped to about 7.1.

5.3.3 FT-IR Spectroscopy

FTIR showed the functional groups present in each sample which indicated the successful removal of unreacted double bonds. The C=C stretching absorbance near 1650 cm^{-1} and the out-of-plane C-H bending of these same double bonds near 950 cm^{-1} were nearly non-existent. Also, the larger presence of etheric bonds in the samples containing PEG tethers, near a frequency of 1100 cm^{-1} (C-O stretching), indicates a higher content of PEG than those simply containing PEG crosslinker. Thus, it is reasonable to assume that the PEG tethers were successfully incorporated into the hydrogel backbone.

5.3.4 NMR Spectroscopy

Water suppression was necessary for all samples analyzed in D_2O; otherwise, the signal-to-noise ratios for the hydrogel peaks were too low for analysis. ^1H NMR was attempted on crushed microparticles in several different solvents, including D_2O and deuterated dimethyl sulphoxide (DMSO-D_6). Unfortunately, due to the limitations of solution NMR on crosslinked microparticles, very little useful information was able to be extracted from the spectra. Solid NMR spectroscopy was a possible alternative, though it was decided not to pursue such a technique due to the lack of availability of the

equipment and the reduced amount of information the technique is able to provide (compared to solution NMR, as discussed in Chapter 6).

5.3.5 Differential Scanning Calorimetry (DSC)

Heat flow curves as a function of temperature were generated for several different polymeric systems and can be seen in Figure 5.5. It is interesting to note that crushed microparticles did not have an observable T_m. This result can be explained by the methods of polymerization and how they alter the polymer structure. The crushed microparticles were synthesized as a film, where the PEG and DEAEM copolymerized without any partitioning and were randomly polymerized into the polymer chain. The T_g of crosslinked hydrogels was unable to be determined, due to the highly restricted polymer chain motion from the of crosslinking. Microparticles did not exhibit a detectable T_g. However, the T_g of uncrosslinked PDEAEM was determined to be -20°C, which agrees with previous reports.

5.3.6 Scanning Electron Microscopy (SEM)

Scanning electron microscopy allowed the visual inspection of the crushed polymer microparticles. Wet sieving of hydrogel films through sieves of 150 μm yielded the particles shown in Figure 5.6 and Figure 5.7. These particles had irregularly shaped features due to the nature of the crushing. These irregular features provided an increased surface area compared to a smooth sphere of a similar diameter, which could potentially affect the dynamics of swelling and insulin release. The PEG surface grafts appeared to soften the surface features of the crushed particles compared to those without PEG grafts, as seen in Figure 5.6. Particles with higher nominal crosslinking ratios had smaller collapsed particle sizes, as seen in Figure 5.7.

5.3.7 Polymer Swelling Characterization

Swelling analyses of the systems showed a sigmoidal response to pH as expected (Figure 5.8), with the transition occurring rapidly near the pK_a of the polymer. The pK_a of DEAEM polymers is a function of molecular weight, comonomer composition, and to some degree, temperature, with a range between pH 7.0-8.0. At 25 °C the transition from fully collapsed to fully swollen occurs over a narrow pH range of less than 1 unit and occurred at about pH 7.2 (Figure 5.8). This pK_a range is important in several applications, most notably in biological systems which are typically buffered at a near neutral pH.

Swelling results for microparticles are reported here as a weight swelling ratio (q),

$q = W_s / W_d$,

where W_s is the swollen weight of the particles and W_d is the dry weight of the particles. Even when fully collapsed, particles retained about equal masses of polymer and solvent, resulting in a collapsed q of 2. As crosslinker content increased, the overall mass swelling decreased due to restrictions in interchain movement. Polymers with a 15% crosslinking ratio swelled from a collapsed weight swelling ratio of 2 (q, weight swollen divided by weight dry) to a ratio of 6, samples that had 10% crosslinking ratio swelled to a ratio of 6.6, while samples that were only crosslinked at 3% swelled to a ratio of 11. Solid lines represent a sigmoidal (hyperbolic tangent) fit to the data, and not just a guide to the eye. These data agree with previous reports of similar systems [12-14].

These swelling values were then used to estimate the mesh size of each sample. Since the mesh size of a hydrogel is essentially the molecular pore size, it can be used to help determine the ability of a given solute to diffuse through the polymer. There are several methods of estimating the mesh size of a hydrogel; however, the Flory-Rehner

model was selected due to the difficulty of measuring such parameters as the relaxed volume (i.e., for the Peppas-Merrill or Brannon-Peppas equation). Thus, these values are rough estimates of the actual values and should not be taken as the actual values themselves.

To determine the polymer parameters, hydrogels were swollen to equilibrium and then mass swelling was determined. The ratio of swollen mass to dry mass, *q*, was calculated for each data point, and the polymer volume fraction in the swollen state, $\upsilon_{2,s}$, was calculated with Equation 5.3:

$$\upsilon_{2,s} = \frac{m\bar{\upsilon}}{m\bar{\upsilon} + mq/\rho_w} \tag{5.3}$$

where *m* is the mass of dry particles, $\bar{\upsilon}$ is the specific volume of the polymer (0.93 g/cm^3), and ρ_w is the density of water.

For the reasons mentioned above, estimation of the average molecular weight between crosslinks was performed by using the Flory-Rehner model:

$$\frac{1}{\overline{M}_c} = \frac{2}{\overline{M}_n} - \frac{\left[\ln\left(1-\upsilon_{2,s}\right) + \upsilon_{2,s} + \chi_1 \upsilon_{2,s}^2\right]}{\left(\frac{V_1}{\bar{\upsilon}}\right)\left[\upsilon_{2,s}^{1/3} - \frac{\upsilon_{2,s}}{2}\right]} \tag{5.4}$$

The parameters are as follows: V_1 is the molar volume of the welling agent (18 cm^3/mol for water), I is the ionic strength (1.7 for PBS, 0.002 for 2mM KCl), χ_1 is the Flory polymer-solvent interaction parameter (0.2, as estimated by Hariharan [5]), and $\overline{M}_n$ is the number average molecular weight of the polymer chains before crosslinking (estimated to be 15 kDa by GPC, though the actual value has negligible influence on estimates beyond a certain value). Once $\overline{M}_c$ was know, the mesh size (ξ) was calculated from equation 5.5,

$$\xi = \upsilon_{2,s}^{-1/3}\left(\frac{C_n \overline{M}_c}{M_r}\right)^{1/2} l \tag{5.5}$$

where C_n is the Flory characteristic ratio (14.6 for vinyl polymers), M_r is the average molecular weight of the repeat units, and *l* is the length of the bond along the polymer backbone (1.54 Å for vinyl polymers).

The results of this analysis are as follows and shown in Figure 5.9. Polymers with a crosslinking ratio of 15% had, as expected, the smallest swollen mesh size at a value of 34 Å. As the crosslinking ration decreased, the hydrogels formed larger molecular pores with values of 40 Å for a 10% crosslinked sample and 78 Å for the 3% crosslinked sample. All samples had a collapsed mesh size on the order of 1 Å. Therefore, it should be feasible to entrap medium molecular weight compounds in the collapsed state, and allow controlled release of these compounds in the swollen state. Small peptides, such as insulin with a monomeric radius of only 1.3 nm [15], were expected to have no trouble being imbibed into the polymer network and then become trapped upon collapse.

5.4 CONCLUSIONS

Hydrogels, in the forms of films and microparticles were successfully synthesized using a redox initiated free-radical polymerization. These systems were characterized by several different techniques. FT-IR confirmed functional group content. DSC indicated the lack of a discernable T_g in these highly crosslinked systems. SEM micrographs provided a visual means of observing the crushed microparticle surface topology. Surface features were also elucidated, indicating that PEG provides different surface properties in the dried state.

These studies have demonstrated that all PDEAEM-based hydrogels synthesized exhibit a sigmoidal response to changes in pH. With this increase in polymer volume, the mesh size increased, and an increase in the diffusion rate of solutes should be present. Thus, these systems are ideal candidates for applications such as controlled

drug delivery of medium-sized molecules such as small peptides based on the estimated changes in mesh sizes that were calculated. These hydrogel particles were further reduced to the nanometer size scale and these nanogels are discussed in Chapter 6. The drug loading and release properties of these systems were characterized in Chapter 7 to determine their feasibility in a drug delivery application, specifically for type I diabetes treatment.

5.5 FIGURES

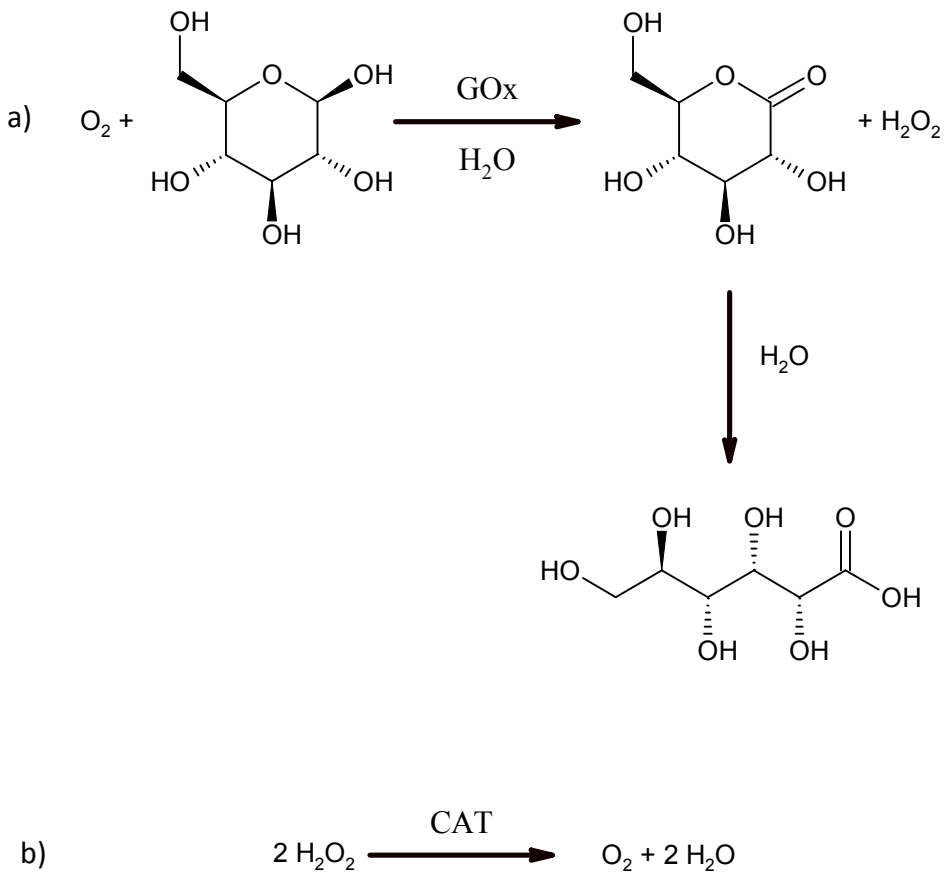

Figure 5.1. Chemical Reaction Catalyzed by Glucose Oxidase

(a) β-D-glucose is first oxidized to β-D-glucono-1,5-lactone while dissolved oxygen is reduced to hydrogen peroxide by the enzyme glucose oxidase (GOx). β-D-glucono-1,5-lactone is then hydrolyzed to gluconic acid in the presence of water.
(b) Hydrogen peroxide is oxidized back into water by catalase (CAT), evolving molecular oxygen in the process.

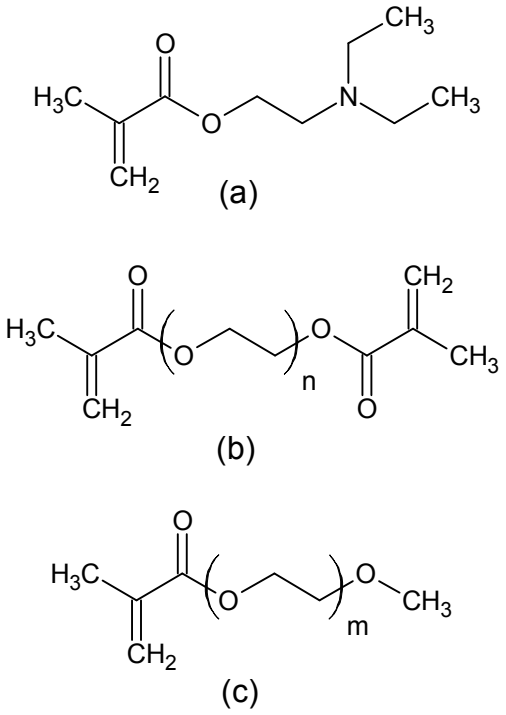

Figure 5.2. Monomers Used in the Synthesis of P(DEAEM-g-EGn)

(a) DEAEM,
(b) PEGDMA-n, n = 4 for TEGDMA, n ≈ 8 for PEGDMA400
(c) PEGMMA-n, n ≈ 8 for PEGMMA400, n = 22 for PEGMMA1000, n ≈ 45 for PEGMMA2000

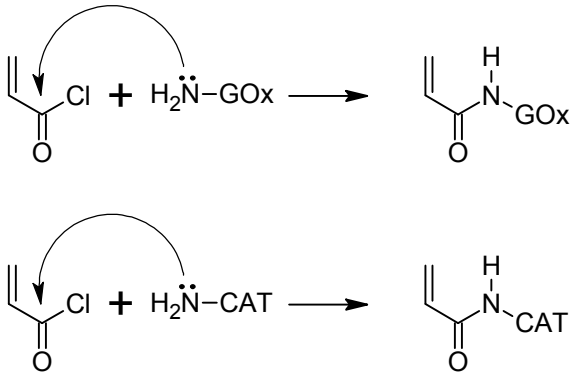

Figure 5.3. Mechanisms of Enzyme Functionalization with Acryloyl Chloride

Mechanisms of the functionalization of Glucose Oxidase (GOx) and Catalase (CAT) with acryloyl chloride. The N-terminus is the most likely amine to attack the carbonyl group on the acryloyl chloride.

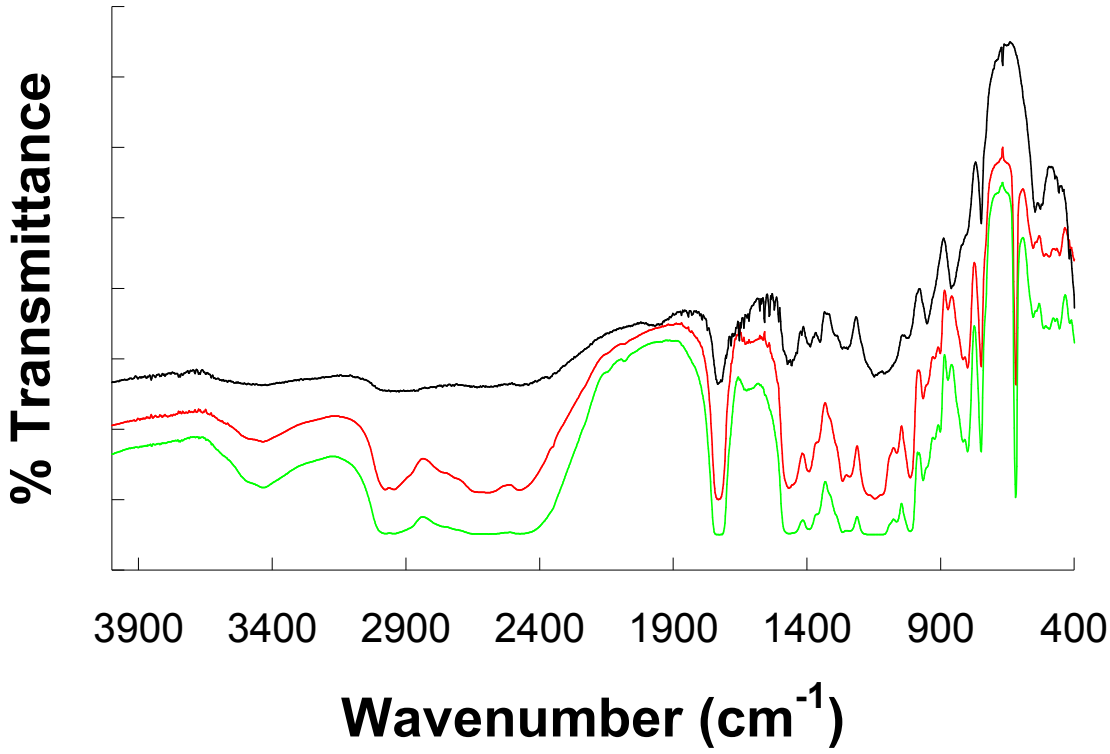

Figure 5.4. Fourier Transform Infrared Spectra of PDEAEM Samples.

FT-IR transmittance spectra of three DEAEM formulations. The top spectrum is from a sample with 3% crosslinking (TEGDMA) and a 10:1 ratio of PEG400MMA grafts to DEAEM. The middle spectrum is from a sample with 5% crosslinking (PEG400DMA) and a 10:1 ratio of PEG400MMA grafts to DEAEM. The bottom spectrum is from a sample with 15% crosslinking (PEG400DMA) and a 10:1 ratio of PEG400MMA grafts to DEAEM. There is very little difference between these spectra, indicating that the amount of crosslinking does not affect the polymerization substantially. PEG etheric peaks at 1100 cm^{-1} appear saturated for the higher crosslinking ratio.

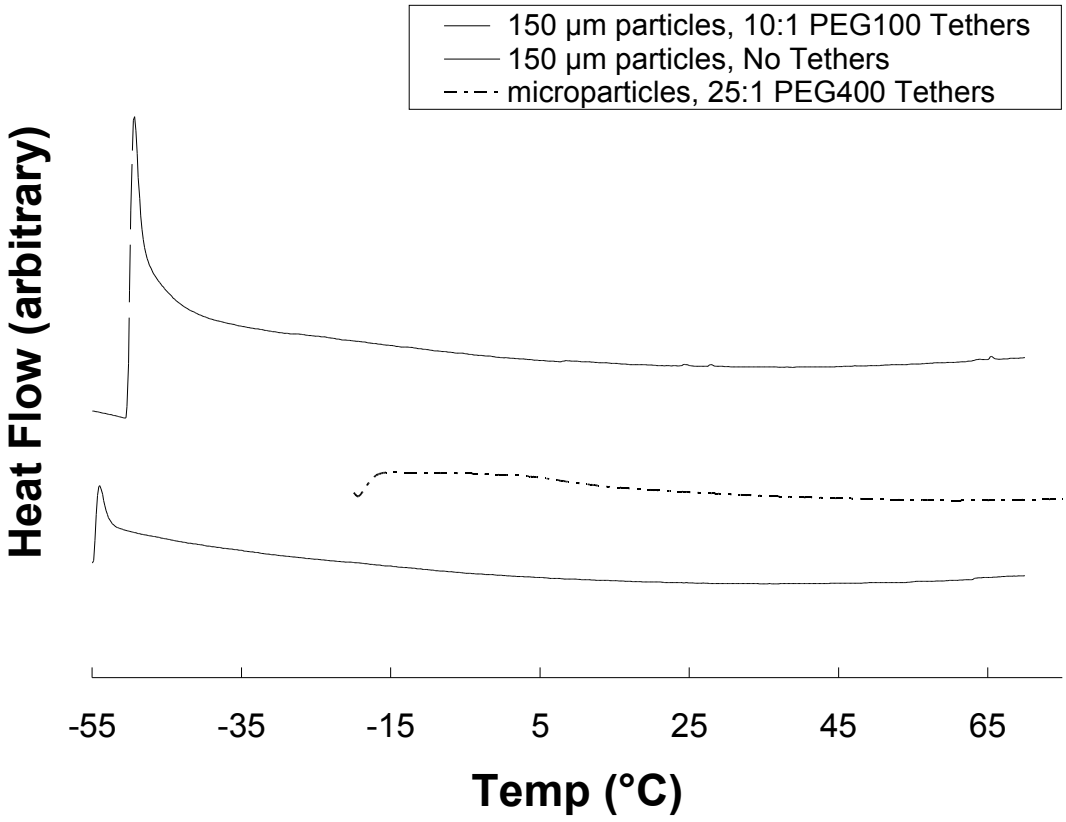

Figure 5.5. Differential Scanning Calorimetry Results for Select Polymer Formulations.

Baselines were straightened and y-axis units are arbitrary heat flow. Initial peaks (at -55, -50, and -15) are artifacts of the initial measurement. Note the lack of T_g for all samples and no other discernable features.

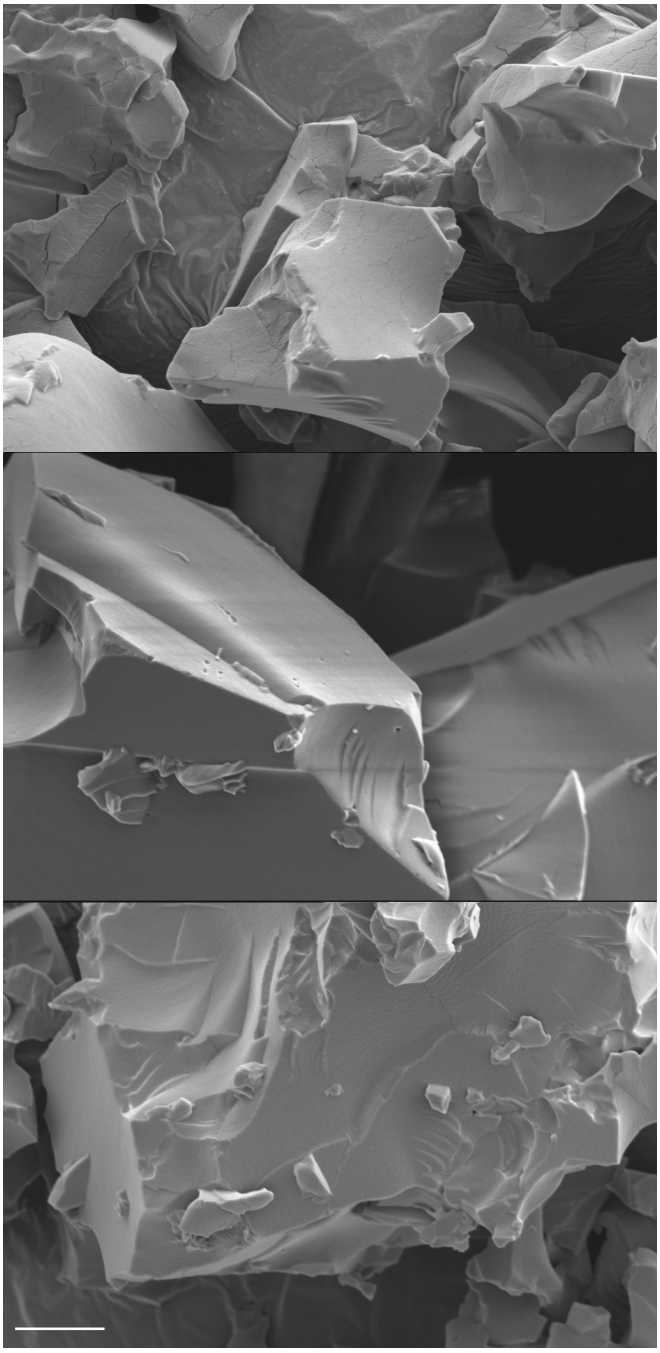

Figure 5.6. SEM Images of Crushed PDEAEM Microparticles, Tight View

a) PDEAEM without PEG tethers, 3% crosslinking; b) PDEAEM without PEG tethers, 10% crosslinking; c) PDEAEM-g-EG1000 with a 10:1 ratio of DEAEM:PEG, 10% crosslinking. Scale bar = 10 µm.

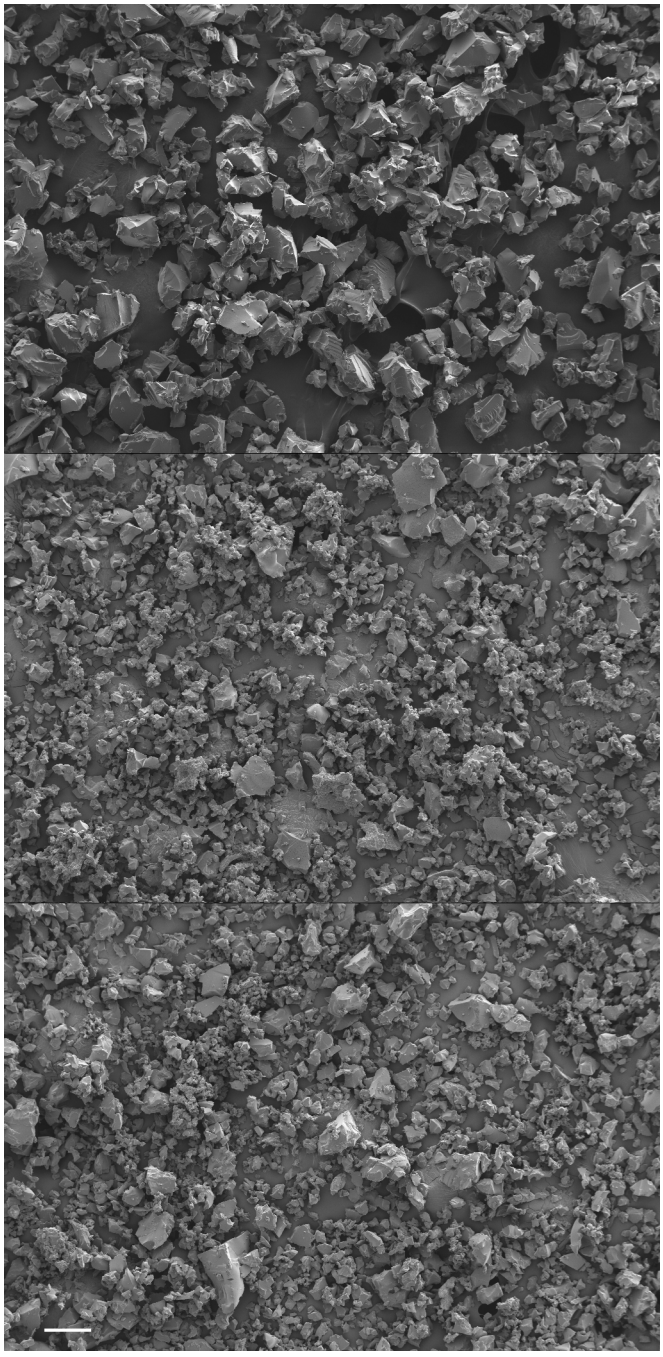

Figure 5.7. SEM Images of Crushed PDEAEM Microparticles, Wide View

a) PDEAEM without PEG tethers, 3% crosslinking; b) PDEAEM without PEG tethers, 10% crosslinking; c) PDEAEM-g-EG1000 with a 10:1 ratio of DEAEM:PEG, 10% crosslinking. Scale bar = 100 μm.

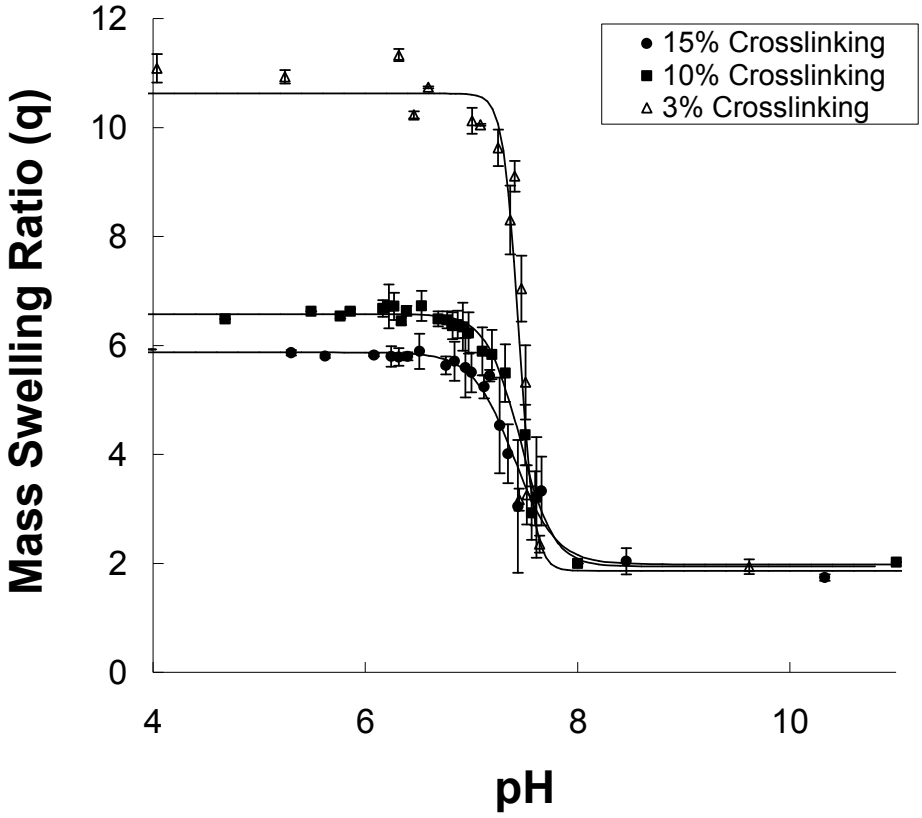

Figure 5.8. Weight Swelling of Crushed Microparticles (150 μm) as a Function of pH

An increase in the crosslinking ratio of the polymers reduced the overall swelling, reducing the amount of water uptake. The transition pH for these particles was right near physiological pH of 7.4, and swelling bean to take place immediately below this pH. (n = 3 ± SD)

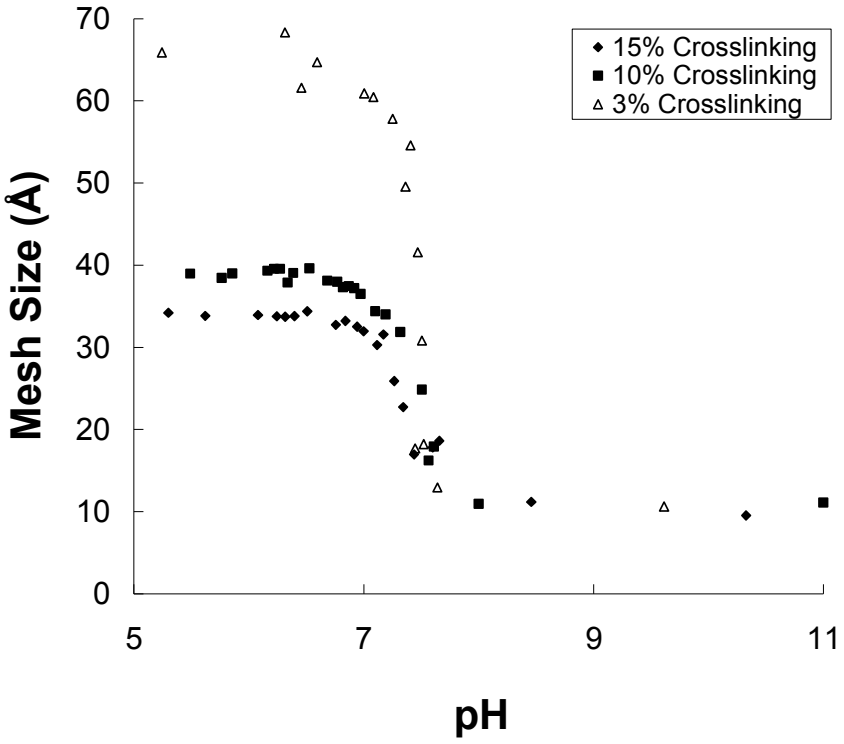

Figure 5.9. Mesh Size Estimations of Crushed Microparticles (150 µm) as a Function of pH

Initially, both systems remain collapsed at a mesh size of 1 nm, small enough to entrap small peptides and other such molecules. At the transition pH, both particle systems swelled dramatically. Samples with a crosslinking of only 10% swelled to a mesh size of 4 nm whereas higher crosslinked samples only swelled to a mesh size of 3.5 nm.

5.6 REFERENCES

1. Kost, J. and R. Langer, *Equilibrium swollen hydrogels in controlled release applications*, in *Hydrogels in medicine and pharmacy*, N.A. Peppas, Editor. 1986, CRC Press: Boca Raton, Fla. p. 95-107.

2. Siegel, R.A. and B.A. Firestone, *pH-dependent equilibrium swelling properties of hydrophobic polyelectrolyte copolymer gels.* Macromolecules, 1988. **21**(11): p. 3254-3259.

3. Siegel, R.A., B.A. Firestone, I. Johannes and J. Cornejo, *Weak Ionic Hydrogels - Effects of Ph, Ionic-Strength and Buffer Composition on Swelling Equilibria, Kinetics and Solute Release.* Abstr Pap Am Chem S, 1990. **199**: p. 119-POLY.

4. Cornejo-Bravo, J.M. and R.A. Siegel, *Water vapour sorption behaviour of copolymers of N,N-diethylaminoethyl methacrylate and methyl methacrylate.* Biomaterials, 1996. **17**(12): p. 1187-1193.

5. Hariharan, D. and N.A. Peppas, *Characterization, dynamic swelling behaviour and solute transport in cationic networks with applications to the development of swelling-controlled release systems.* Polymer, 1996. **37**(1): p. 149-161.

6. Podual, K., F.J. Doyle and N.A. Peppas, *Dynamic behavior of glucose oxidase-containing microparticles of poly(ethylene glycol)-grafted cationic hydrogels in an environment of changing pH.* Biomaterials, 2000. **21**(14): p. 1439-1450.

7. Schwarte, L.M. and N.A. Peppas, *Novel poly(ethylene glycol)-grafted, cationic hydrogels: preparation, characterization and diffusive properties.* Polymer, 1998. **39**(24): p. 6057-6066.

8. Shatkay, A. and I. Michaeli, *Potentiometric Titrations of Polyelectrolytes with Separation of Phases.* The Journal of Physical Chemistry, 1966. **70**(12): p. 3777-3782.

9. Tobolsky, A.V. and M.C. Shen, *THE EFFECT OF HYDROGEN BONDS ON THE VISCOELASTIC PROPERTIES OF AMORPHOUS POLYMER NETWORKS.* The Journal of Physical Chemistry, 2002. **67**(9): p. 1886-1891.

10. Bergmeyer, H.U., J. Bergmeyer and M. Grassl, *Methods of enzymatic analysis*. 3rd ed. 1983, Weinheim ; Deerfield Beach, Fla.: Verlag Chemie.

11. Jaworek, D., H. Botsch and J. Maier, *Preparation and properties of enzymes immobilized by copolymerization.* Methods Enzymol., 1976. **44**: p. 195-20.

12. Fisher, O.Z. and N.A. Peppas, *Polybasic Nanomatrices Prepared by UV-Initiated Photopolymerization.* Macromolecules, 2009. **42**(9): p. 3391-3398.

13. Podual, K., F.J. Doyle and N.A. Peppas, *Preparation and dynamic response of cationic copolymer hydrogels containing glucose oxidase.* Polymer, 2000. **41**(11): p. 3975-3983.

14. Podual, K. and N.A. Peppas, *Relaxational behavior and swelling-pH master curves of poly[(diethylaminoethyl methacrylate)-graft-(ethylene glycol)] hydrogels.* Polym Int, 2005. **54**(3): p. 581-593.

15. Oliva, A., J. Fariña and M. Llabrés, *Development of two high-performance liquid chromatographic methods for the analysis and characterization of insulin and its degradation products in pharmaceutical preparations.* Journal of Chromatography B: Biomedical Sciences and Applications, 2000. **749**(1): p. 25-34.

CHAPTER 6

Preparation and Characterization of Poly(Diethyaminoethyl methacrylate) Based Nanogels

6.1 INTRODUCTION

Nano-sized materials have attracted substantial interest over the last several years due to their unique characteristics and versatility. Nanoparticles, or more specifically nanogels (nanometer-scale hydrogels), have garnered some of this attention due to their wide range of uses, from applications such as paints and thickening agents [1, 2], to drug delivery, diagnostics [3], and other biological applications. However, improved methods of production of such hydrogels are required. Here, a novel inverse emulsion polymerization is described for the synthesis of cationic nanogels that exhibit pH dependent swelling properties in aqueous environments.

In order to accomplish the second specific aim of this dissertation, free-radical initiated cationic hydrogel systems were synthesized. One of the most promising polymeric systems for closed-loop insulin delivery is based on the monomer 2-(diethylamino)ethyl methacrylate (DEAEM) with entrapped glucose oxidase. These polymers are cationic, with a pKa value very near physiological pH. Thus, with an increase in glucose concentration, glucose oxidase catalyzes the formation of gluconic acid. Therefore, the local pH drops, thus protonating the tertiary amines and swelling the system due to charge repulsion and polymer hydration. Optimization was performed to determine the optimal concentrations of glucose oxidase and catalase, as well as the ratio of functional monomers to PEG grafts and crosslinks.

DEAEM is a well studied methacrylate monomer that easily undergoes free-radical polymerizations [4-6]. Several research groups have studied the macroscopic

properties of hydrogels based on DEAEM, either as a homopolymer or copolymerized with such monomers as methyl methacrylate (MMA) [7], 2-hydroxyethyl methacrylate (HEMA) [8], and others [9, 10]. These polymers have an increased hydrophilicity at pH values near and below the pKa of the polymer due to the protonation of the tertiary amine. This process is reversible, and swellability is reduced with increased pH.

Initial studies with DEAEM were performed by Shatkay and Michaeli [11], who identified the phase separation of PDEAEM at 7.48 and measured a pKa of 7.68 via titration. Several factors can influence this pKa value such as polymer chain length, comonomer composition (and thus hydrophobicity), and crosslinking ratio, with other research groups reporting values in the range of 7.0 to 7.4. These polymers also have a Tg below ambient temperature, with values ranging from 16-24°C [7, 12].

Previous reports have indicated that DEAEM polymer particle sizes can be reduced to the nanometer scale. However, most of these methods relied on the hydrophobicity of DEAEM to form emulsions [13-15] or precipitates. The incorporation of hydrophilic components in the interior of these nanogels was not considered, and in practice would be quite difficult with these methods due to the hydrophobicity of deprotonated DEAEM. These reactions also either took over 24 h or relied on UV initiation, both of which could inhibit the scale-up of such materials.

Currently, most attempts at closed-loop drug delivery devices with DEAEM involve the physical entrapment of both glucose oxidase and catalase in the polymeric device. This procedure may allow the slow release of these enzymes into the surrounding medium, thus decreasing the effectiveness of the system as time progresses. The nanoparticles described herein have chemically bound enzymes, which prevent the loss of enzyme over time. It has also been shown that chemically bound enzymes may have increased specific activities when compared to physically entrapped enzymes [16]. The N-terminus of each enzyme was functionalized with acryloyl chloride, essentially turning each enzyme into a very large monomer.

The studies presented here examine the effects of a novel nanoparticle synthesis route of PDEAEM on several polymer properties, including surface charge and swelling response. A new inverse emulsion (water-in-oil) polymerization method is described. The effects of crosslinking ratio and polyethylene glycol (PEG) tether length on physical properties are also examined. The network morphology was also studied. Finally, the potential for these systems to be used as drug delivery agents was evaluated.

6.2 MATERIALS AND METHODS

6.2.1 Poly(Diethylaminoethyl methacrylate) Polymer Nanoparticle Synthesis

Nanoparticle hydrogels of P(DEAEM-g-EGn) were synthesized using a thermally initiated free radical inverse emulsion polymerization. In an inverse emulsion polymerization, the monomer is in the aqueous phase and the continuous phase is the immiscible organic phase, whereas a typical emulsion polymerization has an aqueous continuous phase and an immiscible organic phase of monomer. The initiator is also usually soluble only in the continuous phase; however, the thermal redox initiator ammonium persulfate (APS, Sigma-Aldrich, St. Louis. MO) is soluble in the aqueous monomer phase. Thus, the accelerant used (which allowed the polymerization to progress at room temperature) was N,N,N',N'-tetraethylmethylenediamine (TEMED, Fisher Scientific, Fair Lawn, NJ) which is more soluble in the organic phase than the aqueous phase. To stabilize the emulsion, a mixture of surfactants was used; the 2:1 molar ratio of nonionic surfactants Brij 30 (Sigma-Aldrich) and Triton X-100 (Sigma-Aldrich) gave the best yield of particles with the most monodisperse size distribution.

To form the prepolymer solution, a solution of DEAEM (Sigma-Aldrich), PEGnMMA (Polysciences, Warrington, PA) and the crosslinking agent tetraethylene glycol dimethacrylate (TEGDMA) or polyethylene glycol 400 dimethacrylate

(PEG400DMA) (Acros Organics, Morris Plains, NJ) was made. The DEAEM was passed through a column of basic alumina (Fisher Scientific) prior to use to remove inhibitor. All other reagents were used as received. Phosphate buffered saline (PBS) (Fisher Scientific) was used as the solvent to prevent autoacceleration and was reconstituted from a 10X concentrate with deionized water (Milli-Q Plus system, Millipore, Bedford, MA), in a ratio of about 1:1 by weight of the monomers. Hydrochloric acid (ca. 37 wt%, Fisher Scientific) was used to increase solubility. Ammonium persulfate (APS) (Fisher Scientific) was used to initiate the polymerization and was mixed into the prepolymer solution just prior to being added to the continuous phase. Several different systems were synthesized with varying compositions. The ratio of DEAEM to PEG grafts was either 10:1, 25:1, or no PEG grafts. Crosslinking ratios varied from 3 mol% up to 15 mol%.

To form the emulsion, 85 mL of cyclohexane (Fisher Scientific) was added to a round bottom flask containing 4.7 g Brij 30 (Sigma-Aldrich) and 8.7 g Triton X-100 (Sigma-Aldrich). The aqueous monomer solution, prepared as stated above, was then added to the round bottom. The mixture was homogenized (Ultra-Turrax T25, IKA, Wilmington, NC) at 24,000 rpm for 5 min. The emulsion was then capped with a rubber septum and purged with N_2 for 20 m to remove dissolved oxygen, after which 0.35 mL of TEMED were injected. The reaction proceeded very rapidly, and appeared complete after roughly 30 min. Immediately after injection, the reaction turned slightly cloudy, and then after about 5 min it turned opalescent. Particles of about 220 nm (collapsed) were formed, depending on crosslinker ratio. The cyclohexane was removed under reduced pressure on a rotary evaporator. The particles were precipitated with ethyl ether (Fisher Scientific), which also dissolved most of the surfactant. The solution was centrifuged, the organic layer was poured off, and the process was repeated twice more. Sonication was necessary to resuspend the particles after the first wash, and resuspension became progressively more difficult as more surfactant was removed. The

particles were then washed for one week in a dialysis membrane (SpectraPor, Spectrum Laboratories, Inc., Rancho Dominguez, CA) and the dialysate was changed twice a day. After the washing steps were completed, the particles were lyophilized on a Freezone freeze dryer (Model 77500, Labconco Corp., Kansas City, MO) and stored in a desiccator until use.

6.2.2 Incorporation of Enzymes into Polymer Structure

Polymers were also synthesized with both glucose oxidase and catalase in order to render these polymeric systems glucose sensitive. The enzymes were suspended in PBS and allowed to chill in an ice bath for 30 min. Gentle stirring was used to allow mixing but to prevent flocculation. After chilling, a small amount of acryloyl chloride (Alfa Aesar) was added to the solution. The acid chloride moiety of acryloyl chloride has been shown to be preferentially attacked by the N-terminus of GOx and presumably CAT as well. This step essentially converts the enzymes into very large monomers; the acrylate groups on the enzymes allow them to participate in the copolymerization, incorporating the enzymes covalently into the polymer backbone. It has been reported that chemically immobilizing some enzymes has shown increased stability, and the loss of activity over time due to leeching of enzymes is no longer a concern.

To form the prepolymer solution, a solution of DEAEM, PEGnMMA and the crosslinking agent TEGDMA or PEG400DMA was made. The DEAEM was passed through a column of basic alumina prior to use to remove inhibitor. All other reagents were used as received. Instead of neat PBS, the enzyme solution as prepared above was used as the solvent to prevent autoacceleration, in a ratio of about 1:1 by weight of the monomers. Hydrochloric acid (ca. 37 wt%) was used to increase solubility. APS was used to initiate the polymerization and was mixed into the prepolymer solution just prior to being added to the continuous phase. Several different systems were

synthesized with varying compositions. The ratio of DEAEM to PEG grafts was either 10:1, 25:1, or no PEG grafts. Crosslinking ratios varied from 3 mol% up to 15 mol%.

To form the emulsion, 85 mL of cyclohexane was added to a round bottom flask containing 4.7 g Brij 30 and 8.7 g Triton X-100. The aqueous monomer solution, prepared as stated above, was then added to the round bottom. The mixture was homogenized at 24,000 rpm for 5 min. The emulsion was then capped with a rubber septum and purged with N_2 for 20 m to remove dissolved oxygen, after which 0.35 mL of TEMED were injected. The reaction proceeded very rapidly, and appeared complete after roughly 30 min. Immediately after injection, the reaction turned slightly cloudy, and then after about 5 min it turned opalescent. Particles of about 220 nm (collapsed) were formed, depending on crosslinker ratio. The cyclohexane was removed under reduced pressure on a rotary evaporator. The particles were precipitated with ethyl ether, which also dissolved most of the surfactant. The solution was centrifuged, the organic layer was poured off, and the process was repeated twice more. Sonication was necessary to resuspend the particles after the first wash, and resuspension became progressively more difficult as more surfactant was removed. The particles were then washed for one week in a dialysis membrane and the dialysate was changed twice a day. After the washing steps were completed, the particles were lyophilized on a Freezone freeze dryer and stored in a desiccator until use.

6.2.3 Polymer Characterization via FT-IR

Fourier transform infrared (FT-IR) spectra were obtained on a ThermoNicolet Nexus 470 spectrometer (Thermo Electron Corp., Waltham, MA) with a deuterated triglycine sulfate (DTGS) detector and potassium bromide (KBr) beam splitter. Typically, 128 scans were performed in the wavenumber range of 4000-400/cm, both forward and backward at 10 kHz, with a manual gain of one. Pellets of ca. 10 mg polymer and 200

mg KBr (spectroscopy grade, Acros Organics) were pressed at 15,000 psi using a Carver laboratory press.

6.2.4 Polymer Characterization via NMR

Nuclear magnetic resonance (NMR) spectra were obtained on a Varian Unity+ 300 MHz spectrometer. Deuterated water (D_2O, Cambridge Isotope Laboratories, Inc., Andover, Ma.) was used to suspend nanoparticles for tether analysis. Water suppression was used via the PRESAT macro with a saturation power of -2 and a saturation time of 5 on any samples with significant water signals. Small molecule analysis was obtained by using a suitable deuterated solvent, such as chloroform (CDCl3), dimethylsulfoxide (d6-DMSO), or d¬6-acetone, all obtained from Cambridge Isotope Laboratories. Unless otherwise stated, for all ^1H NMR spectra, the sample was spinning at 20 Hz, the number of transients was 8, and line broadening was 0.1.

6.2.5 Polymer Characterization via DSC

A PerkinElmer DSC 7 differential scanning calorimeter (PerkinElmer, Waltham, MA) using a heat/cool/heat method was used to characterize the polymers. A rapid heating cycle was used to erase any thermal history from the samples, after which the samples were cooled back down to the starting temperature. The final heating cycle had a ramp rate of 10^{o}C/min, which was slow enough to detect a T_g in some samples. Since room temperature was above the T_g of most samples, a nitrogen cooling unit was used with an initial temperature of -55°C.

6.2.6 Polymer Characterization via DLS

Nanoparticle hydrodynamic diameters were characterized using a ZetaPlus Zeta Potential Analyzer with a Multi Angle Particle Sizing Option installed (Brookhaven Instruments Corporation, Holtsville, NY) operating with a 25 mW laser at a wavelength of 635 nm. Detection of scattered light was at 90° to the incident beam. Each sample was subjected to 10 two-minute measurements. Typically, solutions of up to 2 mg/mL were used for the characterizations, at a temperature of 25°C. Freeze-dried particles were suspended in either PBS or 2 mM KCl. The pH of the nanoparticle solution was altered with either 0.1N HCl or 0.1N NaOH (Fisher Scientific), and was measured with an ISFET probe using an IQ Scientific Instruments pH meter.

A DLS measures the amount of a scattered laser beam passed through a suspension of particles. An average intensity of scattered light is determined, usually at a 90º incident angle, which also includes fluctuations associated with the random motion of the particles due to Brownian motion. The decay of these fluctuations can then be correlated to the diffusion coefficient of these particles. Equation (6.1), the Stokes-Einstein equation, is then used to determine the hydrodynamic diameter of the particles.

$$D = \frac{k_B T}{3\pi\eta(T)d} \tag{6.1}$$

In this equation, D is the diffusion coefficient of the particles, k_B is Boltzmann's constant, T is the temperature in Kelvin, η(T) is the temperature-dependent viscosity of the suspension, and d is the hydrodynamic diameter. While there are limitations on the usage of DLS, it was ideal for quickly determining particle sizes in solution. Thus, dynamic measurements were possible on submicron sized particles.

ζ-Potential measurements were conducted using electrophoretic light scattering, also using the Brookhaven ZetaPlus. Freeze-dried particles were suspended in a 10 mM KCl solution and diluted to 2 mM KCl with ddH_2O. Scattered light was detected at 15°

(175° to the incident beam) at a temperature of 25°C. Each sample was subjected to 10 measurements, with a 5 s delay between each measurement.

6.2.7 Polymer Characterization via SEM

A LEO Model 1530 SEM was used to determine the morphology of the synthesized particles. Samples were prepared for imaging in one of two methods. Method one consisted of suspending the particles in a volatile non-solvent and then placing a drop on an aluminum stage. Method two required the use of double-sided conductive carbon tape to hold the lyophilized samples on the aluminum stage. To prevent charging of the samples, they were sputter coated with gold using a Pelco Model 3 sputter coater. Stages were stored in a dessicator until loading into the SEM.

6.3 RESULTS AND DISCUSSION

6.3.1 Poly(diethylaminoethyl methacrylate) Nanoparticle Synthesis

Sub-micron sized particles, or nanoparticles, were successfully synthesized via this novel inverse emulsion polymerization procedure. The necessity for an inverse emulsion stems from the desire for these particles to contain hydrophilic components, such as PEG surface tethers and possibly either proteins or enzymes on the nanogel interior. Previous synthetic approaches inhibited the incorporation of such hydrophilic components due to the hydrophobicity of deprotonated DEAEM. Thus, monomeric DEAEM and hydrophilic comonomers (i.e., functionalized enzymes), did not properly copolymerize. Using this novel polymerization method will allow the copolymerization of DEAEM with several hydrophilic monomers, including functionalized enzymes such as glucose oxidase for the detection of glucose in solution.

It was determined that a 2:1 molar ratio of nonionic surfactants Brij 30 (Sigma-Aldrich) and Triton X-100 (Sigma-Aldrich) was able to form a stable inverse emulsion and provide fairly monodisperse nanogels. This result is somewhat contrary to theory, since the hydrophile-lipophile balance (HLB) of each surfactant is 9 and 13.5, respectively (as provided by the manufacturer). The HLB is a quantification of the ratio of hydrophilic to lipophilic functional groups in the surfactant, where surfactants with values < 10 typically form inverse emulsions, and surfactants with values ≥ 10 form stable emulsions (oil-in-water). Ionic surfactants were investigated, though several problems were encountered. Select cationic surfactants (e.g. MyTAB) would not form inverse emulsions, and anionic surfactants (e.g. AOT) complexed with the partially protonated DEAEM monomers, which prevented proper polymerization.

6.3.2 Incorporation of Enzymes into Polymer Structure

After nanoparticles were synthesized neat, they were also synthesized with glucose oxidase and catalase as co-monomers. These particles were examined and compared to the neat particles to determine if the glucose oxidase or catalase had any effects on the typical response of such systems to a pH stimulus. As shown in Figure 6.5, DLS swelling studies (as explained later in section 6.3.6) indicated that hydrogels both with and without glucose oxidase and catalase swelled to very similar extents over the range of pH values tested. Therefore, it can be concluded that the addition of these enzymes to not negatively affect the swelling characteristics of these nanoparticle systems in any observable way. Nanogels with enzymes were also tested to ensure enzyme activity remained in tact. After a polymerization was performed, a sample of the nanogels was taken and exposed to varying concentrations of glucose solutions. If a batch did not swell in response to glucose levels, it was discarded.

6.3.3 FT-IR Spectroscopy

FT-IR showed several important pieces of information. First, as shown in Figure 6.1, there was no substantial difference in spectra between nanogels with 5% and 15% crosslinking. Thus, the crosslinking does not adversely affect the rest of the polymerization. Second, the spectra indicated the functional groups present in each sample which indicated the successful removal of unreacted double bonds. The C=C stretching absorbance near 1650 cm^{-1} and the out-of-plane C-H bending of these same double bonds near 950 cm^{-1} were nearly non-existent. Also, the larger presence of etheric bonds in the samples containing PEG tethers, near a frequency of 1100 cm^{-1} (C-O stretching), indicates a higher content of PEG than those simply containing PEG crosslinker. Thus, it is reasonable to assume that the PEG tethers were successfully incorporated into the hydrogel backbone. This etheric peak also appears saturated in the highly crosslinked nanoparticles (X = 15%).

6.3.4 NMR Spectroscopy

Water suppression was necessary for all samples analyzed in D_2O; otherwise, the signal-to-noise ratios for the hydrogel peaks were too low for analysis. ^1H NMR was used to confirm the presence of PEG tethers on nanogels in D_2O by identifying the PEG oxyethylene peak at about 3.6 ppm (Figure 6.2). As the PEG tether length or PEG ratio was decreased, the area of the oxyethylene peak also decreased and was practically non-existent in the spectrum of nanogels synthesized without PEG tethers. Lightly crosslinked nanogels were used in these analyses, which also allowed the observance of PDEAEM peaks as well (3.2 ppm, 3.5 ppm). However, directly comparing the PEG oxyethylene peak to the methylamine peak on DEAEM did not provide an accurate

assessment of the ratio of DEAEM to PEG surface grafts due to limitations of NMR on crosslinked nanoparticles.

6.3.5 Differential Scanning Calorimetry (DSC)

Heat flow curves as a function of temperature were generated for several different polymeric systems and can be seen in Figure 6.3. P(DEAEM-g-EG2000) nanogels exhibited a peak T_m at 47°C, which is consistent with the melting temperature of pure PEG at a molecular weight of 2000 Da. These results are further evidence of the inclusion of PEG tethers on the nanogel surface, where tethers from several particles crystallized during the freeze-drying process. Using the melting peak for PEG allowed the calculation of the initial PEG crystallization amount to be about 30% for PEG2000 tethers, which could be recrystallized to 50% after melting; the enthalpy of melting values were obtained from Sanchez-Soto *et al* [17]. These values assume near 100% conversion of PEG monomer, which may not be accurate.

It is interesting to note that crushed microparticles with the same composition as nanogels did not have an observable T_m. This result can be explained by the methods of polymerization and how they alter the polymer structure. The crushed microparticles were synthesized as a film, where the PEG and DEAEM copolymerized without any partitioning and were randomly polymerized into the polymer chain. The nanogels, however, experienced PEG partitioning into the surfactant layer (the surfactants used were based on PEG derivatives). Thus, PEG was more likely to polymerize near the surface of the polymer particles than on the inside. This phenomenon resulted in more PEG protruding from the surface of the nanogels than from the microparticles. These PEG tethers were then able to crystallize with each other during the freeze drying process, which resulted in an observable T_m.

The T_g of crosslinked hydrogels was unable to be determined, due to the highly restricted polymer chain motion from the of crosslinking. Neither nanogels nor microparticles exhibited a detectable T_g. However, the T_g of uncrosslinked PDEAEM was determined to be -20°C, which agrees with previous reports.

6.3.6 DLS and ζ-Potential

DLS provided the solvated hydrodynamic diameter of nanoparticles as a function of pH. Similar to the crushed particles, the transition pH from collapsed to swollen occurred over a narrow range of about 7.4. Due to the limitations of DLS, the swelling properties of some nanogels were not fully investigated. The ability of DLS to measure particle size is dependent on the scattering of laser light off the polymer surface. However, as the nanogels swell with water, the polymer volume fraction can be as low as 1%. Thus, the polymer gel is almost completely solvent (polymer volume fraction approaches zero), and it is difficult for the laser to scatter enough light to collect reliable data. An increase in polymer concentration can help increase the signal to noise ratio, but this step also increases the viscosity of the solution drastically, which has also been shown to produce errant values for particle dimensions [18]. The nanogel suspension was first measured in a viscometer to reduce the possibility of this error.

Several important observations were made via DLS. As shown in Figure 6.4 the swelling response of DEAEM based nanogels was not significantly affected by the presence of PEG tethers. When the crosslinking ratio was held constant, both systems had a transition from collapsed to swollen state at a pH of about 7.2, which agrees with previous reports on similar systems. The particle size in the collapsed state for the non-PEGylated systems was, however, larger than those with surface PEG tethers. This phenomenon was most likely due to slight aggregation, since the deprotonated DEAEM was fairly hydrophobic without PEG tethers. Nanogels viewed in their dried state

tended to have very similar "collapsed" diameters as shown by SEM below. Finally, as mentioned above, as the polymers swelled at low pH, the standard deviation between measurements increased, mainly due to the difficulty in sizing via DLS at such conditions.

The inclusion of the immobilized enzymes did not appear to alter the pK_a of the systems significantly, as discussed earlier. Temperature, however, did affect the pK_a. At 20 °C, the pK_a was very close to 7.4. At a temperature of 37 °C, the pK_a dropped to about 7.1. It was also determined that slight temperature gradients existed in the samples during measurements due to the equipment's ability to maintain sample cell temperature. Thus, with a set point of 40 °C and 3 mL of sample, an average of 37 °C was attained throughout the sample and a temperature of 37 °C was attained at the level of the laser beam. Because the particle sizing relied on Brownian motion, if convective currents were present, reported particle sizes may be lower than actual values.

Systems were also characterized in glucose solutions. Nanoparticles were equilibrated in a salt water solution (0.15 M NaCl) and then glucose was added, enough to raise the concentration to 200 mg/dL. The response of a typical system can be seen in Figure 6.6. The delay before the hydrogels became fully swollen was attributed to a mixture of diffusional limitations on glucose through the gel, which is significantly larger than a hydronium ion, and the reaction kinetics of the enzymes towards oxidizing glucose. These data suggest that a device based on nanoparticles may be able to provide the desired response necessary for a closed-loop insulin delivery device.

The ζ-potential of the nanoparticles was shown to be affected by PEG tether length (Figure 6.7). The longer PEG chains were able to more effectively shield the surface charge of the polymers, thus reducing the measured ζ-potential at all pH values. The PEG tethers were also highly effective at preventing free hydroxide ions from adsorbing to the polymer surface at higher pH ranges. The PEG tethers acted like a

molecular brush, preventing the adsorption of dissolved ions onto the polymer surface. Thus, there was a reduction in the overall surface charge, especially at higher pH values, which can be exploited for biological applications such as drug delivery.

PEG also successfully shielded the positive charges on the protonated amines along the polymer background. However, this shielding effect was less than that of the hydroxide ions at basic pH values. This trend is most likely explained by the nature of PEG and ζ-potentials. PEG is highly effective at preventing ions, proteins, and other molecules from adsorbing to a surface. However, this effect is not fully able to shield the positively charged polymer due to the electric double layer present around such a material. Even longer PEG chains should increase the gap between the polymer and this double layer, thus reducing the ζ-potential. However, there is a practical limit to the PEG tether length due to the polymer synthesis method. Finally, the total number of PEG tethers on the surface of a given particle does not change with swelling, yet the surface area increases by radius squared. Thus, PEG tethers comprise more surface area of the nanogel when in the collapsed state versus the swollen state.

Previous work has shown that the incorporation of PEG tethers can have substantial benefits, such as increased suspension stability and decreased surface adsorption [19]. Moghimi *et al*, showed that PEG grafts of at least 2000 Da were necessary to prevent protein adsorption, while weights over 5000 Da further decreasing overall effectiveness [20]. These observations are consistent with the data above, indicating that PEG tethers of molecular weight 2080 Da were ideal for preliminary studies. Future studies could examine the effect of a tether longer than 2000 Da.

6.3.7 Scanning Electron Microscopy (SEM)

Several important observations can be made from the SEM micrographs shown in Figure 6.8. The nanoparticle synthesis provided fairly monodisperse samples, with

only slight variations in size from particle to particle. These micrographs confirm particle size determinations via DLS to be on the order of 200nm for collapsed particles. While these particles were freeze dried prior to imaging and do not directly provide collapsed particle sizes in solution, these data do agree well with data obtained from the light scattering method.

There is a noticeable difference between nanoparticles synthesized with PEG tethers versus those without. The surface characteristics of the nanoparticles with PEG tethers appear to be softer and more diffuse (Figure 6.8b & c), whereas particles without tethers appear to have more rigid boundaries. This phenomenon could be explained by the hair-like protrusion of the PEG tethers from the surface of the particles, providing a more textured surface for the sputter coated gold layer to adhere to, which in turn could have caused decreased localized resolution. It was reported that PEG tethers of 2000 Da could extend past the particle surface by as much as 7 nm based on the Flory radius of these tethers [21]. The low glass transition temperature of the PEG tethers also may play a role in this observation.

The low glass transition temperatures of the PDEAEM polymers offered an extra challenge during imaging. Deprotonated PDEAEM has a T_g below room temperature, whereas protonated PDEAEM has a somewhat higher T_g. Thus, deprotonated PDEAEM is rubbery and likely to deform during sample preparation and coalesce into a film, making imaging of distinct particles difficult if not impossible. Protonated PDEAEM, on the other hand, has a higher T_g making it glassy at room temperature. This characteristic allows better imaging at the expense of the increased hygroscopic nature of the polymer. These observations agree with previously reported results, which also indicate the difficulty in preventing latex films of PDEAEM during the sample preparation process [15]. Cornejo-Bravo and Siegel quantified the hygroscopic nature of dry, deprotonated PDEAEM by measuring the amount of water vapor absorbed from the air. Polymer weight doubled, and the water acted as a plasticizing agent.

6.4 CONCLUSIONS

Hydrogel nanoparticles, or nanogels, were successfully synthesized using a redox initiated free-radical polymerization. A novel inverse-emulsion polymerization method was described, which allowed nanogels on the order of 200 nm to be synthesized. These systems were characterized by several different techniques. FT-IR confirmed functional group content. ^{1}H NMR indicated successful copolymerization of PEG which resulted in soluble tethers protruding from the surface of the nanogels. DSC indicated the lack of a discernable T_g in these highly crosslinked systems but also confirmed PEG tether content. DLS was used for nanoparticle sizing, though limitations of the equipment were observed which prevented the complete analysis of certain systems. SEM micrographs confirmed that particle sizing measurements provided by DLS were accurate. Surface features were also elucidated, indicating that PEG provides different surface properties in the dried state.

As mentioned in the ζ-potential results above, the PEG tether length directly affected the observed ζ-potential of the nanogels. Longer chain lengths provided better shielding for the positive charges on the polymer backbone. However, a PEG molecular weight of 2000 Da was the largest PEG tested. The possibility of a longer PEG chain providing better shielding for the protonated amines may be worth investigating in future studies.

These studies have demonstrated that all PDEAEM-based systems synthesized exhibit a sigmoidal response to changes in pH. With this increase in polymer volume, the mesh size increased, and an increase in the diffusion rate of solutes should be present. Thus, these systems are ideal candidates for applications such as controlled drug delivery of medium-sized molecules such as small peptides. The loading and release properties of drugs with these systems were characterized in the following chapter to determine their feasibility in a drug delivery application. Finally, since a novel

nanogel synthesis was created using inverse-emulsion polymerization, the option for including hydrophilic comonomers during polymerization is possible. Thus, molecules such as functionalized enzymes (i.e. glucose oxidase) were successfully incorporated into these systems, allowing environmentally responsive systems capable of swelling and deswelling in the presence of an analyte.

6.5 FIGURES

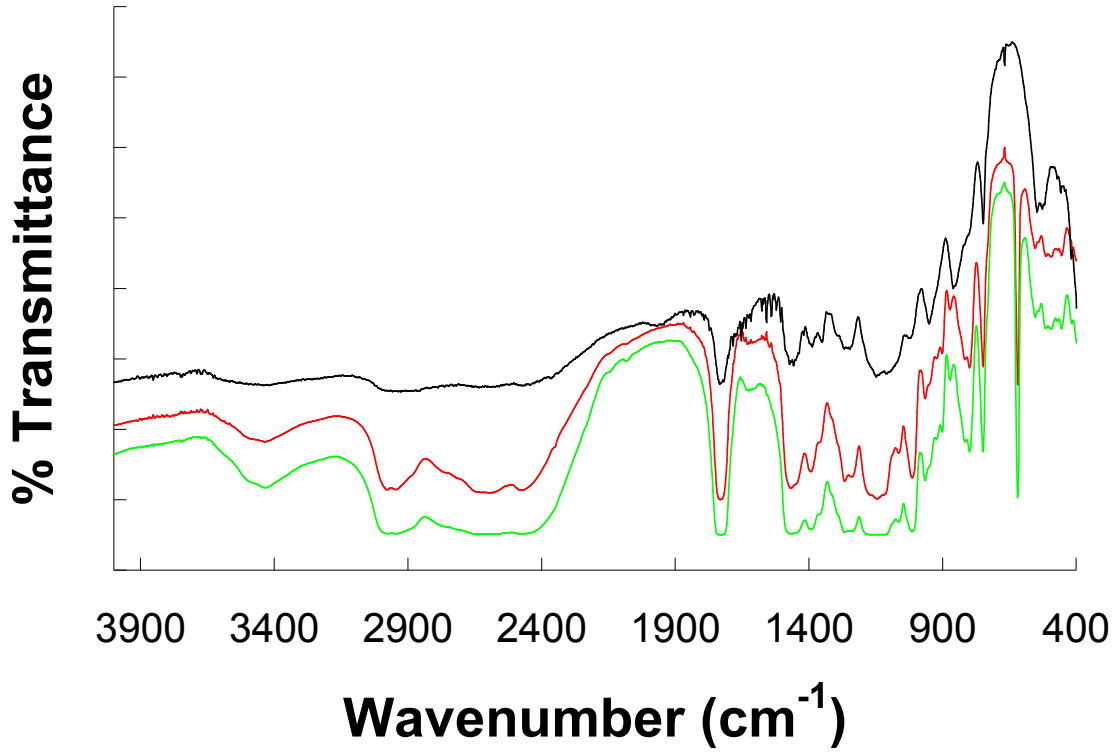

Figure 6.1. Fourier Transform Infrared Spectra of DEAEM Nanogels

FT-IR transmittance spectra of three nanogel formulations. The top spectrum is from a sample with 3% crosslinking (TEGDMA) and a 10:1 ratio of PEG400MMA grafts to DEAEM. The middle spectrum is from a sample with 5% crosslinking (PEG400DMA) and a 10:1 ratio of PEG400MMA grafts to DEAEM. The bottom spectrum is from a sample with 15% crosslinking (PEG400DMA) and a 10:1 ratio of PEG400MMA grafts to DEAEM. There is very little difference between these spectra, indicating that the amount of crosslinking does not affect the polymerization substantially. PEG etheric peaks at 1100 cm^{-1} appear saturated for the higher crosslinking ratio.

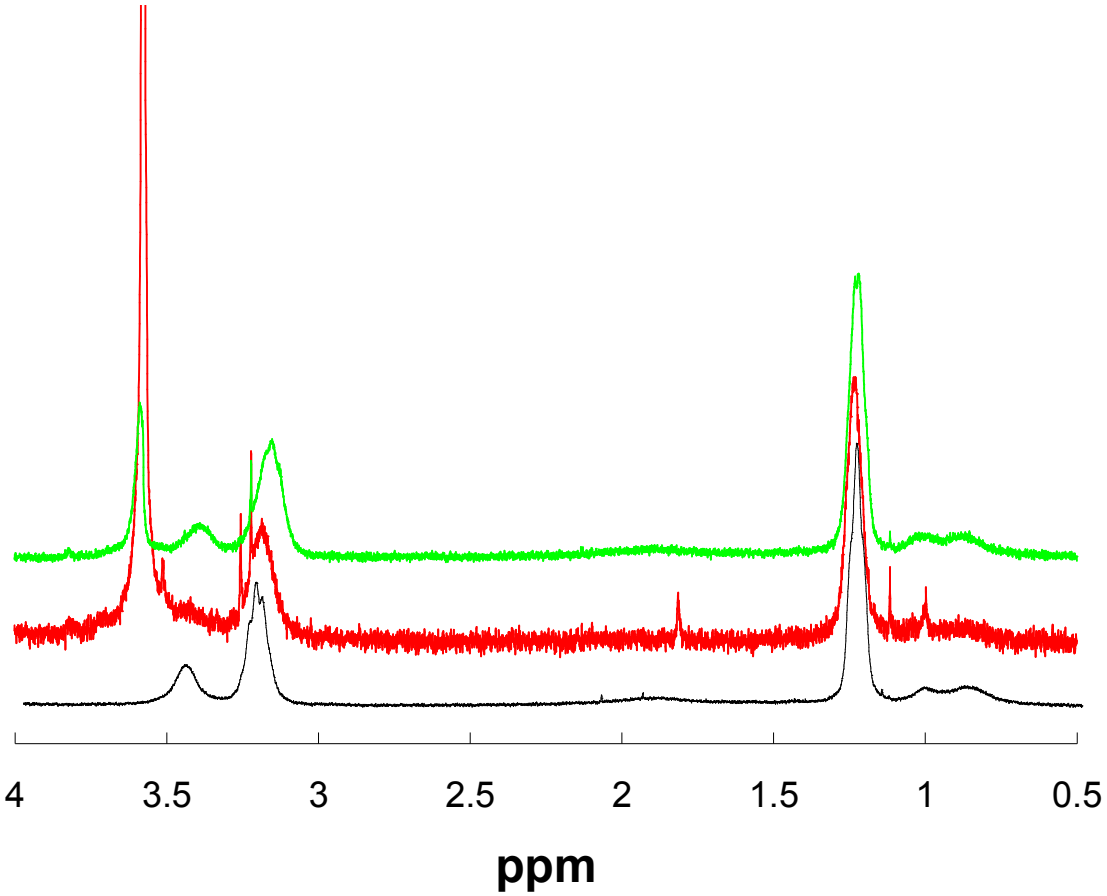

Figure 6.2. ^{1}H Nuclear Magnetic Resonance Spectra of DEAEM Nanogels

^{1}H NMR spectra of different PDEAEM samples in D_2O. The bottom (black) spectrum is linear PDEAEM with no PEG, the top (green) spectrum is P(DEAEM-g-EG400) with 10:1 PEG tethers, and the middle spectrum (red) is P(DEAEM-g-EG2000) with 10:1 PEG tethers. Note the substantial increase in the PEG peak at δ 3.6 ppm.

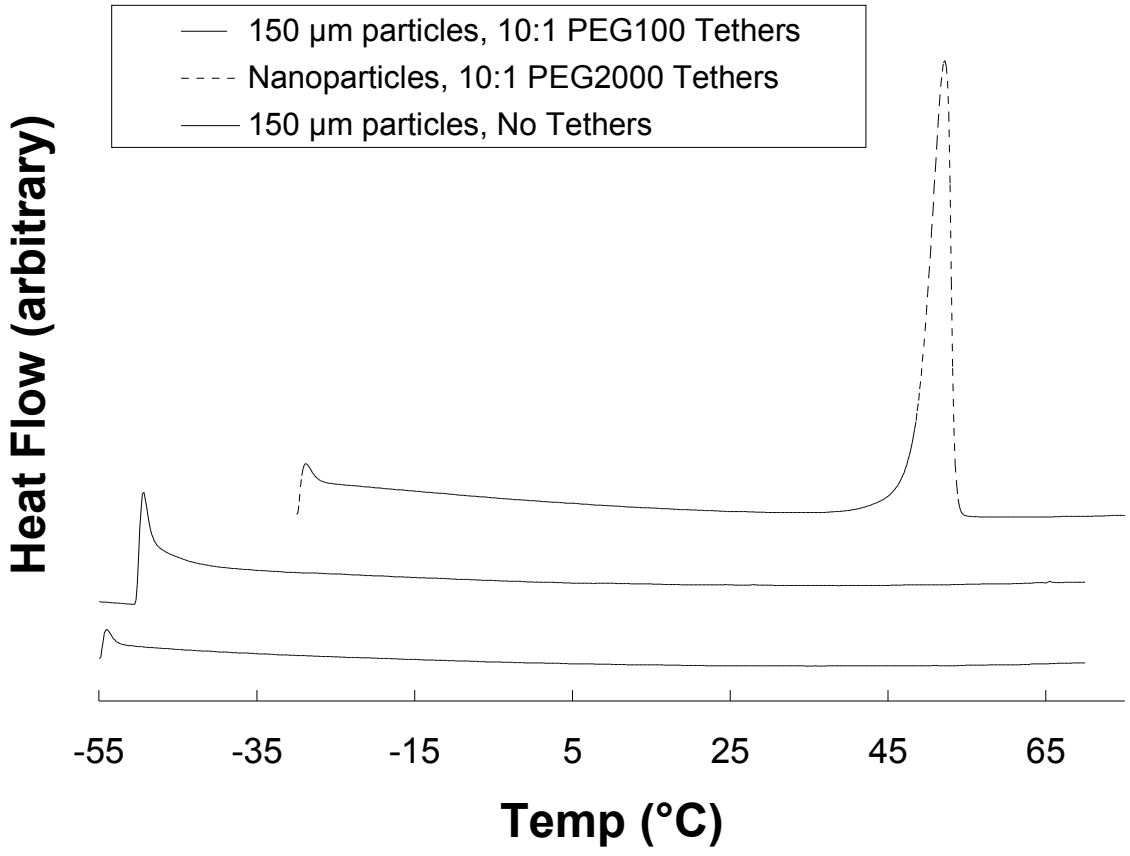

Figure 6.3. Differential Scanning Calorimetry results for select polymer formulations.

Baselines were straightened and y-axis units are arbitrary heat flow. Initial peaks (at -55 °C, -50 °C, and -30 °C) are artifacts of the initial measurement. Note the lack of T_g for all samples.

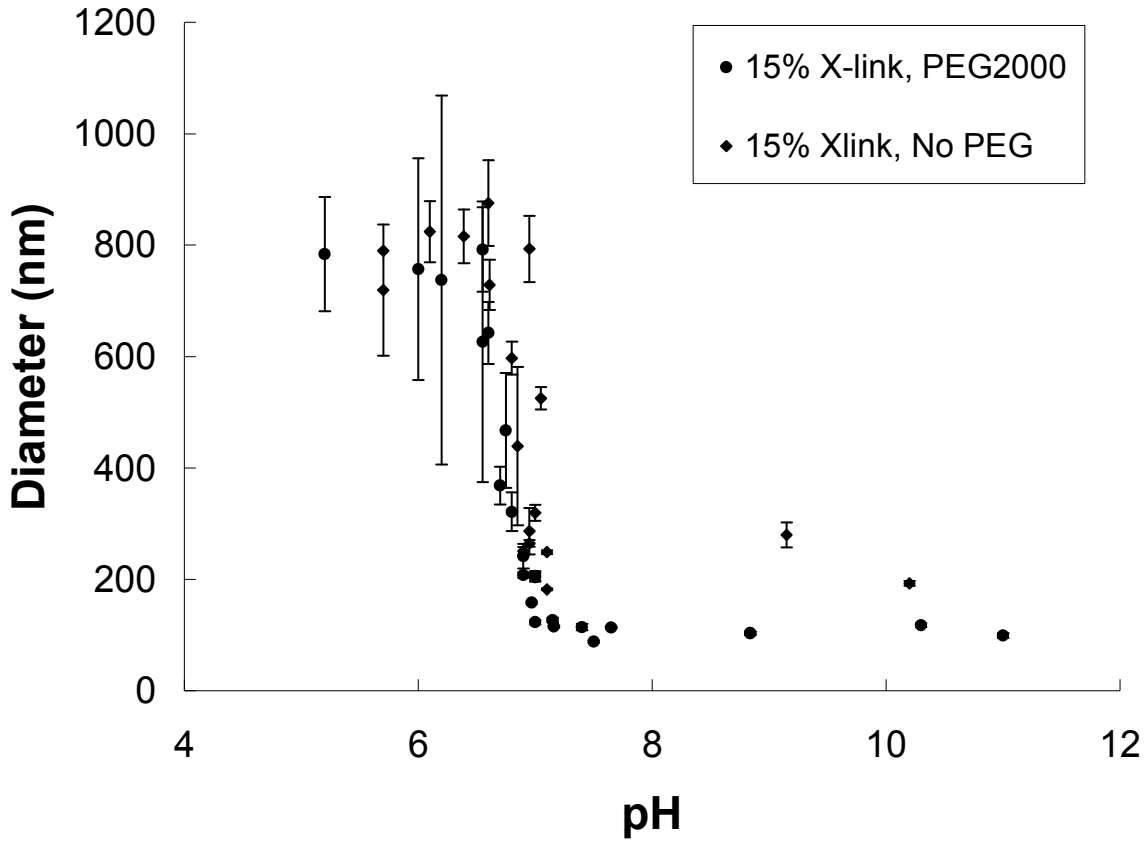

Figure 6.4. Volume Swelling Ratios of DEAEM Nanogels

Swelling response of two sets of particles, those with and those without PEG tethers, were identical. Both samples were collapsed at elevated pH values and fully swollen by pH 6. The transition pH was near physiological pH of 7.4. (n = 10 ± SD)

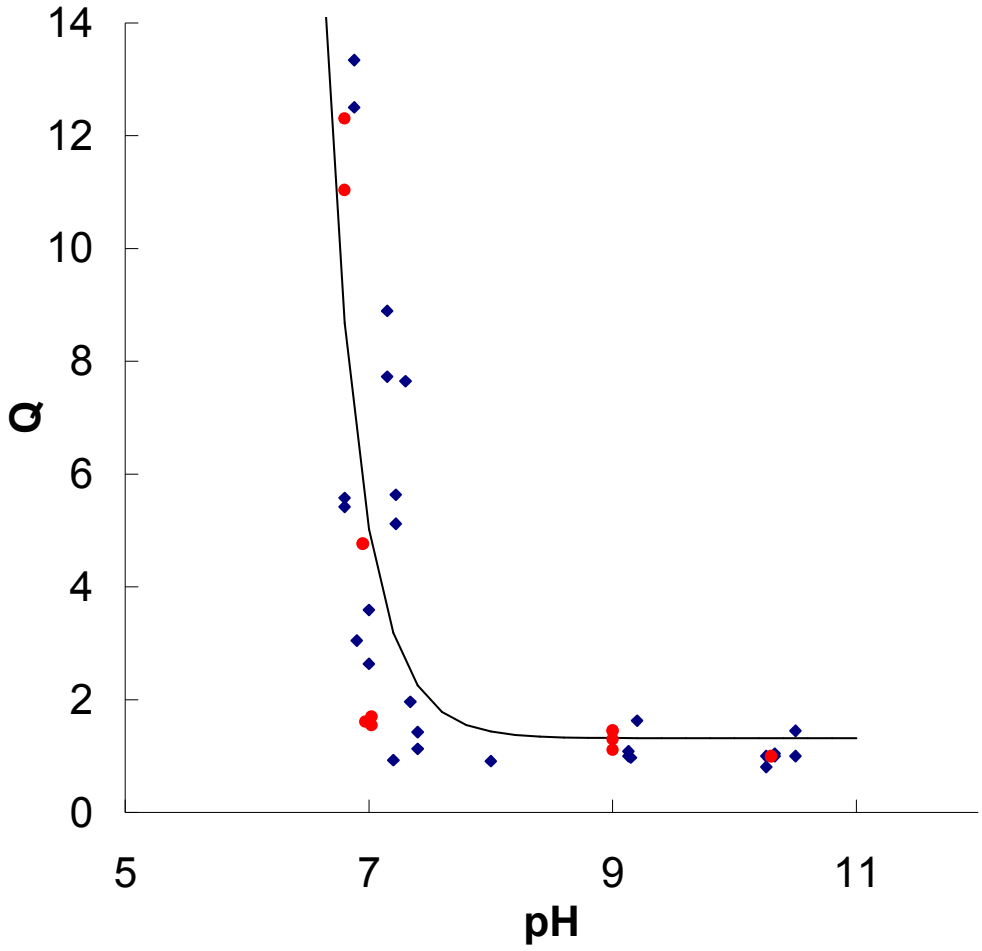

Figure 6.5. Equilibrium Swelling of pH-Sensitive P(DEAEM-g-EG), Both With and Without Glucose Oxidase.

Typical response of a 220 nm p(DEAEM-g-EG) nanoparticles at 20 °C either with or without entrapped glucose oxidase and catalase as a function of pH. Crosslinking ratios were 3% with a PEG to DEAEM ratio of 1:10. Blue dots correspond to particles without enzymes, red dots contained enzymes. Black line is a sigmoidal regression of the data. Q is the measured volume divided by the collapsed (in solution) volume. (n = 10 ± SD)

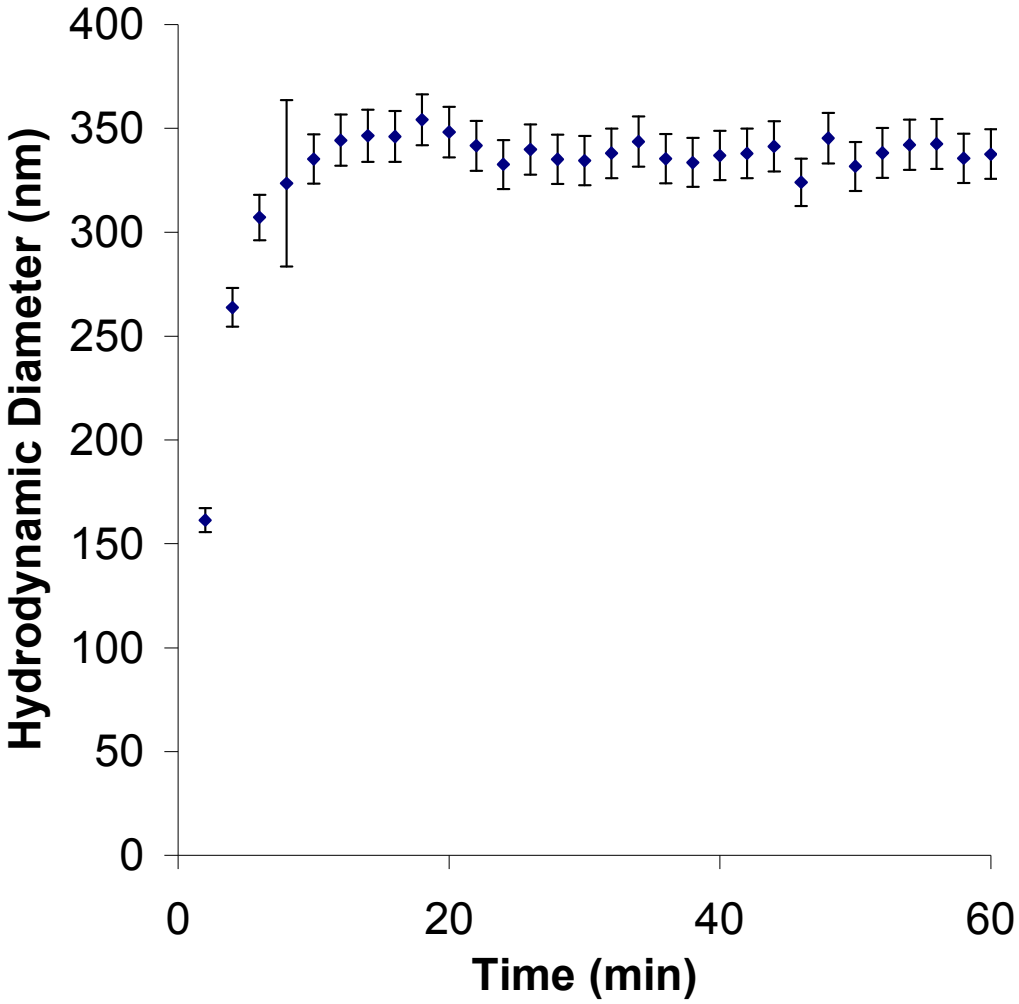

Figure 6.6. Dynamic Swelling of Glucose-Sensitive P(DEAEM-g-EG) Nanoparticles in Response to Step Change in Glucose Concentration.

Typical response of 160 nm p(DEAEM-g-EG) nanoparticles with immobilized glucose oxidase and catalase to a step change in glucose from 0 mg/dL to 200 mg/dL. Particles reached equilibrium in less than 20 minutes. Fluctuations after 20 minutes are due to the standard error associated with DLS. (n = 3 ± SD)

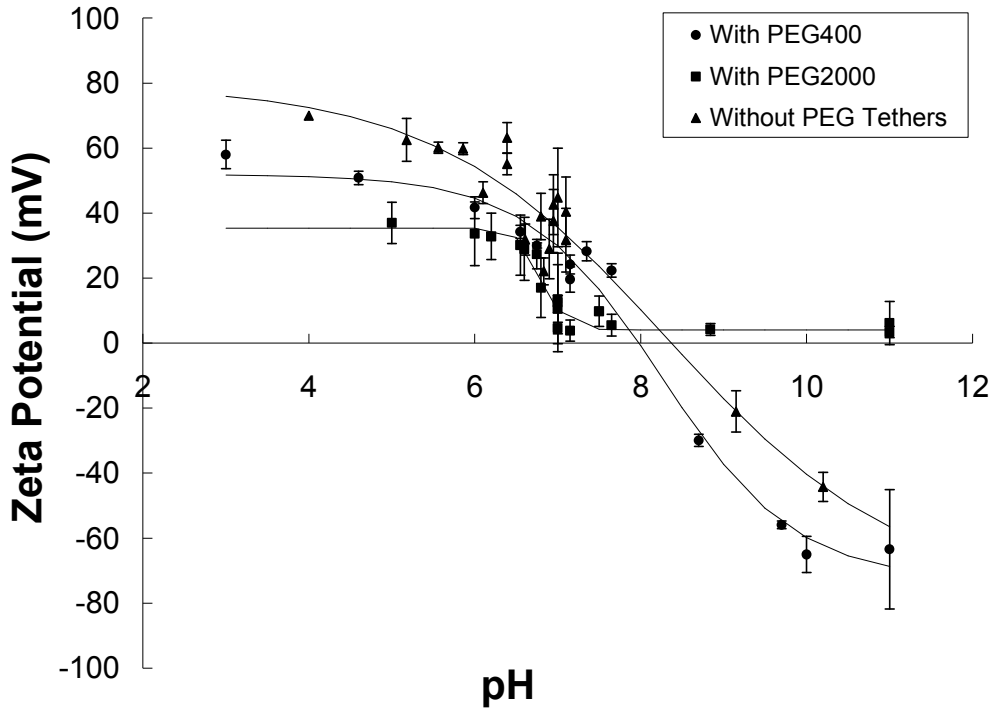

Figure 6.7. ζ-Potential as a Function of pH for DEAEM Nanogels

As PEG tether length increased, overall surface charge decreased, as indicated by the measured ζ-potential of the nanoparticles. Nanogels without PEG adsorbed hydroxide ions at high pH values, while at low pH values the protonated amines were observed. Nanogels with PEG2000 tethers successfully prevented hydroxide ion adsorption in basic solutions and helped shield protonated amines at acidic pH levels. (n = 10 ± SD)

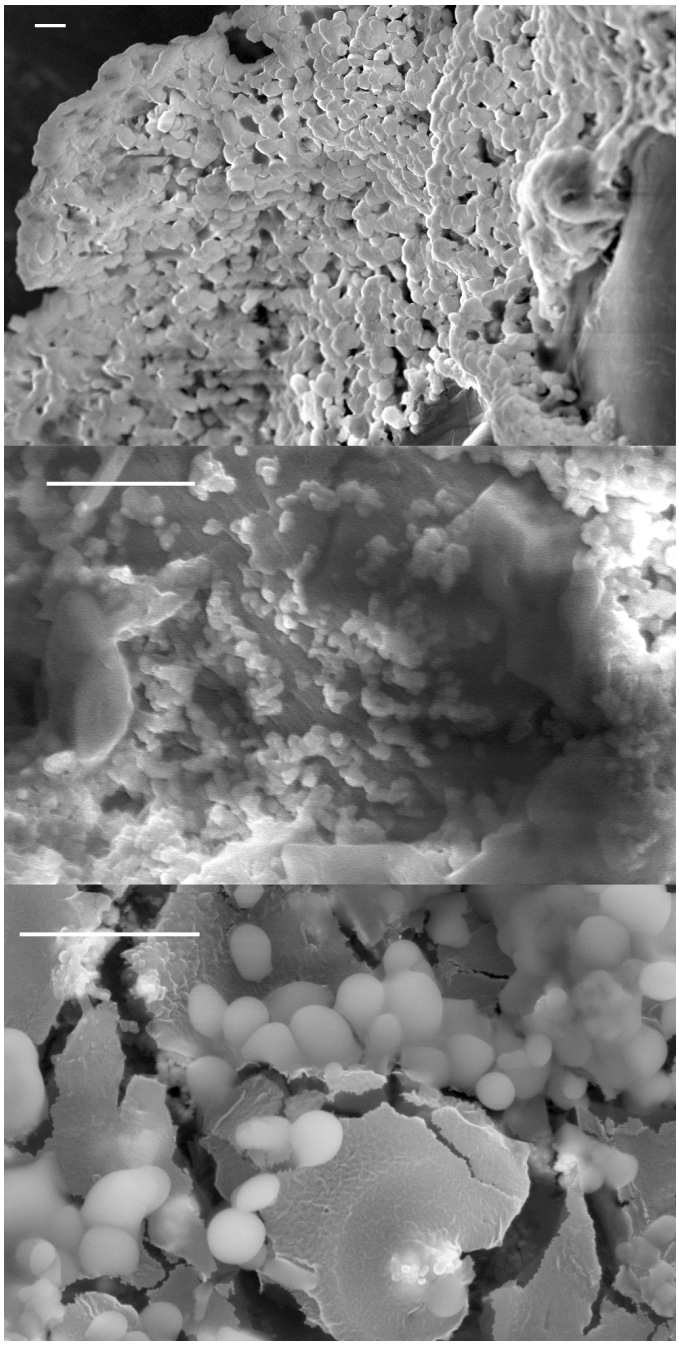

Figure 6.8. Scanning Electron Micrographs of DEAEM Nanogels

a) PDEAEM without PEG tethers; b) PDEAEM-g-EG1000 with a 25:1 DEAEM:PEG ratio; c) PDEAEM-g-EG2000 with a 10:1 ratio of DEAEM:PEG. Scale bars = 2 μm.

6.6 REFERENCES

1. Hellgren, A.-C., P. Weissenborn and K. Holmberg, *Surfactants in water-borne paints.* Prog Org Coat, 1999. **35**(1-4): p. 79-87.

2. Rodriguez, B.E., M.S. Wolfe and M. Fryd, *Nonuniform Swelling of Alkali Swellable Microgels.* Macromolecules, 2002. **27**(22): p. 6642-6647.

3. Bromberg, L. and L. Salvati, *Bioactive Surfaces via Immobilization of Self-Assembling Polymers onto Hydrophobic Materials.* Bioconjugate Chem, 1999. **10**(4): p. 678-686.

4. Kost, J. and R. Langer, *Equilibrium swollen hydrogels in controlled release applications*, in *Hydrogels in medicine and pharmacy*, N.A. Peppas, Editor. 1986, CRC Press: Boca Raton, Fla. p. 95-107.

5. Siegel, R.A. and B.A. Firestone, *pH-dependent equilibrium swelling properties of hydrophobic polyelectrolyte copolymer gels.* Macromolecules, 1988. **21**(11): p. 3254-3259.

6. Siegel, R.A., B.A. Firestone, I. Johannes and J. Cornejo, *Weak Ionic Hydrogels - Effects of Ph, Ionic-Strength and Buffer Composition on Swelling Equilibria, Kinetics and Solute Release.* Abstr Pap Am Chem S, 1990. **199**: p. 119-POLY.

7. Cornejo-Bravo, J.M. and R.A. Siegel, *Water vapour sorption behaviour of copolymers of N,N-diethylaminoethyl methacrylate and methyl methacrylate.* Biomaterials, 1996. **17**(12): p. 1187-1193.

8. Hariharan, D. and N.A. Peppas, *Characterization, dynamic swelling behaviour and solute transport in cationic networks with applications to the development of swelling-controlled release systems.* Polymer, 1996. **37**(1): p. 149-161.

9. Podual, K., F.J. Doyle and N.A. Peppas, *Dynamic behavior of glucose oxidase-containing microparticles of poly(ethylene glycol)-grafted cationic hydrogels in an environment of changing pH.* Biomaterials, 2000. **21**(14): p. 1439-1450.

10. Schwarte, L.M. and N.A. Peppas, *Novel poly(ethylene glycol)-grafted, cationic hydrogels: preparation, characterization and diffusive properties.* Polymer, 1998. **39**(24): p. 6057-6066.

11. Shatkay, A. and I. Michaeli, *Potentiometric Titrations of Polyelectrolytes with Separation of Phases.* The Journal of Physical Chemistry, 1966. **70**(12): p. 3777-3782.

12. Tobolsky, A.V. and M.C. Shen, *THE EFFECT OF HYDROGEN BONDS ON THE VISCOELASTIC PROPERTIES OF AMORPHOUS POLYMER NETWORKS.* The Journal of Physical Chemistry, 2002. **67**(9): p. 1886-1891.

13. Hayashi, H., M. Iijima, K. Kataoka and Y. Nagasaki, *pH-sensitive nanogel possessing reactive PEG tethered chains on the surface.* Macromolecules, 2004. **37**(14): p. 5389-5396.

14. Fisher, O.Z. and N.A. Peppas, *Polybasic Nanomatrices Prepared by UV-Initiated Photopolymerization.* Macromolecules, 2009. **42**(9): p. 3391-3398.

15. Amalvy, J.I., E.J. Wanless, Y. Li, V. Michailidou, S.P. Armes and Y. Duccini, *Synthesis and characterization of novel pH-responsive microgels based on tertiary amine methacrylates.* Langmuir, 2004. **20**(21): p. 8992-8999.

16. Jaworek, D., H. Botsch and J. Maier, *Preparation and properties of enzymes immobilized by copolymerization.* Methods Enzymol., 1976. **44**: p. 195-20.

17. Sanchez-Soto, P.J., J.M. Gines, M.J. Arias, C. Novak and A. Ruiz-Conde, *Effect of molecular mass on the melting temperature, enthalpy and entropy of hydroxy-terminated PEO.* J Therm Anal Calorim, 2002. **67**(1): p. 189-197.

18. Malvern, *The importance of sample viscosity in dynamic light scattering measurements*, in *Application note. Recognising the quality of data from photon correlation spectroscopy measurements. Technical note.* 2005, Malvern Instruments.

19. Owens, D.E. and N.A. Peppas, *Opsonization, biodistribution, and pharmacokinetics of polymeric nanoparticles.* Int J Pharm, 2006. **307**(1): p. 93-102.

20. Moghimi, S.M., A.C. Hunter and J.C. Murray, *Long-circulating and target-specific nanoparticles: Theory to practice.* Pharmacol Rev, 2001. **53**(2): p. 283-318.

21. Wong, J.Y., T.L. Kuhl, J.N. Israelachvili, N. Mullah and S. Zalipsky, *Direct Measurement of a Tethered Ligand-Receptor Interaction Potential.* Science, 1997. **275**(5301): p. 820-822.

CHAPTER 7

Insulin Loading and Release from Poly(Diethylaminoethyl Methacrylate) Hydrogels

7.1 INTRODUCTION

It is essential for the loading and release properties of a controlled drug delivery device to be quantified. The drug delivery device needs to provide the appropriate amount of drug loading and bioavailability, and the desired release profile. A low loading efficiency would indicate difficulties associated with entrapping the drug of interest into the polymer matrix. Low bioavailability would cause waste of the drug in the delivery device, since not all of the loaded drug would be released from the matrix and would not be available to the patient. Finally, an incorrect drug release profile would not correctly treat the disease.

Several previous studies have been performed on similar hydrogel systems to determine the loading and release behavior of different solutes. Siegel and Firestone looked at the release of caffeine from dimethylaminoethyl methacrylate (DMAEMA) as a model drug [1, 2]. Oscillatory swelling and deswelling were achieved by varying the pH, and caffeine release was dependent on the pH of the media. These gels exhibited a moving front mechanism of water sorption, which allowed the caffeine release from within these hydrogels.

Ishihara, *et al.*, investigated the release of imbibed insulin out of membranes made of 2-hydroxyethyl methacrylate (HEMA) and methyl methacrylate (MMA) [3, 4]. This research showed that the release rate of insulin increased as the HEMA concentration increased, likely due to the increased hydrophilicity of the hydrogel at higher HEMA concentrations. Zero order release out of these membranes was achieved

because of the relatively constant concentration of insulin inside the membrane device. However, diabetes patients require fluctuating insulin release depending on their body's current condition; thus, zero order release is not ideal for an insulin delivery device.

Schwarte and Peppas [5] also investigated several different systems for intelligent, controlled release. They studied the permeation of proxyphylline, vitamin B_{12}, and several different dextran molecules from P(DEAEM-g-EG) hydrogel discs. All solutes of interest were neutral, thus having no attraction or repulsion to the cationic hydrogels. The authors noted that the proxyphylline and vitamin B_{12} had much lower permeation values than expected, due to their molecular weights and the mesh sizes of the hydrogels investigated.

Finally, Hariharan and Peppas [6] investigated several other solutes of interest. Several different hydrogel matrices were synthesized, including P(DEAEM-co-HEMA) and poly(diethylaminoethyl acrylate-co-HEMA). Oxprenolol HCl, insulin, albumin, and myoglobin were loaded and released from these hydrogel discs. It was determined that the release rate of certain drugs (i.e., oxprenolol) was due primarily to polymer chain relaxation whereas the others were Fickian controlled.

A type I diabetic patient typically has to have a very specific insulin dosage regimen. A general rule of thumb is that a diabetic patient needs to inject subcutaneously about 0.2 IU/kg/day of basal insulin, and between 0.05 and 0.1 IU/kg before consuming a meal. One IU, or international unit, of insulin is precisely defined as 1/22 mg (ca. 45.5 μg) of pure crystalline insulin. Thus, for a patient with a body mass of 75 kg (165 lb), these values correspond to a total daily insulin intake of about 30 mg. The basal insulin dose corresponds to roughly half of the daily dose, about 15 mg, whereas between 3.7 and 7.5 mg is necessary before the consumption of each meal [7, 8].

Insulin is a peptide hormone of 51 amino acids with a monomeric molecular weight of ~5.8 kDa. However, in the presence of zinc, it tends to form a hexameric

structure of approximately 35 kDa. At physiological relevant conditions (pH 7.4), x-ray scattering has shown that the average radius of gyration of insulin is 1.98 nm, which corresponds to the hexameric structure. The active form of insulin is the monomeric structure, and hexameric insulin will not bind to cellular receptors. Thus, hexameric insulin remains in equilibrium with its monomeric form, and it slowly breaks down into monomeric insulin [9, 10].

The inactivity of hexameric insulin has been exploited in the treatment of diabetes. Pharmaceutical companies synthesize several different analogs of insulin, each have differing abilities to form hexamers. Thus, "long acting" insulin analogs such as Sanofi-Aventis's Lantus (insulin glargine) are less soluble at physiological pH and take a longer time to dissolve into the monomeric insulin form. These types of insulin are ideal for a long-term basal insulin delivery, such as a daily basal injection. Lispro insulin, on the other hand, was modified to prevent the formation of dimers and hexamers. This analog is entirely in its monomeric form, which makes it a "fast-acting" insulin ideal for postprandial subcutaneous delivery [8]. Hexamers can also be prevented *in vitro* by using ethylenediaminetetraacetic acid (EDTA) to chelate the zinc ion.

Chapter 5 discussed the physical properties of crushed microparticles of P(DEAEM-g-EG). There, the mesh size was estimated for polymer samples with a crosslinking ratio of 3%, 10%, and 15%. These estimates indicated that a collapsed mesh size of roughly 1 nm would potentially trap insulin, which has a monomeric hydrodynamic radius of 1.3 nm [11]. Thus, experiments were conducted to determine if these hydrogel particles could indeed entrap insulin and release insulin only under certain conditions, specifically acidic pH or increased solution glucose concentrations.

Insulin loading and release studies were performed to determine the feasibility of using a polycationic based hydrogel system for treatment of type 1 diabetes. Physiologically relevant conditions *in vitro* were used to simulate how these polymers might respond *in vivo*. Insulin was loaded into the hydrogels via both equilibrium

partitioning and ionic interactions. The release on insulin from these cationic hydrogels was measured as a function of time. Insulin release was triggered by either pH or glucose concentrations.

7.2 MATERIALS AND METHODS

7.2.1 Insulin Loading

A stock solution of bovine insulin (Sigma-Aldrich, 30 USP U/mg) was prepared in phosphate buffered saline (PBS, Fisher Scientific) with ethylenediaminetetraacetic acid (EDTA, Sigma Aldrich) at a concentration of 1.0 mg/mL. Insulin will only fully dissolve at acidic pH or after the addition of EDTA; thus, 0.04 mg EDTA per mg insulin was added to the PBS solution to facilitate insulin dissolution and loading. EDTA chelates the zinc ion which lies at the center of a hexameric insulin unit; thus, this procedure forced insulin into its monomeric form. After the insulin was dissolved, typically 7 mg/mL polymer sample (150 μm crushed microparticles) was added to the solution and the pH was lowered to about 5.6-5.8 using 1N HCl (Fisher Scientific).

After allowing a suitable amount of time for loading, typically 4 hr, the gels were collapsed by raising the pH to 9 with 1 M NaOH. This collapse physically trapped the insulin inside the microparticles. Excess insulin was washed off the surface of the particles with dilute (10 μM) NaOH and finally ddH_2O using a porcelain Büchner funnel atop a glass side-arm Erlynmeyer flask. A plastic centrifuge tube was put in place below the funnel and inside the flask to catch the filtrate, allowing the measurement of insulin in the filtrate after each wash step. The particles were then lyophilized and stored in a freezer until use.

To perform the washings on nanoparticles, special centrifuge tubes with dialysis membranes of a molecular weight cut-off of 20 kDa were used (iCON Concentrators

#89886, Pierce, Rockford, IL). These membranes allowed the surface insulin to be washed away, while retaining the collapsed nanoparticles inside the dialysis membrane.

7.2.2 Insulin Release

Insulin-loaded particles were suspended in appropriate media (i.e., PBS, saline) in SigmaCoted® glassware. Typically, a particle concentration of 1 mg/mL was used. To maintain physiological relevance, the temperature was kept at 37 °C using a recirculating water bath. A dissolution apparatus (Distek Dissolution System 2100B, North Brunswick, NJ) was operated at 100 rpm using flat anchor impellers.

At each desired time point, 100 µL of solution was extracted via pipette and ejected into a syringe attached to a 0.22 µm PVDF filter (Millipore Millex-GV filter unit, Bedford, MA). This solution was filtered into a vial suitable for high performance liquid chromatography (HPLC, Waters Corp., Milford, MA). All samples were analyzed via a Waters 2695 separations module (Waters Corp.) with a Waters 2487 Dual λ Absorbance detector and a Symmetry300™ C4 column (particle size 5 µm; dimensions 3.0 mm ID x 150 mm length, Waters Corp.). A mobile phase of 70% water (0.1% trifluoroacetic acid) and 30% acetonitrile (0.08% trifluoroacetic acid) was used.

Insulin release was measured as a function of time. Both pH and glucose concentration was used as the trigger for insulin release, and will be discussed separately below.

7.3 RESULTS AND DISCUSSION

7.3.1 Insulin Loading

7.3.1.1 Insulin Loading Efficiency

The loading of insulin into PDEAEM microparticles was performed at a pH between 5.6 and 5.8. This pH range allowed insulin to retain a net negative charge, while still swelling the hydrogels with a net positive charge (Figure 7.1). Ionic interactions between the insulin and the polymer increased total loading of insulin into the hydrogels. Previous experiments relied solely on equilibrium partitioning of insulin into the polymer; however, these techniques yielded lower overall insulin loading.

The loading efficiency of insulin into the particles is defined in Equation (7.1):

$$Loading\ Efficieny = \frac{m_0 - m_i}{m_0} \times 100\% \qquad (7.1)$$

where m_0 was the initial mass of insulin in solution and m_i was the mass of insulin in solution at condition *i*. Samples of the suspension medium were analyzed for insulin content using HPLC at the following conditions of interest: pre-collapse, post-collapse, and post-rinse. Pre-collapse was the time immediately before the addition of NaOH (to raise the pH above the pK_a), which was after particles had been suspended in the insulin solution and time was allowed for the particles to imbibe insulin. Post-collapse refers to the time after the particles were collapsed to entrap insulin using NaOH, but prior to any surface rinsing. Post-rinse was after rinsing surface-bound insulin from the particles using a filtration device, and consisted of the total mass of insulin recovered from the supernatant of the loading step plus all insulin collected after each wash step.

Figure 7.2 shows the relationship between the concentration of particles in the insulin loading solution to the loading efficiency of the particles. The concentration of insulin remained constant at 1 mg/mL during these studies. As the concentration of 150 µm crushed microparticles was increased from 4.78 mg/mg insulin to 10.54 mg/mg insulin, the total amount of insulin imbibed into the particles increased from 72% to 93%, after the rinsing step. These results indicate that as the concentration of polymer particles was increased, more polymer was able to interact with the available insulin in solution, thus creating more ionic insulin-polymer interactions. Therefore, more insulin was removed from solution and imbibed into the hydrogel particles as the concentration of particles increased.

Even though these results indicated that increasing the particle concentration during insulin loading resulted in an increased amount of insulin being removed from solution, there was a practical limit to what polymer concentration was desired. This optimization is discussed below in section 7.3.1.2.

As shown in Figure 7.3, the loading efficiency for crushed microparticles was a function of crosslinking ratio. Particles with a crosslinking ratio of 10% yielded the highest loading efficiency, at a value of almost 92% after rinsing, whereas particles with a crosslinking ratio of 3% provided only a 63% efficiency and particles with a crosslinking ratio of 15% only entrapped about 58% of the insulin in solution. It is interesting that as the particles with a 3% crosslinking ratio were collapsed and rinsed, the loading efficiency dropped from nearly 87% down to 77% and 63%, respectively. These results are due to the more loosely defined polymer network, which allowed the slight diffusion (and ultimately loss) of insulin out of the particles even in the collapsed state.

The particles with higher nominal crosslinking ratios, 10% and 15%, also exhibited some interesting characteristics. The amount of insulin entrapped in the polymer particles increased slightly between the pre-collapse and post-collapse steps. This result, which may be contrary to what was expected, could be explained by the

extent of ionic interactions. As the particles were being collapsed, the negative charge density of the insulin increased. Therefore, more insulin was imbibed into the hydrogel matrices due to increased ionic interactions. Since the highly crosslinked hydrogels had smaller overall mesh sizes, the insulin was not squeezed out after collapse. Finally, there was almost no difference between the post-collapse and the post-rinse steps, indicating that nearly all insulin that was entrapped in the particles occurred on the inside of these particles. This result also indicates that the collapsed particles were bound tightly enough to prevent the premature diffusion of insulin out of the particles.

7.3.1.2 Insulin Weight Fraction

A second important means of characterizing the amount of insulin loaded into the particles was the insulin weight fraction, defined in Equation (7.2):

$$Insulin\ Weight\ Fraction = \frac{m_0 - m_i}{m_0 - m_i + m_p} \times 100\% \qquad (7.2)$$

where m_p was the mass of particles added to the insulin solution for loading. This relationship indicates what mass percent of a given loaded particle is insulin. In other words, if the insulin weight fraction is 10%, with a basis of 100 g of insulin-loaded particles, there would be 10 g of insulin and 90 g of polymer.

Figure 7.4 identifies the relationship between the concentration of particles in the insulin loading solution to the insulin weight fraction of the particles. The concentration of insulin remained constant at 1 mg/mL during these studies. As the concentration of 150 µm crushed microparticles was increased from 4.78 mg/mg insulin to 10.54 mg/mg insulin, the relative amount of insulin per mass of particles imbibed into the particles decreased from 13% to 8%, after the rinsing step. These results indicate that as the concentration of polymer particles was increased, less total insulin was available per hydrogel microparticle. Therefore, even though more insulin was removed

from the solution at higher particle concentrations, the total amount of insulin in each particle decreased.

These results indicated that a higher concentration of particles during the insulin loading was not necessary ideal. For a drug formulation, the amount of drug loaded into each particle is an important parameter. If the insulin weight fraction is very low for a given set of microparticles, then it would take more particles to deliver the same amount of insulin compared to a set of microparticles with a high insulin weight fraction. For example, 5 g of particles with an insulin weight fraction of 8% has 400 mg of insulin. However, 5 g of particles with an insulin weight fraction of 13% has 650 mg of insulin, more than 60% more insulin per mass of particles. Thus, it would take 60% more particles of the lower insulin weight fraction to be able to deliver the same total amount of insulin as the particles with the higher insulin weight fraction.

The ratio of 7 mg particles per 1 mg insulin was used for all further studies due to the high loading efficiency and relatively high insulin weight fraction of microparticles loaded at these conditions.

As shown in Figure 7.5, the insulin weight fraction for crushed microparticles was also a function of crosslinking ratio. Particles with a crosslinking ratio of 10% yielded the highest mass of insulin loaded per total mass, at a value of over 10% after rinsing, whereas particles with a crosslinking ratio of 3% provided only an 8% weight fraction and particles with a crosslinking ratio of 15% only contained about 6% of insulin per mass. Similar to the loading efficiency, after the particles with a 3% crosslinking ratio were collapsed and rinsed, the insulin weight fraction dropped from nearly 11% down to 10% and 8%, respectively. Again, this phenomenon is most likely due to the more loosely defined polymer network which allowed some of the entrapped insulin to diffuse out during the hydrogel collapse.

The particles with higher crosslinking ratios, 10% and 15%, exhibited some interesting characteristics in the insulin weight fraction as well. The amount of insulin

entrapped in the polymer particles increased slightly between the pre-collapse and post-collapse steps. This result, which may be contrary to what was expected, could be explained by the extent of ionic interactions. As the particles were being collapsed, the negative charge density of the insulin increased. Therefore, more insulin was imbibed into the hydrogel matrices due to increased ionic interactions. Since the highly crosslinked hydrogels had smaller overall mesh sizes, the insulin was not squeezed out after collapse. Again, since there was almost no difference between the post-collapse and the post-rinse steps, nearly all insulin that was entrapped in the particles occurred on the inside of these particles and there was very little surface-bound insulin to be washed off. This result also indicates that the collapsed particles were bound tightly enough to prevent the premature diffusion of insulin out of the particles.

As determined by the mesh size estimates in Chapter 5, the crushed microparticles were indeed able to entrap insulin in basic media. However, the ability to load insulin into the nanoparticles discussed in Chapter 6 was more problematic. Studies were inconclusive as to the effectiveness of trapping insulin inside these nanoparticles at elevated pH values. In acidic media, negatively charged insulin was attracted to the positively charged nanogels. However, upon addition of NaOH to collapse the nanogels and trap the imbibed insulin, most insulin appeared to simply diffuse out. This result is due to the substantially increased surface-area-to-volume ratio of the nanogels compared with the microparticles, which substantially increased the diffusional surface per unit mass by orders of magnitude. These results were further investigated with release studies performed with the nanogels, and discussed below.

7.3.2 Insulin Release

7.3.2.1 pH-Sensitivity for Insulin Release

Initial studies were first performed on crushed microparticles that were exposed to different pH media. This proof-of-concept was used to ensure that insulin could be trapped in the hydrogel particles at elevated pH values (physiological pH of 7.4) and then be released at acidic conditions. Crushed microparticles were used in the study represented by Figure 7.6, where the pH of the media was 7.4 until time 120 min, at which time an injection of HCl was used to reduce the pH to 4.0. As desired, the insulin remained entrapped inside the hydrogel microparticles at the physiological pH. After the addition of acid, the tertiary amines of DEAEM became protonated, and the insulin took on a net negative charge (pI = 5.3). This charge repulsion caused particle swelling and the expulsion of imbibed insulin from the microparticles.

Rapid insulin release occurred after the addition of hydrochloric acid, releasing most releasable insulin after 30 min and nearly 100% after about 50 min. This experiment confirmed the ability to retain the insulin inside the hydrogel microparticles at elevated pH values and only release the insulin once the pH became acidic. Attempts were made to release insulin in a controlled manner from nanoparticles (Figure 7.7). However, large errors were encountered in acidic media and the pH of the media did not affect the release in a desirable manner, even in basic media. Thus, nanoparticle release was not exhaustively analyzed.

7.3.2.2 Glucose-Sensitivity for Insulin Release

The proof-of-concept results discussed above were promising, and indicated that further studies were necessary to determine the release profile for hydrogels exposed

to glucose solutions. Since the mechanism of insulin delivery with the proposed system is during elevated glucose levels, it was necessary to determine the effect glucose had on the release of insulin.

The first comparison was between two sets of crushed hydrogel microparticles which had differing crosslinking ratios. Figure 7.8 shows the insulin release profile of microparticles with a crosslinking ratio of 3% and 10%. Since the microparticles with only 3% crosslinking swelled substantially more than those with 10% crosslinking (see Chapter 5), more insulin was able to easily diffuse out during the insulin release study. Thus, 70% of the total amount of insulin that was releasable in the microparticles was released for the particles having 3% crosslinking. This polymeric system would not be ideal for multiple, pulsed release due to over two-thirds of the total drug payload being released on the first pulse.

The higher crosslinked particles exhibited more ideal characteristics for an insulin delivery device. These microparticles released closer to one-third of the available insulin from within the matrix instead of 70%. Thus, multiple dosages of insulin would be possible with such a hydrogel, potentially up to three for the particles investigated. The actual amount of insulin released per mass of particles was 24 μg/mg for the 3% crosslinked microparticles and 6 μg/mg for the 10% crosslinked microparticles. Therefore, for a typical patient of about 75 kg that would require a postprandial insulin dose of between 3.75-7.5 IU, roughly 30-60 mg of dry microparticles (10% crosslinking ratio) would be required per day.

Figure 7.9 shows how the total amount of insulin able to be released from the particles was determined. This value may differ from M_∞ due to the method used. After the insulin release due to the glucose stimulus, hydrochloric acid was added to the solution to lower the pH to below the pI of insulin. At a pH of 4, both the insulin and the hydrogel microparticles had net positive charges. Thus, ionic repulsion helped force out any excess insulin still entrapped in the hydrogel after the glucose stimulus. This

amount of insulin was quantified, and used as the total amount of insulin that was able to be released from the microparticles. M_∞, on the other hand, typically just refers to the amount of drug released at infinite time.

Figure 7.10 indicated the effect a buffering system had on the release of insulin from the hydrogel microparticles. The ionic strength of each solution was kept constant at 150 mM, and the only difference was whether there was a phosphate buffer (5 mM) present. The buffered media reduced the total amount of insulin released due to the Donnan equilibrium effect, which has an effect on the overall swelling of the particles [12]. This effect indicates that a semi-permeable membrane, such as the hydrogel itself, may balance net charges by partitioning certain ions into either the membrane or the solvent phase [13]. Previous modeling studies indicated that the buffered medium substantially hindered the pH drop inside these particles [14]. It was also modeled that a pH profile along the radius of each particle, thus preventing total swelling. With a decrease in the particle swelling, each insulin molecule was presented with a more tortuous diffusional path and was thus less likely to be able to leave the microparticle.

7.4 CONCLUSIONS

Several important conclusions were drawn from the above mentioned studies. First, the ideal insulin loading procedure for crushed microparticles was determined to be a particle concentration of 7 mg/mL, at an insulin concentration of 1 mg/mL. These conditions yielded a high insulin loading efficiency (over 90%) and a relatively high insulin weight fraction in the particles. It was also determined that particles with a crosslinking ratio of 10% provided the highest insulin loading efficiency compared to particles with 3% and 15% crosslinking. Finally, particles with a crosslinking ratio of 10% only released about one-third of the total releasable insulin after a single glucose stimulus, compared to nearly 70% in the case of 3% crosslinked particles. Thus,

microparticles with a crosslinking ratio of 10% were determined to have the optimal characteristics for insulin loading and release, both as a function of pH and as a function of glucose concentrations.

The insulin release properties of these microparticles had several desirable characteristics. The release of insulin was controlled by either pH or glucose concentration, and insulin release was minimal at physiological pH values. The total amount of insulin released from the particles was a function of the crosslinking ratio, which would allow the tuning of the particles to provide a specific number of doses of insulin (each pulse of glucose causing the release of one of these insulin "doses"). It was also possible to obtain physiologically relevant amounts of insulin release from these microparticle systems. A patient of 75 kg would only need between 30-60 mg of microparticles per day for postprandial insulin delivery.

However, some scientific concerns must also be noted. Donnan equilibrium was determined to cause decreased release rates of insulin out of the swollen microparticles. This phenomenon substantially decreased the amount of released insulin, as shown by the difference in release rates and amounts for hydrogel microparticles suspended in saline compared to buffer.

Nanoparticles, which were expected to have the fastest response to a given stimulus (either pH or glucose), were very difficult to work with when it came to insulin loading and release. Loading of nanoparticles after synthesis had challenges associated with washing and collection. Due to the small size and the necessity to prevent premature diffusion of insulin out of the particles, rapid methods of collapse and collection were necessary. Ultracentrifugation was not an option because it may have squeezed the loaded drug out of the matrix.

Finally, the release of insulin from the nanoparticles was difficult. These studies yielded unreliable data with large errors. The large surface area to volume ratio of these nanoparticles substantially increased the diffusional driving force by increasing the area

for mass transfer flux. These results agree with modeling attempts of similar systems, which indicated that the submicron particle size would not properly work as an injectable controlled drug delivery device [14].

7.5 FIGURES

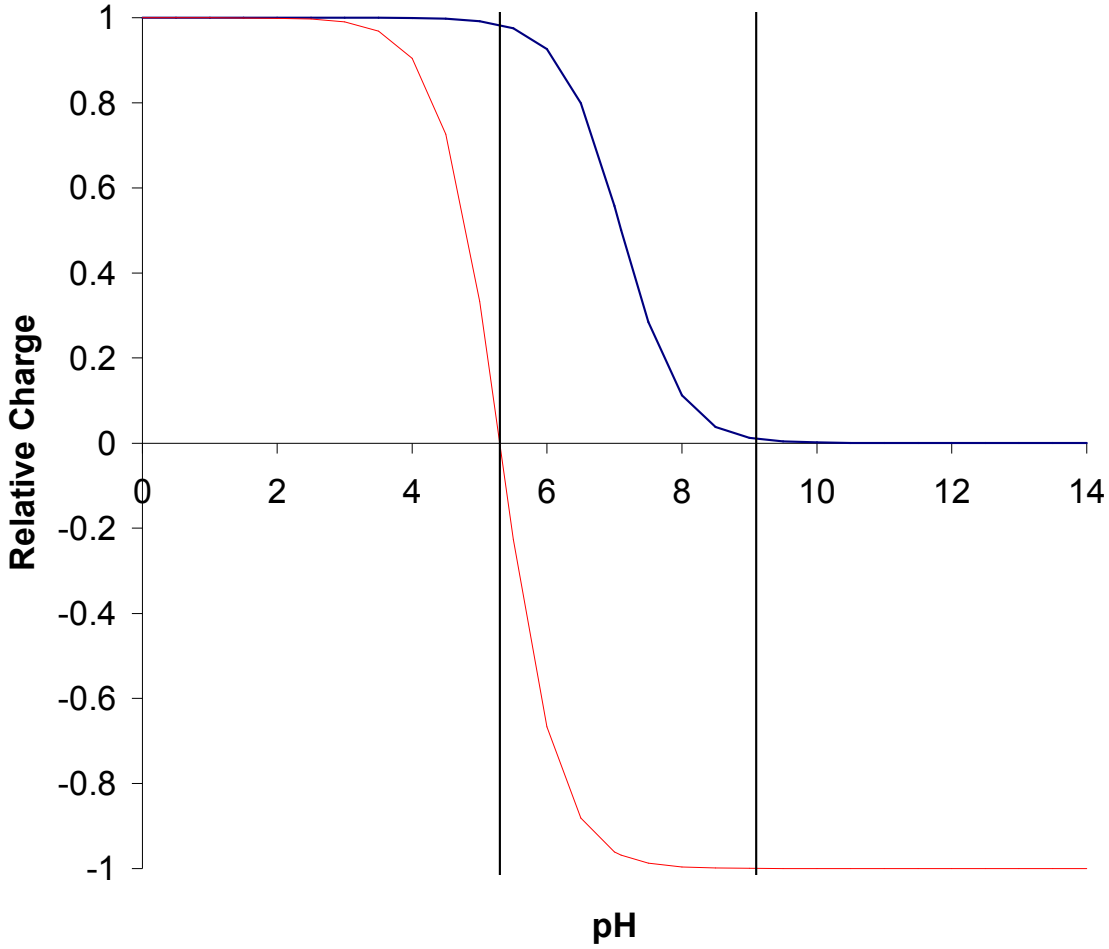

Figure 7.1. Theoretical Charges for Insulin Loading

The theoretical charges on insulin (pI = 5.6) and PDEAEM (pK_a = 7.4) indicate a window above pH 5.6 and below pH 9 where optimal ionic interactions will occur to increase insulin loading. Since PDEAEM is not swollen above pH 7.4, this window is further reduced to above pH 5.6 and below pH 7.4.

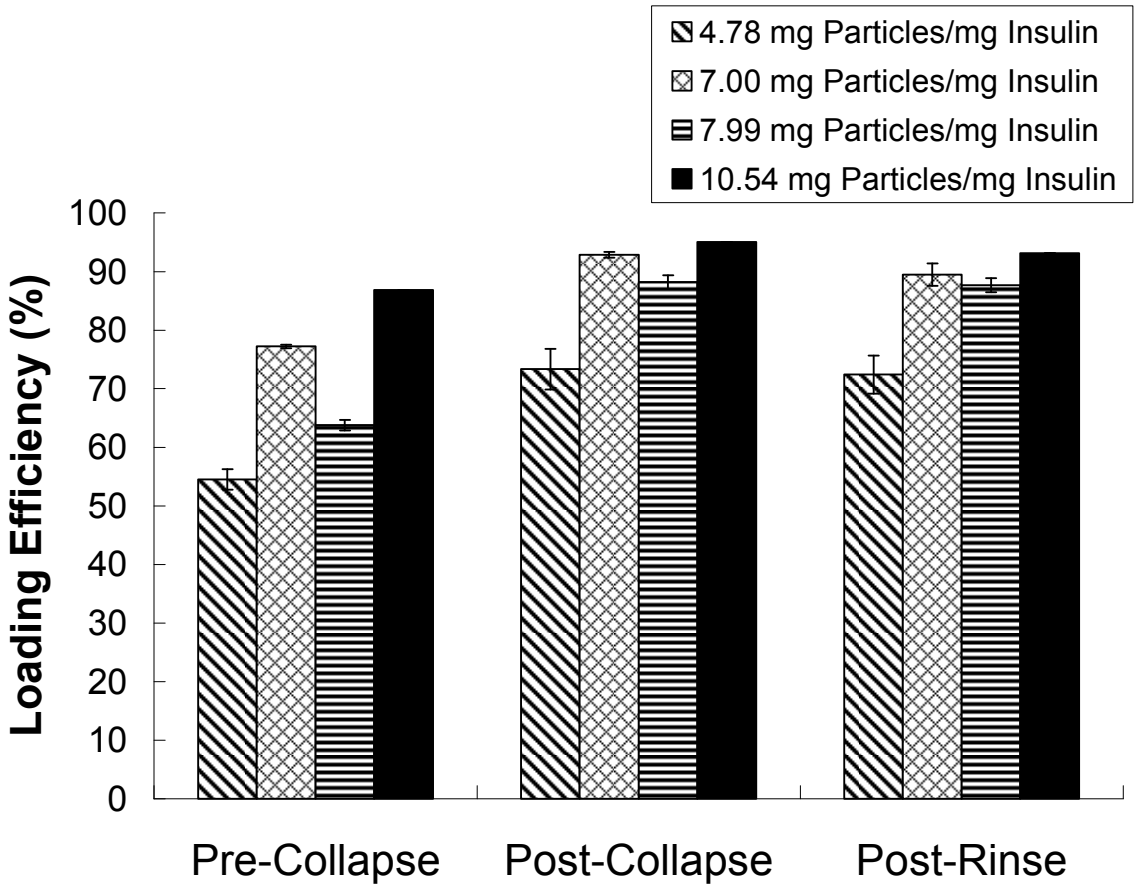

Figure 7.2. Insulin Loading Efficiency Insulin into Microparticles With 10% Crosslinking

The loading efficiency of insulin into 150 µm crushed microparticles having a crosslinking ratio of 10%. As the concentration of particles increased (with constant insulin concentration) from 4.78 mg/mg insulin to 10.54 mg/mg insulin, the loading efficiency also increased, from a low of 72% to a high of 93%. These results were due to a larger polymer-insulin interaction since there were more available particles per mass of insulin.

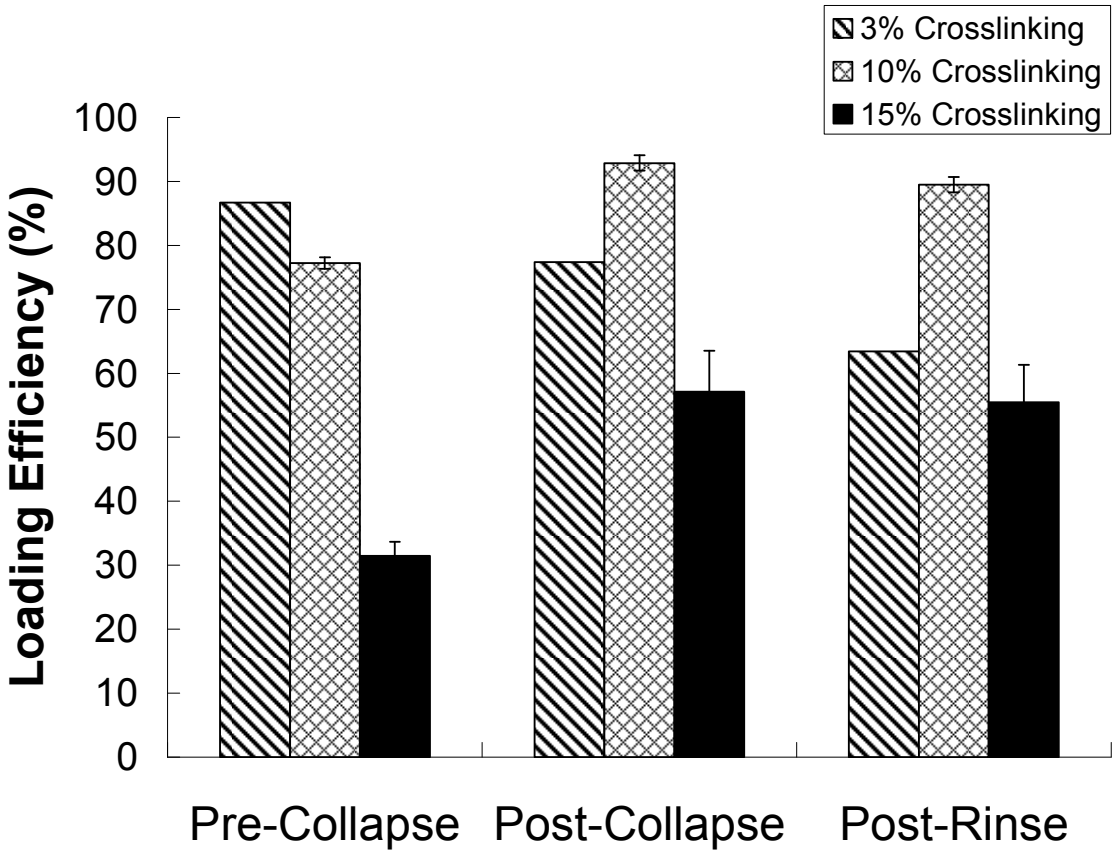

Figure 7.3. Insulin Loading Efficiency Insulin into Microparticles With Varying Crosslinking Ratios

Insulin loading efficiency of crushed microparticles, indicating the amount of insulin in solution that was imbibed into the polymers during insulin loading.

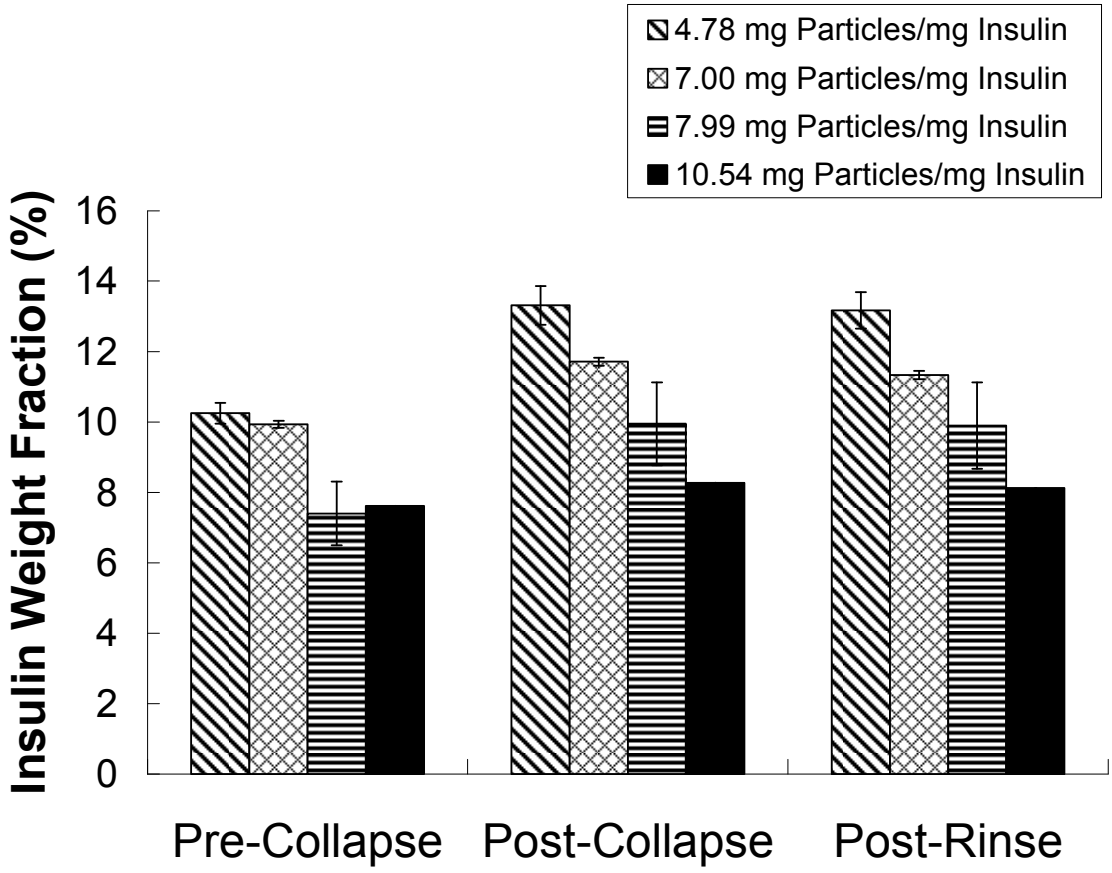

Figure 7.4. Insulin Weight Fraction of Loaded Microparticles With 10% Crosslinking

The insulin weight fraction of loaded insulin into 150 µm crushed microparticles having a crosslinking ratio of 10%. As the concentration of particles increased (with constant insulin concentration) from 4.78 mg/mg insulin to 10.54 mg/mg insulin, the insulin weight fraction of the particles decreased from a high of 13% to a low of 8%, after the rinsing step. These results were because there was less insulin available for each particle, and so less insulin was loaded into each particle.

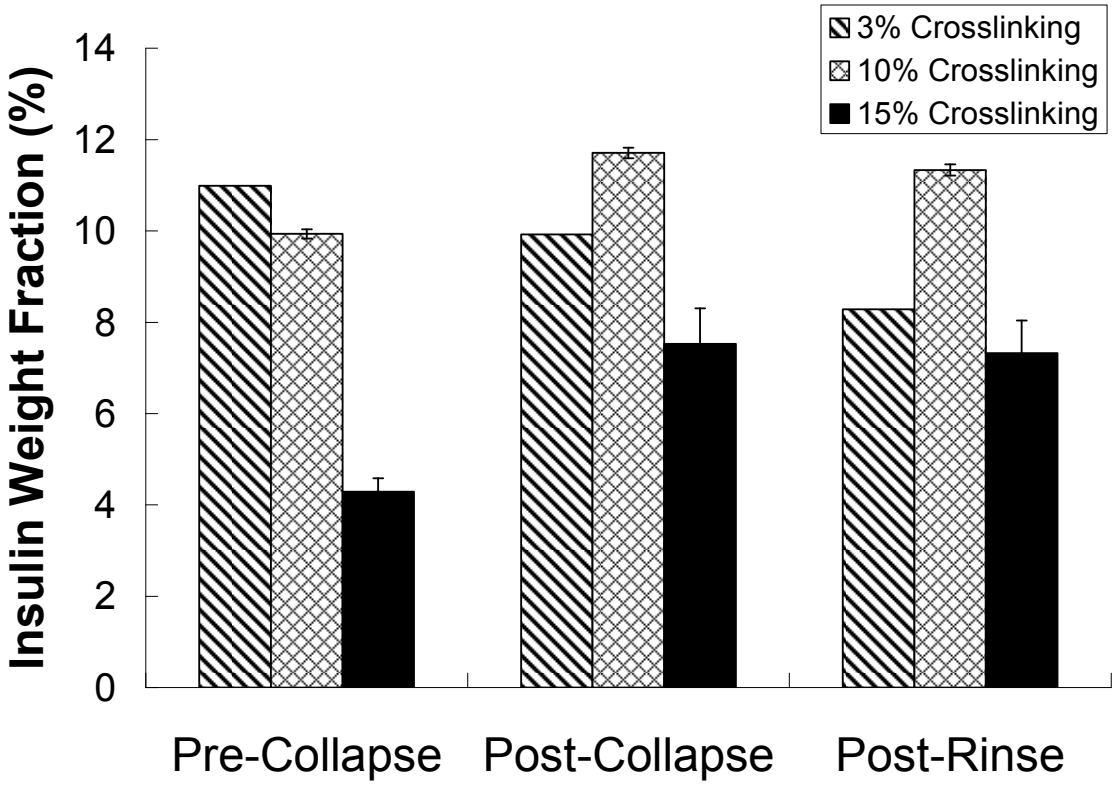

Figure 7.5. Insulin Weight Fraction of Loaded Microparticles With Varying Crosslinking Ratios

Weight fraction of insulin in loaded crushed microparticles. For example, a weight fraction of 10% indicates that for every 100 g of loaded particles, 10 g is insulin and 90 g is polymer.

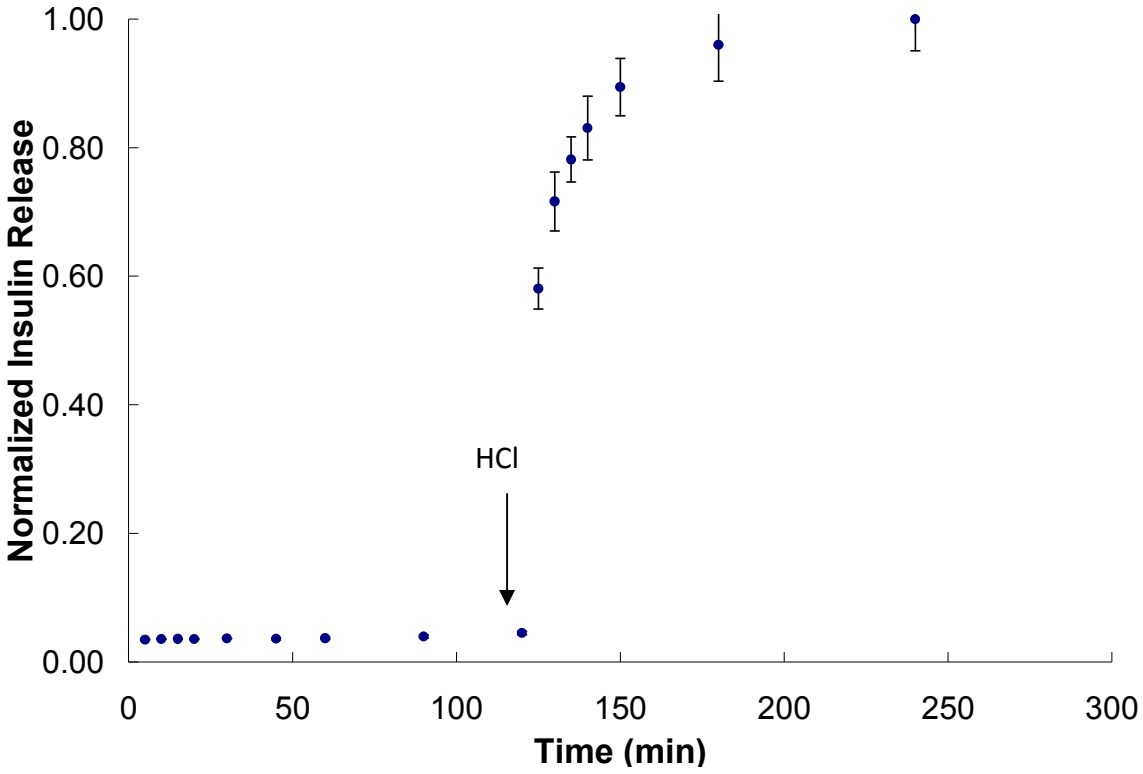

Figure 7.6. Insulin Release in Response to pH Change

Insulin release from microparticles in response to a step change in pH. At time 120 min, 1N HCl was added to the solution to decrease the pH, and increase the amount of hydrogel swelling. This swelling in turn increased the amount of insulin released drastically over the course of about one hour. (n = 3 ± SD)

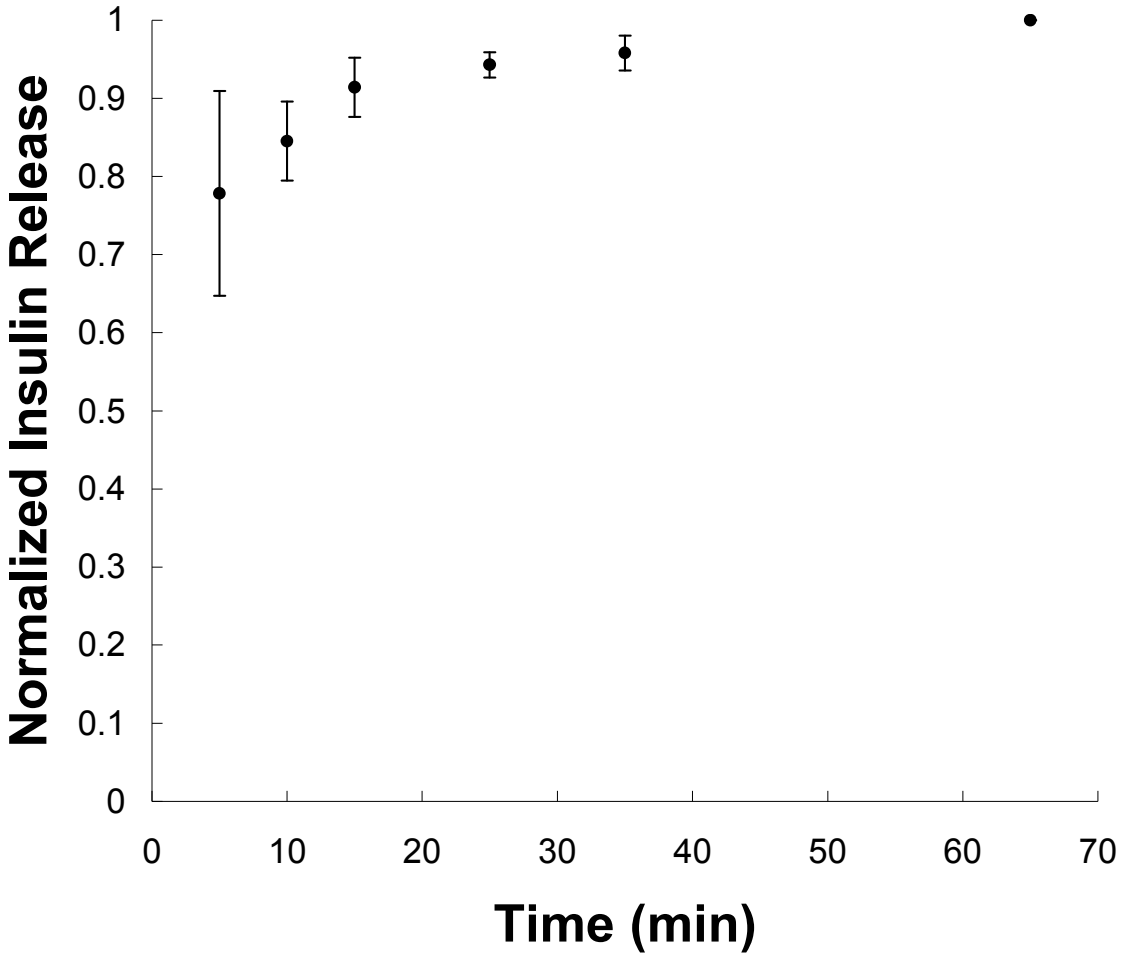

Figure 7.7. Insulin Release from Nanogels at Physiological pH

Release profile of insulin from loaded nanoparticles which were suspended in buffered media at pH 7.4. While microparticles were able to retain the loaded insulin at this pH, the nanogels were not. (n = 3 ± SD)

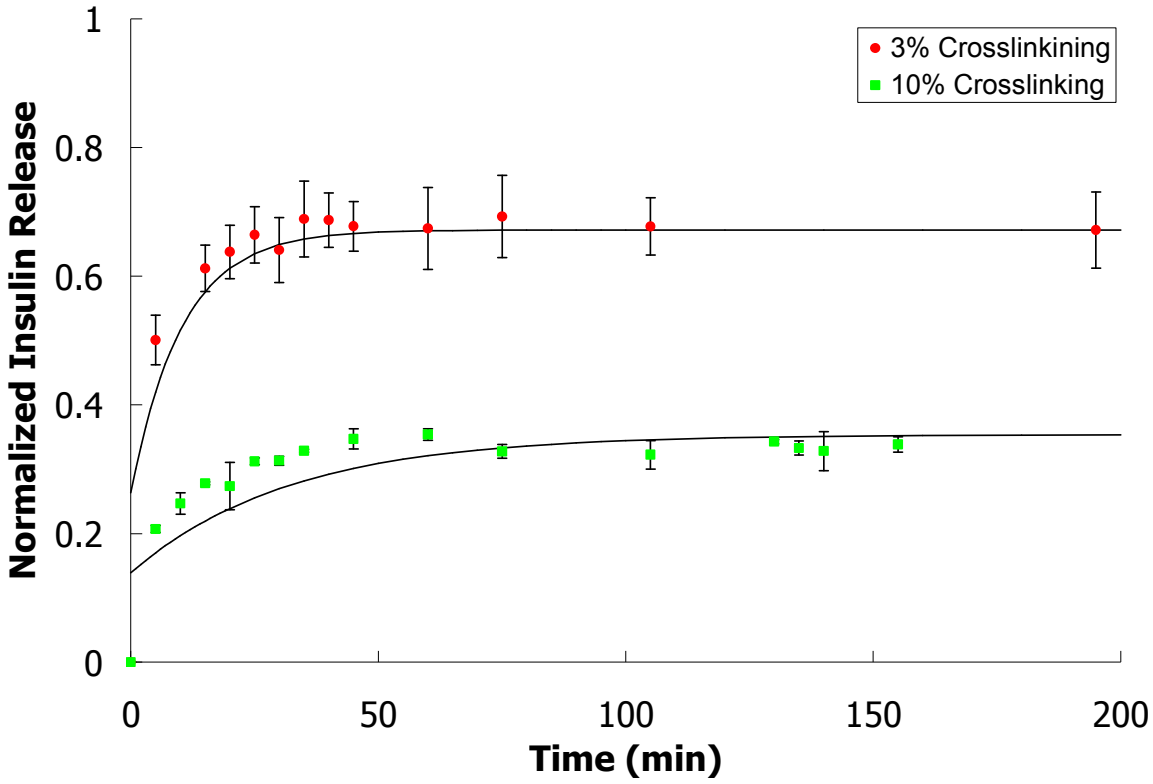

Figure 7.8. Insulin Release in Response to Glucose Stimulus

The effect of crosslinking ratio on amount of insulin released in response to a glucose stimulus. At time 0, a glucose bolus was delivered to the particle suspension and the amount of insulin released was observed. Higher crosslinking ratios yielded in less fractional insulin release (amount released compared to amount loaded) thus allowing the possibility of multiple pulses of insulin release. (n = 3 ± SD)

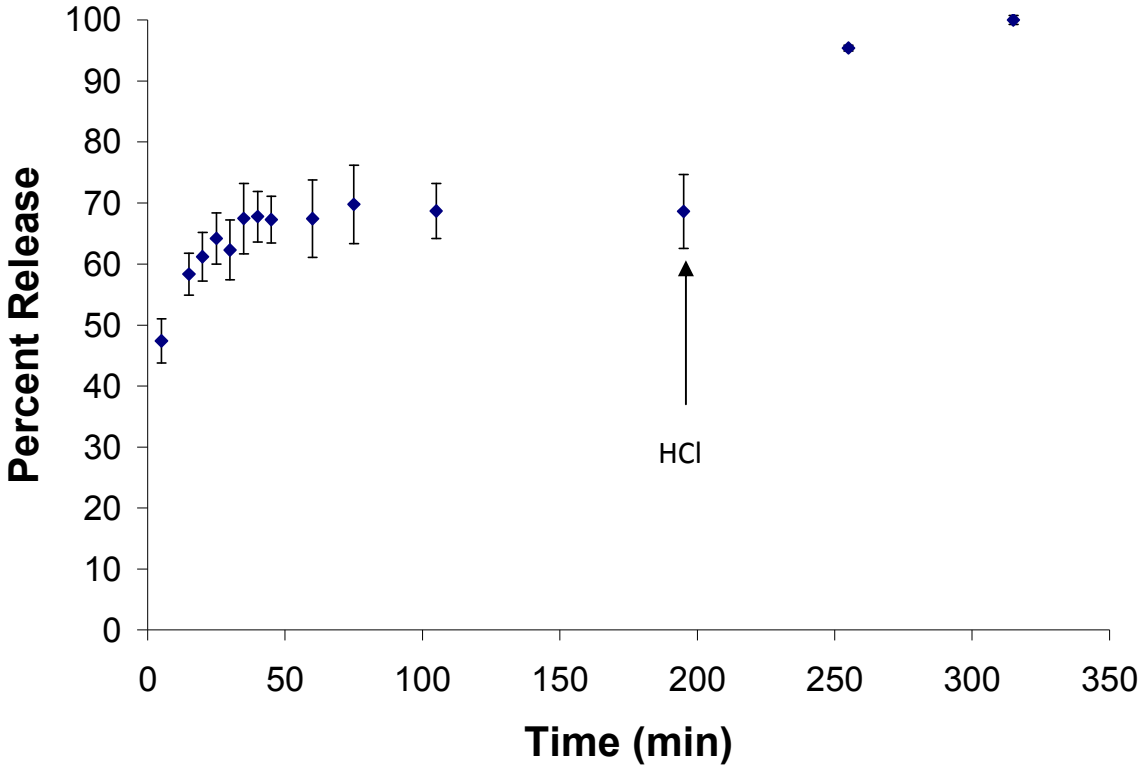

Figure 7.9. Insulin Release in Response to Glucose and pH Change

To determine the total amount of insulin that is able to be released in Figure 7.8, 1 N HCl was added after the insulin release caused by a glucose bolus. This change in pH caused the pH to drop below the pI of insulin, forming ionic repulsion between the positively charged insulin and the positively charged hydrogel. (n = 3 ± SD)

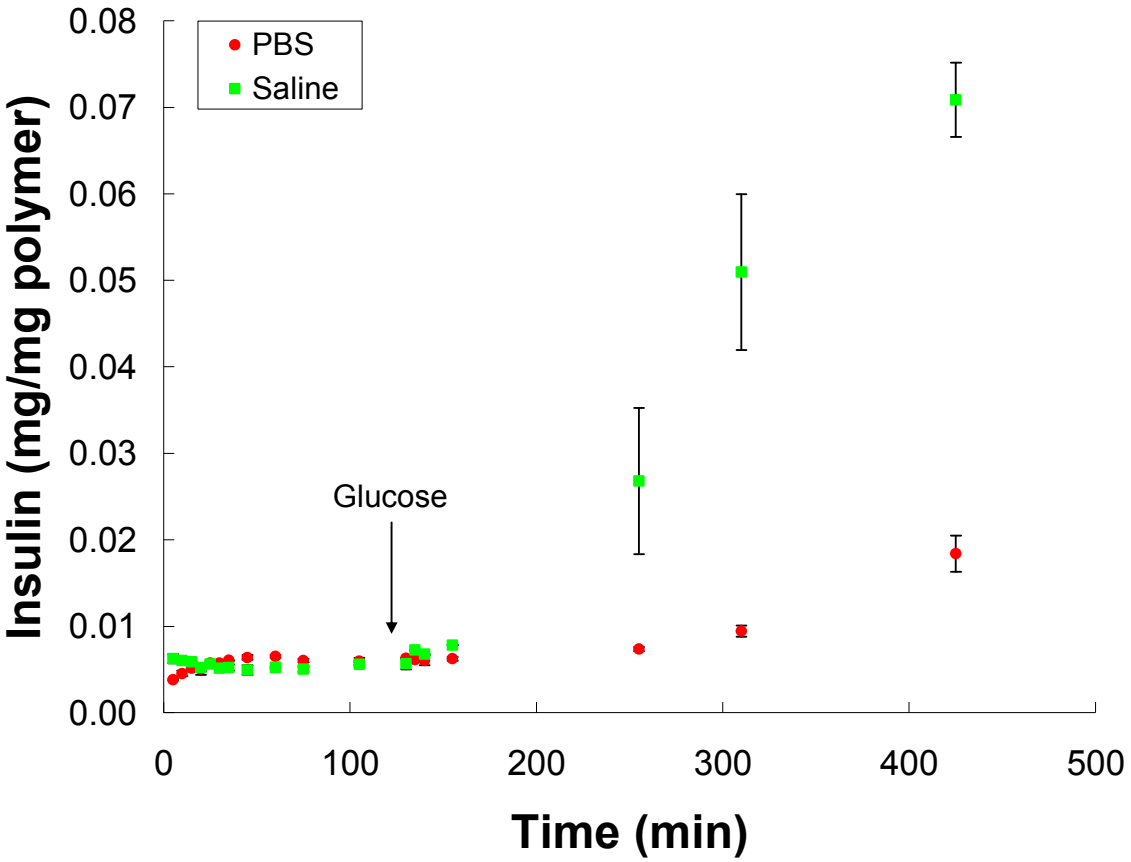

Figure 7.10. Insulin Release in Response to Glucose, Solvent

Release of insulin from 150 µm crushed microparticles. At a time of 125 min, 300 mg/dL glucose was added to each sample. Release of insulin in unbuffered saline (ionic strength I = 0.15 M) was much higher than in buffered PBS (I = 0.15 M) due to the buffering capacity of PBS. (n = 3 ± SD)

7.6 REFERENCES

1. Firestone, B.A. and R.A. Siegel, *Dynamic Ph-Dependent Swelling Properties of a Hydrophobic Poly-Electrolyte Gel.* Polym Commun, 1988. **29**(7): p. 204-208.

2. Siegel, R.A., M. Falamarzian, B.A. Firestone and B.C. Moxley, *Ph-Controlled Release from Hydrophobic Poly-Electrolyte Copolymer Hydrogels.* J Control Release, 1988. **8**(2): p. 179-182.

3. Ishihara, K., M. Kobayashi and I. Shionohara, *Control of Insulin Permeation through a Polymer Membrane with Responsive Function for Glucose.* Makromol Chem-Rapid, 1983. **4**(5): p. 327-331.

4. Ishihara, K., M. Kobayashi, N. Ishimaru and I. Shinohara, *Glucose-Induced Permeation Control of Insulin through a Complex Membrane Consisting of Immobilized Glucose-Oxidase and a Poly(Amine).* Polym J, 1984. **16**(8): p. 625-631.

5. Schwarte, L.M. and N.A. Peppas, *Novel poly(ethylene glycol)-grafted, cationic hydrogels: preparation, characterization and diffusive properties.* Polymer, 1998. **39**(24): p. 6057-6066.

6. Hariharan, D. and N.A. Peppas, *Characterization, dynamic swelling behaviour and solute transport in cationic networks with applications to the development of swelling-controlled release systems.* Polymer, 1996. **37**(1): p. 149-161.

7. Lepore, M., S. Pampanelli, C. Fanelli, F. Porcellati, L. Bartocci, A. Di Vincenzo, C. Cordoni, E. Costa, P. Brunetti and G.B. Bolli, *Pharmacokinetics and pharmacodynamics of subcutaneous injection of long-acting human insulin*

analog glargine, NPH insulin, and ultralente human insulin and continuous subcutaneous infusion of insulin lispro. Diabetes, 2000. **49**(12): p. 2142-2148.

8. Ahmad, B., *Pharmacology of insulin.* British Journal of Diabetes & Vascular Disease, 2004. **4**(10): p. 10-14.

9. Nielsen, L., R. Khurana, A. Coats, S. Frokjaer, J. Brange, S. Vyas, V.N. Uversky and A.L. Fink, *Effect of environmental factors on the kinetics of insulin fibril formation: Elucidation of the molecular mechanism.* Biochemistry-Us, 2001. **40**(20): p. 6036-6046.

10. Chang, X.Q., A.M.M. Jorgensen, P. Bardrum and J.J. Led, *Solution structures of the R-6 human insulin hexamer.* Biochemistry-Us, 1997. **36**(31): p. 9409-9422.

11. Oliva, A., J. Fariña and M. Llabrés, *Development of two high-performance liquid chromatographic methods for the analysis and characterization of insulin and its degradation products in pharmaceutical preparations.* Journal of Chromatography B: Biomedical Sciences and Applications, 2000. **749**(1): p. 25-34.

12. Siegel, R.A., I. Johannes, C.A. Hunt and B.A. Firestone, *Buffer Effects on Swelling Kinetics in Polybasic Gels.* Pharmaceut Res, 1992. **9**(1): p. 76-81.

13. Cooney, D.O., *Biomedical engineering principles : an introduction to fluid, heat, and mass transport processes*. Biomedical engineering and instrumentation series. 1976, New York: M. Dekker. xvi, 458 p.

14. Farmer, T.G., T.F. Edgar and N.A. Peppas, *In Vivo Simulations of the Intravenous Dynamics of Submicrometer Particles of pH-Responsive Cationic Hydrogels in Diabetic Patients.* Ind Eng Chem Res, 2008. **47**(24): p. 10053-10063.

CHAPTER 8

Preparation of Custom Monomers and Crosslinking Agents

8.1 INTRODUCTION

8.1.1 Alternate Cationic Monomers

Since PDEAEM has a pK_a very close to physiological pH, it may not be in its fully collapsed state when in a physiological environment. Therefore, it may be beneficial to find polymers with even lower values of pK_a and so other cationic monomers were also considered for intelligent insulin delivery devices. Using small molecule analogs as a basis, one such monomer of interest was 2-(diethylamino)ethyl methacrylamide. 2-(diethylamino)ethanol has a slightly higher pK_a value than the corresponding amine, 2-(diethylamino)ethylamine, and acrylates tend to have a slightly higher pK_a value than methacrylates [1-3]. The methacrylamide moiety also has the potential for hydrogen bonding with the PEG grafts in a hydrogel, thus allowing an even more collapsed state (Figure 8.1) similar to copolymers of methacrylic acid and PEG. This information was used to synthesize a new tertiary amine containing methacrylamide based monomer for possible use as an intelligent drug delivery hydrogel system.

8.2.1 Biodegradable Crosslinking Agents

To render these systems biodegradable, degradable crosslinking agents are necessary. Often, methacrylate-based hydrogels are turned into degradable polymers by using biodegradable acrylated poly(lactide-co-glycolide) (PLGA) crosslinks. However,

there are several problems with using PLGA based crosslinks in the described system. PLGA polymers exhibit acid-catalyzed degradation rates. However, the PDEAEM system described in previous chapters uses glucose oxidase to detect glucose by producing gluconic acid. This local drop in pH causes hydrogel swelling, which would also increase the rate of degradation of PLGA-based crosslinks. The complexity of determining the appropriate amount of PLGA crosslinks for a desired degradation profile in such a system is quite large.

A second problem with PLGA-based crosslinks is that they degrade into lactic acid and glycolic acid. While these byproducts have been shown to be safe and for the most part cytocompatible, their interaction with the proposed PDEAEM systems may be adverse. These degradation products may cause swelling of the system even without the presence of a high glucose concentration, since PDEAEM responds to changes in pH. This problem would potentially lead to premature or sustained insulin release, which is not desired in a type I diabetes insulin delivery device. Thus, a crosslinking agent that does not exhibit acid catalyzed degradation is ideal.

One promising crosslinking agent is based on a labile carbonate bond. These crosslinking agents show no increased degradation rates in acidic media compared to neutral media [4, 5]. Also, the degradation byproducts are carbon dioxide and a hydroxyl-terminated polymer. The human body is already very capable in handling small shifts in the carbon dioxide equilibrium. As shown in Figure 8.3b, the synthesis of the desired carbonate-containing crosslinking agent closely follows the synthetic steps of Bruining, *et al.* [5] (Figure 8.3a). Bruining, *et al.*, reported significant cytotoxicity in PDMAEM polymers that used these degradable crosslinks. In this research, the triethylene glycol spacer was omitted, since small molecular weight PEGs have been known to be toxic [6, 7]. Degradation of the triethylene glycol containing hydrogels occurred rapidly, within about 4 days; adjusting the hydrophobicity of such a crosslink

was hypothesized to also alter the degradation rate since the mechanism of degradation is the hydrolysis of the carbonate bond.

8.2 MATERIALS AND METHODS

8.2.1 Synthesis of 2-(Diethylamino)ethyl acrylamide

The synthetic route of 2-(diethylamino)ethyl acrylamide can be seen in Figure 8.2. All glassware was dried overnight in an oven at 120 °C, allowed to cool in a dessicator, and then subjected to three vacuum/nitrogen purge cycles before use. 2-(diethylamino)ethylamine (16.54 g, DEAEA, Sigma-Aldrich) was dissolved in 75 mL dry DCM and chilled in an ice bath under nitrogen. Acryloyl chloride (13.9 mL, Alfa Aesar) was added dropwise to prevent the reaction from progressing too quickly and the reaction mixture from becoming too hot.

The reaction was allowed to proceed for a few hours, after which it was washed three times with 1 N NaOH, once with brine, and then dried over $MgSO_4$. The washed and dry crude product was filtered and then concentrated and stored in the refrigerator until use. ^1H NMR was used to confirm the molecular structure. Similar monomers could be synthesized in a similar fashion. Analogs such as 2-(diethylamino)ethyl methacrylamide were considered for synthesis by replacing the acryloyl chloride with methacryloyl chloride.

The pK_a of monomers was measured by titration. Briefly, 0.5 g monomer was dissolved in 10 mL ethanol and 100 mL ddH_2O. The pH was continuously monitored as increments of between 0.25 and 0.5 mL 0.1 N hydrochloric acid were added.

Methacryloyl chloride was synthesized to be used in the synthesis of 2-(diethylamino)ethyl methacrylamide. Methacrylic acid (Fisher Scientific) was dissolved in dry DCM and chilled in an ice bath under nitrogen. An equimolar amount of

thionyl chloride (Sigma-Aldrich) was added dropwise to prevent the reaction from progressing too quickly and the reaction mixture from becoming too hot. Triethyl amine (TEA, Sigma-Aldrich) was used in equal molar amounts to complex the liberated hydrochloric acid during the reaction, which then precipitated out as the TEA-HCl salt. The salt was filtered and the solvent was removed under reduced pressure to afford the acid chloride of methacrylic acid.

8.2.2 Synthesis of Poly[2-(Diethylamino)ethyl acrylamide]

Hydrogels of 2-(diethylamino)ethyl acrylamide and poly(ethylene glycol)-400 monomethyl ether monomethacrylate, henceforth P(DEAEAAm-g-EG400) were synthesized using a free radical thermal polymerization in solution, where 400 refers to the average molecular weight of the ethylene glycol repeat units. To synthesize these systems, a solution of DEAEAAm (synthesized above), PEG400MMA (Polysciences, Warrington, PA) and the crosslinking agent tetraethylene glycol dimethacrylate (TEGDMA) (Acros Organics, Morris Plains, NJ) was made. All other reagents were used as received. Phosphate buffered saline (PBS) (Fisher Scientific) was used as the solvent to prevent autoacceleration and was reconstituted from a 10X concentrate with deionized water (Milli-Q Plus system, Millipore, Bedford, MA), in a ratio of about 1:1 by weight of the monomers. Ammonium persulfate (APS) (Fisher Scientific) and sodium metabisulfite (NaMBS) (Fisher Scientific) were used to initiate the polymerization in a ratio of 4:1 by mole, and the chemicals were pre-mixed before polymerization in distilled deionized water (ddH_2O) at a 1 wt% concentration of APS. The initiator solution was used in an amount of 0.5% by moles of monomers.

Two different systems were synthesized with varying compositions. The ratio of DEAEAAm to PEG grafts was either 25:1 or no PEG grafts. Crosslinking ratios were 3 mol% for both samples Once all compounds had been well mixed in a test tube, the

solution was transported to a glove box where it was purged with nitrogen for 20 min to remove dissolved oxygen, a free-radical scavenger. The initiator solution was then added, mixed via aspiration, and then pipette between two glass slides, separated by a 760 µm Teflon spacer. The glass slide assembly was then placed in an acrylic air-tight polymerization box, sealed, and transported to an incubator at 37°C for 24 h. This procedure resulted in polymer films. The films were then washed in a jar of PBS for one week to remove unreacted monomers and small molecular weight polymers.

8.2.3 Synthesis of Biodegradable Crosslinking Agents

Paraformaldehyde (9.384 g, Sigma-Aldrich) was dissolved in hydroxyethyl methacrylate (40.0 g. HEMA, Sigma-Aldrich) and cooled in an ice bath. Thionyl chloride (15.2 mL, Sigma-Aldrich) was added dropwise to the solution, and the reaction was allowed to proceed for about 15 minutes. The reaction mixture was then quenched with ice water and extracted twice with methylene chloride (DCM, Fisher Scientific). The organic layers were combined, dried over $MgSO_4$ (Fisher Scientific), and filtered. The washed and dried reaction mixture was concentrated under reduced pressure. The crude product, 2-chloromethoxy ethylmethacrylate, was purified by vacuum distillation to afford pure product, which was then characterized by ^1H NMR.

The second step of this synthesis proceeded as follows, and was varied to alter the spacer that was incorporated in the final structure. Initial crosslinks did not contain PEG spacers.

Silver carbonate (7.77 g, Alfa Aesar, Ward Hill, MA) was suspended in a solution of HEMA in 10 mL dry dimethylformamide (DMF, Alfa Aesar) and cooled to -15°C under nitrogen gas. Crude 2-chloromethoxy ethylmethacrylate (7 mL, with unreacted HEMA) was added to the flask dropwise, with the exclusion of light, and allowed to react for an hour. Cold acetone was added to quench the reaction, and the mixture was allowed to

warm to room temperature. The crude product was filtered through a short packed silica column using ethyl acetate as the mobile phase. After removing the solvent under reduced pressure, the crude product was dissolved in toluene and washed with brine. The organic layer was dried over $MgSO_4$, filtered, and concentrated again under reduced pressure to afford degradable crosslinker 2 (DC2, Figure 8.3).

To incorporate PEG spacers between the two HEMA analogs, the above procedure was slightly modified. Silver carbonate (7.77 g) was suspended in a solution of 0.564 g PEG (i.e., PEG 200) in 10 mL dry DMF and cooled to -15°C under nitrogen gas. Pure (distilled) 2-chloromethoxy ethylmethacrylate (3.3 mL) was added to the flask dropwise, with the exclusion of light, and allowed to react for an hour. Cold acetone was added to quench the reaction, and the mixture was allowed to warm to room temperature. The crude product was filtered through a short packed silica column using ethyl acetate as the mobile phase. After removing the solvent under reduced pressure, the crude product was dissolved in toluene and washed with brine. The organic layer was dried over $MgSO_4$, filtered, and concentrated again under reduced pressure to afford degradable crosslinker 1 (DC1, Figure 8.3).

8.2.4 Molecular Characterization via NMR

Nuclear magnetic resonance (NMR) spectra were obtained on a Varian Unity+ 300 MHz spectrometer. Both ^{1}H and ^{13}C spectra were obtained for most small molecular weight compounds. Water suppression was used via the PRESAT macro with a saturation power of 2 and a saturation delay of 5 s on any samples with significant water signals. Small molecule analysis was obtained by using a suitable deuterated solvent, such as chloroform (CDCl3), dimethylsulfoxide (d6-DMSO), or d¬6-acetone, all obtained from Cambridge Isotope Laboratories. Unless otherwise stated, for all ^{1}H NMR spectra, the sample was spinning at 20 Hz, the number of transients was 8, and line

broadening was 0.1. Unless otherwise stated, for all ^{13}C NMR spectra, the sample was spinning at 20 Hz and line broadening was 0.1. The number of transients was typically greater than 128, but was ultimately dependent on the signal-to-noise ratio.

8.3 RESULTS AND DISCUSSION

8.3.1 Synthesis of 2-(Diethylamino)ethyl acrylamide

Successful synthesis of the monomer 2-(diethylamino)ethyl acrylamide, was confirmed via ^{1}H and ^{13}C NMR spectroscopy. Structural analyses by NMR can be seen in Figure 8.4. ^{1}H NMR peaks in $CDCl_3$ had the following assignment: δ 0.98 (6H, s, CH_3), 2.52 (6H, m, CH_2), 3.36 (2H, q, CH_2), 5.61 (1H, dd, NH), 6.10 (1H, m, vinyl H), 6.26 (2H, dd, vinyl H). The pK_a of the DEAEAAm monomer was estimated to be about 0.1 pH units higher than DEAEM monomer (8.4 versus 8.5), as measured by titration with sodium hydroxide. Cationic polymers tend to have lower pK_a values than their corresponding monomers, in part due to steric concerns and ionic repulsion [8, 9].

8.3.2 Synthesis of Poly[2-(Diethylamino)ethyl acrylamide]

Ultimately, the physical properties of poly[2-(diethylamino)ethyl acrylamide)] (PDEAEAAm) prevented it from further use as a potential intelligent insulin delivery device. The theoretical hydrogen bonding in Figure 8.1 did not appear to occur as desired. Instead, the acrylamide functional group increased the overall hydrophilicity of both the monomer and the polymer (compared to PDEAEM). Thus, the polymer swelled in the presence of water despite the pH of the surrounding medium. Controlled swelling and deswelling was difficult to achieve, even when the pH of the medium was substantially above the pK_a of the monomer. Structural integrity was also difficult to

maintain due to the extent of swelling. Thus, PDEAEAAm was not used in insulin release experiments and it was not fully characterized.

8.3.3 Synthesis of Biodegradable Crosslinking Agents

Successful synthesis of the intermediate compound, 2-chloromethoxy ethylmethacrylate, was confirmed via ^{1}H and ^{13}C NMR spectroscopy. Structural analyses by NMR can be seen in Figure 8.5 and Figure 8.6. ^{1}H NMR peaks in $CDCl_3$ had the following assignment: δ 1.95 (3H, singlet, CH_3), 3.92 (2H, triplet, $OCH_2C\underline{H}_2OCH_2Cl$), 4.34 (2H, triplet, $OC\underline{H}_2CH_2OCH_2Cl$), 5.48 (2H, singlet, $OCH_2CH_2OC\underline{H}_2Cl$), 5.60 (1H, multiplet, vinyl H), 6.15 (1H, multiplet, vinyl H). ^{13}C NMR peaks in $CDCl_3$ had the following assignment: δ 17.7, 62.2, 67.5, 82.1, 125.4, 135.4, 166.5.

Vacuum distillation yielded a clear liquid product and occurred at either a temperature of 55 °C and pressure of 455 µbar, or a temperature of 34 °C and pressure of about 140 µbar. The density was measured to be 1.15 g/mL. Long-term stability of this compound was determined by comparing ^{1}H NMR spectra of the same sample, taken several months apart. Storage away from light at 4 °C provided at least 3 months of stability. A yield of about 50% conversion was obtained, and for some syntheses (which used HEMA in the second step), the unreacted HEMA was left in the product since the second step required HEMA in excess.

Successful synthesis of the degradable crosslinking agents DC1 was confirmed via ^{1}H and ^{13}C NMR spectroscopy. Structure analyses by NMR can be seen in Figure 8.7 and Figure 8.8. ^{1}H NMR peaks in $CDCl_3$ had the following assignment: δ 1.93 (6H, singlet, CH_3), 3.65 (4H, singlet, $CO_3CH_2CH_2OC\underline{H}_2C\underline{H}_2OCH_2CH_2OCO_2$), 3.72 (4H, triplet, $CO_3CH_2C\underline{H}_2O$), 3.92 (4H, triplet, $OCH_2C\underline{H}_2OCH_2CO_3$), 4.29 (8H, multiplet, $CO_2C\underline{H}_2CH_2$-OCH_2CO_3 and $CO_3C\underline{H}_2CH_2O$), 5.31 (4H, singlet, $OCH_2CH_2OC\underline{H}_2O$), 5.57 (1H, multiplet, vinyl H), 6.11 (1H, multiplet, vinyl H). ^{13}C NMR peaks in $CDCl_3$ had the following

assignment: δ 17.7, 62.8, 66.6, 67.8, 68.34, 70.1, 91.7, 125.4, 135.4, 154.0, 166.6. Long-term stability of this compound was determined by comparing ^{13}C NMR spectra of the same sample, taken one month apart (Figure 8.8 and Figure 8.9). Storage away from light at 4 °C did not provide stability for one month, and this compound partially degraded into its precursory compounds.

Successful synthesis of the degradable crosslinking agents DC2 was confirmed via ^{1}H NMR spectroscopy, as seen in Figure 8.10. ^{1}H NMR peaks in $CDCl_3$ had the following assignment: δ 1.21 (6H, multiplet, CH_3), 1.90 (4H, singlet), 2.00 (4H, triplet), 3.77 (4H, multiplet), 4.08 (4H, quartet), 4.28 (2H, multiplet), 4.41 (2H, multiplet), 5.31 (2H, multiplet), 5.55 (2H, multiplet, vinyl H), 6.09 (2H, multiplet, vinyl H).

8.4 CONCLUSIONS

There are several conclusions that can be made from the research presented above. The monomer 2-(diethylamino)ethyl acrylamide was successfully synthesized and purified. Polymers were successfully synthesized using this monomer, and the polymers were partially characterized. A novel family of degradable crosslinking agents was presented, and the synthetic steps necessary were elucidated. The intermediate compound necessary for these syntheses was successfully isolated and characterized. Some of these crosslinking agents were successfully synthesized and purified as well.

Unfortunately, the hydrophilicity of pure crosslinked P(DEAEAAm) was too great to form polymers which would collapse enough for the controlled drug delivery devices that this research focused on. The extent of hydrogen bonding between PEG and DEAEAAm was not elucidated. Further studies could be performed, however, on this monomer and these hydrogels, to determine if there are other potential uses.

The degradable crosslinking agents synthesized showed promise as short-term degradable crosslinkers. Due to the hydrolysis of the carbonate bond, each crosslinking

agent could potentially release up to two carbon dioxide molecules. While in an aqueous environment such as bodily fluids, the carbon dioxide would dissolve as carbonate. This carbonate anion could potentially affect the pH of the media, but at the low concentrations in a hydrogel, and the biological fluid's natural buffering capacity, this pH variation was expected to be negligible. Degradation of the pure crosslinking agents was apparent after less than a month of storage. More studies would be necessary to fully characterize the degradation of these crosslinking agents for usage in hydrogel drug delivery systems, such as the kinetics of degradation and the analysis of the cytotoxicity of degradation byproducts.

8.5 FIGURES

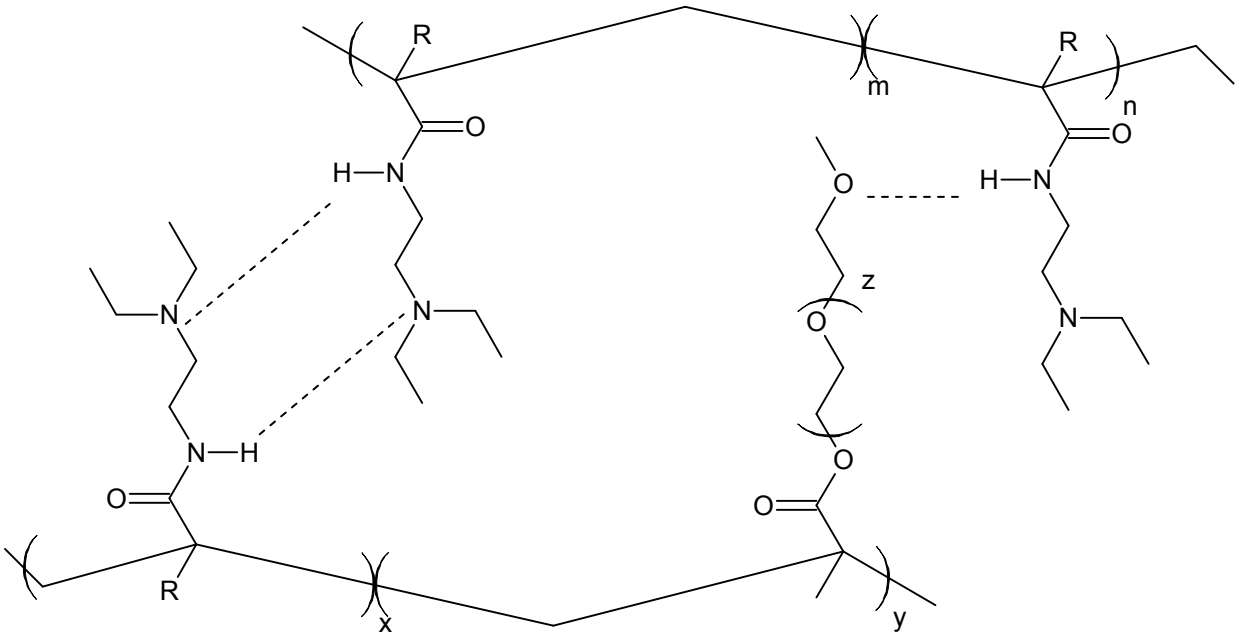

Figure 8.1. Theoretical Hydrogen Bonding in P(DEAEAAm-g-EG)

Theoretical hydrogen bonding between the amide hydrogen and either the tertiary amines or the ethereal oxygens.

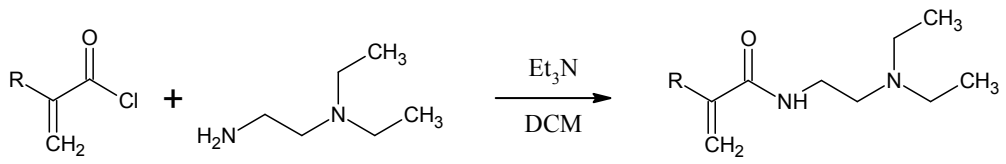

(a)

Figure 8.2. 2-(Diethylamino)ethyl (Meth)acrylamide Synthetic Route

Synthesis of 2-(diethylamino)ethyl (meth)acrylamide cationic monomer, where R=H for acrylamide and R=CH_3 for methacrylamide.

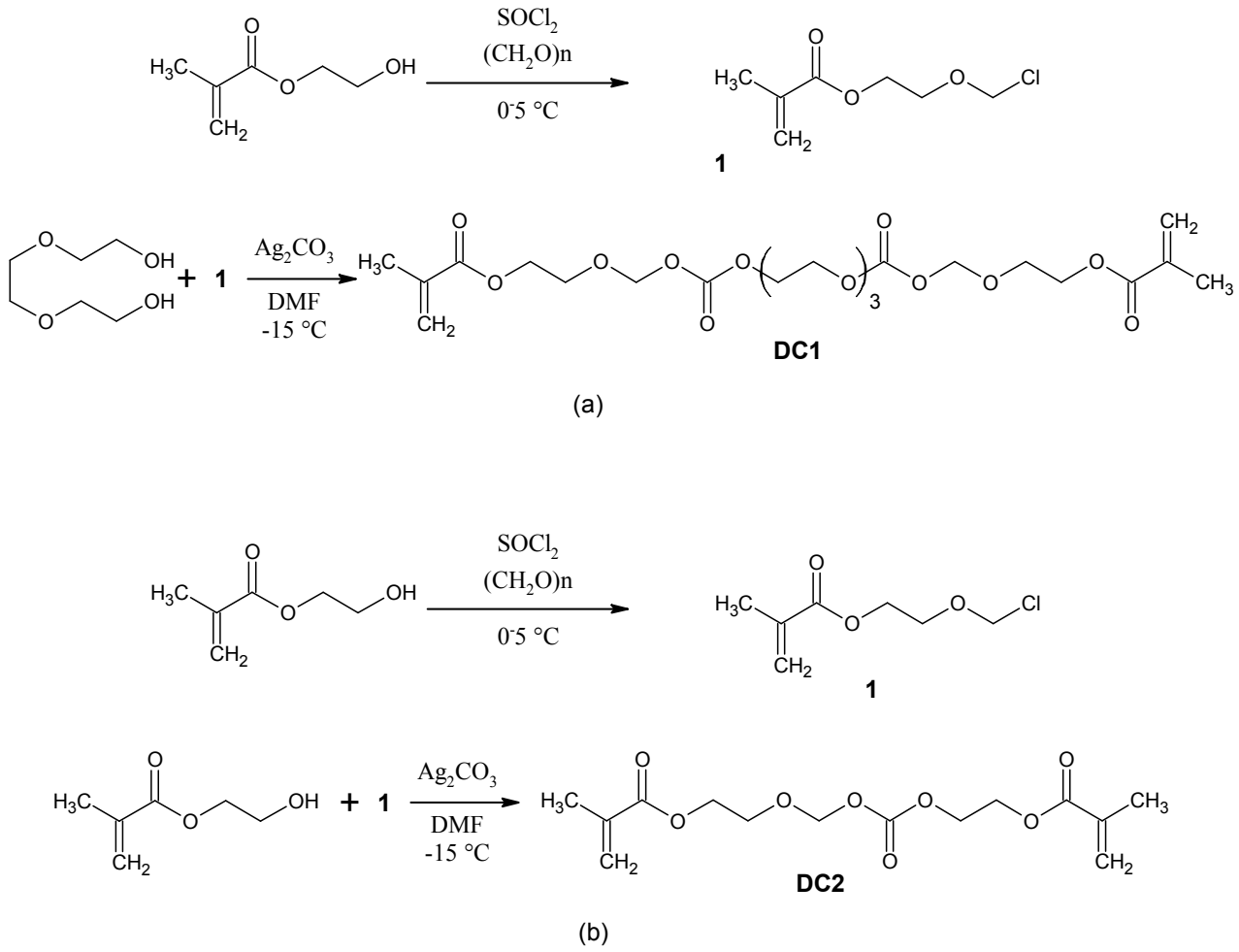

Figure 8.3. Biodegradable Crosslinking Agent Synthetic Routes

Synthesis of (a) Degradable carbonate dimethacrylate crosslinking agent, with triethylene glycol spacer, degradable crosslinking agent #1 (DC1) [5];
(b) Degradable carbonate dimethacrylate crosslinking agent, without triethylene glycol spacer, degradable crosslinking agent #2 (DC2).

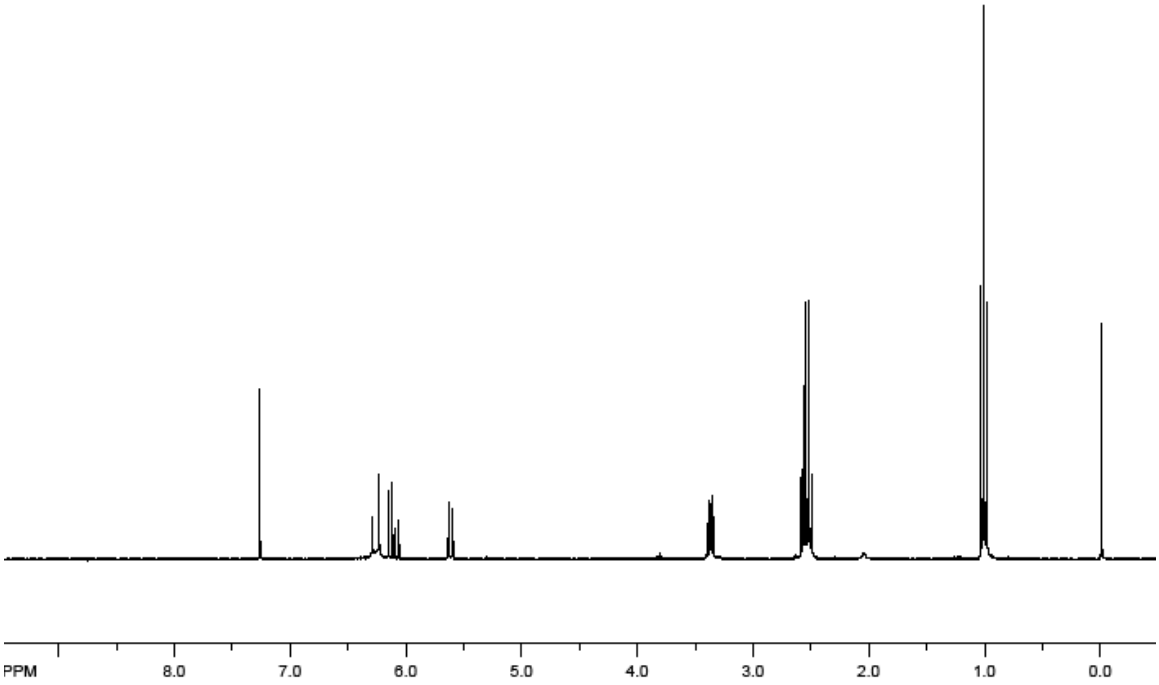

Figure 8.4. ^{1}H NMR Spectrum of 2-(Diethylamino)ethyl Acrylamide

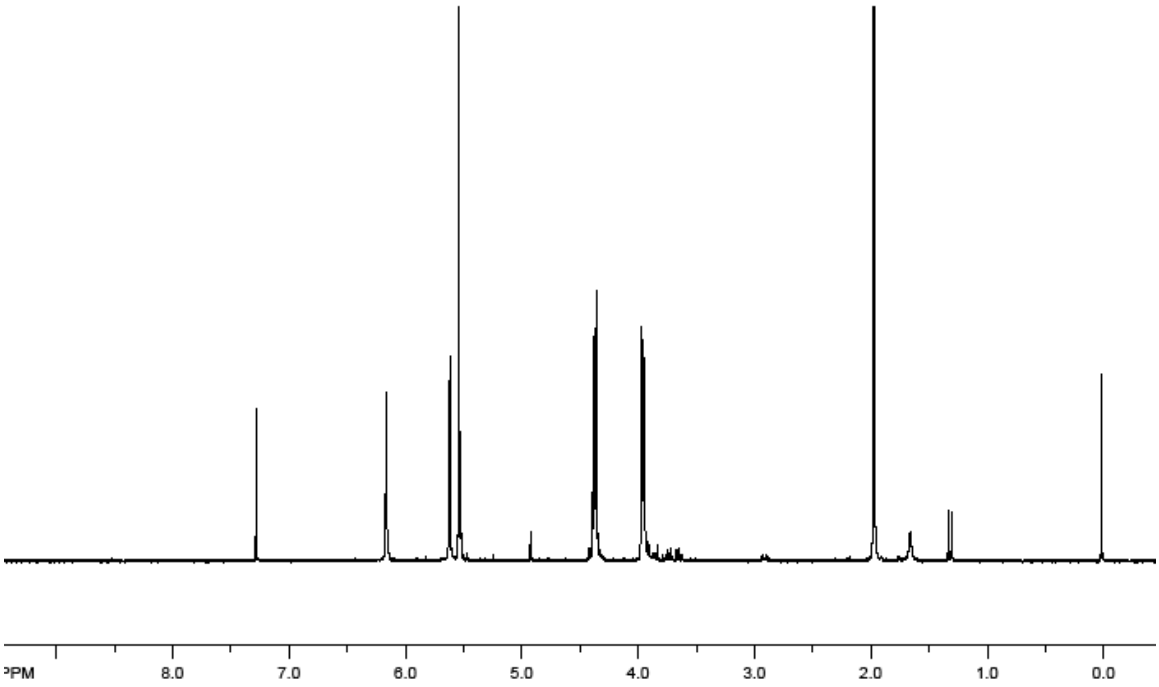

Figure 8.5. ^{1}H NMR Spectrum of 2-(Chloromethoxy)ethyl Methacrylate

^{1}H NMR of 2-(chloromethoxy)ethyl methacrylate, the precursor to the degradable crosslinking agents, in $CDCl_3$.

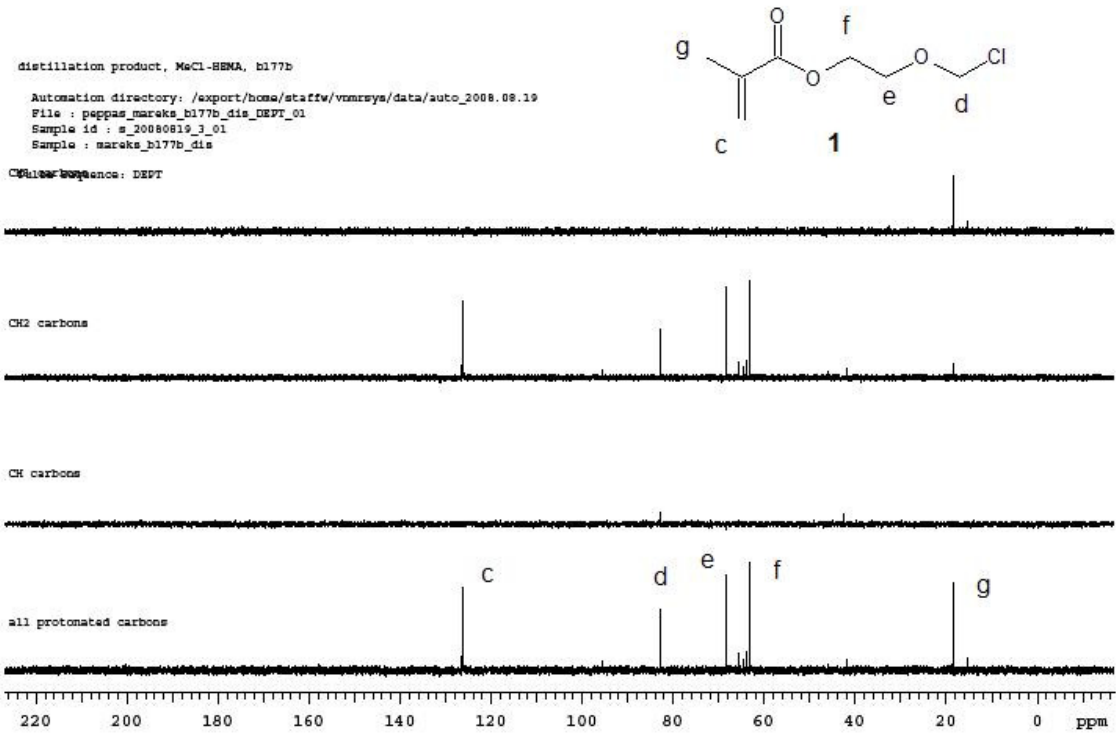

Figure 8.6. DEPT ^{13}C NMR of 2-(Chloromethoxy)ethyl Methacrylate

DEPT ^{13}C NMR of 2-(chloromethoxy)ethyl methacrylate, the precursor to the degradable crosslinking agents, in $CDCl_3$. Each carbon peak is labeled. The top spectrum only contains CH_3 carbons, the second one only displays CH_2 carbons, the third spectrum displays only CH carbons, and the final spectrum displays all carbons. The peaks between (e) and (f) correspond to the solvent.

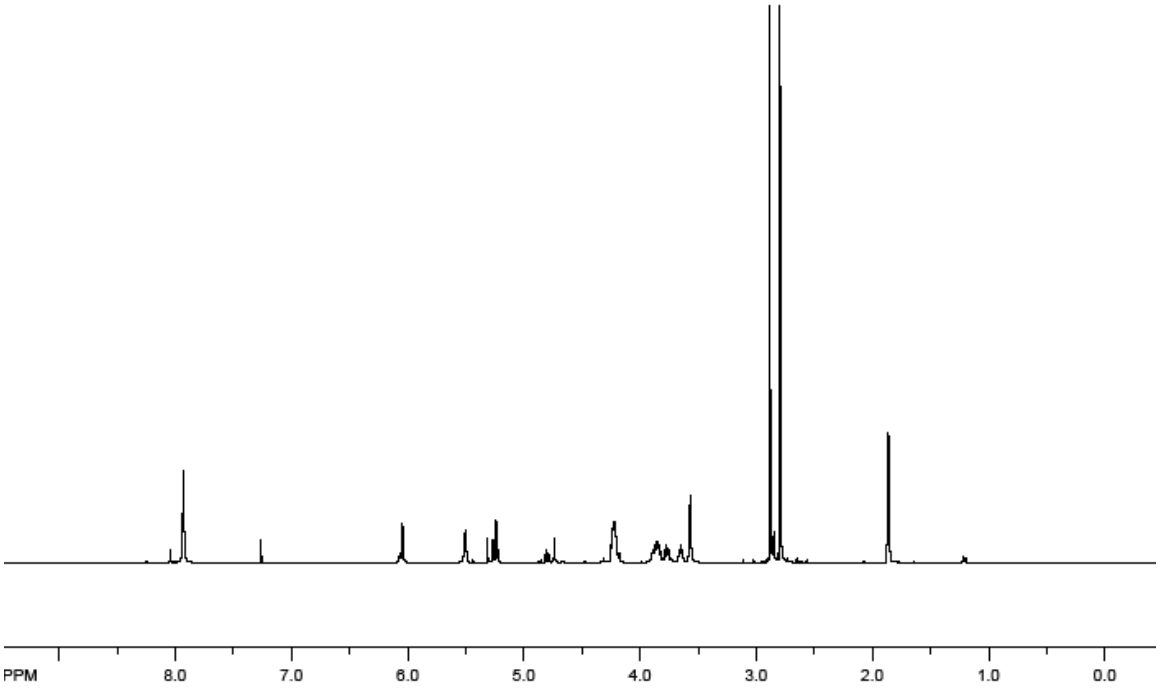

Figure 8.7. ^{1}H NMR Spectrum of Degradable Crosslinker 1

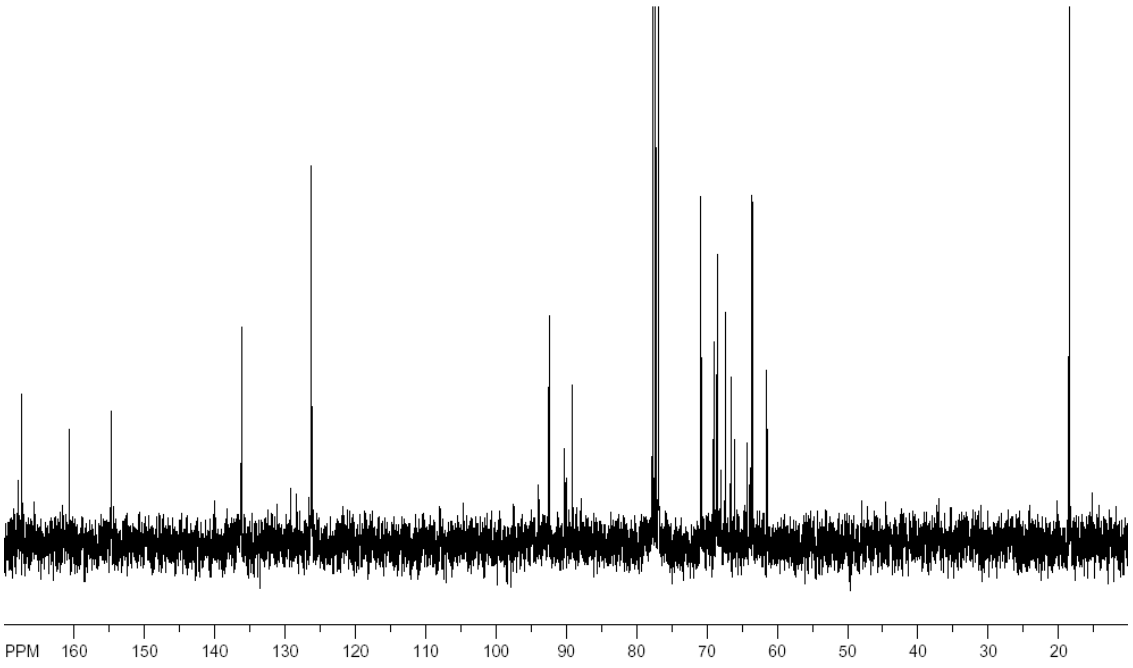

Figure 8.8. ^{13}C NMR of Freshly Synthesized Degradable Crosslinker 1

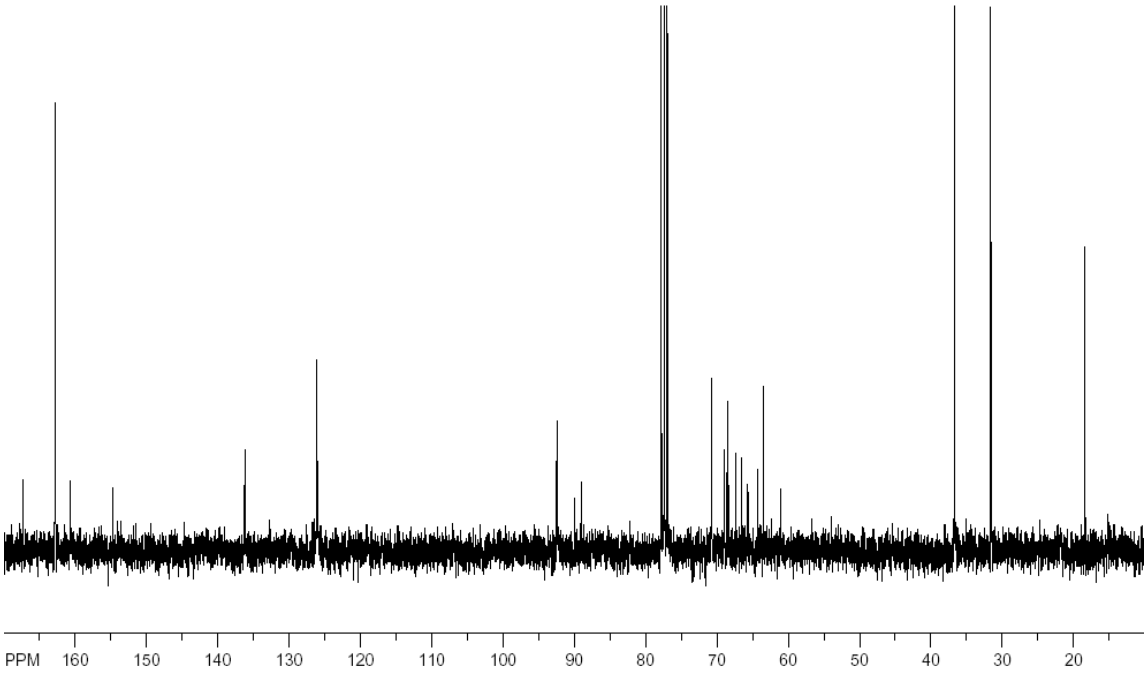

Figure 8.9. ^{13}C NMR of Partially Degraded Degradable Crosslinker 1

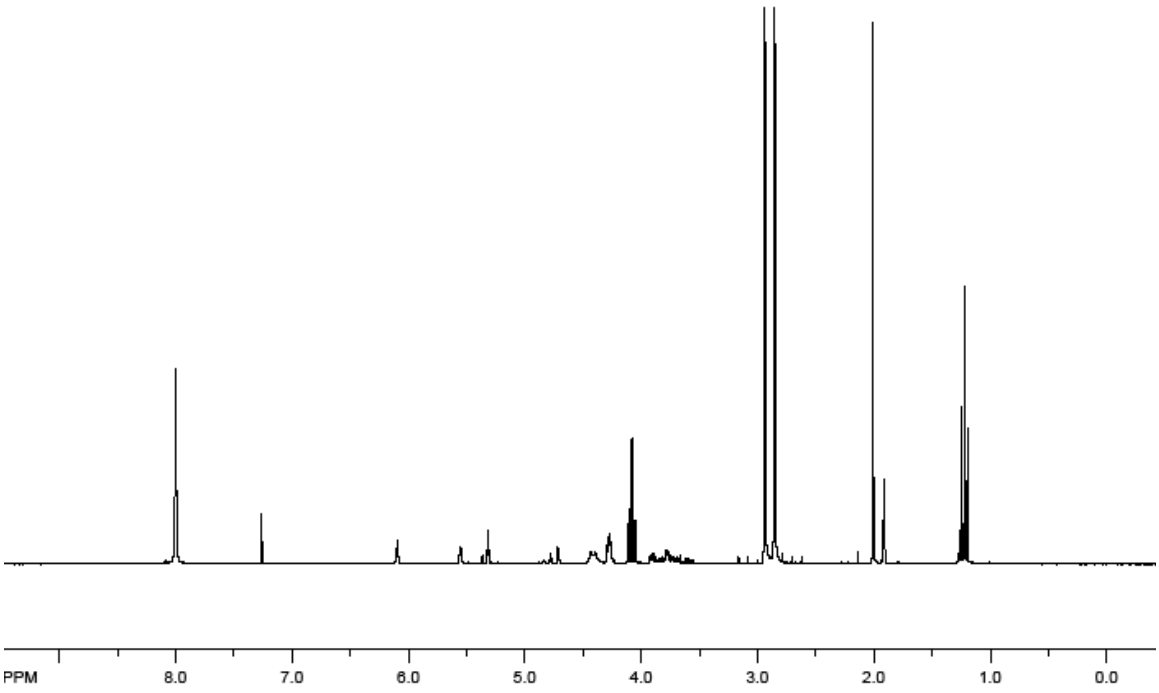

Figure 8.10. ^{1}H NMR Spectrum of Degradable Crosslinker 2

8.6 REFERENCES

1. Hariharan, D. and N.A. Peppas, *Characterization, dynamic swelling behaviour and solute transport in cationic networks with applications to the development of swelling-controlled release systems.* Polymer, 1996. **37**(1): p. 149-161.

2. Podual, K., *Glucose-sensitive cationic hydrogels for insulin release*. 1998, Purdue University, CHE, DEC, 1998. p. xviii, 263 p.

3. Butun, V., S.P. Armes and N.C. Billingham, *Synthesis and aqueous solution properties of near-monodisperse tertiary amine methacrylate homopolymers and diblock copolymers.* Polymer, 2001. **42**(14): p. 5993-6008.

4. Bruining, M.J., H.G.T. Blaauwgeers, R. Kuijer, E. Pels, R. Nuijts and L.H. Koole, *Biodegradable three-dimensional networks of poly(dimethylamino ethyl methacrylate). Synthesis, characterization and in vitro studies of structural degradation and cytotoxicity.* Biomaterials, 2000. **21**(6): p. 595-604.

5. Bruining, M.J., P.S. Edelbroek-Hoogendoorn, H.G.T. Blaauwgeers, C.M. Mooy, F.H. Hendrikse and L.H. Koole, *New biodegradable networks of poly(N-vinylpyrrolidinone) designed for controlled nonburst degradation in the vitreous body.* J Biomed Mater Res, 1999. **47**(2): p. 189-197.

6. Biondi, O., S. Motta and P. Mosesso, *Low molecular weight polyethylene glycol induces chromosome aberrations in Chinese hamster cells cultured in vitro.* Mutagenesis, 2002. **17**(3): p. 261-264.

7. Pang, S.N.J., *Final Report on the Safety Assessment of Polyethylene Glycols (Pegs) -6, -8, -32, -75, -150, -14m, -20m.* J Am Coll Toxicol, 1993. **12**(5): p. 429-457.

8. Hoogeveen, N.G., M.A.C. Stuart, G.J. Fleer, W. Frank and M. Arnold, *Novel water-soluble block copolymers of dimethylaminoethyl methacrylate and dihydroxypropyl methacrylate.* Macromol Chem Physic, 1996. **197**(8): p. 2553-2564.

9. Pradny, M. and S. Sevcik, *PRECURSORS OF HYDROPHILIC POLYMERS .3. THE POTENTIOMETRIC BEHAVIOR OF ISOTACTIC AND ATACTIC POLY(2-DIMEHTYLAMINOETHYL METHACRYLATE) IN WATER ETHANOL SOLUTIONS.* Makromol Chem, 1985. **186**(1): p. 111-121.

CHAPTER 9

Conclusions and Recommendations

9.1 Intelligent Insulin Delivery Device Design Considerations

The goals of this research were to develop novel hydrogels for the intelligent delivery of insulin. These hydrogels were then characterized in several ways, including determining the swelling as well as the insulin loading and release, as a function of both pH and glucose concentrations. Finally, these hydrogel systems were evaluated as potential intelligent insulin delivery devices, and guidance is provided for potential designs.

We were able to successfully synthesize pH responsive cationic hydrogels having various morphologies. Polymer slabs, microparticles, and nanoparticles were synthesized and characterized in several ways. These hydrogels were then made glucose responsive by the addition of glucose oxidase and catalase, which transduced a glucose signal into a pH signal. We were able to load insulin into these hydrogel systems with a fairly high efficiency and then determine their efficacy as intelligent controlled drug delivery devices. Thus, a glucose stimulus was successfully able to cause the release of an insulin bolus.

Microparticles were successfully synthesized by first synthesizing a polymer film. This film was wet sieved through sieves of varying meshes (i.e., 150 μm, 35 μm) to produce relatively uniform particle size distributions. Particles were successfully synthesized on the nanoscale using a novel inverse emulsion polymerization, with diameters as small as 120 nm in the collapsed state. This process also allowed the

incorporation of hydrophilic components (i.e., enzymes) on the interior of the particles and PEG grafts on the surface of the particles for increased biocompatibility.

The ideal insulin loading procedure for crushed microparticles was determined, which yielded a high insulin loading efficiency (over 90%) and a relatively high insulin weight fraction in the particles (over 10%). It was also determined that particles with a crosslinking ratio of 10% provided the highest insulin loading efficiency compared to particles with 3% and 15% crosslinking. Finally, particles with a crosslinking ratio of 10% only released about one-third of the total releasable insulin after a single glucose stimulus. Thus, microparticles with a crosslinking ratio of 10% were determined to have the optimal characteristics for insulin loading and release for a cyclic intelligent insulin delivery device, both as a function of pH and as a function of glucose concentrations.

The insulin release properties of these highly crosslinked microparticles had several desirable characteristics. The release of insulin was controlled by either pH or glucose concentration, and insulin release was minimal at physiological pH values. The total amount of insulin released from the particles was a function of the crosslinking ratio, which would allow the tuning of the particles to provide a specific number of doses of insulin (each pulse of glucose causing the release of one of these insulin "doses"). It was also possible to obtain physiologically relevant amounts of insulin release from these microparticle systems. A patient of 75 kg would only need between 30-60 mg of microparticles per day for postprandial insulin delivery.

Donnan equilibrium concerns with hydrogels as feedback controlled intelligent delivery devices were partially overcome by altering the hydrogel morphology. Work performed has indicated that the swelling rate is significantly faster than the collapsing rate for macroscopic hydrogels. Thus, collapsing the hydrogels rapidly to promptly cut off insulin release was difficult on macroscopically sized hydrogels. To overcome this challenge, smaller gel sizes were used. Microparticles and nanoparticles were synthesized, which offered superior swelling rates, equilibrating in minutes or less.

Thus, as delivery device sizes decrease, this deswelling rate complication was diminished.

However, there were some challenges encountered while trying to design a feedback-controlled intelligent insulin delivery device based on hydrogels. Loosely crosslinked hydrogels released up to 70% of the available insulin after the first stimulus. These hydrogels were able to respond more quickly due to their more loosely bound polymer chains, but were less able to be useful as repeated drug delivery devices. Nanoparticles, on the other hand, were almost impossible to control the release of insulin. Insulin diffused out whether the particle was swollen or collapsed, and the release profile was not what was desired for a type I diabetes treatment.

Donnan equilibrium also may play a part in preventing the gels from fully deswelling under cyclic conditions. This behavior may also be in part due to the buffering nature of the hydrogel itself. Therefore, when trying to collapse the hydrogels, significant amounts of H^+ ions had to be released from the gels, mostly via conjugate bases. This phenomenon substantially decreased the amount of released insulin, as shown by the difference in release rates and amounts for hydrogel microparticles suspended in saline compared to buffer. With *in vivo* studies, however, there would be a significantly higher solvent-to-particle ratio, and thus this effect should be minimized.

Finally, the release of insulin from the nanoparticles was problematic. These studies yielded unreliable data with large errors. The large surface area to volume ratio of these nanoparticles substantially increased the diffusional driving force by increasing the area for mass transfer flux. These results agree with modeling attempts of similar systems, which indicated that the submicron particle size would not properly work as an injectable controlled drug delivery device. Thus, it was determined that nanoparticles alone would not provide the desired insulin delivery characteristics.

9.2 FINAL RECOMMENDATIONS AND FUTURE WORK

Ultimately, an intelligent insulin delivery device for type I diabetes treatment would need to have several specific features. It would need to be able to replace the current insulin therapy methods employed today, which primarily consists of three insulin injections a day. Thus, the delivery device would at least need to replace an entire day's worth of insulin injections, but three to seven days worth would be preferable and insulin stability on such a time scale would not be a concern. These delivery devices would also need to be able to degrade and be excreted on a similar time scale in order to prevent a large build up of hydrogels in the patient's body.

Initial aspirations and design considerations during this research were for an intravenous injectable hydrogel device which could respond to glucose levels and release insulin in the presence of elevated glucose levels. Due to the small diameter of capillaries (5-9 μm), circulating particles could not possibly be larger than about 5 μm when swollen. This limitation led the research towards the use of nanoparticles for insulin loading and release. However, mathematical modeling determined that these particles would not be feasible due to the uncontrolled release of insulin, and experimental studies confirmed these conclusions. Also, intravenous particles would be subjected to more immune response and current technologies have only been able to extend circulation to less than a day, even with PEG surface tethers.

Thus, it is recommended that intravenous injectable hydrogels are not pursued for insulin delivery based on this body of work. Crushed microparticles were shown to have acceptable glucose response and insulin release for type I diabetes treatment. Instead of injectable nanoparticles, microparticles could be implanted either in a synthetic matrix intraperitonealy or simply as free microparticles. The proposed matrix would only need to entrap the microparticles until degradation, and not have an environmental response to the glucose; therefore, a hydrogel with an LCST is suggested,

which would allow the injection of a solution which would then gel upon warming to body temperature and entrap the microparticles.

Degradable crosslinks are an obvious method of creating degradable hydrogel delivery devices. Since the hydrogels investigated in this research respond to pH changes, lactic acid and similarly based degradable polymers would not be acceptable due to their elevated degradation in acidic media and the production of acidic byproducts. Thus, this work described a whole family of possible degradable crosslinks based on labile carbonate bonds, whose hydrophilicity (and presumably degradation rate) was tunable by adjusting the PEG spacer length between carbonate bonds. These crosslinking agents need to be fully characterized to determine their feasibility in an actual drug delivery device.

Future work should include the characterization of these crosslinking agents and the investigation of microparticles implanted intraperitonealy either neat or contained in a secondary matrix. This matrix would need to be investigated for its effects on glucose response and insulin release rates. Finally, *in vitro* and *in vivo* biocompatibility studies would need to be conducted to determine the feasibility of such a drug delivery device. Hydrogels exhibit several important features necessary for an intelligent drug delivery device, though many complications lie in the path to the development of a feedback controlled delivery device.

APPENDIX A

The Biocompatibility of poly(ethylene glycol) Containing Biomaterials

A.1 INTRODUCTION

Biomaterials are natural or man-made materials used to replace, assist, or improve a component of a living system. A biomaterial can range anywhere from an artificial skin graft [1, 2] to a dental implant [3, 4] to a drug delivery device [5, 6] to a synthetic heart [7]. They can range from nano-scale sizes up to macroscopic scale. These materials have intimate contact with biological surfaces, and thus a major problem in the development of new biomaterials has been the compatibility of the new material with its surrounding tissues. This compatibility has been addressed in a number of ways, including using natural materials as a construct and decorating the material's surface with more biocompatible materials [8].

It must be noted that there is a difference between toxicity and biocompatibility. Therefore, toxicity *and* biocompatibility tests must be performed on a new biomaterial to ensure limited or no complications will occur during usage. Toxicity is generally caused by compounds leaching out of the biomaterial, such as unreacted monomer or degraded biomaterial byproducts. Biocompatibility, on the other hand, is determined by the material itself and depends on the way the host immune system responds to the biomaterial's bulk and surface properties [9]. The bulk properties of the new biomaterial must be similar to the surrounding tissue to prevent damage to either the implant or the nearby tissue. The interfacial properties of the implant and surrounding tissues must be tuned to reduce or eliminate an immune response, or else risk

degrading or losing the function of the device. There are also numerous methods of testing for biocompatibility, both *in vitro* [10] and *in vivo* [11].

Different materials inherently elicit different strengths of an immune response. Highly hydrophilic polymers, such as hydrogels, tend to mimic soft bodily tissue [12] and thus exhibit less immunogenicity [13, 14] than a much more rigid and hydrophobic polyethylene. It has been shown that untreated titanium can even cause activation of platelets causing clotting [15]. In order to help make a material biocompatible, it is typically desirable to decrease protein adsorption, complement activation, and cell adhesion. There are, however, certain instances where cell proliferation is desired on a biomaterial. These devices, commonly referred to as scaffolds, are not covered in this review since they have entirely different properties from what one would want in a non-cellular based biomaterial.

A.2 IMMUNE RESPONSE

The immune system is what springs to life when the host identifies some sort of injury or foreign material. The foreign material can either be infectious, such as a bacterium or virus, or noninfectious, such as a biomaterial implant. There are two parts to the immune system, the innate (rapid) and the adaptive immune systems, which distinguish "self" from "non-self" materials, cells, proteins, and molecules. The goal of these systems is to destroy, remove, or segregate unwanted components from the rest of the host. Without a defense mechanism as intricate as the human immune system, a simple laceration could potentially turn from a common annoyance to a very lethal problem [16].

The innate system produces a non-specific response to and is the first line of defense against foreign materials. While it is able to quickly respond, within hours, to an infection, it can only recognize general motifs associated with "non-self" material. It

is also not able to "remember" the last infection, and so the response is always the same. The innate system is composed of cells (leukocytes) and circulating proteins, including cytokines and those composing the complement system. It can also detect injuries to tissue, anticipating that the tissue damage was either caused by a foreign material or will allow a foreign material entry into the body [17-19]. This response is particularly important for biomaterial implants [16].

The innate system is strongly contrasted by the adaptive system, which is able to produce a much more specific response to each individual threat. Humoral cells and proteins circulate through the host, and can either be activated directly by the foreign material or by the signals produced by the innate system. Since they are able to adapt, they are able to respond to nearly an infinite array of "non-self" materials. The adaptive system also "remembers" the invader from the last infection, and is able to respond more quickly to subsequent infections [8, 16].

These two pieces of the immune system work together to keep the host healthy and free of foreign substances. After a biomaterial is introduced to the host, there is typically some sort of immune response. It is very common during this process to coat the foreign object with numerous proteins to help aid in the detection of the intruder. If the biomaterial is cell-based, the host will respond with its adaptive system; T-cell activation and B-cell antibody production will occur. However, if the biomaterial is synthetic, it will most likely induce the innate system's response. A nonspecific reaction to the material will occur, by macrophages or the complement system, which can then lead to damage of the surrounding tissue. It is therefore extremely important to prevent this cascade of events during the usage of a biomaterial [8, 16].

A.3 COMPLEMENT SYSTEM

The complement system was first described by Paul Ehrlich as the plasma proteins necessary for a host to recognize and dispose of bacteria via antibodies. There are over 30 known plasma and surface proteins involved in the complement system which work together in a cascade to amplify the response to a foreign material [20, 21]. The complement system has three known components: classical, lectin, and alternative pathway. It plays an essential role in the immune system's ability to identify "non-self" surfaces due to the ability of these proteins to adsorb to surfaces, and the ability of "self" cells to easily desorb or remove these proteins from their surfaces. This process allows the complement system to coat a foreign surface and then recruit cells to either destroy or encapsulate it [16, 22].

All three components of the complement system are initiated differently but then converge with the activation of C3 [16, 20]. These earlier components, as well as C3 itself, are proenzymes which, upon cleavage, activate the next component. This order of events allows an amplification of this cascade, since once activated, a component can then activate numerous more components. Once activated, C3 is split into C3a and C3b [20]; C3a circulates through the blood to act as a signal, whereas C3b binds to the surface of the foreign material [23-25]. The classical pathway is activated by IgG or IgM [16] with C1 initiation on the surface of the foreign material, which then eventually activates C3. The lectin pathway is initiated with mannan-binding lectin, which binds either mannose or fructose on the foreign surface [22]. The alternative pathway is directly initiated by activated C3, which circulates at very low concentrations, and then attaches to the foreign substance [26, 27]. Normal autonomous cells have specific proteins coating their surface to prevent buildup of activated C3, C3b, which prevents complement activation [16].

It appears that this activation of C3 could be the most important aspect of the complement system [25, 28]. It has been shown that a conformational change in C3 allows a hidden thioester group to become available on the surface of the protein [25], which is able to easily bind to free amino or hydroxyl groups on the biomaterial. C3 can also changes its conformation and noncovalently bind to a polymer surface [29]. Therefore, activation of C3 is an aid in determining foreign materials [24]. Prevention of this binding step is a potential target for increasing the biocompatibility of many biomaterial systems [25].

There are numerous methods of detecting complement activation, ranging from methods that measure levels of complement proteins adsorbed to the surface of the biomaterial, to the measurement of soluble factors in the medium surrounding the biomaterial. With the way the complement system performs its cascade and amplification, for each proenzyme cleavage, there results in a smaller soluble factor which circulates and a larger enzymatic factor that tends to localize around or adsorb to the biomaterial itself. The soluble factor can be detected with numerous analytical techniques, such as Enzyme-Linked ImmunoSorbent Assay (ELISA) [30, 31], precipitation tests using PEG [32], or 2-D electrophoresis [33]. Measurement of the bound C3b was performed by direct radioimmunoassay [34], the CH50 method [35, 36], and others.

A.4 THROMBOGENICITY

Thrombogenicity is the ability of a material to induce clotting upon contact with the blood. This clot can form locally and remain local, form locally and detach (forming emboli), or form at some satellite location due to the presence of the biomaterial [8]. This process is mediated by numerous proteins as well as cells and cell fragments. As with many immunological responses, the clotting procedure follows a cascade of events which are amplified until a full-blown clot is formed [21, 37]. If a blood clot forms on a

newly introduced biomaterial, there could be dire consequences for either the biomaterial itself or the patient.

There are two distinct pathways towards a blood clot, which then converge upon the formation of thrombin and fibrin. The intrinsic pathway begins with protein adsorption to negatively charged surfaces, which produces a cascade of factor activations ultimately activating factor X. The extrinsic pathway, which is more specific to biomaterials [38], activates factor VII with the aid of tissue factors released from locally damaged cells. Once thrombin is formed, it catalyzes the polymerization of fibrinogen into fibrin. Unless streptokinase or urokinase degrades this fibrin clot, platelets will adhere forming a white clot. The platelets adhere to the fibrin, becoming sticky and forming pseudopods. The next step involves the entrapment of red blood cells, forming a red clot [8, 38]. By this time, the clot has reached a size of 30 μm or more and has become quite dangerous.

As alluded to above, there are certain circulating proteins that specifically attract platelets, and adhesion of vitronectin, fibronectin [8], fibrinogen, or von Willebrand factor [39] onto a surface mediates platelet adhesion. These proteins adhereing to the surface of the biomaterial propagate the clotting cascade. Fibrinogen provides an irreversible means of attachment, which decreases as blood shear rate increases, whereas von Willebrand factor slowly provides more and more adhesion as shear rate increases [39].

There are a number of methods that may potentially delay or inhibit clot formation [37]. If protein adsorption is prevented, then the clotting cascade cannot be initiated. Antithrombin III and tissue factor pathway inhibitor (TFPI) are such proteins which can decrease clotting [8]. It has been shown that coating a surface with albumin can actually decrease the thrombogenicity of a material [40-43]. These data provide means of decreasing the clotting cascade that would otherwise retard or inhibit the usage of a biomaterial.

A.5 POLY(ETHYLENE GLYCOL)

Poly(ethylene glycol) (PEG) is a biocompatible polymer of repeating ethylene glycol units. In an aqueous environment, each ethylene glycol repeat unit binds multiple molecules of water. This phenomenon allows the PEG chains to repel each other and form a "brush-like" conformation when the appropriate PEG density is achieved [44]. PEG is soluble in both aqueous and organic environments while similar polyethers are not [45]. PEG in aqueous solutions also has a large excluded volume, which helps impart some of its interesting properties.

PEG has long been known for its resistance to protein adsorption [46-48] which can be attributed to its steric repulsion, hydrophilicity, and chain mobility [49]. Two surfaces coated with PEG will develop repulsive forces when brought close enough, due to the steric stabilization of each PEG chain. The interaction between infinitely sized [47] to small sized [46] proteins has been modeled, showing that van der Waals interactions between the PEG and protein are negligible. Numerous groups have tried to model the ability of PEG to prevent protein adsorption [44, 46, 47], including using the single-chain mean-field analysis [50]. There are some studies that show an adhesive force between PEG and protein can be achieved [45], but high compressive forces were needed to obtain this adhesion and the PEG chains were possibly forced to envelope the protein. While PEG itself is able to decrease protein adsorption, there are many other factors that influence whether an entire biomaterial will adsorb proteins.

There are many groups working on PEG containing biomaterials [51-56]. Many times, a material with the correct physical characteristics to solve a biomedical problem just does not have the biocompatibility characteristics needed in a biomaterial. Therefore, a strong thrust towards increasing biocompatibility while retaining the

function of the biomaterial has been undertaken. Following is a review of numerous attempts at using PEG in materials to make them more biocompatible; specifically, PEG has been used with biomaterials to decrease protein adsorption, decrease cell adhesion, increase blood compatibility, and decrease the activation of the complement system.

A.5.1 PEG Coatings

Many natural materials have been decorated with PEG in attempt to increase biocompatibility by decreasing protein adsorption, decreasing cell adhesion, and/or decreasing thrombogenicity [57-61]. Kishida, *et al.*, took cellulose membranes and grafted PEG to the surface. Both a mono-acid and di-acid form of PEG were used, which were covalently bound to the free hydroxyls of the cellulose. The di-acid actually increased adsorption of bovine serum albumin as well as γ-globulin, whereas the mono-acid did not change the protein adsorption from the neat cellulose. Both did, however decrease complement activation. It was suspected that the free carboxylic acid on the di-acid allowed ionic interactions between proteins and the surface, which increased adsorption [57].

Chitosan is another commonly used natural polymer for biomaterials [58-61]. Five types of chitosan-PEG blends were studied to test their physical, chemical, and biological properties. PEGs with molecular weights of 6000 and 8000 Da were used, in ratios of 2:1 and 4:1 by weight. They showed that, for low levels of PEG, protein adsorption and cell adhesion and proliferation increased. However, once the PEG surface coverage was high enough, protein adsorption decreased as did cell adhesion. While the study was for new cellular scaffolds, it was shown that an increase in the PEG content will also increase biocompatibility with the immune response [62].

There has been a significant amount of research in coating polymeric materials with PEG [63-68]. PEG has been adsorbed to the surface [65-68], covalently bound to

the surface, and formed interpenetrating networks [63] on the surface of numerous polymeric materials. The advantages and disadvantages of each method have been studied. Adsorbing to the surface can involve an easier synthetic route, such as ionic interactions or hydrophilic or hydrophobic interactions, but has the disadvantage of desorption over time. If the device will be *in vivo* for prolonged periods of time, the biocompatibility of the device will decrease over time. Covalently bound PEG, whether to the surface, copolymerized with the polymer, or polymerized as an interpenetrating network, appears to offer much longer compatibility.

The effect of hydrophilic and hydrophobic components has also been studied on polymers composed of PEG and poly(tetramethylene oxide) (PTMO) or poly(dimethyl siloxane) (PDMS). Both random and block copolymers were formed. Measurements indicated that longer PEG lengths, as well as usage of PDMS instead of PTMO, increased hydrophilicity. Significantly lower adsorption of human serum albumin, human fibrinogen, and IgG was measured on the PEG containing polymers. With this decrease in protein adsorption, a decrease in platelet adhesion was also detected. The most promising material was PDMS with a 3400 Da PEG graft [64].

A.5.2 PEG as a Copolymer

Since hydrogels are similar to bodily tissue [12], it is only natural that they are used in biomaterial devices. It is also only natural that an increase in biocompatibility would be desired. Interpenetrating networks of acrylamide and ethylene glycol have been made {Bearinger, 1997 #44}, as have acrylonitrile membranes [69, 70] and other biomaterials. Other forms of hydrogels containing PEG have also been synthesized [64, 71-73]. These hydrogel systems have been tested for protein adsorption, cell adhesion, and complement activation in order to determine overall biocompatibility and resistance to blood clotting.

Instead of a traditional copolymerization procedure, interpenetrating networks of PEG have also been studied [63 , 74-76]. An interpenetrating network consists of two independent polymeric systems, both of which are crosslinked with themselves but not crosslinked with each other. The chains of each network actually interpenetrate each other, thus producing a polymeric system of two entangled networks which cannot be separated without breaking chemical bonds [77, 78]. The advantage of this approach is that the PEG component of the device can be added after the fact; the original biomaterial can be prepared as usual, and provided that it has some sort of porosity, the PEG network can be formed around and through the existing material. This procedure can make the synthetic route for the biomaterial significantly easier, since pre-made devices can easily be PEGylated.

Interpenetrating networks of acrylamide and PEG were made on silicon wafers. The silicon was first coated with an acrylamide network by silanization and then photoinitiated polymerization of acrylamide with N,N-methylenebis(acrylamide) as a crosslinker. PEG monomethylether monomethacrylate of molecular weight 1000 Da was then polymerized through the acrylamide network, also using N,N-methylenebis (acrylamide) as a crosslinker. There was no statistically relevant adsorption of bovine serum albumin on either acrylamide or acrylamide-PEG interpenetrating networks; however, there was a statistical amount of adsorption on the untreated silicon. Cell adhesion was also significantly decreased on the polymer-coated silicon surfaces. Therefore, it was shown that PEG does not have to be tethered to a surface to help impart resistance to protein adsorption [63].

Mixtures of hydrophobic polymers with PEG have been tested for their biocompatibilities. Polymers of octadecylacrylate were synthesized, some of which were functionalized with either PEG or PEG-sulfate groups. Free radical polymerization in toluene was performed. Coagulation tests indicated that the PEG coated polymers had decreased protein adsorption and decreased thrombogenicity. The PEG-sulfate

polymers had superior blood clotting characteristics, and improved complement activation over the normal PEG polymers. Both C3 and C5 levels were decreased, markedly decreasing other factors indicating the improved complement system compatibility. It was thought that the negative charge held on the sulfate group played a significant role in the decreased activation of the complement system [79].

A.5.3 PEG and Polyurethane

Polyurethane is one of the longest used biomaterial. It was one of the original materials used in an artificial heart; however, it was plagued with problems of blood coagulation [8]. Polyurethane elastomers were synthesized, initiated from a PEG, PPO, or PTMO chain. Human serum albumin adsorption was significantly reduced in the urethanes containing PEG. However, there were no clear cut results as to whether bacterial adhesion was increased or decreased. There were significant variations depending on species of bacterium used [80].

Other results were interesting. Surface modified Pellethane 2363-80AE was made using multiple coatings. Both surface adsorption, using ampiphilic block copolymers, and surface grafting were performed. The ampiphilic polymers used were Pluronic PE9400 and a custom made segmented polyurethane using PEG of molecular weight 1500 Da. The adsorption of fibrinogen and albumin was measured, and both were significantly decreased from the normal polyurethane sample. The Pluronic results were very similar to the PEG grafting of molecular weight 20000 Da. Blood clotting *in vitro* was also shown to have decreased with the surface coatings of PEG, indicating higher biocompatibility [81].

One last group indicated a much more promising outlook for PEGylated polyurethane [81, 82]. Segmented polyurethane, with dicumyl peroxide crosslinks, containing PEG, was synthesized. The number of PEG repeat units varied from 0 to 98,

and both UV and temperature initiated polymerizations were used. As little as 5% PEG was necessary to elicit changes in surface properties. Platelet adhesion from fresh human blood, and therefore most likely protein adsorption, decreased with an increase in PEG content. There was not much difference between UV and thermally initiated polymerizations. These data follow more hydrophilic polymeric systems trends, indicating that PEG is able to shield the polyurethane core from the surrounding environment. It was also noticed that the addition of PEG acts as a plasticizer of the polyurethane, decreasing the tensile strength and increasing the elongation at break [82].

A.5.4 PEG on Membranes

Membranes of acrylonitrile-co-maleic acid have been synthesized [69, 70, 83]. Hydrophilicity of these membranes was increased significantly on the addition of PEG grafts. PEG chains of molecular weight 200, 400, 600, and 1000 Da were used. As PEG chain length increased or maleic acid content increased, bovine serum albumin adsorption decreased. The same trends yielded improved filtration as well, which was attributed to the increased hydrophilicity. Platelet and macrophage adhesion also decreased with increasing PEG content. Therefore, these biomembranes have much lower fouling properties than the neat acrylonitrile-co-maleic acid membranes.

A commonly used biomaterial is expanded poly(tetrafluoroethylene) (ePTFE) [84-88]. It is highly inert, nontoxic, and microporous. These properties combined were suspected to work well in a biological membrane device. However, the extreme hydrophobicity can cause complications. Atmospheric pressure glow discharge of PEG, with molecular weight of 600 Da, was used to coat ePTFE surfaces, which were then tested for biological use. Albumin adsorption increased, while γ-globulin did not change and fibrinogen decreased. More than 3% coverage with PEG seemed to induce platelet

adhesion, which could lead to clot formation. However, with the decreased fibrinogen adsorption and the slight adhesion of platelets without conformational changes, the modified ePTFE appeared to be a fairly non-thrombogenic material [89]. The benefits of this improved membrane device could have implications in artificial kidneys, allowing improved dialysis with less membrane fouling, therefore reducing the maintenance costs of the devices.

A.5.5 PEG on Non-Biological Surfaces

Decorating material surfaces with PEG has been used with completely non-biologically similar materials such as silicon [49, 90], glass [91], and gold [92]. Grafting linear PEG of molecular weights of 3400, 10000, and 20000 Da, as well as star PEG, to silicon wafers was achieved via aminosilane treatments of the silicon and tresyl treatments of the PEG. The adsorption of cytochrome-*c*, albumin, and fibronectin were all studied, and grafting densities of 100 ng/cm^2 yielded nearly zero adsorption for all proteins. It was observed that, with the tested molecular weight PEGs, chain overlap was necessary for the protein adsorption resistance. Therefore, as the molecular weight of the PEG chain decreased, the grafting density needed to increase. However, star PEG chains were effective at preventing protein adsorption provided the gaps between chains were smaller than the proteins themselves [90].

Sharma, *et al.*, were able to surface coat silicon squares with both a solution-based and vapor-based approach. The silicon may have micron or nano scale channels etched into the surface to provide functionality to the device, where the viscosity or surface tension of the PEG-silane solution could inhibit the formation of a confluent PEG layer. Therefore, the vapor deposition of ethylene oxide appears to be a better method of obtaining an even PEG coating. They demonstrated that both methods of PEGylation were able to significantly decrease fibrinogen and albumin adsorption over the neat

silicon, and there was no significant difference in adsorption between the two methods of PEGylation [49]. These data imply decreased cell adhesion and better biocompatibility over uncoated silicon devices.

Glass can also be silanized with PEG to increase biocompatibility. PEG of molecular weights 750 and 5000 Da were functionalized with silane and then allowed to self-assemble on the glass surface, thus the term "self-assembled monolayers" (SAMs) of PEG. The lower molecular weight PEG formed brush-like structures, with the chains extending about 85% of their total lengths. The higher molecular weight PEG tended to form a mushroom configuration, with significant entanglement away from the glass surface as shown by the approximately 25% extension of their total lengths. Adsorption of bovine serum albumin on both PEGylated surfaces was significantly decreased, to about 6% of that adsorbed to uncoated glass. There were, however, differences in diffusion and aggregation of bovine serum albumin on the different length PEGs, which was attribute to aqueous content and conformational differences [91].

SAMs can be used to coat gold slabs as well, by using PEG with thiol derivatives to form the self-assembled monolayer. The reaction between gold and thiol groups has been well established [93-95]. The work done by Prime and Whitesides is interesting because they were able to find an empirical method of determining the molar coverage by PEGylation that is necessary for prevention of protein adsorption, specifically, $n^{0.4}$ where n is the number of ethylene glycol repeat units. Alkanethiols with varying ethylene glycol repeat units were used to coat gold slabs, after which the adsorption of fibrinogen, lysozyme, pyruvate kindase and RNAse A were measured. It was shown that, on average, there was no difference between hydroxy terminated and methoxy terminated PEGs, an increase in the number of PEG repeat units decreased the total surface coverage needed for the prevention of protein adsorption, and higher surface coverage prevented more adsorption [92].

One last similar approach is the coating of silica with PEG. The silica layer was deposited by plasma-enhanced vapor deposition of SiH_4 and O_2, which was then activated with water plasma to coat the silica layers with hydroxyl groups. PEG with a molecular weight of 400 Da was used to coat the silica, also via plasma deposition. Protein adsorption experiments were carried out to measure how much bovine serum albumin adsorbed to each surface. While treating the silica with water plasma only slightly decreased the amount of adsorbed protein, treating with PEG significantly dropped to protein adsorption. The interesting part of this research is the flexibility of the process [96]. Since the PEG is covalently bound to the silica, nearly any surface that can have silica plasma-deposited on it has the potential to be PEGylated via this method. This can decrease problems with finding reactive functional groups for a biomaterial or even issues with the shape and size of the biomaterial. Therefore, it is possible to functionalize surfaces that would not normally be considered for use in biomaterials due to their inherent non-biocompatibility.

A.5.6 PEG and the Complement System

The majority of the previous work mainly focused on two aspects of biocompatibility, namely, adsorption of proteins and adhesion of cells to the surface of the biomaterial. To test for complete nonimmunogenicity, the activation of the complement system must also be analyzed. Without prevention of the activation of the complement system, biomaterial devices will rapidly be flagged by the body and either opsonized or isolated. Decreased adsorption of serum proteins is not the only feature needed to decrease complement activation, as shown below.

One common area of research for biomaterials is in the drug delivery field. The general trend is to decrease the size of the devices, in hopes of decreasing the immune response to the device. What started at macroscale oral tablets has shrunk to micro-

and nano-sized particles, allowing more rapid release and even allowing intravenous injections of long-circulating drug delivery devices. The implications of improved drug delivery devices are to increase the patient compliance by increasing the bioavailability of the drug, as well as increasing the length of time between dosings. This will ultimately result in improved control over the diseased state, as well as lower chances of falling out of the therapeutic window of the drug, either above (toxic) or below (ineffective). These devices can be liposomic or polymeric in nature, and can be formed by a wide variety of methods [33, 35, 36, 97-100].

Liposomes are composed of amphiphilic lipid molecules that can self-assemble into spherical capsules. The lipid molecules have hydrophilic heads and hydrophobic tails, and thermodynamics drives the molecules into spherical conformations. Monolayers, bilayers, and higher ordered systems can be formed; a monolayer would be preferred for a slightly water-soluble drug, whereas a bilayer would be preferred for a highly water-soluble drug. Sizes can range from 10 nm to over 10 μm. The inherent interest in liposomes lies in the fact that all known cells are composed of these lipid bilayers, and therefore even a synthetic liposome appears more natural than polymeric systems [36, 97, 98]. Unfortunately, non-functionalized liposomes are easily sequestered by the immune system and highly activate the complement system.

The introduction of PEGylated liposomes was a significant breakthrough in the development of sustained release drug delivery devices [98]. These liposomes can be created in many different ways, but one common method is to link a methoxy terminated PEG to the phospholipids using a carbamate bond [98]. Other methods include terminal amino and epoxy group functionalizations [100]. It has been shown that, to yield the desired lack of protein adsorption, PEG of molecular weights between 2000 and 5000 Da are necessary. PEG chains larger than this size may cause instability of the liposome, whereas smaller chains may not provide the necessary coverage to prevent protein adsorption. Sizes in the range of 70-200 nm seem to be ideal;

liposomes larger tend to be noticed and opsonized much more quickly, whereas liposomes smaller tend to get lost in the leaky vasculature of certain organs [98, 100]. These modifications have increased circulation times, but not necessarily decreased complement activation [36]. Vonarbourg attributed this problem to too dense a PEG coating on small particles, which decreased the ability to shield the particles from protein adsorption and therefore phagocytosis.

A second method of drug delivery is using polymeric micro and nano particles or capsules. Common systems include poly(lactic acid) (PLA), poly(glycolic acid) (PGA), or mixtures of the two. These systems are hydrolysable in aqueous media, and therefore are biodegradable *in vivo*. Numerous research groups are working on PLA/PGA based devices for delivering drugs, whether targeted or not. One specifically tested adsorption versus covalent grafting of PEG to nanocapsules and nanospheres. Data indicate that capsules tend to activate the complement system less than spheres, but could potentially be due to residual lecithin on the capsule surfaces. As the PEG chain length increased, biocompatibility also increased [33].

Other groups had much better success using PLA and PGA particles containing PEG. Diblock copolymers of PLA-PEG were synthesized, using PEG of a molecular weight of 2000 Da. Human serum was used in a CH50 test to determine complement activation. PLA particles without PEG produced a strong and rapid complement activation, whereas PLA-PEG diblock copolymers having an average PEG surface density of greater than 0.2 molecules per square nanometer had significantly reduced complement activation. Therefore, below the threshold PEG levels, the PEG is unable to produce its brush-like conformation, decreasing its ability to inhibit complement activation. Once the PEG content was brought up above the threshold, complement activation was decreased drastically. There still is the possibility of C3 activation by non-covalent binding, but more tests needed to be performed to test that potential complement activation method [29].

In contrast to covalently bonded microparticles, there are ionically stabilized microparticles. One such device is a PEG-graft-poly(L-lysine) (PEG-g-PLL) copolymer, forced into microparticles by the ionic interaction with sodium alginate. A noticeable decrease in protein adsorption, cell adhesion, and complement activation was observed for the PEG containing PLL polymers over the neat PLL polymers. IT was also recorded that the microcapsules became leakier; that is, solutes diffused more rapidly out of the PEG-g-PLL/alginate systems than the PLL/alginate systems. To compensate for this, multilayered devices were synthesized, using layers of alginate, then PLL, then alginate, then PEG-g-PLL, and then alginate once more. This process yielded a more ideal device, as it retained its ability to prevent protein adsorption as well as decrease the activation of the complement system. At the same time, it also decreased the diffusion of solutes out of the system, allowing a tunable delivery device. These systems have also been determined to be stable for at least one month, providing the ability of mass-produced off-the-shelf delivery devices [34].

It must be noted that all articles reviewed thus far have been using an *in vitro* approach to measuring biocompatibility, and at most, have used blood plasma for the thrombogenicity studies. Some work has been done to test the protein adsorption and blood clotting of PEGylated surfaces using whole blood. Titanium is a common metal in medical applications due to its high strength-to-weight ratio. Uncoated titanium, however, has been shown to elicit clotting of blood. Ionically bonding a PEG layer, by treatment with poly(L-lysine)-g-PEG, was shown to increase clotting time threefold. The treated titanium also showed no antibodies binding fibrinogen, kininogen, or C3. These data indicate that a decreased clotting and decreased complement activation occurs when coating titanium with PEG [15]. Again, the evidence suggests that PEG can help decrease complement activation while decreasing protein adsorption and cell adhesion.

A.5.7 PEG and Polystyrene

Polystyrene has an interesting place in the review of PEG biomaterials. Untreated, polystyrene is highly non-biocompatible, and will induce protein adsorption quite rapidly. However, attempts were made to PEGylate polystyrene in order to model cellular behavior. PEG chains with mono and bi functionalities, including amino, methoxy, and hydroxyl, were used in this study. Molecular weights of 1500, 3400, and 5000 Da were used. The control used was polystyrene coated with carboxylic acid functional groups. Protein adsorption was measured by incubating samples in human plasma and then separating the particle out with centrifugation. The proteins were then desorbed via sonication, and once again the particles were separated out. Complement system activation was also measured with fresh human blood. As PEG surface concentrations approached 40 pmol/cm^2, the amount of protein adsorbed dropped to 90% or less than the control. The end group of the PEG did not appear to make any significant difference in protein adsorption. Over 30% of the adsorbed proteins were albumin, or similar, and therefore are potentially beneficial. As PEG concentrations increased above 55 pmol/cm^2, substantial complement activation occurred. Hydroxyl terminated PEG chains also induced much higher complement activation [101].

Another method of PEGylation involves using Pluronic™ materials. Pluronics™ are made of poly(propylene oxide) (PPO) blocks with PEG blocks on each end. This block copolymer was adsorbed to polystyrene surfaces. The hydrophobicity of both the polystyrene and PPO provided a means of immobilizing the Pluronic™ chains. Protein adsorption and complement activation were measured. Factor H, a cofactor for inactivating C3 and a competing binding partner for B and Bb (parts of the C3 complement activation cascade), was also bound to these polymeric devices. The inertness of the PEG decreased protein adsorption, whereas the bound factor H helped decrease the complement activation. However, a possible cause for slight complement

activation was the PPO block in the Pluronic™ [20]. It appears that there tends to be a tradeoff between decreased coagulation and decreased complement activation.

Gorbet and Sefton concur with this tradeoff between complement activation and protein adsorption. They also used polystyrene beads, TentaGel™, of 45 µm diameters to perform their experiments. PEG chains of roughly 3000 Da were used. Fresh whole blood from humans was used in the complement activation tests, of which serum was extracted. Both the coated and uncoated polystyrene beads elicited C3b binding. Leukocyte adhesion was also fairly high. Again, they attributed these issues to hydroxyl groups allowing the covalent attachment of C3 proteins to the ends of the PEG chains, thereby increasing complement activation [38].

A.5.8 Problems with PEG

While nearly all other reports indicate significant improvements in biocompatibility by the addition of PEG, some research indicates PEG may not be as bioinert as previously thought. As noted earlier, liposomes are an interesting biomaterial for drug delivery. Significant increases in circulating half-lives have been shown, simply by PEGylating the surface. However, there may possibly be an "accelerated blood clearance phenomenon" which decreases the half-life of circulating liposomes instead. Contrary to what would be expected, an increase in the initial dose of PEGylated liposomes actually *decreases* this phenomenon [102], while decreasing the time between injections increases this phenomenon [103]. There are certain serum factors circulating in the blood that help contribute to this phenomenon, notably IgM, which appear to bind to the PEG portion of the liposomes. Even in "naïve" serum, slight complement activation was noted. It is suggested that the IgM bound directly to the PEG, since it did not bind to non-PEGylated liposomes after the accelerated blood clearance phenomenon had been observed. This may, however, be misleading since

PEG alone did not induce IgM binding until it had been coated on a liposome [104]. A similar phenomenon has been called the hypersensitivity reactions (HSRs) which have been common with liposomal drug delivery devices [105].

A second report shows similar results, when a red blood cell was PEGylated to decrease the immune response to non-matching ABO antigens. Typically, upon transfusion, if the ABO are not correctly matched, an immune response occurs, lysing the foreign red blood cell. Upon PEGylation with cyanuric chloride activated PEG, molecular weight 5000 Da, the recognition of the red blood cell by antibodies. Unfortunately, it also *increased* the complement activation via the classical pathway. Again, an increase in IgM was noticed on the mismatched red blood cells, indicating that the possible cause of complement activation was the PEG itself. It is interesting that PEGylation decreased the adaptive immune response while increasing the innate immune response [106].

A.6 SUMMARY AND CONCLUSIONS

As shown above, the biocompatibility of a new biomaterial is one of the most important design criteria for the device. There are numerous issues with trying to introduce new materials and devices into the body, whether the construct be of synthetic or natural materials. The immune response to a material, whether it is complement activation, the formation of a fibrotic encapsulation, or blood coagulation, poses a serious threat to the deployment of mass-produced biomaterial devices. All of these responses are due to cascades of events which amplify even a small immunological response to a scale that can cause significant problems to both the biomaterial device and the patient himself.

One method of avoiding the immunological response has been to use poly(ethylene glycol) to prevent adsorption of proteins, adhesion of cells, and decrease

complement activation and blood coagulation. The hydrophilicity, lack of ionic charge, and steric repulsion characteristics of PEG are what give it a place in biomaterial design. A plethora of articles have reported decreased protein adsorption and decreased cell adhesion with numerous variants of PEGylation and even more variations of devices and biomaterial systems. With the range of problems that biomaterials can potentially fix, it is promising to see that an even larger range of materials are being tested for usage in biomaterials. These data provide hope to the research and medical communities for finding a mechanism of creating truly "stealth" biomaterials to improve or repair the ailments of a patient.

It is interesting that there are numerous ways to add PEG to a biomaterial surface. Free hydroxyl groups are easy to react PEG on to, but many other functional groups such as amines, siloxanes, carbamates, and thiols can be used. The biomaterial itself does not even have to be functionalized; silica or gold could be plasma deposited on the surface, and then the silica or gold surface can easily be functionalized. This versatility increases the ability of researchers to be able to use PEG in the creation of new biomaterials and devices.

There are, however, numerous problems with the usage of PEG. If the PEG is not covalently bound to the device, then it will elute out of the system over time. If it is not coated consistently enough or densely enough, then it will not provide the necessary protection from the immune system. It has even been observed that PEG could possibly elicit a direct immune response, causing the formation of IgM that can actually bind PEG itself. Several research groups observed that hydroxyl terminated PEG chains tend to elicit higher complement activation than methoxy terminated PEG chains. Numerous groups have noted that PEG alone tends to have a tradeoff with improving biocompatibility properties. As the protein adsorption, cell adhesion, and blood coagulation decrease with increasing PEG lengths and/or densities, the complement activation tends to increase.

It is therefore the view of the author that, while PEG offers significant advantages over neat biomaterial devices, it is still a long ways away from solving the total biocompatibility issue. It also appears that PEG alone will not be able to provide the necessary protection of a new device from the immune response. Coating the biomaterial with peptide fragments or proteins, in addition to the PEG, will most likely be necessary to produce truly "stealth" systems that can avoid the immune response. The human body is full of cells and biological molecules, and trying to trick the body with strictly synthetic methods will be a more frustrating and less fruitful endeavor than trying to use what nature has already provided.

A.7. REFERENCES

1. De Filippo, R.E., J.J. Yoo and A. Atala, *Urethral replacement using cell seeded tubularized collagen matrices.* J. Urol., 2002. **168**(4): p. 1789-1792.

2. Rhee, P.H., C.D. Friedman, J.A. Ridge and J. Kusiak, *The use of processed allograft dermal matrix for intraoral resurfacing - An alternative to split-thickness skin grafts.* Archives of Otolaryngology-Head & Neck Surgery, 1998. **124**(11): p. 1201-1204.

3. Watari, F., A. Yokoyama, F. Saso, M. Uo and T. Kawasaki, *Fabrication and properties of functionally graded dental implant.* Composites Part B-Engineering, 1997. **28**(1-2): p. 5-11.

4. Smith, D.C., R.M. Pilliar and R. Chernecky, *Dental Implant Materials .1. Some Effects of Preparative Procedures on Surface-Topography.* Journal of Biomedical Materials Research, 1991. **25**(9): p. 1045-1068.

5. Siepmann, J. and N.A. Peppas, *Modeling of drug release from delivery systems based on hydroxypropyl methylcellulose (HPMC).* Advanced Drug Delivery Reviews, 2001. **48**(2-3): p. 139-157.

6. Peppas, N.A. and J.J. Sahlin, *Hydrogels as mucoadhesive and bioadhesive materials: A review.* Biomaterials, 1996. **17**(16): p. 1553-1561.

7. Gristina, A.G., J.J. Dobbins, B. Giammara, J.C. Lewis and W.C. Devries, *Biomaterial-Centered Sepsis and the Total Artificial-Heart - Microbial Adhesion Vs Tissue Integration.* Jama-Journal of the American Medical Association, 1988. **259**(6): p. 870-874.

8. Ratner, B.D., A.S. Hoffman, F.J. Schoen and J.E. Lemons, eds. *Biomaterials Science: An Introduction to Materials in Medicine*. 2nd ed. 2004, Elsevier Academic Press: Amsterdam ; Boston.

9. Ikada, Y., *Surface Modification of Polymers for Medical Applications.* Biomaterials, 1994. **15**(10): p. 725-736.

10. Hanks, C.T., J.C. Wataha and Z. Sun, *In vitro models of biocompatibility: A review.* Dental Materials, 1996. **12**(3): p. 186-193.

11. Ryhanen, J., M. Kallioinen, J. Tuukkanen, J. Junila, E. Niemela, P. Sandvik and W. Serlo, *In vivo biocompatibility evaluation of nickel-titanium shape memory metal alloy: Muscle and perineural tissue responses and encapsule membrane thickness.* Journal of Biomedical Materials Research, 1998. **41**(3): p. 481-488.

12. Peppas, N.A., P. Bures, W. Leobandung and H. Ichikawa, *Hydrogels in pharmaceutical formulations.* European Journal of Pharmaceutics and Biopharmaceutics, 2000. **50**(1): p. 27-46.

13. Nickel, J.C., M.E. Olson and J.W. Costerton, *In vivo coefficient of kinetic friction: Study of urinary catheter biocompatibility.* Urology, 1987. **29**(5): p. 501-503.

14. Graiver, D., R.L. Durall and T. Okada, *Surface morphology and friction coefficient of various types of Foley catheter.* Biomaterials, 1993. **14**(6): p. 465-469.

15. Hansson, K.M., S. Tosatti, J. Isaksson, J. Wettero, M. Textor, T.L. Lindahl and P. Tengvall, *Whole blood coagulation on protein adsorption-resistant PEG and peptide functionalised PEG-coated titanium surfaces.* Biomaterials, 2005. **26**(8): p. 861-872.

16. Alberts, B., A. Johnson, J. Lewis, M. Raff, K. Roberts and P. Walter, *Molecular Biology of the Cell*. 4th ed. 2002, New York: Garland Science.

17. Babensee, J.E., J.M. Anderson, L.V. McIntire and A.G. Mikos, *Host response to tissue engineered devices.* Advanced Drug Delivery Reviews, 1998. **33**(1-2): p. 111-139.

18. Khouw, I., P.B. van Wachem, L. de Leij and M.J.A. van Luyn, *Inhibition of the tissue reaction to a biodegradable biomaterial by monoclonal antibodies to IFN-gamma.* Journal of Biomedical Materials Research, 1998. **41**(2): p. 202-210.

19. Sennerby, L. and P. Thomsen, *Tissue-Response to Titanium Implants in Experimental Antigen-Induced Arthritis.* Biomaterials, 1993. **14**(6): p. 413-422.

20. Andersson, J., K.N. Ekdahl, J.D. Lambris and B. Nilsson, *Binding of C3 fragments on top of adsorbed plasma proteins during complement activation on a model biomaterial surface.* Biomaterials, 2005. **26**(13): p. 1477-1485.

21. Sefton, M.V., C.H. Gemmel and M.B. Gorbet, *What really is blood compatibility?* Journal of Biomaterials Science -- Polymer Edition, 2000. **11**(11): p. 1165.

22. Carroll, M.C., *The role of complement and complement receptors in induction and regulation of immunity.* Annual Review of Immunology, 1998. **16**: p. 545-568.

23. Ajees, A.A., K. Gunasekaran, J.E. Volanakis, S.V.L. Narayana, G.J. Kotwal and H.M.K. Murthy, *The structure of complement C3b provides insights into complement activation and regulation.* Nature, 2006. **444**(7116): p. 221-225.

24. Dempsey, P.W., M.E.D. Allison, S. Akkaraju, C.C. Goodnow and D.T. Fearon, *C3d of complement as a molecular adjuvant: Bridging innate and acquired immunity.* Science, 1996. **271**(5247): p. 348-350.

25. Janssen, B.J.C., A. Christodoulidou, A. McCarthy, J.D. Lambris and P. Gros, *Structure of C3b reveals conformational changes that underlie complement activity.* Nature, 2006. **444**(7116): p. 213-216.

26. Janeway, C., *Immunobiology: The Immune System in Health and Disease*. 5th ed. 2001, New York: Garland Science.

27. Reid, K.B.M., D.R. Bentley, R.D. Campbell, L.P. Chung, R.B. Sim, T. Kristensen and B.F. Tack, *Complement system proteins which interact with C3b or C4b A superfamily of structurally related proteins.* Immunology Today, 1986. **7**(7-8): p. 230-234.

28. Bergmann-Leitner, E.S., W.W. Leitner and G.C. Tsokos, *Complement 3d: From molecular adjuvant to target of immune escape mechanisms.* Clinical Immunology, 2006. **121**(2): p. 177-185.

29. Vittaz, M., D. Bazile, G. Spenlehauer, T. Verrecchia, M. Veillard, F. Puisieux and D. Labarre, *Effect of PEO surface density on long-circulating PLA-PEO nanoparticles which are very low complement activators.* Biomaterials, 1996. **17**(16): p. 1575-1581.

30. Bruins, P., H.T. Velthuis, A.P. Yazdanbakhsh, P.G.M. Jansen, F.W.J. vanHardevelt, E. deBeaumont, C.R.H. Wildevuur, L. Eijsman, A. Trouwborst and C.E. Hack, *Activation of the complement system during and after cardiopulmonary bypass surgery - Postsurgery activation involves C-reactive protein and is associated with postoperative arrhythmia.* Circulation, 1997. **96**(10): p. 3542-3548.

31. Adams, E.M., M.C. Brown, M. Nunge, M. Krych and J.P. Atkinson, *Contribution of the Repeating Domains of Membrane Cofactor Protein (Cd46) of the*

Complement-System to Ligand-Binding and Cofactor Activity. Journal of Immunology, 1991. **147**(9): p. 3005-3011.

32. Digeon, M., M. Laver, J. Riza and J.F. Bach, *Detection of circulating immune complexes in human sera by simplified assays with polyethylene glycol.* Journal of Immunological Methods, 1977. **16**(2): p. 165-183.

33. Mosqueira, V.C.F., P. Legrand, A. Gulik, O. Bourdon, R. Gref, D. Labarre and G. Barratt, *Relationship between complement activation, cellular uptake and surface physicochemical aspects of novel PEG-modified nanocapsules.* Biomaterials, 2001. **22**(22): p. 2967-2979.

34. Sawhney, A.S. and J.A. Hubbell, *Poly(Ethylene Oxide)-Graft-Poly(L-Lysine) Copolymers to Enhance the Biocompatibility of Poly(L-Lysine)-Alginate Microcapsule Membranes.* Biomaterials, 1992. **13**(12): p. 863-870.

35. Vonarbourg, A., C. Passirani, P. Saulnier and J.-P. Benoit, *Parameters influencing the stealthiness of colloidal drug delivery systems.* Biomaterials, 2006. **27**(24): p. 4356-4373.

36. Vonarbourg, A., C. Passirani, P. Saulnier, P. Simard, J.C. Leroux and J.P. Benoit, *Evaluation of pegylated lipid nanocapsules versus complement system activation and macrophage uptake.* Journal of Biomedical Materials Research Part A, 2006. **78A**(3): p. 620-628.

37. Elbert, D.L. and J.A. Hubbell, *Surface treatments of polymers for biocompatibility.* Annual Review of Materials Science, 1996. **26**: p. 365-394.

38. Gorbet, M.B. and M.V.M.V. Sefton, *Biomaterial-associated thrombosis: roles of coagulation factors, complement, platelets and leukocytes.* Biomaterials, 2004. **25**(26): p. 5681-5703.

39. Savage, B., E. Saldivar and Z.M. Ruggeri, *Initiation of Platelet Adhesion by Arrest onto Fibrinogen or Translocation on von Willebrand Factor.* Cell, 1996. **84**(2): p. 289-297.

40. Amiji, M. and K. Park, *Surface Modification of Polymeric Biomaterials with Poly(Ethylene Oxide), Albumin, and Heparin for Reduced Thrombogenicity.* Journal of Biomaterials Science-Polymer Edition, 1993. **4**(3): p. 217-234.

41. Kamath, K.R. and K. Park, *Surface Modification of Polymeric Biomaterials by Albumin Grafting Using Gamma-Irradiation.* Journal of Applied Biomaterials, 1994. **5**(2): p. 163-173.

42. Tseng, Y.C., T. McPherson, C.S. Yuan and K. Park, *Grafting of Ethylene Glycol-Butadiene Block-Copolymers onto Dimethyl-Dichlorosilane-Coated Glass by Gamma-Irradiation.* Biomaterials, 1995. **16**(13): p. 963-972.

43. Tseng, Y.C., W.M. Mullins and K. Park, *Albumin Grafting on to Polypropylene by Thermal-Activation.* Biomaterials, 1993. **14**(5): p. 392-400.

44. Halperin, A., *Polymer brushes that resist adsorption of model proteins: Design parameters.* Langmuir, 1999. **15**(7): p. 2525-2533.

45. Sheth, S.R. and D. Leckband, *Measurements of attractive forces between proteins and end-grafted poly(ethylene glycol) chains.* PNAS, 1997. **94**(16): p. 8399-8404.

46. Jeon, S.I. and J.D. Andrade, *Protein--surface interactions in the presence of polyethylene oxide : II. Effect of Protein Size.* Journal of Colloid and Interface Science, 1991. **142**(1): p. 159-166.

47. Jeon, S.I., J.H. Lee, J.D. Andrade and P.G. De Gennes, *Protein--surface interactions in the presence of polyethylene oxide : I. Simplified theory.* Journal of Colloid and Interface Science, 1991. **142**(1): p. 149-158.

48. Seifert, L.M. and R.T. Greer, *Evaluation of in vivo adsorption of blood elements onto hydrogel-coated silicone rubber by scanning electron microscopy and fourier transform infrared spectroscopy.* Journal Of Biomedical Materials Research, 1985. **19**(9): p. 1043-1071.

49. Sharma, S., K.C. Popat and T.A. Desai, *Controlling nonspecific protein interactions in silicon biomicrosystems with nanostructured poly(ethylene glycol) films.* Langmuir, 2002. **18**(23): p. 8728-8731.

50. McPherson, T., A. Kidane, I. Szleifer and K. Park, *Prevention of protein adsorption by tethered poly(ethylene oxide) layers: Experiments and single-chain mean-field analysis.* Langmuir, 1998. **14**(1): p. 176-186.

51. Parrish, B., R.B. Breitenkamp and T. Emrick, *PEG- and peptide-grafted aliphatic polyesters by click chemistry.* Journal of the American Chemical Society, 2005. **127**(20): p. 7404-7410.

52. Massia, S.P. and J. Stark, *Immobilized RGD peptides on surface-grafted dextran promote biospecific cell attachment.* Journal of Biomedical Materials Research, 2001. **56**(3): p. 390-399.

53. Kenausis, G.L., J. Voros, D.L. Elbert, N.P. Huang, R. Hofer, L. Ruiz-Taylor, M. Textor, J.A. Hubbell and N.D. Spencer, *Poly(L-lysine)-g-poly(ethylene glycol) layers on metal oxide surfaces: Attachment mechanism and effects of polymer architecture on resistance to protein adsorption.* Journal of Physical Chemistry B, 2000. **104**(14): p. 3298-3309.

54. Suggs, L.J., M.S. Shive, C.A. Garcia, J.M. Anderson and A.G. Mikos, *In vitro cytotoxicity and in vivo biocompatibility of poly(propylene fumarate-co-ethylene glycol) hydrogels.* Journal of Biomedical Materials Research, 1999. **46**(1): p. 22-32.

55. Black, F.E., M. Hartshorne, M.C. Davies, C.J. Roberts, S.J.B. Tendler, P.M. Williams and K.M. Shakesheff, *Surface engineering and surface analysis of a biodegradable polymer with biotinylated end groups.* Langmuir, 1999. **15**(9): p. 3157-3161.

56. Park, J.H., K.D. Park and Y.H. Bae, *PDMS-based polyurethanes with MPEG grafts: synthesis, characterization and platelet adhesion study.* Biomaterials, 1999. **20**(10): p. 943-953.

57. Kishida, A., K. Mishima, E. Corretge, H. Konishi and Y. Ikada, *Interactions of Poly(Ethylene Glycol)-Grafted Cellulose Membranes with Proteins and Platelets.* Biomaterials, 1992. **13**(2): p. 113-118.

58. Liu, L., F.Z. Li, Y.E. Fang and S.R. Guo, *Regioselective grafting of poly(ethylene glycol) onto chitosan and the properties of the resulting copolymers.* Macromolecular Bioscience, 2006. **6**(10): p. 855-861.

59. Zahr, A.S., C.A. Davis and M.V. Pishko, *Macrophage uptake of core-shell nanoparticles surface modified with poly(ethylene glycol).* Langmuir, 2006. **22**(19): p. 8178-8185.

60. Drury, J.L. and D.J. Mooney, *Hydrogels for tissue engineering: scaffold design variables and applications.* Biomaterials, 2003. **24**(24): p. 4337-4351.

61. Sugimoto, M., M. Morimoto, H. Sashiwa, H. Saimoto and Y. Shigemasa, *Preparation and characterization of water-soluble chitin and chitosan derivatives.* Carbohydrate Polymers, 1998. **36**(1): p. 49-59.

62. Zhang, M., X.H. Li, Y.D. Gong, N.M. Zhao and X.F. Zhang, *Properties and biocompatibility of chitosan films modified by blending with PEG.* Biomaterials, 2002. **23**(13): p. 2641-2648.

63. Bearinger, J.P., D.G. Castner, S.L. Golledge, A. Rezania, S. Hubchak and K.E. Healy, *P(AAm-co-EG) interpenetrating polymer networks grafted to oxide surfaces: Surface characterization, protein adsorption, and cell detachment studies.* Langmuir, 1997. **13**(19): p. 5175-5183.

64. Park, J.H. and Y.H. Bae, *Hydrogels based on poly(ethylene oxide) and poly(tetramethylene oxide) or poly(dimethyl siloxane): synthesis, characterization, in vitro protein adsorption and platelet adhesion.* Biomaterials, 2002. **23**(8): p. 1797-1808.

65. Chibowski, S., M. Paszkiewicz and E. Mazur-Opala, *Investigation of the structure of polyethylene glycol (PEG) layers adsorbed at the alumina-polymer solution interface.* Adsorption Science & Technology, 2004. **22**(5): p. 385-392.

66. Muller, M., S. Lee, H.A. Spikes and N.D. Spencer, *The influence of molecular architecture on the macroscopic lubrication properties of the brush-like co-polyelectrolyte poly(L-lysine)-g-poly(ethylene glycol) (PLL-g-PEG) adsorbed on oxide surfaces.* Tribology Letters, 2003. **15**(4): p. 395-405.

67. Chibowski, S. and M. Paszkiewicz, *Studies of some properties and the structure of polyethylene glycol (PEG) macromolecules adsorbed on a TiO2 surface.* Adsorption Science & Technology, 2001. **19**(5): p. 397-407.

68. Woodle, M.C., M.S. Newman and F.J. Martin, *Liposome Leakage and Blood-Circulation - Comparison of Adsorbed Block Copolymers with Covalent Attachment of Peg.* International Journal of Pharmaceutics, 1992. **88**(1-3): p. 327-334.

69. Nie, F.-Q., Z.-K. Xu, Q. Yang, J. Wu and L.-S. Wan, *Surface modification of poly(acrylonitrile-co-maleic acid) membranes by the immobilization of poly(ethylene glycol).* Journal of Membrane Science, 2004. **235**(1-2): p. 147-155.

70. Nie, F.-Q., Z.-K. Xu, P. Ye, J. Wu and P. Seta, *Acrylonitrile-based copolymer membranes containing reactive groups: effects of surface-immobilized poly(ethylene glycol)s on anti-fouling properties and blood compatibility.* Polymer, 2004. **45**(2): p. 399-407.

71. Hern, D.L. and J.A. Hubbell, *Incorporation of adhesion peptides into nonadhesive hydrogels useful for tissue resurfacing.* Journal of Biomedical Materials Research, 1998. **39**(2): p. 266-276.

72. Jeong, B., Y.H. Bae and S.W. Kim, *Drug release from biodegradable injectable thermosensitive hydrogel of PEG-PLGA-PEG triblock copolymers.* Journal of Controlled Release, 2000. **63**(1-2): p. 155-163.

73. Sawhney, A.S., C.P. Pathak and J.A. Hubbell, *Bioerodible Hydrogels Based on Photopolymerized Poly(Ethylene Glycol)-Co-Poly(Alpha-Hydroxy Acid) Diacrylate Macromers.* Macromolecules, 1993. **26**(4): p. 581-587.

74. Kim, G.M. and W.H. Jo, *Synthesis and physical properties of pH-sensitive semi-IPN hydrogels based on poly(dimethylaminoethyl methaerylate-co-PEG dimethacrylate) and poly(acrylic acid).* Fibers and Polymers, 2006. **7**(3): p. 223-228.

75. Barber, T.A., L.J. Gamble, D.G. Castner and K.E. Healy, *In vitro characterization of peptide-modified p(AAm-co-EG/AAc) IPN-coated titanium implants.* Journal of Orthopaedic Research, 2006. **24**(7): p. 1366-1376.

76. Kumar, H., Siddaramaiah, R. Somashekar, S.S. Mahesh, S. Abhishek, T.N.G. Row and G.S. Kini, *Structure-property relationship of polyethylene glycol-based PU/PAN semi-interpenetrating polymer networks.* Journal of Applied Polymer Science, 2006. **99**(1): p. 177-187.

77. Aoki, T., M. Kawashima, H. Katono, K. Sanui, N. Ogata, T. Okano and Y. Sakurai, *Temperature-Responsive Interpenetrating Polymer Networks Constructed with Poly(Acrylic Acid) and Poly(N,N-Dimethylacrylamide).* Macromolecules, 1994. **27**(4): p. 947-952.

78. Okano, T., *Molecular Design of Temperature-Responsive Polymers as Intelligent Materials.* Advances in Polymer Science, 1993. **110**: p. 179-197.

79. Jang, H.S., K.E. Ryu, W.S. Ahn, H.J. Chun, H. Dal Park, K.D. Park and Y.H. Kim, *Complement activation by sulfonated poly(ethylene glycol)-acrylate copolymers through alternative pathway.* Colloids and Surfaces B: Biointerfaces, 2006. **50**(2): p. 141-146.

80. Corneillie, S., P.N. Lan, E. Schacht, M. Davies, A. Shard, R. Green, S. Denyer, M. Wassall, H. Whitfield and S. Choong, *Polyethylene glycol-containing polyurethanes for biomedical applications.* Polymer International, 1998. **46**(3): p. 251-259.

81. Wesslen, B., M. Kober, C. Freijlarsson, A. Ljungh and M. Paulsson, *Protein Adsorption of Poly(Ether Urethane) Surfaces Modified by Amphiphilic and Hydrophilic Polymers.* Biomaterials, 1994. **15**(4): p. 278-284.

82. Lee, J.H., Y.M. Ju and D.M. Kim, *Platelet adhesion onto segmented polyurethane film surfaces modified by addition and crosslinking of PEO-containing block copolymers.* Biomaterials, 2000. **21**(7): p. 683-691.

83. Xu, Z.-K., F.-Q. Nie, C. Qu, L.-S. Wan, J. Wu and K. Yao, *Tethering poly(ethylene glycol)s to improve the surface biocompatibility of poly(acrylonitrile-co-maleic acid) asymmetric membranes.* Biomaterials, 2005. **26**(6): p. 589-598.

84. Kidane, A., G.C. Lantz, S. Jo and K. Park, *Surface modification with PEO-containing triblock copolymer for improved biocompatibility: In vitro and ex vivo studies.* Journal of Biomaterials Science-Polymer Edition, 1999. **10**(10): p. 1089-1105.

85. Maas, C.S., T. Eriksson, T. McCalmont, M. Mabry, D. Cooke and R. Schindler, *Evaluation of expanded polytetrafluoroethylene as a soft-tissue filling substance: An analysis of design-related implant behavior using the porcine skin model.* Plastic and Reconstructive Surgery, 1998. **101**(5): p. 1307-1314.

86. Salzmann, D.L., L.B. Kleinert, S.S. Berman and S.K. Williams, *The effects of porosity on endothelialization of ePTFE implanted in subcutaneous and adipose tissue.* Journal of Biomedical Materials Research, 1997. **34**(4): p. 463-476.

87. Bellon, J.M., J. Bujan, L.A. Contreras, A. Hernando and F. Jurado, *Similarity in behavior of polytetrafluoroethylene (ePTFE) prostheses implanted into different interfaces.* Journal of Biomedical Materials Research, 1996. **31**(1): p. 1-9.

88. Greisler, H.P., D.J. Cziperle, D.U. Kim, J.D. Garfield, D. Petsikas, P.M. Murchan, E.O. Applegren, W. Drohan and W.H. Burgess, *Enhanced Endothelialization of Expanded Polytetrafluoroethylene Grafts by Fibroblast Growth-Factor Type-1 Pretreatment.* Surgery, 1992. **112**(2): p. 244-255.

89. Zhang, Q., C.R. Wang, Y. Babukutty, T. Ohyama, M. Kogoma and M. Kodama, *Biocompatibility evaluation of ePTFE membrane modified with PEG in atmospheric pressure glow discharge.* Journal of Biomedical Materials Research, 2002. **60**(3): p. 502-509.

90. Sofia, S.J., V. Premnath and E.W. Merrill, *Poly(ethylene oxide) grafted to silicon surfaces: Grafting density and protein adsorption.* Macromolecules, 1998. **31**(15): p. 5059-5070.

91. Yang, Z.H., J.A. Galloway and H.U. Yu, *Protein interactions with poly(ethylene glycol) self-assembled monolayers on glass substrates: Diffusion and adsorption.* Langmuir, 1999. **15**(24): p. 8405-8411.

92. Prime, K.L. and G.M. Whitesides, *Adsorption of Proteins onto Surfaces Containing End-Attached Oligo(Ethylene Oxide) - a Model System Using Self-Assembled Monolayers.* Journal of the American Chemical Society, 1993. **115**(23): p. 10714-10721.

93. Hostetler, M.J., A.C. Templeton and R.W. Murray, *Dynamics of place-exchange reactions on monolayer-protected gold cluster molecules.* Langmuir, 1999. **15**(11): p. 3782-3789.

94. Laibinis, P.E. and G.M. Whitesides, *Self-Assembled Monolayers of N-Alkanethiolates on Copper Are Barrier Films That Protect the Metal against Oxidation by Air.* Journal of the American Chemical Society, 1992. **114**(23): p. 9022-9028.

95. Hickman, J.J., D. Ofer, C.F. Zou, M.S. Wrighton, P.E. Laibinis and G.M. Whitesides, *Selective Functionalization of Gold Microstructures with Ferrocenyl Derivatives Via Reaction with Thiols or Disulfides - Characterization by Electrochemistry and Auger-Electron Spectroscopy.* Journal of the American Chemical Society, 1991. **113**(4): p. 1128-1132.

96. Alcantar, N.A., E.S. Aydil and J.N. Israelachvili, *Polyethylene glycol-coated biocompatible surfaces.* Journal of Biomedical Materials Research, 2000. **51**(3): p. 343-351.

97. Allen, T.M., *Long-circulating (sterically stabilized) liposomes for targeted drug delivery.* Trends in Pharmacological Sciences, 1994. **15**(7): p. 215-220.

98. Lasic, D.D. and D. Needham, *The ''Stealth'' liposome: A prototypical biomaterial.* Chemical Reviews, 1995. **95**(8): p. 2601-2628.

99. Moghimi, S.M., I. Hamad, R. Bunger, T.L. Andresen, K. Jorgensen, A.C. Hunter, L. Baranji, L. Rosivall and J. Szebeni, *Activation of the human complement system by cholesterol-rich and pegylated liposomes - Modulation of cholesterol-rich liposome-mediated complement activation by elevated serum LDL and HDL levels.* Journal of Liposome Research, 2006. **16**(3): p. 167-174.

100. Moghimi, S.M., A.C. Hunter and J.C. Murray, *Long-circulating and target-specific nanoparticles: Theory to practice.* Pharmacological Reviews, 2001. **53**(2): p. 283-318.

101. Meng, F.H., G.H.M. Engbers, A. Gessner, R.H. Muller and J. Feijen, *Pegylated polystyrene particles as a model system for artificial cells.* Journal of Biomedical Materials Research Part A, 2004. **70A**(1): p. 97-106.

102. Ishida, T., M. Harada, X.Y. Wang, M. Ichihara, K. Irimura and H. Kiwada, *Accelerated blood clearance of PEGylated liposomes following preceding liposome injection: Effects of lipid dose and PEG surface-density and chain length of the first-dose liposomes.* Journal of Controlled Release, 2005. **105**(3): p. 305-317.

103. Ishida, T., R. Maeda, M. Ichihara, K. Irimura and H. Kiwada, *Accelerated clearance of PEGylated liposomes in rats after repeated injections.* Journal of Controlled Release, 2003. **88**(1): p. 35-42.

104. Ishida, T., M. Ichihara, X. Wang, K. Yamamoto, J. Kimura, E. Majima and H. Kiwada, *Injection of PEGylated liposomes in rats elicits PEG-specific IgM, which is responsible for rapid elimination of a second dose of PEGylated liposomes.* Journal of Controlled Release, 2006. **112**(1): p. 15-25.

105. Szebeni, J., *Complement activation-related pseudoallergy: A new class of drug-induced acute immune toxicity.* Toxicology, 2005. **216**(2-3): p. 106-121.

106. Bradley, A.J., S.T. Test, K.L. Murad, J. Mitsuyoshi and M.D. Scott, *Interactions of IgM ABO antibodies and complement with methoxy-PEG-modified human RBCs.* Transfusion, 2001. **41**(10): p. 1225-1233.

References

Effect of Intensive Diabetes Management on Macrovascular Events and Risk-Factors in the Diabetes Control and Complications Trial. Am J Cardiol, 1995. **75**(14): p. 894-903.

Effect of Intensive Therapy on the Development and Progression of Diabetic Nephropathy in the Diabetes Control and Complications Trial. Kidney Int, 1995. **47**(6): p. 1703-1720.

Influence of Intensive Diabetes Treatment on Quality-of-Life Outcomes in the Diabetes Control and Complications Trial. Diabetes Care, 1996. **19**(3): p. 195-203.

Adams, E.M., M.C. Brown, M. Nunge, M. Krych, and J.P. Atkinson, *Contribution of the Repeating Domains of Membrane Cofactor Protein (Cd46) of the Complement-System to Ligand-Binding and Cofactor Activity.* Journal of Immunology, 1991. **147**(9): p. 3005-3011.

Ahmad, B., *Pharmacology of Insulin.* British Journal of Diabetes & Vascular Disease, 2004. **4**(10): p. 10-14.

Ajees, A.A., K. Gunasekaran, J.E. Volanakis, S.V.L. Narayana, G.J. Kotwal, and H.M.K. Murthy, *The Structure of Complement C3b Provides Insights into Complement Activation and Regulation.* Nature, 2006. **444**(7116): p. 221-225.

Albers, J.W., D.J. Kenny, M. Brown, D. Greene, P.A. Cleary, J.M. Lachin, and D.M. Nathan, *Effect of Intensive Diabetes Treatment on Nerve Conduction in the Diabetes Control and Complications Trial.* Ann Neurol, 1995. **38**(6): p. 869-880.

Alberts, B., A. Johnson, J. Lewis, M. Raff, K. Roberts, and P. Walter, *Molecular Biology of the Cell*. 4th ed. 2002, New York: Garland Science.

Albin, G., T.A. Horbett, and B.D. Ratner, *Glucose Sensitive Membranes for Controlled Delivery of Insulin: Insulin Transport Studies.* J Control Release, 1985. **2**: p. 153-164.

Alcantar, N.A., E.S. Aydil, and J.N. Israelachvili, *Polyethylene Glycol-Coated Biocompatible Surfaces.* Journal of Biomedical Materials Research, 2000. **51**(3): p. 343-351.

Allen, T.M., *Long-Circulating (Sterically Stabilized) Liposomes for Targeted Drug Delivery.* Trends in Pharmacological Sciences, 1994. **15**(7): p. 215-220.

Alton, G., S. Kjaergaard, J.R. Etchison, F. Skovby, and H.H. Freeze, *Oral Ingestion of Mannose Elevates Blood Mannose Levels: A First Step toward a Potential Therapy*

for Carbohydrate-Deficient Glycoprotein Syndrome Type I. Biochem Mol Med, 1997. **60**(2): p. 127-133.

Amalvy, J.I., E.J. Wanless, Y. Li, V. Michailidou, S.P. Armes, and Y. Duccini, *Synthesis and Characterization of Novel Ph-Responsive Microgels Based on Tertiary Amine Methacrylates.* Langmuir, 2004. **20**(21): p. 8992-8999.

Amende, M.T., D. Hariharan, and N.A. Peppas, *Factors Influencing Drug and Protein-Transport and Release from Ionic Hydrogels.* React Polym, 1995. **25**(2-3): p. 127-137.

Amiji, M. and K. Park, *Surface Modification of Polymeric Biomaterials with Poly(Ethylene Oxide), Albumin, and Heparin for Reduced Thrombogenicity.* Journal of Biomaterials Science-Polymer Edition, 1993. **4**(3): p. 217-234.

Anderson, B.C. and S.K. Mallapragada, *Synthesis and Characterization of Injectable, Water-Soluble Copolymers of Tertiary Amine Methacrylates and Poly(Ethylene Glycol) Containing Methacrylates.* Biomaterials, 2002. **23**(22): p. 4345-4352.

Andersson, J., K.N. Ekdahl, J.D. Lambris, and B. Nilsson, *Binding of C3 Fragments on Top of Adsorbed Plasma Proteins During Complement Activation on a Model Biomaterial Surface.* Biomaterials, 2005. **26**(13): p. 1477-1485.

Aoki, T., M. Kawashima, H. Katono, K. Sanui, N. Ogata, T. Okano, and Y. Sakurai, *Temperature-Responsive Interpenetrating Polymer Networks Constructed with Poly(Acrylic Acid) and Poly(N,N-Dimethylacrylamide).* Macromolecules, 1994. **27**(4): p. 947-952.

Babensee, J.E., J.M. Anderson, L.V. Mcintire, and A.G. Mikos, *Host Response to Tissue Engineered Devices.* Advanced Drug Delivery Reviews, 1998. **33**(1-2): p. 111-139.

Bagshaw, S.M. and R.T.N. Gibney, *Conventional Markers of Kidney Function.* Crit Care Med, 2008. **36**(4): p. S152-S158.

Baker, J.P., L.H. Hong, H.W. Blanch, and J.M. Prausnitz, *Effect of Initial Total Monomer Concentration on the Swelling Behavior of Cationic Acrylamide-Based Hydrogels.* Macromolecules, 1994. **27**(6): p. 1446-1454.

Ballerstadt, R., C. Evans, R. Mcnichols, and A. Gowda, *Concanavalin a for in Vivo Glucose Sensing: A Biotoxicity Review.* Biosens Bioelectron, 2006. **22**(2): p. 275-284.

Barber, T.A., L.J. Gamble, D.G. Castner, and K.E. Healy, *In Vitro Characterization of Peptide-Modified P(Aam-Co-Eg/Aac) Ipn-Coated Titanium Implants.* Journal of Orthopaedic Research, 2006. **24**(7): p. 1366-1376.

Bearinger, J.P., D.G. Castner, S.L. Golledge, A. Rezania, S. Hubchak, and K.E. Healy, *P(Aam-Co-Eg) Interpenetrating Polymer Networks Grafted to Oxide Surfaces: Surface Characterization, Protein Adsorption, and Cell Detachment Studies.* Langmuir, 1997. **13**(19): p. 5175-5183.

Bellon, J.M., J. Bujan, L.A. Contreras, A. Hernando, and F. Jurado, *Similarity in Behavior of Polytetrafluoroethylene (Eptfe) Prostheses Implanted into Different Interfaces.* Journal of Biomedical Materials Research, 1996. **31**(1): p. 1-9.

Bergmann-Leitner, E.S., W.W. Leitner, and G.C. Tsokos, *Complement 3d: From Molecular Adjuvant to Target of Immune Escape Mechanisms.* Clinical Immunology, 2006. **121**(2): p. 177-185.

Bergmeyer, H.U., J. Bergmeyer, and M. Grassl, *Methods of Enzymatic Analysis*. 3rd ed. 1983, Weinheim ; Deerfield Beach, Fla.: Verlag Chemie.

Bermejo, F., D. Boixeda, J.P. Gisbert, V. Defarges, J.M. Sanz, C. Redondo, C.M. De Argila, and A.G. Plaza, *Rapid Urease Test Utility for Helicobacter Pylori Infection Diagnosis in Gastric Ulcer Disease.* Hepato-Gastroenterol, 2002. **49**(44): p. 572-575.

Biondi, O., S. Motta, and P. Mosesso, *Low Molecular Weight Polyethylene Glycol Induces Chromosome Aberrations in Chinese Hamster Cells Cultured in Vitro.* Mutagenesis, 2002. **17**(3): p. 261-264.

Bjork, S., *The Cost of Diabetes and Diabetes Care.* Diabetes Res Clin Pr, 2001. **54**: p. S13-S18.

Black, F.E., M. Hartshorne, M.C. Davies, C.J. Roberts, S.J.B. Tendler, P.M. Williams, and K.M. Shakesheff, *Surface Engineering and Surface Analysis of a Biodegradable Polymer with Biotinylated End Groups.* Langmuir, 1999. **15**(9): p. 3157-3161.

Bodde, H.E., E.A.C. Vanaalten, and H.E. Junginger, *Hydrogel Patches for Transdermal Drug Delivery - Invivo Water Exchange and Skin Compatibility.* J Pharm Pharmacol, 1989. **41**(3): p. 152-155.

Bradley, A.J., S.T. Test, K.L. Murad, J. Mitsuyoshi, and M.D. Scott, *Interactions of Igm Abo Antibodies and Complement with Methoxy-Peg-Modified Human Rbcs.* Transfusion, 2001. **41**(10): p. 1225-1233.

Bromberg, L. and L. Salvati, *Bioactive Surfaces Via Immobilization of Self-Assembling Polymers onto Hydrophobic Materials.* Bioconjugate Chem, 1999. **10**(4): p. 678-686.

Brownlee, M. and A. Cerami, *Glucose-Controlled Insulin-Delivery System - Semi-Synthetic Insulin Bound to Lectin.* Science, 1979. **206**(4423): p. 1190-1191.

Bruining, M.J., H.G.T. Blaauwgeers, R. Kuijer, E. Pels, R. Nuijts, and L.H. Koole, *Biodegradable Three-Dimensional Networks of Poly(Dimethylamino Ethyl Methacrylate). Synthesis, Characterization and in Vitro Studies of Structural Degradation and Cytotoxicity.* Biomaterials, 2000. **21**(6): p. 595-604.

Bruining, M.J., P.S. Edelbroek-Hoogendoorn, H.G.T. Blaauwgeers, C.M. Mooy, F.H. Hendrikse, and L.H. Koole, *New Biodegradable Networks of Poly(N-Vinylpyrrolidinone) Designed for Controlled Nonburst Degradation in the Vitreous Body.* J Biomed Mater Res, 1999. **47**(2): p. 189-197.

Bruins, P., H.T. Velthuis, A.P. Yazdanbakhsh, P.G.M. Jansen, F.W.J. Vanhardevelt, E. Debeaumont, C.R.H. Wildevuur, L. Eijsman, A. Trouwborst, and C.E. Hack, *Activation of the Complement System During and after Cardiopulmonary Bypass Surgery - Postsurgery Activation Involves C-Reactive Protein and Is Associated with Postoperative Arrhythmia.* Circulation, 1997. **96**(10): p. 3542-3548.

Butun, V., S.P. Armes, and N.C. Billingham, *Synthesis and Aqueous Solution Properties of near-Monodisperse Tertiary Amine Methacrylate Homopolymers and Diblock Copolymers.* Polymer, 2001. **42**(14): p. 5993-6008.

Byrne, M.E., E. Oral, J.Z. Hilt, and N.A. Peppas, *Networks for Recognition of Biomolecules: Molecular Imprinting and Micropatterning Poly(Ethylene Glycol)-Containing Films.* Polym Advan Technol, 2002. **13**(10-12): p. 798-816.

Carroll, M.C., *The Role of Complement and Complement Receptors in Induction and Regulation of Immunity.* Annual Review of Immunology, 1998. **16**: p. 545-568.

Chang, X.Q., A.M.M. Jorgensen, P. Bardrum, and J.J. Led, *Solution Structures of the R-6 Human Insulin Hexamer.* Biochemistry-Us, 1997. **36**(31): p. 9409-9422.

Chen, J., Y.Q. Yang, P.B. Qian, Z.T. Ma, W.B. Wu, P.Z. Sung, X.G. Wang, and J.H. Li, *Drug Carrying Hydrogel Base Wound Dressing.* Radiat Phys Chem, 1993. **42**(4-6): p. 915-918.

Chibowski, S. and M. Paszkiewicz, *Studies of Some Properties and the Structure of Polyethylene Glycol (Peg) Macromolecules Adsorbed on a Tio2 Surface.* Adsorption Science & Technology, 2001. **19**(5): p. 397-407.

Chibowski, S., M. Paszkiewicz, and E. Mazur-Opala, *Investigation of the Structure of Polyethylene Glycol (Peg) Layers Adsorbed at the Alumina-Polymer Solution Interface.* Adsorption Science & Technology, 2004. **22**(5): p. 385-392.

Chung, D.J., Y. Ito, and Y. Imanishi, *An Insulin-Releasing Membrane System on the Basis of Oxidation Reaction of Glucose.* J Control Release, 1992. **18**(1): p. 45-53.

Cooney, D.O., *Biomedical Engineering Principles : An Introduction to Fluid, Heat, and Mass Transport Processes*. Biomedical Engineering and Instrumentation Series. 1976, New York: M. Dekker. xvi, 458 p.

Corneillie, S., P.N. Lan, E. Schacht, M. Davies, A. Shard, R. Green, S. Denyer, M. Wassall, H. Whitfield, and S. Choong, *Polyethylene Glycol-Containing Polyurethanes for Biomedical Applications.* Polymer International, 1998. **46**(3): p. 251-259.

Cornejo-Bravo, J.M. and R.A. Siegel, *Water Vapour Sorption Behaviour of Copolymers of N,N-Diethylaminoethyl Methacrylate and Methyl Methacrylate.* Biomaterials, 1996. **17**(12): p. 1187-1193.

De Filippo, R.E., J.J. Yoo, and A. Atala, *Urethral Replacement Using Cell Seeded Tubularized Collagen Matrices.* J Urol, 2002. **168**(4): p. 1789-1792.

Dempsey, P.W., M.E.D. Allison, S. Akkaraju, C.C. Goodnow, and D.T. Fearon, *C3d of Complement as a Molecular Adjuvant: Bridging Innate and Acquired Immunity.* Science, 1996. **271**(5247): p. 348-350.

Dhanarajan, A.P. and R.A. Siegel, *Time-Dependent Permeabilities of Hydrophobic, Ph-Sensitive Hydrogels Exposed to Ph Gradients.* Macromol Symp, 2005. **227**: p. 105-114.

Digeon, M., M. Laver, J. Riza, and J.F. Bach, *Detection of Circulating Immune Complexes in Human Sera by Simplified Assays with Polyethylene Glycol.* Journal of Immunological Methods, 1977. **16**(2): p. 165-183.

Dorski, C.M., F.J. Doyle, and N.A. Peppas, *Glucose-Responsive, Complexation Hydrogels.* Abstr Pap Am Chem S, 1996. **211**: p. 417-POLY.

Dorski, C.M., F.J. Doyle, and N.A. Peppas, *Preparation and Characterization of Glucose-Sensitive P(Maa-G-Eg) Hydrogels.* Abstr Pap Am Chem S, 1997. **213**: p. 172-PMSE.

Drury, J.L. and D.J. Mooney, *Hydrogels for Tissue Engineering: Scaffold Design Variables and Applications.* Biomaterials, 2003. **24**(24): p. 4337-4351.

Elbert, D.L. and J.A. Hubbell, *Surface Treatments of Polymers for Biocompatibility.* Annual Review of Materials Science, 1996. **26**: p. 365-394.

Farmer, T.G., T.F. Edgar, and N.A. Peppas, *In Vivo Simulations of the Intravenous Dynamics of Submicrometer Particles of Ph-Responsive Cationic Hydrogels in Diabetic Patients.* Ind Eng Chem Res, 2008. **47**(24): p. 10053-10063.

Firestone, B.A. and R.A. Siegel, *Dynamic Ph-Dependent Swelling Properties of a Hydrophobic Poly-Electrolyte Gel.* Polym Commun, 1988. **29**(7): p. 204-208.

Firestone, B.A. and R.A. Siegel, *Kinetics and Mechanisms of Water Sorption in Hydrophobic, Ionizable Copolymer Gels.* J Appl Polym Sci, 1991. **43**(5): p. 901-914.

Firestone, B.A. and R.A. Siegel, *Ph, Salt, and Buffer Dependent Swelling in Ionizable Copolymer Gels - Tests of the Ideal Donnan Equilibrium-Theory.* J Biomat Sci-Polym E, 1994. **5**(5): p. 433-450.

Fisher, O.Z. and N.A. Peppas, *Polybasic Nanomatrices Prepared by Uv-Initiated Photopolymerization.* Macromolecules, 2009. **42**(9): p. 3391-3398.

Genuth, S., J. Lipps, G. Lorenzi, D.M. Nathan, M.D. Davis, J.M. Lachin, and P.A. Cleary, *Effect of Intensive Therapy on the Microvascular Complications of Type 1 Diabetes Mellitus.* Jama-J Am Med Assoc, 2002. **287**(19): p. 2563-2569.

Goldraich, M. and J. Kost, *Glucose-Sensitive Polymeric Matrices for Controlled Drug Delivery.* Clin Mater, 1993. **13**(1-4): p. 135-142.

Gorbet, M.B. and M.V.M.V. Sefton, *Biomaterial-Associated Thrombosis: Roles of Coagulation Factors, Complement, Platelets and Leukocytes.* Biomaterials, 2004. **25**(26): p. 5681-5703.

Graiver, D., R.L. Durall, and T. Okada, *Surface Morphology and Friction Coefficient of Various Types of Foley Catheter.* Biomaterials, 1993. **14**(6): p. 465-469.

Greisler, H.P., D.J. Cziperle, D.U. Kim, J.D. Garfield, D. Petsikas, P.M. Murchan, E.O. Applegren, W. Drohan, and W.H. Burgess, *Enhanced Endothelialization of Expanded Polytetrafluoroethylene Grafts by Fibroblast Growth-Factor Type-1 Pretreatment.* Surgery, 1992. **112**(2): p. 244-255.

Gristina, A.G., J.J. Dobbins, B. Giammara, J.C. Lewis, and W.C. Devries, *Biomaterial-Centered Sepsis and the Total Artificial-Heart - Microbial Adhesion Vs Tissue Integration.* Jama-Journal of the American Medical Association, 1988. **259**(6): p. 870-874.

Guyton, A.C. and J.E. Hall, *Textbook of Medical Physiology*. 11th ed. 2006, Philadelphia: Elsevier Saunders. xxxv, 1116 p.

Halperin, A., *Polymer Brushes That Resist Adsorption of Model Proteins: Design Parameters.* Langmuir, 1999. **15**(7): p. 2525-2533.

Hanks, C.T., J.C. Wataha, and Z. Sun, *In Vitro Models of Biocompatibility: A Review.* Dental Materials, 1996. **12**(3): p. 186-193.

Hansson, K.M., S. Tosatti, J. Isaksson, J. Wettero, M. Textor, T.L. Lindahl, and P. Tengvall, *Whole Blood Coagulation on Protein Adsorption-Resistant Peg and Peptide*

Functionalised Peg-Coated Titanium Surfaces. Biomaterials, 2005. **26**(8): p. 861-872.

Hariharan, D. and N.A. Peppas, *Characterization, Dynamic Swelling Behaviour and Solute Transport in Cationic Networks with Applications to the Development of Swelling-Controlled Release Systems.* Polymer, 1996. **37**(1): p. 149-161.

Hariharan, D., N.A. Peppas, R. Bettini, and P. Colombo, *Mathematical-Analysis of Drug-Delivery from Swellable Systems with Partial Physical Restrictions or Impermeable Coatings.* Int J Pharm, 1994. **112**(1): p. 47-54.

Hassan, C.M., F.J. Doyle, and N.A. Peppas, *Dynamic Behavior of Glucose-Responsive Poly(Methacrylic Acid-G-Ethylene Glycol) Hydrogels.* Macromolecules, 1997. **30**(20): p. 6166-6173.

Hayashi, H., M. Iijima, K. Kataoka, and Y. Nagasaki, *Ph-Sensitive Nanogel Possessing Reactive Peg Tethered Chains on the Surface.* Macromolecules, 2004. **37**(14): p. 5389-5396.

Heller, A., *Integrated Medical Feedback Systems for Drug Delivery.* AIChE J, 2005. **51**(4): p. 1054-1066.

Heller, A., *Electron-Conducting Redox Hydrogels: Design, Characteristics and Synthesis.* Curr Opin Chem Biol, 2006. **10**(6): p. 664-672.

Heller, J., A.C. Chang, G. Rood, and G.M. Grodsky, *Release of Insulin from Ph-Sensitive Poly(Ortho Esters).* J Control Release, 1990. **13**(2-3): p. 295-302.

Hellgren, A.-C., P. Weissenborn, and K. Holmberg, *Surfactants in Water-Borne Paints.* Prog Org Coat, 1999. **35**(1-4): p. 79-87.

Hern, D.L. and J.A. Hubbell, *Incorporation of Adhesion Peptides into Nonadhesive Hydrogels Useful for Tissue Resurfacing.* Journal of Biomedical Materials Research, 1998. **39**(2): p. 266-276.

Hickman, J.J., D. Ofer, C.F. Zou, M.S. Wrighton, P.E. Laibinis, and G.M. Whitesides, *Selective Functionalization of Gold Microstructures with Ferrocenyl Derivatives Via Reaction with Thiols or Disulfides - Characterization by Electrochemistry and Auger-Electron Spectroscopy.* Journal of the American Chemical Society, 1991. **113**(4): p. 1128-1132.

Hilt, J.Z., M.E. Byrne, and N.A. Peppas, *Microfabrication of Intelligent Biomimetic Networks for Recognition of D-Glucose.* Chem Mater, 2006. **18**(25): p. 5869-5875.

Hirotsu, S., *Coexistence of Phases and the Nature of 1st-Order Phase-Transition in Poly-N-Isopropylacrylamide Gels.* Adv Polym Sci, 1993. **110**: p. 1-26.

Hoffman, A.S., *Hydrogels for Biomedical Applications.* Ann Ny Acad Sci, 2001. **944**(1): p. 62-73.

Hoogeveen, N.G., M.A.C. Stuart, G.J. Fleer, W. Frank, and M. Arnold, *Novel Water-Soluble Block Copolymers of Dimethylaminoethyl Methacrylate and Dihydroxypropyl Methacrylate.* Macromol Chem Physic, 1996. **197**(8): p. 2553-2564.

Hostetler, M.J., A.C. Templeton, and R.W. Murray, *Dynamics of Place-Exchange Reactions on Monolayer-Protected Gold Cluster Molecules.* Langmuir, 1999. **15**(11): p. 3782-3789.

Ikada, Y., *Surface Modification of Polymers for Medical Applications.* Biomaterials, 1994. **15**(10): p. 725-736.

Ishida, T., M. Harada, X.Y. Wang, M. Ichihara, K. Irimura, and H. Kiwada, *Accelerated Blood Clearance of Pegylated Liposomes Following Preceding Liposome Injection: Effects of Lipid Dose and Peg Surface-Density and Chain Length of the First-Dose Liposomes.* Journal of Controlled Release, 2005. **105**(3): p. 305-317.

Ishida, T., M. Ichihara, X. Wang, K. Yamamoto, J. Kimura, E. Majima, and H. Kiwada, *Injection of Pegylated Liposomes in Rats Elicits Peg-Specific Igm, Which Is Responsible for Rapid Elimination of a Second Dose of Pegylated Liposomes.* Journal of Controlled Release, 2006. **112**(1): p. 15-25.

Ishida, T., R. Maeda, M. Ichihara, K. Irimura, and H. Kiwada, *Accelerated Clearance of Pegylated Liposomes in Rats after Repeated Injections.* Journal of Controlled Release, 2003. **88**(1): p. 35-42.

Ishihara, K., M. Kobayashi, N. Ishimaru, and I. Shinohara, *Glucose-Induced Permeation Control of Insulin through a Complex Membrane Consisting of Immobilized Glucose-Oxidase and a Poly(Amine).* Polym J, 1984. **16**(8): p. 625-631.

Ishihara, K., M. Kobayashi, and I. Shinohara, *Insulin Permeation through Amphiphilic Polymer Membranes Having 2-Hydroxyethyl Methacrylate Moiety.* Polym J, 1984. **16**(8): p. 647-651.

Ishihara, K., M. Kobayashi, and I. Shionohara, *Control of Insulin Permeation through a Polymer Membrane with Responsive Function for Glucose.* Makromol Chem-Rapid, 1983. **4**(5): p. 327-331.

Ishihara, K. and K. Matsui, *Glucose-Responsive Insulin Release from Polymer Capsule.* J Polym Sci Pol Lett, 1986. **24**(8): p. 413-417.

Ito, Y., M. Casolaro, K. Kono, and Y. Imanishi, *An Insulin-Releasing System That Is Responsive to Glucose.* J Control Release, 1989. **10**(2): p. 195-203.

Janeway, C., *Immunobiology: The Immune System in Health and Disease*. 5th ed. 2001, New York: Garland Science.

Jang, H.S., K.E. Ryu, W.S. Ahn, H.J. Chun, H. Dal Park, K.D. Park, and Y.H. Kim, *Complement Activation by Sulfonated Poly(Ethylene Glycol)-Acrylate Copolymers through Alternative Pathway.* Colloids and Surfaces B: Biointerfaces, 2006. **50**(2): p. 141-146.

Janssen, B.J.C., A. Christodoulidou, A. Mccarthy, J.D. Lambris, and P. Gros, *Structure of C3b Reveals Conformational Changes That Underlie Complement Activity.* Nature, 2006. **444**(7116): p. 213-216.

Jaworek, D., H. Botsch, and J. Maier, *Preparation and Properties of Enzymes Immobilized by Copolymerization.* Methods Enzymol, 1976. **44**: p. 195-20.

Jeon, S.I. and J.D. Andrade, *Protein--Surface Interactions in the Presence of Polyethylene Oxide : Ii. Effect of Protein Size.* Journal of Colloid and Interface Science, 1991. **142**(1): p. 159-166.

Jeon, S.I., J.H. Lee, J.D. Andrade, and P.G. De Gennes, *Protein--Surface Interactions in the Presence of Polyethylene Oxide : I. Simplified Theory.* Journal of Colloid and Interface Science, 1991. **142**(1): p. 149-158.

Jeong, B., Y.H. Bae, and S.W. Kim, *Drug Release from Biodegradable Injectable Thermosensitive Hydrogel of Peg-Plga-Peg Triblock Copolymers.* Journal of Controlled Release, 2000. **63**(1-2): p. 155-163.

Joyce, D.E. and T. Kurucsev, *Hydrogen-Ion Equilibria in Poly(Methacrylic Acid) and Poly(Ethacrylic Acid) Solutions.* Polymer, 1981. **22**(3): p. 415-417.

Ju, H.K., S.Y. Kim, and Y.M. Lee, *Ph/Temperature-Responsive Behaviors of Semi-Ipn and Comb-Type Graft Hydrogels Composed of Alginate and Poly (N-Isopropylacrylamide).* Polymer, 2001. **42**(16): p. 6851-6857.

Kamath, K.R. and K. Park, *Surface Modification of Polymeric Biomaterials by Albumin Grafting Using Gamma-Irradiation.* Journal of Applied Biomaterials, 1994. **5**(2): p. 163-173.

Kataoka, K., H. Miyazaki, M. Bunya, T. Okano, and Y. Sakurai, *Totally Synthetic Polymer Gels Responding to External Glucose Concentration: Their Preparation and Application to on-Off Regulation of Insulin Release.* J Am Chem Soc, 1998. **120**(48): p. 12694-12695.

Kenausis, G.L., J. Voros, D.L. Elbert, N.P. Huang, R. Hofer, L. Ruiz-Taylor, M. Textor, J.A. Hubbell, and N.D. Spencer, *Poly(L-Lysine)-G-Poly(Ethylene Glycol) Layers on Metal Oxide Surfaces: Attachment Mechanism and Effects of Polymer*

Architecture on Resistance to Protein Adsorption. Journal of Physical Chemistry B, 2000. **104**(14): p. 3298-3309.

Khouw, I., P.B. Van Wachem, L. De Leij, and M.J.A. Van Luyn, *Inhibition of the Tissue Reaction to a Biodegradable Biomaterial by Monoclonal Antibodies to Ifn-Gamma.* Journal of Biomedical Materials Research, 1998. **41**(2): p. 202-210.

Kidane, A., G.C. Lantz, S. Jo, and K. Park, *Surface Modification with Peo-Containing Triblock Copolymer for Improved Biocompatibility: In Vitro and Ex Vivo Studies.* Journal of Biomaterials Science-Polymer Edition, 1999. **10**(10): p. 1089-1105.

Kim, G.M. and W.H. Jo, *Synthesis and Physical Properties of Ph-Sensitive Semi-Ipn Hydrogels Based on Poly(Dimethylaminoethyl Methaerylate-Co-Peg Dimethacrylate) and Poly(Acrylic Acid).* Fibers and Polymers, 2006. **7**(3): p. 223-228.

Kim, S.W., *Hydrogel Drug Delivery Systems.* Pharm Int, 1983. **4**(7): p. 182-182.

Kishida, A., K. Mishima, E. Corretge, H. Konishi, and Y. Ikada, *Interactions of Poly(Ethylene Glycol)-Grafted Cellulose Membranes with Proteins and Platelets.* Biomaterials, 1992. **13**(2): p. 113-118.

Kopecek, J. and R. Duncan, *Targetable Polymeric Prodrugs.* J Control Release, 1987. **6**(1): p. 315-327.

Kost, J., T.A. Horbett, B.D. Ratner, and M. Singh, *Glucose-Sensitive Membranes Containing Glucose-Oxidase - Activity, Swelling, and Permeability Studies.* J Biomed Mater Res, 1985. **19**(9): p. 1117-1133.

Kost, J. and R. Langer, *Equilibrium Swollen Hydrogels in Controlled Release Applications*, in *Hydrogels in Medicine and Pharmacy*, N.A. Peppas, Editor. 1986, CRC Press: Boca Raton, Fla. p. 95-107.

Kumar, H., Siddaramaiah, R. Somashekar, S.S. Mahesh, S. Abhishek, T.N.G. Row, and G.S. Kini, *Structure-Property Relationship of Polyethylene Glycol-Based Pu/Pan Semi-Interpenetrating Polymer Networks.* Journal of Applied Polymer Science, 2006. **99**(1): p. 177-187.

Laibinis, P.E. and G.M. Whitesides, *Self-Assembled Monolayers of N-Alkanethiolates on Copper Are Barrier Films That Protect the Metal against Oxidation by Air.* Journal of the American Chemical Society, 1992. **114**(23): p. 9022-9028.

Lasic, D.D. and D. Needham, *The ''Stealth'' Liposome: A Prototypical Biomaterial.* Chemical Reviews, 1995. **95**(8): p. 2601-2628.

Lee, J.H., Y.M. Ju, and D.M. Kim, *Platelet Adhesion onto Segmented Polyurethane Film Surfaces Modified by Addition and Crosslinking of Peo-Containing Block Copolymers.* Biomaterials, 2000. **21**(7): p. 683-691.

Lee, P.I., *Kinetics of Drug Release from Hydrogel Matrices.* J Control Release, 1985. **2**: p. 277-288.

Lee, S.J. and K. Park, *Synthesis and Characterization of Sol-Gel Phase-Reversible Hydrogels Sensitive to Glucose.* J Mol Recognit, 1996. **9**(5-6): p. 549-557.

Lei, M., A. Baldi, E. Nuxoll, R.A. Siegel, and B. Ziaie, *A Hydrogel-Based Implantable Micromachined Transponder for Wireless Glucose Measurement.* Diabetes Technology & Therapeutics, 2006. **8**(1): p. 112-122.

Lepore, M., S. Pampanelli, C. Fanelli, F. Porcellati, L. Bartocci, A. Di Vincenzo, C. Cordoni, E. Costa, P. Brunetti, and G.B. Bolli, *Pharmacokinetics and Pharmacodynamics of Subcutaneous Injection of Long-Acting Human Insulin Analog Glargine, Nph Insulin, and Ultralente Human Insulin and Continuous Subcutaneous Infusion of Insulin Lispro.* Diabetes, 2000. **49**(12): p. 2142-2148.

Liu, L., F.Z. Li, Y.E. Fang, and S.R. Guo, *Regioselective Grafting of Poly(Ethylene Glycol) onto Chitosan and the Properties of the Resulting Copolymers.* Macromolecular Bioscience, 2006. **6**(10): p. 855-861.

Lowman, A.M., M. Morishita, M. Kajita, T. Nagai, and N.A. Peppas, *Oral Delivery of Insulin Using Ph-Responsive Complexation Gels.* J Pharm Sci, 1999. **88**(9): p. 933-937.

Lowman, A.M. and N.A. Peppas, *Molecular Analysis of Interpolymer Complexation in Graft Copolymer Networks.* Polymer, 2000. **41**(1): p. 73-80.

Maas, C.S., T. Eriksson, T. Mccalmont, M. Mabry, D. Cooke, and R. Schindler, *Evaluation of Expanded Polytetrafluoroethylene as a Soft-Tissue Filling Substance: An Analysis of Design-Related Implant Behavior Using the Porcine Skin Model.* Plastic and Reconstructive Surgery, 1998. **101**(5): p. 1307-1314.

Malvern, *The Importance of Sample Viscosity in Dynamic Light Scattering Measurements*, in *Application note Recognising the quality of data from photon correlation spectroscopy measurements Technical note*. 2005, Malvern Instruments.

Mandel, M., *The Potentiometric Titration of Weak Polyacids.* Eur Polym J, 1970. **6**(6): p. 807-822.

Massia, S.P. and J. Stark, *Immobilized Rgd Peptides on Surface-Grafted Dextran Promote Biospecific Cell Attachment.* Journal of Biomedical Materials Research, 2001. **56**(3): p. 390-399.

Mccluskey, A., C.I. Holdsworth, and M.C. Bowyer, *Molecularly Imprinted Polymers (Mips): Sensing, an Explosive New Opportunity?* Organic & Biomolecular Chemistry, 2007. **5**(20): p. 3233-3244.

Mcpherson, T., A. Kidane, I. Szleifer, and K. Park, *Prevention of Protein Adsorption by Tethered Poly(Ethylene Oxide) Layers: Experiments and Single-Chain Mean-Field Analysis.* Langmuir, 1998. **14**(1): p. 176-186.

Meng, F.H., G.H.M. Engbers, A. Gessner, R.H. Muller, and J. Feijen, *Pegylated Polystyrene Particles as a Model System for Artificial Cells.* Journal of Biomedical Materials Research Part A, 2004. **70A**(1): p. 97-106.

Miyata, M., A. Jikihara, K. Nakamae, T. Uragami, A.S. Hoffman, K. Kinomura, and M. Okumura, *Preparation of Glucose-Sensitive Hydrogels by Entrapment or Copolymerization of Concanavalin a in a Glucosyloxyethyl Methacrylate Hydrogel*, in *Advanced Biomaterials in Biomedical Engineering and Drug Delivery Systems*, N. Ogata, Editor. 1996, Springer: Tokyo ; New York. p. 237-240.

Miyata, T., T. Uragami, and K. Nakamae, *Biomolecule-Sensitive Hydrogels.* Adv Drug Deliver Rev, 2002. **54**(1): p. 79-98.

Moghimi, S.M., I. Hamad, R. Bunger, T.L. Andresen, K. Jorgensen, A.C. Hunter, L. Baranji, L. Rosivall, and J. Szebeni, *Activation of the Human Complement System by Cholesterol-Rich and Pegylated Liposomes - Modulation of Cholesterol-Rich Liposome-Mediated Complement Activation by Elevated Serum Ldl and Hdl Levels.* Journal of Liposome Research, 2006. **16**(3): p. 167-174.

Moghimi, S.M., A.C. Hunter, and J.C. Murray, *Long-Circulating and Target-Specific Nanoparticles: Theory to Practice.* Pharmacological Reviews, 2001. **53**(2): p. 283-318.

Moore, K.B., C.D. Saudek, A. Greene, and A. Dackiw, *Implantable Insulin Pump Therapy: An Unusual Presentation of a Catheter-Related Complication.* Diabetes Technology & Therapeutics, 2006. **8**(3): p. 397-401.

Morishita, M., A.M. Lowman, K. Takayama, T. Nagai, and N.A. Peppas, *Elucidation of the Mechanism of Incorporation of Insulin in Controlled Release Systems Based on Complexation Polymers.* J Control Release, 2002. **81**(1-2): p. 25-32.

Mosbach, K., *Molecular Imprinting.* Trends Biochem Sci, 1994. **19**(1): p. 9-14.

Mosqueira, V.C.F., P. Legrand, A. Gulik, O. Bourdon, R. Gref, D. Labarre, and G. Barratt, *Relationship between Complement Activation, Cellular Uptake and Surface Physicochemical Aspects of Novel Peg-Modified Nanocapsules.* Biomaterials, 2001. **22**(22): p. 2967-2979.

Muller, M., S. Lee, H.A. Spikes, and N.D. Spencer, *The Influence of Molecular Architecture on the Macroscopic Lubrication Properties of the Brush-Like Co-Polyelectrolyte Poly(L-Lysine)-G-Poly(Ethylene Glycol) (Pll-G-Peg) Adsorbed on Oxide Surfaces.* Tribology Letters, 2003. **15**(4): p. 395-405.

Nickel, J.C., M.E. Olson, and J.W. Costerton, *In Vivo Coefficient of Kinetic Friction: Study of Urinary Catheter Biocompatibility.* Urology, 1987. **29**(5): p. 501-503.

Nie, F.-Q., Z.-K. Xu, Q. Yang, J. Wu, and L.-S. Wan, *Surface Modification of Poly(Acrylonitrile-Co-Maleic Acid) Membranes by the Immobilization of Poly(Ethylene Glycol).* Journal of Membrane Science, 2004. **235**(1-2): p. 147-155.

Nie, F.-Q., Z.-K. Xu, P. Ye, J. Wu, and P. Seta, *Acrylonitrile-Based Copolymer Membranes Containing Reactive Groups: Effects of Surface-Immobilized Poly(Ethylene Glycol)S on Anti-Fouling Properties and Blood Compatibility.* Polymer, 2004. **45**(2): p. 399-407.

Nielsen, L., R. Khurana, A. Coats, S. Frokjaer, J. Brange, S. Vyas, V.N. Uversky, and A.L. Fink, *Effect of Environmental Factors on the Kinetics of Insulin Fibril Formation: Elucidation of the Molecular Mechanism.* Biochemistry-Us, 2001. **40**(20): p. 6036-6046.

Nir, Y., A. Paz, E. Sabo, and I. Potasman, *Fear of Injections in Young Adults: Prevalence and Associations.* Am J Trop Med Hyg, 2003. **68**(3): p. 341-344.

Nomura, M., M. Shichiri, R. Kawamori, Y. Yamasaki, N. Iwama, and H. Abe, *A Mathematical Insulin-Secretion Model and Its Validation in Isolated Rat Pancreatic Islets Perifusion.* Comput Biomed Res, 1984. **17**(6): p. 570-579.

Okano, T., *Molecular Design of Temperature-Responsive Polymers as Intelligent Materials.* Advances in Polymer Science, 1993. **110**: p. 179-197.

Oliva, A., J. Fariña, and M. Llabrés, *Development of Two High-Performance Liquid Chromatographic Methods for the Analysis and Characterization of Insulin and Its Degradation Products in Pharmaceutical Preparations.* Journal of Chromatography B: Biomedical Sciences and Applications, 2000. **749**(1): p. 25-34.

Owens, D.E., Y.C. Jian, J.E. Fang, B.V. Slaughter, Y.H. Chen, and N.A. Peppas, *Thermally Responsive Swelling Properties of Polyacrylamide/Poly(Acrylic Acid) Interpenetrating Polymer Network Nanoparticles.* Macromolecules, 2007. **40**(20): p. 7306-7310.

Owens, D.E. and N.A. Peppas, *Opsonization, Biodistribution, and Pharmacokinetics of Polymeric Nanoparticles.* Int J Pharm, 2006. **307**(1): p. 93-102.

Oya, T., T. Enoki, A.Y. Grosberg, S. Masamune, T. Sakiyama, Y. Takeoka, K. Tanaka, G.Q. Wang, Y. Yilmaz, M.S. Feld, et al., *Reversible Molecular Adsorption Based on Multiple-Point Interaction by Shrinkable Gels.* Science, 1999. **286**(5444): p. 1543-1545.

Pang, S.N.J., *Final Report on the Safety Assessment of Polyethylene Glycols (Pegs) -6, -8, -32, -75, -150, -14m, -20m.* J Am Coll Toxicol, 1993. **12**(5): p. 429-457.

Park, J.H. and Y.H. Bae, *Hydrogels Based on Poly(Ethylene Oxide) and Poly(Tetramethylene Oxide) or Poly(Dimethyl Siloxane): Synthesis, Characterization, in Vitro Protein Adsorption and Platelet Adhesion.* Biomaterials, 2002. **23**(8): p. 1797-1808.

Park, J.H., K.D. Park, and Y.H. Bae, *Pdms-Based Polyurethanes with Mpeg Grafts: Synthesis, Characterization and Platelet Adhesion Study.* Biomaterials, 1999. **20**(10): p. 943-953.

Parker, R.S., *Insulin Delivery*, in *Encyclopedia of Biomaterials and Biomedical Engineering*, G.E. Wnek and G.L. Bowlin, Editors. 2004, Marcel Dekker: New York. p. 857-866.

Parrish, B., R.B. Breitenkamp, and T. Emrick, *Peg- and Peptide-Grafted Aliphatic Polyesters by Click Chemistry.* Journal of the American Chemical Society, 2005. **127**(20): p. 7404-7410.

Peppas, N.A., P. Bures, W. Leobandung, and H. Ichikawa, *Hydrogels in Pharmaceutical Formulations.* European Journal of Pharmaceutics and Biopharmaceutics, 2000. **50**(1): p. 27-46.

Peppas, N.A. and J.J. Sahlin, *Hydrogels as Mucoadhesive and Bioadhesive Materials: A Review.* Biomaterials, 1996. **17**(16): p. 1553-1561.

Podual, K., *Glucose-Sensitive Cationic Hydrogels for Insulin Release*. 1998, Purdue University, CHE, DEC, 1998. p. xviii, 263 p.

Podual, K., F. Doyle, and N.A. Peppas, *Modeling of Water Transport in and Release from Glucose-Sensitive Swelling-Controlled Release Systems Based on Poly(Diethylaminoethyl Methacrylate-G-Ethylene Glycol).* Ind Eng Chem Res, 2004. **43**(23): p. 7500-7512.

Podual, K., F.J. Doyle, and N.A. Peppas, *Release of Insulin from Glucose-Sensitive Hydrogels.* Abstr Pap Am Chem S, 1996. **211**: p. 221-PMSE.

Podual, K., F.J. Doyle, and N.A. Peppas, *Dynamic Behavior of Glucose Oxidase-Containing Microparticles of Poly(Ethylene Glycol)-Grafted Cationic Hydrogels in an Environment of Changing Ph.* Biomaterials, 2000. **21**(14): p. 1439-1450.

Podual, K., F.J. Doyle, and N.A. Peppas, *Glucose-Sensitivity of Glucose Oxidase-Containing Cationic Copolymer Hydrogels Having Poly(Ethylene Glycol) Grafts.* J Control Release, 2000. **67**(1): p. 9-17.

Podual, K., F.J. Doyle, and N.A. Peppas, *Preparation and Dynamic Response of Cationic Copolymer Hydrogels Containing Glucose Oxidase.* Polymer, 2000. **41**(11): p. 3975-3983.

Podual, K. and N.A. Peppas, *Relaxational Behavior and Swelling-Ph Master Curves of Poly[(Diethylaminoethyl Methacrylate)-Graft-(Ethylene Glycol)] Hydrogels.* Polym Int, 2005. **54**(3): p. 581-593.

Pradny, M. and S. Sevcik, *Precursors of Hydrophilic Polymers .3. The Potentiometric Behavior of Isotactic and Atactic Poly(2-Dimehtylaminoethyl Methacrylate) in Water Ethanol Solutions.* Makromol Chem, 1985. **186**(1): p. 111-121.

Prime, K.L. and G.M. Whitesides, *Adsorption of Proteins onto Surfaces Containing End-Attached Oligo(Ethylene Oxide) - a Model System Using Self-Assembled Monolayers.* Journal of the American Chemical Society, 1993. **115**(23): p. 10714-10721.

Ratner, B.D., A.S. Hoffman, F.J. Schoen, and J.E. Lemons, eds. *Biomaterials Science: An Introduction to Materials in Medicine*. 2nd ed. 2004, Elsevier Academic Press: Amsterdam ; Boston.

Reid, K.B.M., D.R. Bentley, R.D. Campbell, L.P. Chung, R.B. Sim, T. Kristensen, and B.F. Tack, *Complement System Proteins Which Interact with C3b or C4b a Superfamily of Structurally Related Proteins.* Immunology Today, 1986. **7**(7-8): p. 230-234.

Rhee, P.H., C.D. Friedman, J.A. Ridge, and J. Kusiak, *The Use of Processed Allograft Dermal Matrix for Intraoral Resurfacing - an Alternative to Split-Thickness Skin Grafts.* Archives of Otolaryngology-Head & Neck Surgery, 1998. **124**(11): p. 1201-1204.

Rice, C.V., *Phase-Transition Thermodynamics of N-Isopropylacrylamide Hydrogels.* Biomacromolecules, 2006. **7**(10): p. 2923-2925.

Rodriguez, B.E., M.S. Wolfe, and M. Fryd, *Nonuniform Swelling of Alkali Swellable Microgels.* Macromolecules, 2002. **27**(22): p. 6642-6647.

Rosiak, J., K. Burozak, and W. Pekala, *Polyacrylamide Hydrogels as Sustained Release Drug Delivery Dressing Materials.* Radiation Physics and Chemistry (1977), 1983. **22**(3-5): p. 907-915.

Ryhanen, J., M. Kallioinen, J. Tuukkanen, J. Junila, E. Niemela, P. Sandvik, and W. Serlo, *In Vivo Biocompatibility Evaluation of Nickel-Titanium Shape Memory Metal Alloy: Muscle and Perineural Tissue Responses and Encapsule Membrane Thickness.* Journal of Biomedical Materials Research, 1998. **41**(3): p. 481-488.

Salzmann, D.L., L.B. Kleinert, S.S. Berman, and S.K. Williams, *The Effects of Porosity on Endothelialization of Eptfe Implanted in Subcutaneous and Adipose Tissue.* Journal of Biomedical Materials Research, 1997. **34**(4): p. 463-476.

Sanchez-Soto, P.J., J.M. Gines, M.J. Arias, C. Novak, and A. Ruiz-Conde, *Effect of Molecular Mass on the Melting Temperature, Enthalpy and Entropy of Hydroxy-Terminated Peo.* J Therm Anal Calorim, 2002. **67**(1): p. 189-197.

Savage, B., E. Saldivar, and Z.M. Ruggeri, *Initiation of Platelet Adhesion by Arrest onto Fibrinogen or Translocation on Von Willebrand Factor.* Cell, 1996. **84**(2): p. 289-297.

Sawhney, A.S. and J.A. Hubbell, *Poly(Ethylene Oxide)-Graft-Poly(L-Lysine) Copolymers to Enhance the Biocompatibility of Poly(L-Lysine)-Alginate Microcapsule Membranes.* Biomaterials, 1992. **13**(12): p. 863-870.

Sawhney, A.S., C.P. Pathak, and J.A. Hubbell, *Bioerodible Hydrogels Based on Photopolymerized Poly(Ethylene Glycol)-Co-Poly(Alpha-Hydroxy Acid) Diacrylate Macromers.* Macromolecules, 1993. **26**(4): p. 581-587.

Schaumberg, D.A., R.J. Glynn, A.J. Jenkins, T.J. Lyons, N. Rifai, J.E. Manson, P.M. Ridker, and D.M. Nathan, *Effect of Intensive Glycemic Control on Levels of Markers of Inflammation in Type 1 Diabetes Mellitus in the Diabetes Control and Complications Trial.* Circulation, 2005. **111**(19): p. 2446-2453.

Schwarte, L.M. and N.A. Peppas, *Novel Poly(Ethylene Glycol)-Grafted, Cationic Hydrogels: Preparation, Characterization and Diffusive Properties.* Polymer, 1998. **39**(24): p. 6057-6066.

Sefton, M.V., C.H. Gemmel, and M.B. Gorbet, *What Really Is Blood Compatibility?* Journal of Biomaterials Science -- Polymer Edition, 2000. **11**(11): p. 1165.

Seifert, L.M. and R.T. Greer, *Evaluation of in Vivo Adsorption of Blood Elements onto Hydrogel-Coated Silicone Rubber by Scanning Electron Microscopy and Fourier Transform Infrared Spectroscopy.* Journal Of Biomedical Materials Research, 1985. **19**(9): p. 1043-1071.

Sellergren, B., M. Lepisto, and K. Mosbach, *Highly Enantioselective and Substrate-Selective Polymers Obtained by Molecular Imprinting Utilizing Noncovalent Interactions - Nmr and Chromatographic Studies on the Nature of Recognition.* J Am Chem Soc, 1988. **110**(17): p. 5853-5860.

Seminoff, L.A., G.B. Olsen, and S.W. Kim, *A Self-Regulating Insulin Delivery System .1. Characterization of a Synthetic Glycosylated Insulin Derivative.* Int J Pharm, 1989. **54**(3): p. 241-249.

Sennerby, L. and P. Thomsen, *Tissue-Response to Titanium Implants in Experimental Antigen-Induced Arthritis.* Biomaterials, 1993. **14**(6): p. 413-422.

Shamoon, H., H. Duffy, N. Fleischer, S. Engel, P. Saenger, M. Strelyzn, M. Litwak, J. Wylierosett, A. Farkash, D. Geiger, et al., *The Effect of Intensive Diabetes Treatment on the Progression of Diabetic-Retinopathy in Insulin-Dependent Diabetes-Mellitus - the Diabetes Control and Complications Trial.* Arch Ophthalmol-Chic, 1995. **113**(1): p. 36-51.

Shamoon, H., H. Duffy, N. Fleischer, S. Engel, P. Saenger, M. Strelzyn, M. Litwak, J. Wylierosett, A. Farkash, D. Geiger, et al., *The Effect of Intensive Treatment of Diabetes on the Development and Progression of Long-Term Complications in Insulin-Dependent Diabetes-Mellitus.* New Engl J Med, 1993. **329**(14): p. 977-986.

Sharma, S., K.C. Popat, and T.A. Desai, *Controlling Nonspecific Protein Interactions in Silicon Biomicrosystems with Nanostructured Poly(Ethylene Glycol) Films.* Langmuir, 2002. **18**(23): p. 8728-8731.

Shatkay, A. and I. Michaeli, *Potentiometric Titrations of Polyelectrolytes with Separation of Phases.* The Journal of Physical Chemistry, 1966. **70**(12): p. 3777-3782.

Shawky, H.A., M.H. El-Sayed, A.E. Ali, and M.S.A. Mottaleb, *Treatment of Polluted Water Resources Using Reactive Polymeric Hydrogel.* J Appl Polym Sci, 2006. **100**(5): p. 3966-3973.

Sheth, S.R. and D. Leckband, *Measurements of Attractive Forces between Proteins and End-Grafted Poly(Ethylene Glycol) chains.* PNAS, 1997. **94**(16): p. 8399-8404.

Siegel, R.A., M. Falamarzian, B.A. Firestone, and B.C. Moxley, *Ph-Controlled Release from Hydrophobic Poly-Electrolyte Copolymer Hydrogels.* J Control Release, 1988. **8**(2): p. 179-182.

Siegel, R.A. and B.A. Firestone, *Ph-Dependent Equilibrium Swelling Properties of Hydrophobic Poly-Electrolyte Copolymer Gels.* Macromolecules, 1988. **21**(11): p. 3254-3259.

Siegel, R.A. and B.A. Firestone, *Ph-Dependent Equilibrium Swelling Properties of Hydrophobic Polyelectrolyte Copolymer Gels.* Macromolecules, 1988. **21**(11): p. 3254-3259.

Siegel, R.A. and B.A. Firestone, *Mechanochemical Approaches to Self-Regulating Insulin Pump Design.* J Control Release, 1990. **11**(1-3): p. 181-192.

Siegel, R.A., B.A. Firestone, I. Johannes, and J. Cornejo, *Weak Ionic Hydrogels - Effects of Ph, Ionic-Strength and Buffer Composition on Swelling Equilibria, Kinetics and Solute Release.* Abstr Pap Am Chem S, 1990. **199**: p. 119-POLY.

Siegel, R.A., Y.D. Gu, A. Baldi, and B. Ziaie, *Novel Swelling/Shrinking Behaviors of Glucose-Binding Hydrogels and Their Potential Use in a Microfluidic Insulin Delivery System.* Macromol Symp, 2004. **207**: p. 249-256.

Siegel, R.A., I. Johannes, C.A. Hunt, and B.A. Firestone, *Buffer Effects on Swelling Kinetics in Polybasic Gels.* Pharmaceut Res, 1992. **9**(1): p. 76-81.

Siepmann, J. and N.A. Peppas, *Modeling of Drug Release from Delivery Systems Based on Hydroxypropyl Methylcellulose (Hpmc).* Advanced Drug Delivery Reviews, 2001. **48**(2-3): p. 139-157.

Smith, D.C., R.M. Pilliar, and R. Chernecky, *Dental Implant Materials .1. Some Effects of Preparative Procedures on Surface-Topography.* Journal of Biomedical Materials Research, 1991. **25**(9): p. 1045-1068.

Sofia, S.J., V. Premnath, and E.W. Merrill, *Poly(Ethylene Oxide) Grafted to Silicon Surfaces: Grafting Density and Protein Adsorption.* Macromolecules, 1998. **31**(15): p. 5059-5070.

Stayton, P.S., A.S. Hoffman, N. Murthy, C. Lackey, C. Cheung, P. Tan, L.A. Klumb, A. Chilkoti, F.S. Wilbur, and O.W. Press. *Molecular Engineering of Proteins and Polymers for Targeting and Intracellular Delivery of Therapeutics*. 2000.

Suggs, L.J., M.S. Shive, C.A. Garcia, J.M. Anderson, and A.G. Mikos, *In Vitro Cytotoxicity and in Vivo Biocompatibility of Poly(Propylene Fumarate-Co-Ethylene Glycol) Hydrogels.* Journal of Biomedical Materials Research, 1999. **46**(1): p. 22-32.

Sugimoto, M., M. Morimoto, H. Sashiwa, H. Saimoto, and Y. Shigemasa, *Preparation and Characterization of Water-Soluble Chitin and Chitosan Derivatives.* Carbohydrate Polymers, 1998. **36**(1): p. 49-59.

Sung, W.K., M.P. Chaul, K. Makino, L.A. Seminoff, D.L. Holmberg, J.M. Gleeson, D.E. Wilson, and E.J. Mack, *Self-Regulated Glycosylated Insulin Delivery.* J Control Release, 1990. **11**(1-3): p. 193-201.

Suzuki, K., T. Shimizu, and T. Nakata, *The Cholesterol Metabolite Cholest-4-En-3-One and Its 3-Oxo Derivatives Suppress Body Weight Gain, Body Fat Accumulation and Serum Lipid Concentration in Mice.* Bioorg Med Chem Lett, 1998. **8**(16): p. 2133-2138.

Szebeni, J., *Complement Activation-Related Pseudoallergy: A New Class of Drug-Induced Acute Immune Toxicity.* Toxicology, 2005. **216**(2-3): p. 106-121.

Tobolsky, A.V. and M.C. Shen, *The Effect of Hydrogen Bonds on the Viscoelastic Properties of Amorphous Polymer Networks.* The Journal of Physical Chemistry, 2002. **67**(9): p. 1886-1891.

Tseng, Y.C., T. Mcpherson, C.S. Yuan, and K. Park, *Grafting of Ethylene Glycol-Butadiene Block-Copolymers onto Dimethyl-Dichlorosilane-Coated Glass by Gamma-Irradiation.* Biomaterials, 1995. **16**(13): p. 963-972.

Tseng, Y.C., W.M. Mullins, and K. Park, *Albumin Grafting on to Polypropylene by Thermal-Activation.* Biomaterials, 1993. **14**(5): p. 392-400.

Vittaz, M., D. Bazile, G. Spenlehauer, T. Verrecchia, M. Veillard, F. Puisieux, and D. Labarre, *Effect of Peo Surface Density on Long-Circulating Pla-Peo Nanoparticles Which Are Very Low Complement Activators.* Biomaterials, 1996. **17**(16): p. 1575-1581.

Vonarbourg, A., C. Passirani, P. Saulnier, and J.-P. Benoit, *Parameters Influencing the Stealthiness of Colloidal Drug Delivery Systems.* Biomaterials, 2006. **27**(24): p. 4356-4373.

Vonarbourg, A., C. Passirani, P. Saulnier, P. Simard, J.C. Leroux, and J.P. Benoit, *Evaluation of Pegylated Lipid Nanocapsules Versus Complement System Activation and Macrophage Uptake.* Journal of Biomedical Materials Research Part A, 2006. **78A**(3): p. 620-628.

Watari, F., A. Yokoyama, F. Saso, M. Uo, and T. Kawasaki, *Fabrication and Properties of Functionally Graded Dental Implant.* Composites Part B-Engineering, 1997. **28**(1-2): p. 5-11.

Wesslen, B., M. Kober, C. Freijlarsson, A. Ljungh, and M. Paulsson, *Protein Adsorption of Poly(Ether Urethane) Surfaces Modified by Amphiphilic and Hydrophilic Polymers.* Biomaterials, 1994. **15**(4): p. 278-284.

Wheeler, J.C., J.A. Woods, M.J. Cox, R.W. Cantrell, F.H. Watkins, and R.F. Edlich, *Evolution of Hydrogel Polymers as Contact Lenses, Surface Coatings, Dressings, and Drug Delivery Systems.* J Long-Term Eff Med, 1996. **6**(3-4): p. 207-217.

Wong, J.Y., T.L. Kuhl, J.N. Israelachvili, N. Mullah, and S. Zalipsky, *Direct Measurement of a Tethered Ligand-Receptor Interaction Potential.* Science, 1997. **275**(5301): p. 820-822.

Woodle, M.C., M.S. Newman, and F.J. Martin, *Liposome Leakage and Blood-Circulation - Comparison of Adsorbed Block Copolymers with Covalent Attachment of Peg.* International Journal of Pharmaceutics, 1992. **88**(1-3): p. 327-334.

Xu, Z.-K., F.-Q. Nie, C. Qu, L.-S. Wan, J. Wu, and K. Yao, *Tethering Poly(Ethylene Glycol)S to Improve the Surface Biocompatibility of Poly(Acrylonitrile-Co-Maleic Acid) Asymmetric Membranes.* Biomaterials, 2005. **26**(6): p. 589-598.

Yang, Z.H., J.A. Galloway, and H.U. Yu, *Protein Interactions with Poly(Ethylene Glycol) Self-Assembled Monolayers on Glass Substrates: Diffusion and Adsorption.* Langmuir, 1999. **15**(24): p. 8405-8411.

Yu, H. and D.W. Grainger, *Thermosensitive Swelling Behavior in Cross-Linked N-Isopropylacrylamide Networks - Cationic, Anionic, and Ampholytic Hydrogels.* J Appl Polym Sci, 1993. **49**(9): p. 1553-1563.

Zahr, A.S., C.A. Davis, and M.V. Pishko, *Macrophage Uptake of Core-Shell Nanoparticles Surface Modified with Poly(Ethylene Glycol).* Langmuir, 2006. **22**(19): p. 8178-8185.

Zhang, M., X.H. Li, Y.D. Gong, N.M. Zhao, and X.F. Zhang, *Properties and Biocompatibility of Chitosan Films Modified by Blending with Peg.* Biomaterials, 2002. **23**(13): p. 2641-2648.

Zhang, Q., C.R. Wang, Y. Babukutty, T. Ohyama, M. Kogoma, and M. Kodama, *Biocompatibility Evaluation of Eptfe Membrane Modified with Peg in Atmospheric Pressure Glow Discharge.* Journal of Biomedical Materials Research, 2002. **60**(3): p. 502-509.

Zhang, R., M. Tang, A. Bowyer, R. Eisenthal, and J. Hubble, *Synthesis and Characterization of a D-Glucose Sensitive Hydrogel Based on Cm-Dextran and Concanavalin A.* Reactive and Functional Polymers, 2006. **66**(7): p. 757-767.

Zhao, B. and J.S. Moore, *Fast Ph- and Ionic Strength-Responsive Hydrogels in Microchannels.* Langmuir, 2001. **17**(16): p. 4758-4763.

Zhao, Y.B., W.Y. Chen, Y.J. Yajiang, X.L. Yang, and H.B. Xu, *Swelling Behavior of Ionically Cross-Linked Polyampholytic Hydrogels in Varied Salt Solutions.* Colloid Polym Sci, 2007. **285**(12): p. 1395-1400.

Vita

Stephen Richard Marek was born and raised in Virginia. He graduated from The Chesterfield County Mathematics and Science High School at Clover Hill High School in 2001. He pursued his undergraduate studies at The Georgia Institute of Technology, where he majored in chemical engineering. He was also a highly active photographer for the Georgia Tech newspaper and yearbook, and he performed research in the chemistry lab of Dr. Suzanne Shuker. He graduated with a Bachelor of Science in chemical and biomolecular engineering with Highest Honors from Georgia Tech in May, 2005. After completing his bachelor's degree, Stephen accepted the invitation to attend The University of Texas at Austin to pursue his doctoral degree in chemical engineering. He performed his research in the Laboratory of Biomaterials, Drug Delivery, Bionanotechnology, and Molecular Recognition under the guidance of Professor Nicholas Peppas. He is currently residing in Austin, Texas.

Permanent address: 1748 Ohlen Rd #100, Austin, TX 78757

This dissertation was typed by the author.